



**HAL**  
open science

# Implantable microelectrode biosensors for neurochemical monitoring of brain functioning

Natalia Vasylieva

► **To cite this version:**

Natalia Vasylieva. Implantable microelectrode biosensors for neurochemical monitoring of brain functioning. Agricultural sciences. INSA de Lyon, 2012. English. NNT : 2012ISAL0078 . tel-00861119

**HAL Id: tel-00861119**

**<https://theses.hal.science/tel-00861119>**

Submitted on 12 Sep 2013

**HAL** is a multi-disciplinary open access archive for the deposit and dissemination of scientific research documents, whether they are published or not. The documents may come from teaching and research institutions in France or abroad, or from public or private research centers.

L'archive ouverte pluridisciplinaire **HAL**, est destinée au dépôt et à la diffusion de documents scientifiques de niveau recherche, publiés ou non, émanant des établissements d'enseignement et de recherche français ou étrangers, des laboratoires publics ou privés.

Thèse

## **Implantable microelectrode biosensors for neurochemical monitoring of brain functioning**

Présentée devant  
L'institut national des sciences appliquées de Lyon

Pour obtenir  
Le grade de docteur

École doctorale: Electronique, électrotechnique, automatique

par

**Natalia Vasylieva**

Soutenue le 11 septembre 2012 devant la Commission d'examen

### **JURY**

Présidente	Eliane Souteyrand	Directeur de recherches (INL, E.C de Lyon)
Rapporteur	Christian Amatore	Directeur de recherches (ENS, Paris)
Rapporteur	Pierre Temple Boyer	Directeur de recherches (LAAS, Toulouse)
Rapporteur	Olivier Frey	Chargé de recherches (ETH Zurich)
Examineur	Alain Walcarius	Directeur de recherches (LCPME, Nancy)
Directeur de thèse	Daniel Barbier	Professeur d'Université (INL, INSA-Lyon)
Directeur de thèse	Stéphane Marinesco	Chargé de recherches (CRNL, UCBL)
Membre invité	Andrei Sabac	Ingénieur de Recherches (INL, INSA-Lyon)



INSA Direction de la Recherche - Ecoles Doctorales – Quinquennal 2011-2015

SIGLE	ECOLE DOCTORALE	NOM ET COORDONNEES DU RESPONSABLE
CHIMIE	<b><u>CHIMIE DE LYON</u></b>  <a href="http://www.edchimie-lyon.fr">www.edchimie-lyon.fr</a>  Insa : R. GOURDON	M. Jean Marc LANCELIN Université de Lyon – Collège Doctoral Bât ESCPE 43 bd du 11 novembre 1918 69622 VILLEURBANNE Cedex Tél : 04.72.43 13 95 <a href="mailto:directeur@edchimie-lyon.fr">directeur@edchimie-lyon.fr</a>
E.E.A.	<b><u>ELECTRONIQUE,</u></b> <b><u>ELECTROTECHNIQUE,</u></b> <b><u>AUTOMATIQUE</u></b> <a href="http://edeea.ec-lyon.fr">edeea.ec-lyon.fr</a> Secrétariat : M.C. HAVGOUDOUKIAN <a href="mailto:eea@ec-lyon.fr">eea@ec-lyon.fr</a>	M. Gérard SCORLETTI Ecole Centrale de Lyon 36 avenue Guy de Collongue 69134 ECULLY Tél : 04.72.18 60 97 Fax : 04 78 43 37 17 <a href="mailto:Gerard.scorletti@ec-lyon.fr">Gerard.scorletti@ec-lyon.fr</a>
E2M2	<b><u>EVOLUTION, ECOSYSTEME,</u></b> <b><u>MICROBIOLOGIE,</u></b> <b><u>MODELISATION</u></b>  <a href="http://e2m2.universite-lyon.fr">e2m2.universite-lyon.fr</a>  Insa : H. CHARLES	Mme Gudrun BORNETTE CNRS UMR 5023 LEHNA Université Claude Bernard Lyon Bât Forel 43 bd du 11 novembre 1918 69622 VILLEURBANNE Cédex Tél : 04.72.43.12.94 <a href="mailto:e2m2@biomserv.univ-lyon1.fr">e2m2@biomserv.univ-lyon1.fr</a>
EDISS	<b><u>INTERDISCIPLINAIRE</u></b> <b><u>SCIENCES-SANTE</u></b>  <a href="http://ww2.ibcp.fr/ediss">ww2.ibcp.fr/ediss</a>  Sec : Safia AIT CHALAL Insa : M. LAGARDE	M. Didier REVEL Hôpital Louis Pradel Bâtiment Central 28 Avenue Doyen Lépine 69677 BRON Tél : 04.72.68 49 09 Fax : 04 72 35 49 16 <a href="mailto:Didier.revel@creatis.uni-lyon1.fr">Didier.revel@creatis.uni-lyon1.fr</a>
INFOMATHS	<b><u>INFORMATIQUE ET</u></b> <b><u>MATHEMATIQUES</u></b>  <a href="http://infomaths.univ-lyon1.fr">infomaths.univ-lyon1.fr</a>	M. Johannes KELLENDONK Université Claude Bernard Lyon INFOMATHS Bâtiment Braconnier 43 bd du 11 novembre 1918 69622 VILLEURBANNE Cedex Tél : 04.72. 44.82.94 Fax 04 72 43 16 87 <a href="mailto:infomaths@univ-lyon1.fr">infomaths@univ-lyon1.fr</a>
Matériaux	<b><u>MATERIAUX DE LYON</u></b>  Secrétariat : M. LABOUNE PM : 71.70 –Fax : 87.12 Bat. Saint Exupéry  <a href="mailto:Ed.materiaux@insa-lyon.fr">Ed.materiaux@insa-lyon.fr</a>	M. Jean-Yves BUFFIERE INSA de Lyon, MATEIS Bâtiment Saint Exupéry 7 avenue Jean Capelle 69621 VILLEURBANNE Cédex Tél : 04.72.43 83 18 Fax 04 72 43 85 28 <a href="mailto:Jean-yves.buffiere@insa-lyon.fr">Jean-yves.buffiere@insa-lyon.fr</a>
MEGA	<b><u>MECANIQUE, ENERGETIQUE,</u></b> <b><u>GENIE CIVIL, ACOUSTIQUE</u></b>  Secrétariat : M. LABOUNE PM : 71.70 –Fax : 87.12 Bat. Saint Exupéry  <a href="mailto:mega@insa-lyon.fr">mega@insa-lyon.fr</a>	M. Philippe BOISSE INSA de Lyon Laboratoire LAMCOS Bâtiment Jacquard 25 bis avenue Jean Capelle 69621 VILLEURBANNE Cedex Tél : 04.72.43.71.70 Fax : 04 72 43 72 37 <a href="mailto:Philippe.boisse@insa-lyon.fr">Philippe.boisse@insa-lyon.fr</a>
ScSo	<b><u>ScSo*</u></b>  M. OBADIA Lionel  Sec : Viviane POLSINELLI Insa : J.Y. TOUSSAINT	M. OBADIA Lionel Université Lyon 2 86 rue Pasteur 69365 LYON Cedex 07 Tél : 04.78.69.72.76 Fax : 04.37.28.04.48 <a href="mailto:Lionel.Obadia@univ-lyon2.fr">Lionel.Obadia@univ-lyon2.fr</a>

\*ScSo : Histoire, Géographie, Aménagement, Urbanisme, Archéologie, Science politique, Sociologie, Anthropologie



## ACKNOWLEDGEMENTS

The multi-disciplinary nature of my thesis has permitted me to benefit from the experience of my colleagues in the fields of analytical chemistry applied to biological studies, neurobiology, and microelectromechanical system fabrication. Besides the technical skills and scientific reasoning, I have got an enriching experience in social adaptation, communication, collaboration, project organization and managing. Benevolent atmosphere of the host laboratories promoted my assimilation to French culture and facilitated the learning of French language.

I am particularly grateful to my supervisor *Stéphane Marinesco*. I am thankful for his trust and confidence in my work, for his help in technical difficulties. I am grateful for our efficient discussions and his competent advices. I am glad to adapt his manner of scientific writing which is simple, clear but nevertheless strongly logic and substantiated. I appreciate very much the possibility that I had to observe him during scientific negotiations and to learn his manner of scientific presentations. Finally, I am grateful for his support, attention, patience and amicability during these 4 years.

I would like to thank my second supervisor *Daniel Barbier* who gave me the opportunity to participate in this project and obtained the financial support for me. I appreciate the flexibility I had in my developments, his readiness to help me with advices, his support, motivation and stimulating discussions.

I am thankful to NanoLyon Platform for technical support. I would like to address my thanks to *Andrei Sabac* who contributed in development and fabrication of multisensing micro-needles: advices in masques design, metals deposition and development of DRIE protocol. I am grateful to *Joelle Gregoire*, *Khaled Ayadi* (NanoLyon, INSA) for their help in metal deposition and technical advices; to Radoslaw Mazurczyk (NanoLyon, ECL) for his help and implication in early steps of microfabrication development, his encouragements and trainings in English communication; to *Patrick Pittet* and his team (NanoLyon, UCBL) for technical assistance with diamond saw equipment. I am also very much thankful to *Irène Pheng* (CIME nanotech, Grenoble) for her help in microdevices packaging.

I am very much grateful to the INSERM U1028 team and the Technological Platform AniRA-Neurochem. It was my special pleasure to work with *Anne Meiller*, with whom I performed my first animal experiments, whose good humor and kind attention made me particularly comfortable during my first months in France. It was a great pleasure to work with *Caroline Maucier*, who shared with me the difficulties of PhD students and who lent me her rats for experiments in awake animals. She also contributed a lot in my French learning and improvement. I would also like to thank the students, *Estelle Enriquez* and *Quentin Chalvet*, for their important help and contribution to my thesis progress. I thank *Sandrine Parrot* and *Gabriel Debilly* for their technical support. I am thankful to all the colleagues of INSERM U1028 laboratory for collaboration, assistance, their amicability and good humor, for shared joyous occasions during these four years.

My special thanks go to my husband *Bogdan*, whose expertise in chemical questions and high quality organic synthesis were indispensable for success of my thesis work. I am grateful for my dear parents and sister for their belief in me and unconditional help.



## ABSTRACT

Identification, monitoring and quantification of biomolecules in the CNS is a field of growing interest for identifying biomarkers of neurological diseases. Implantable enzymatic microelectrode biosensors are a unique minimally invasive tool for real-time monitoring. Progress in microfabrication technologies has opened new possibilities in the preparation of complex biosensor architectures with numerous electrodes to respond to the needs of neurobiologists and neurochemists for simultaneous monitoring of numerous biomarkers.

In this thesis, silicon needle-shaped multisensing microprobes were developed. Our microelectrode array design comprises a needle length of 6mm with 100x50  $\mu\text{m}^2$  cross-section bearing three platinum electrodes with a size of 40x200  $\mu\text{m}$  and 200 $\mu\text{m}$  spacing between them. We have used these microprobes for simultaneous glucose and lactate monitoring, using the third electrode for control of non-specific current variations. Local microdroplet protein deposition on the electrode surface was achieved using a pneumatic picopump injection system.

Enzyme immobilization on the electrode surface is a key step in microelectrode biosensor fabrication. We have developed a simple, low cost, non-toxic enzyme immobilization method employing poly(ethyleneglycol) diglycidyl ether (PEGDE). Successful biosensor fabrication was demonstrated with glucose oxidase, D-amino acid oxidase, and glutamate oxidase. We found that these biosensors exhibited high sensitivity and short response time sufficient for observing biological events *in vivo* on a second-by-second timescale. PEGDE-based biosensors demonstrated an excellent long-term stability and reliably monitored changes in brain glucose levels induced by sequential administration of insulin and glucose solution. We then carried out a comparative study of five enzyme immobilization procedures commonly used in Neuroscience: covalent immobilization by cross-linking using glutaraldehyde, PEGDE, or a hydrogel matrix and enzyme entrapment in a sol-gel or polypyrrole-derived matrices. Enzymatic microelectrodes prepared using these different procedures were compared in terms of sensitivity, response time, linear range, apparent Michaelis-Menten constant, stability and selectivity. We conclude that PEGDE and sol-gel techniques are potentially promising procedures for *in vivo* laboratory studies. The comparative study also revealed that glutaraldehyde significantly decreased enzyme selectivity while PEGDE preserved it. The effects that immobilization can have on enzyme substrate specificity, produce dramatic consequences on glutamate detection in complex biological samples and in the CNS. Our biosensor's results were systematically controlled by HPLC or capillary electrophoresis. The highly selective PEGDE-based biosensors allowed accurate measurements glutamate concentrations in the anesthetized and awaked rats at physiological conditions and under pharmacological and electrical stimulations.

The microfabricated multielectrodes based on silicon needles coupled to the simple, non-toxic and mild immobilization method based on PEGDE, open new possibilities for specific neurotransmitter detection in the central nervous system and the study of cell-cell communication *in vivo*.

**KEYWORDS:** *biosensor, electrochemistry, amperometry, enzyme, immobilization, PEGDE, micro-needle, silicon, MEMS, in vivo, rat, glucose oxidase, glutamate oxidase.*

**MOTS-CLES:** *biocapteur, électrochimie, amperometry, enzyme, immobilisation, PEGDE, micro-aiguille, silicium, MEMS, in vivo, rat, glucose oxidase, glutamate oxidase.*





**Table of content**

ABSTRACT .....	7
Glossary .....	13
List of figures and tables.....	15
Introduction.....	19
Chapter 1: Neurochemical monitoring <i>in vivo</i> (state of the art) .....	23
I. Small molecules monitoring in the brain .....	25
1. Neurotransmitters .....	26
2. Metabolites .....	32
3. Small molecules monitoring in the brain for diagnostics of neurological disorders: example of subarachnoid hemorrhage and traumatic brain injury. ....	35
II. Techniques for monitoring the brain extracellular fluid: microdialysis and microelectrode biosensors.....	36
1. Microdialysis.....	36
1.1 Methods for biomolecules analysis: High-performance analytical techniques .....	37
1.1.1 Liquid chromatography (LC).....	38
1.1.2 Capillary electrophoresis (CE).....	40
1.1.3 HPLC and EC detection systems .....	41
1.2 Methods for biomolecules analysis: Point of care units (Ex-vivo biosensors).....	43
1.2.1 MEMS technology .....	45
1.2.2 Biosensing part of analytical devices.....	49
1.2.3 Optical detection of biomolecules .....	51
1.2.4 Electrochemical detection of biomolecules.....	53
1.2.5 Mass sensitive detection systems .....	54
2. Implantable enzymatic microbiosensors (In vivo biosensors).....	56
2.1 Microelectrodes: configuration and materials.....	56
2.2 Biosensing part – enzyme .....	60
2.3 Non-specific interaction suppression .....	65
2.4 Requirements for implantable microbiosensors .....	66
2.5 Implantable multisensing microprobes in Neuroscience .....	67
III. Experimental strategy .....	73
Chapter 2:.....	75
Covalent enzyme immobilization by poly(ethylene glycol) diglycidyl ether (PEGDE) for microelectrode biosensors preparation .....	75

ABSTRACT .....	78
1. Introduction.....	79
2. Materials and Methods .....	79
3. Results.....	81
4. Discussion .....	88
Chapter 3:.....	93
Comparative study of immobilization methods for biosensor construction .....	93
ABSTRACT .....	96
1. Introduction.....	97
2. Immobilization methods and protocols.....	97
2.1 Cross-linking.....	97
2.1.1 Glutaraldehyde .....	98
2.1.2 PEGDE matrix .....	99
2.1.3 Redox hydrogel .....	100
Polymer synthesis.....	102
Biosensor construction.....	102
2.2. Enzyme entrapment.....	103
2.2.1 Sol-gel matrix .....	103
2.2.2 Polypyrrole-derived matrix .....	105
3. Quantitative comparison of different immobilization methods.....	107
3.1. Apparent Michaelis – Menten constant and linear range.....	107
3.2. Biosensor sensitivity .....	109
3.3 Response time.....	110
3.4 Stability.....	111
4. Conclusions .....	111
Chapter 4:.....	113
Effect of enzyme immobilization on biosensors substrate-specificity: consequences for glutamate detection in the central nervous system.....	113
ABSTRACT .....	116
1. Introduction.....	117
2. Materials and Methods .....	117
3. Results.....	122

4. Discussion .....	129
5. Conclusion.....	132
Chapter 5:.....	137
Multi-sensing bioprobes on silicon.....	137
1. Microprobes fabrication .....	140
2. Electrochemical (diffusion) cross-talk .....	142
3. Enzyme integration.....	145
Enzyme deposition in chitosan matrix and cross-talk studies.....	146
Enzyme local drop deposition and cross-talk studies.....	148
4. Microprobe biosensor validation for in vivo experiments .....	150
Conclusion and perspectives.....	155
Bibliography.....	159
Annexes.....	175
Annex 1. Microfabrication .....	177
Microfabrication protocol.....	177
SU8 patterning conditions.....	178
SU8 oxygen plasma etch conditions.....	178
Design evolution within project .....	179
Annex 2. Enzyme-immobilization protocols .....	181
PEGDE.....	181
Glutaraldehyde .....	181
Annex 3. Thesis summary in French .....	183
Annex 4. List of publications related to the thesis project.....	197



## Glossary

ATP	Adenosine-5'-triphosphate
ANLSH	Astrocytes-neuron lactate shuttle hypothesis
CE	Capillary Electrophoresis
CNS	Central Nervous System
CPG	(S)-4-carboxyphenylglycine
CSF	Cerebrospinal fluid
CV	Cerebral vasospasm
CV	Cyclic voltammetry
CVD	Chemical vapor deposition
EAAC	Excitatory Amino Acid Carrier
EAAT	Excitatory Amino Acid Transporter
ECF	Extracellular fluid
EIS	Electrochemical impedance spectroscopy
EOF	Electroosmotic flow
ESI	Electrospray ionization
FAD	Flavin adenine dinucleotide (quinon form)
FADH <sub>2</sub>	Flavin adenine dinucleotide (hydroquinon form)
FSCV	Fast cyclic voltammetry
GLAST	Glutamate-aspartate transporter
GLT	Glutamate Transporter
GLU	Glutamate
HCA	Homocysteic acid
HPLC	High Performance Liquid Chromatography
LIF	Laser-induced fluorescence
MEA	Microelectrode array
MEMS	Microelectromechanical systems

MS	Mass-spectrometry
NADH/NAD <sup>+</sup>	Nicotinamide adenine dinucleotide
PGC	Porous graphitic carbon
POC	Point-of-care
<sup>1</sup> HMRS	Proton magnetic resonance spectroscopy
QCM	Quartz crystal microbalances
RP-HPLC	Reversed Phase Chromatography
SAH	Subarachnoid hemorrhage
SPR	Surface-plasmon resonance
ssDNA	Single stranded DNA
TBI	Traumatic Brain Injury
TBOA	<sub>DL</sub> -threo-β-benzyloxyaspartate
TFA	Trifluoroacetic acid
TTX	Tetrodotoxin

## List of figures and tables

Figure 1.1 SEM picture of a brain slice .....	25
Figure 1.2 Neuron structure and connection with other nerve cells.....	27
Figure 1.3 The glutamine-glutamate cycle .....	29
Figure 1.4 Glutamate transporters .....	30
Figure 1.5 Glucose metabolism in the brain, the classical model.....	33
Figure 1.6 Glucose metabolism in the brain, ANLSH hypothesis. ....	34
Figure 1.7 Microdialysis technique .....	37
Figure 1.8 Capillary electrophoresis technique .....	41
Figure 1.9 Cylindrical glass-capillary microelectrode .....	57
Figure 1.10 Processed wafer.....	58
Figure 1.11 Glucose biosensor.....	61
Figure 1.12 Multienzymatic biosensor design .....	62
Figure 1.13 Michaelis–Menten kinetics.....	64
Figure 1.14 Multisensing microprobes .....	67
Figure 1.15 Schema of cross-talk effect .....	70
Scheme 2.1 Reaction scheme of protein with PEGDE .....	82
Figure 2.1 Dependence of glucose biosensor sensitivity on PEGDE concentration .....	83
Figure 2.2 Glucose biosensors .....	84
Figure 2.3 D-Serine and glutamate biosensors.....	86
Figure 2.4 Examples of biosensor recordings <i>in vivo</i> .....	88
Figure S2.5 Biosensor sensitivity towards the endogenous electroactive molecules in physiological concentrations.....	91
Table 2.1 Comparison of biosensor characteristics with proteins immobilized by glutaraldehyde versus PEGDE.....	90
Figure 3.1 Glutaraldehyde method .....	98
Figure 3.2 Poly(ethylene glycol) diglycidyl ether (PEGDE) method.....	99
Figure 3.3 Redox hydrogel matrix method.....	101
Figure 3.4 Sol-gel method .....	104
Figure 3.5 Polypyrrole method.....	106
Figure 3.6 Apparent Michaelis-Menten constant and linear range .....	108
Figure 3.7 Biosensor sensitivity and response time .....	110
Figure 4.1 Effect of enzyme immobilization method on glucose oxidase substrate-specificity	



.....	123
Figure 4.2 Effect of enzyme immobilization method on glutamate oxidase substrate-specificity.....	124
Figure 4.3 Biosensor specificity in biological samples .....	127
Figure 4.4 <i>In vivo</i> glutamate detection in the cortex.....	128
Figure 4.5 Detection of Glutamate spillover in the dentate gyrus .....	130
Figure S4.6 HPLC analysis of sugars in brain homogenates .....	134
Figure S4.7 HPLC analysis of amino acids in brain homogenate.....	135
Figure S4.8 Covalent immobilization techniques .....	136
Table 4.1 HPLC identification of sugars in serum and brain homogenates .....	125
Table 4.2 HPLC identification of proteinogenic amino acids in brain dialysate and homogenate .....	126
Figure 5.1 Microprobe fabrication process.....	141
Figure 5.2 Fabricated microelectrode array .....	142
Figure 5.3 Diffusion cross-talk .....	144
Figure 5.4 Impact of top layer thickness on cross-talk currents.....	145
Figure 5.5 Local enzyme deposition by entrapment in chitosan matrix .....	147
Figure 5.6. Enzyme drop dispensing on microelectrode .....	148
Figure 5.7 <i>In vitro</i> simultaneous glucose and lactate calibration. ....	150
Figure 5.8 Optimization of immobilization conditions .....	151
Figure 5.9 Correction of the linearity response range .....	152
Figure 5.10 Simultaneous <i>in vivo</i> recording of glucose and lactate -Proof of the concept...	153
Table 5.1. Cross-talk study on microprobes with enzyme entrapped in chitosan matrix.....	147
Table 5.2. Cross-talk study on microprobes with enzyme applied by drop dispensing .....	149
Figure A. 1. Microprobe design.....	179

*“Understanding the human mind in biological terms has emerged as the central challenge for science in the twenty-first century. We want to understand the biological nature of perception, learning, memory, thought, consciousness, and the limits of free will” (2).*

Eric Kandel



# Introduction



Enzymatic implantable biosensors are widely used for *in vivo* monitoring applications. They are used in neuroscience research to detect neurotransmitters and metabolites with outstanding temporal resolution. In addition to animal studies, medical diagnostics is increasingly oriented to the detection and monitoring of biomarkers and biochemical components in patients to improve the detection of specific illnesses. In animal research, these biosensors are usually made of platinum microelectrodes constructed from a glass capillary, on which an enzymatic layer is immobilized. Their fabrication involves simple assembling procedures without high-cost equipment and materials. Such microelectrodes are minimally invasive and cause minor damage to biological tissues. However, to meet the severe requirements of clinical practice, implantable enzymatic biosensors have to be approved in terms of safety, biocompatibility, operational stability, chemical specificity etc.

Recent studies have been oriented on the development of multisensing probes with an increasing number of electrodes to allow simultaneous monitoring of several neurotransmitters or metabolites during physiological or pathological neurological states. Such devices can also monitor the same molecule in different areas of the brain. Up to now, a few research groups have succeeded in fabricating such integrated biosensor probes and applied them *in vivo*. However, minor attention has been paid so far to clinical applications and to their drastic requirements. Important attention must be paid to the protein immobilization procedure that impacts the overall biosensor performance. A wide variety of enzyme immobilization techniques are now available for biosensor construction. However, most methods involve toxic components that make potential clinical applications difficult. Moreover, the chemicals used for biosensor preparation are often expensive or imply some organic synthesis. Overall, there is a need for simple, safe and clean way for enzyme immobilization on biosensors. Additionally, the resulting biosensors have to possess sufficient selectivity to target the biomarker of interest and ensure accurate interpretation of biological data.

The main objective of this thesis work is to develop a biomedical tool that permits parallel, simultaneous monitoring of neurotransmitters or metabolites, such as glutamate, D-serine, glucose or lactate with high selectivity, and validate it in the central nervous system (CNS) of the laboratory animals. The long term goal of this study is to allow biologists to improve their understanding of chemical communication between brain cells and its role in physiological and pathological brain functioning.

This experimental work is at the interface between microfabrication technologies, analytical chemistry and neurobiology. We first sought to optimize enzyme immobilization by testing several immobilization procedures that have already been validated in Neuroscience research, and compared the corresponding biosensors in terms of sensitivity, *in vitro* and *in vivo* stability, response time as well as toxicity in view of potential clinical applications. We then developed a simple and non-toxic PEGDE assisted enzyme immobilization method that is especially mild in order to preserve the substrate specificity of natural enzymes, and fulfill the safety requirements of *in vivo* recordings in the CNS. We constructed glutamate biosensors using either PEGDE or the more conventional glutaraldehyde method to immobilize Glutamate oxidase. We then studied *in vivo* glutamate dynamics with both biosensor types, and determined the consequences of the immobilization method on glutamate concentration estimates in the CNS of laboratory rats. We then developed a multisensing implantable microelectrode array exploiting MEMS-microfabrication technologies, in which enzymes were immobilized by the PEGDE-based method. This multisensing array was applied for simultaneous glucose and lactate monitoring.

This manuscript comprises an Introduction, 5 chapters, annexes and summary report in French.

The Chapter 1 is a bibliographical review of methods for biomolecules analysis in complex media, especially *in vivo* monitoring. This chapter reviews the developments in the field of micromachining and microfabrication of analytical devices with specific attention to enzymatic microelectrode biosensors. Finally, the current developments, problems and applications of the implantable biosensors and multisensing probes are summarized.

The main results and discussion are presented in the Chapters 2-5. Chapter 2 presents an innovative enzyme immobilization method using polyethylene glycol diglycidyl ether (PEGDE). Chapter 3 represents a comparative study of the widely used methods for enzyme immobilization on biosensors applied in neuroscience research. Chapter 4 discusses the influence of enzyme immobilization methods on biosensor selectivity and the consequences on glutamate detection in the CNS. Chapter 5 presents the development and characterization of multisensing arrays on silicon and their application for glucose and lactate simultaneous monitoring in the cortex of anesthetized rats.

The annexes contain: (1) the detailed protocol of multielectrode array fabrication; (2) conditions of enzyme immobilization by PEGDE and Glutaraldehyde; (3) extended summary of thesis results in French and (4) a list of publications related to the thesis.

# Chapter 1: Neurochemical monitoring *in vivo* (state of the art)

This chapter covers the field of biomolecule analysis in complex biological media and particularly, the interest of small biomolecules monitoring *in vivo*. It reviews the current approaches for *in vivo* quantification of metabolites and neurotransmitters. The use of *in vivo* microdialysis coupled to High performance liquid chromatography (HPLC) or capillary electrophoresis (CE) is also discussed. Finally, this chapter discusses the developments in the field of micromachining and microfabrication of “lab on a chip” devices for analysis of complex biological media. It reviews the principal components of these devices: sensing elements, detection configurations etc. Much attention is devoted to enzymatic biosensors: microelectrode design and materials, enzyme theory and the requirements for implantable biosensor are discussed. Finally, the current developments, problems and applications of the implantable biosensors and multisensing probes are reviewed.





## I. Small molecules monitoring in the brain

*In this section I specify the general interest of monitoring molecules in neuroscience (cells communication in brain functioning); why these studies are performed in the interstitial milieu*

The brain is the most complex biological organ in mammals, controlling vital functions of living organism and causing neurological diseases. It is no wonder that a lot of research studies are oriented on understanding brain functioning and in particular, brain cells connection and reciprocal communication. Cell-to-cell signaling mostly occurs through electric nerve impulses, neurotransmitter release in the extracellular space and intracellular biochemical cascades. The monitoring of neurotransmitter dynamics, metabolic molecules and hormones during physiological or pathological brain functioning is an important approach for understanding neuronal and glial cell communication.

More precisely, cell-to-cell chemical communication occurs through release of neurotransmitters into the interstitial fluid (Fig.1.1 (3)), followed by their binding to specific receptors that trigger intracellular biochemical cascades susceptible to change the cellular activity and gene expression. Metabolic molecules like glucose or lactate are used as energetic sources for biochemical reactions. Neurochemical changes in the brain are therefore accompanied by changes in the concentration of metabolic molecules in the interstitial fluid. Thus, the extracellular space represents a rich chemical environment containing substances with diverse chemical structures that are involved in neural activity. Mental processes and physiological states are probably characterized by changes in the

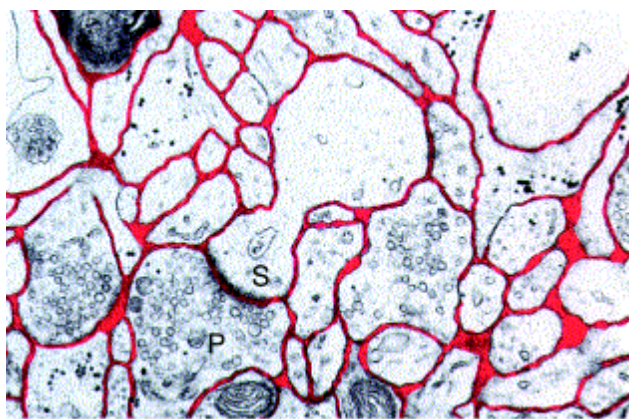


**Figure 1.1:** SEM picture of a brain slice with interstitial milieu in red, taking 20% of the overall brain space (adapted from (1))

concentrations of specific chemicals. Therefore, the study of the chemical composition of the extracellular milieu and the variations in concentration of neurotransmitters and metabolites in response to chemical, physical or physiological stimulations is of particular interest and permits a deeper understanding of the mechanisms and laws of brain functioning.

Modern techniques allow the advantageous non-invasive tracking of molecules in the brain. Proton magnetic resonance spectroscopy ( $^1\text{HMR}$ S) is a noninvasive imaging technique that relies on the interaction of electromagnetic radiation with tissues.

The resonance frequency of atomic nuclei depends on the local magnetic field to which they are exposed. Depending on the chemical structure of the molecule, an atomic nucleus can absorb or emit specific radiations at different frequencies allowing identification of different molecules present in the brain. This method allows obtaining *in vivo* information about N-acetylaspartate, choline, myo-inositol, creatine and phosphocreatine, lactate, glutamine and glutamate in the living brain (4, 5). Another noninvasive technology for measuring the cerebral oxygen saturation is a near-infrared spectroscopy (6). It measures the absorption of the near-infrared light by hemoglobin, which absorbs different wavelengths at oxidized or

reduced states. These techniques are sensitive and allow good temporal resolution, though they are voluminal and reflect the overall brain concentration of molecules of interest. They cannot differentiate the concentration of molecules between intracellular and extracellular milieus which is usually not homogeneous. For instance, the majority of glutamate is stored in neuronal vesicles while only trace amounts are present in the extracellular fluid for signaling (7, 8). Moreover metabolites like glucose and lactate are largely concentrated inside the cell for energetic supply and can be shuttled between neurons and glial cells in response to neuronal activity (9). Therefore, despite the great interest of non invasive imaging techniques, especially in humans, there is also a need for methods and technologies allowing local detection of extracellular molecules.

Studying the composition of the interstitial fluid is a difficult task, as a wide variety of molecules are present and therefore, highly selective techniques and methods must be employed to obtain accurate data. Moreover, the changes in the chemical composition of the interstitial fluid can be very rapid, especially when neurotransmitters are released, requiring techniques with high temporal resolution. Finally, the probes for *in vivo* monitoring must be minimally invasive to ensure the physiological functioning of the brain tissue under study.

Despite the complexity of the interstitial fluid composition, our interest and development of appropriate technique is basically focused on detecting and monitoring neurotransmitters and metabolites concentration and dynamics.

## 1. Neurotransmitters

*In this section I introduce the neurons as main users of neurotransmitters; I discuss what a neurotransmitter is, and give detailed information about the neurochemistry of glutamate, because it is one of the most important neurotransmitters in the CNS. Glutamate will be the focus of chapter 4.*

Neurons are the basic building blocks of the Central Nervous System (CNS), and use neurotransmitters to communicate with other cells.

A typical neuron possesses a cell body, dendrites and axon as illustrated in Figure 1.2A. The *cell body (soma)* is a central part of the neuron and is usually of 10-25  $\mu\text{m}$  in diameter. It contains all necessary components of the cell, such as the nucleus that stores genetic information, endoplasmic reticulum and ribosomes for protein synthesis and mitochondria for energy production. *Dendrites* are the branchlike extensions that arise from the cell body. Dendrites serve to receive signals from axonal termini of other neurons and to transmit them to the cell body. Dendrites often extend over hundreds of micrometers and form a so called "dendritic tree" that forms synapses and receives signals from a large number of other neurons. The *axon* is the main conducting unit of the neuron. It arises from the cell body. Neurons possess only one axon and multiple dendrites. The axon can extend over 2 meters in humans and thus is capable of conveying electrical signals over long distances in the CNS. The axon can conduct and distribute an electrical signal to thousand of neurons simultaneously. Even if a given neuron gives a rise to only one axon, the axon in turn can branch into hundreds of synaptic terminals. At the end of the terminal button is a gap known as a *synapse*. Synapses transmit signals between neurons in only one direction: from the axon terminal of the presynaptic cell to the postsynaptic cell. There are two general types of synapses: the relatively rare electric synapse and the chemical synapse, illustrated in Figure 1.2B. In a chemical synapse, the axon terminal of the presynaptic cell contains vesicles filled with a particular neurotransmitter. The postsynaptic cell can be a dendrite or cell body of another neuron or even another axon, and possesses specific receptors on their

plasma membrane, that specifically bind to the neurotransmitter released by the presynaptic terminal.

When an action potential (or electric impulse) in the presynaptic cell reaches an axon terminal, it triggers vesicles to fuse with the plasma membrane, releasing their contents into the synaptic cleft. The neurotransmitters diffuse across the synaptic cleft (within 0.5 ms) and bind to receptors on postsynaptic cells. Neurotransmitter binding provokes changes in the ion permeability of the postsynaptic plasma membrane and subsequently changes in the membrane's electrical potential. The result of action potential firing can be muscle contraction if the postsynaptic cell is a muscle cell, hormone secretion if the postsynaptic cell is a gland cell, or more generally, changes in neuronal activity when the postsynaptic cell is a neuron. Thus, synaptic communication between neurons allows them to function as a network interconnected through neurotransmitters actions.

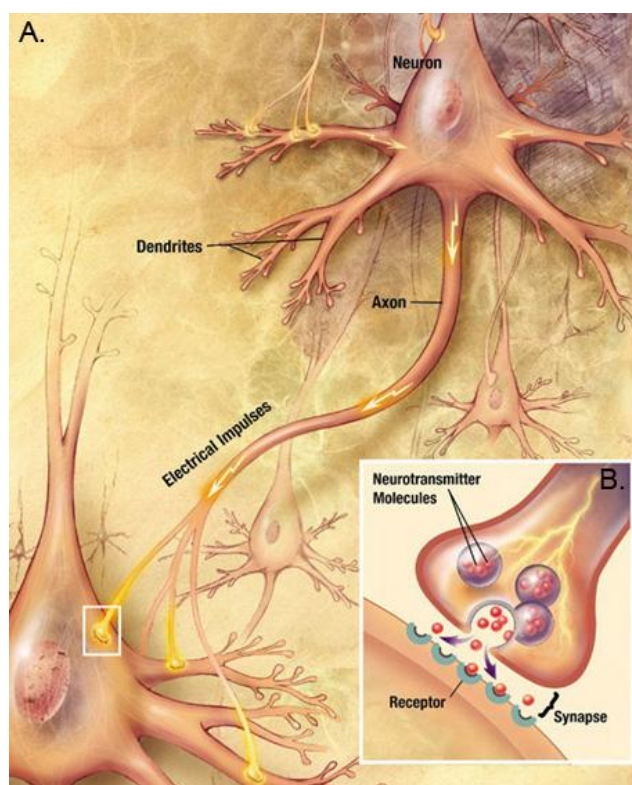


**Figure 1.2: Neuron structure and connection with other nerve cells.** A. Neuron contains a cell body, dendrites, an axon, conducting electrical impulses and the axon terminals. B. Axon terminals of the presynaptic cell with the postsynaptic cell form the synapse. Neurotransmitters stored in the vesicles of axon terminal are released into the synaptic cleft in response to action potential firing (illustration is adopted from Wikipedia).

To understand the nature and chemistry of neuronal communication neuroscientists search to identify active neurotransmitters and characterize their changes in concentration during physiological or pathological brain functioning.

Chemically, neurotransmitters are relatively small and simple molecules. Each brain neurotransmitter may have a different effect according to receptor that it activates. Some 60 neurotransmitters have been identified. They fall into several classes:

1. cholines – of which acetylcholine is the most important one;
2. biogenic amines – serotonin, histamine, and the catecholamines - dopamine and norepinephrine, epinephrine;

3. amino acids - glutamate and aspartate are excitatory transmitters, while gamma-aminobutyric acid (GABA) and glycine are inhibitory neurotransmitters;
4. neuropeptides,- these are formed by longer chains of amino acids (like a small protein molecule). Over 50 of them are known to act in the brain, and many of them have been implicated in the modulation or transmission of neural information;
5. gases – nitric oxide, carbon monoxide.

Among these neurotransmitters, the present work is largely focused on glutamate monitoring in the brain interstitial fluid.

The amino acid **L-glutamate (GLU)** is the most abundant amino acid in the brain and is considered to be the major mediator of excitatory signals in the mammalian central nervous system. It plays a central role in cellular metabolism and is widely recognized as the principal excitatory neurotransmitter in the CNS. It is involved in most aspects of normal brain function including cognition, memory and learning (10) as well as in psychiatric and neurological diseases. Glutamate also plays major roles in the development of the central nervous system, including synapse induction and elimination, neuronal and glial cell migration, differentiation and death. Glutamate also plays a signaling role in peripheral organs and tissues as well as in endocrine cells (11, 12).

The brain contains large amounts of glutamate but its distribution is not uniform. Thus, red blood cells cytoplasmic glutamate is ~500  $\mu\text{M}$  whereas in muscle cells, cytoplasmic glutamate is ~5 mM. The concentration of glutamate in the cytoplasm of glutamatergic neurons is ~10 mM and synaptic vesicles of these neurons contain glutamate at ~100 mM (7, 13, 14). However, the glutamate concentration in the cerebrospinal fluid (CSF) and in the extracellular fluid was found to be very low compared to its intracellular concentration – about 10  $\mu\text{M}$  in the CSF (11), and up to 5  $\mu\text{M}$  in the extracellular fluid (8, 15-18). It is of critical importance that the extracellular glutamate concentration is kept low because excessive activation of glutamate receptors is harmful. Glutamate is toxic at high concentrations and produces neuronal injury: in cell cultures maintained in 1-20  $\mu\text{M}$  glutamate swelling and apoptosis are observed and fast necrosis develops at > 100  $\mu\text{M}$  glutamate (19). For example, large extracellular glutamate levels can cause excessive influx of calcium ions through NMDA receptors and allow intracellular calcium to reach cytotoxic levels resulting in neuronal damage or cell death. By contrast, intracellular glutamate represents a storage pool with no signaling properties which is generally considered non-toxic. The over-stimulation of glutamate receptors also produces multiple adverse effects including compromise of organelle functions, increase in nitric oxide (NO) production and free radicals, persistent activation of proteases and kinases, increases in expression of pro-death transcription factors and immediate early genes (20).

It is known that the extracellular glutamate concentration is a result of its release and uptake. There is no extracellular enzyme identified to degrade glutamate in significant amounts. Consequently, the only rapid way to remove glutamate from the extracellular fluid is by cellular uptake (21). There are five principal glutamate transporters: EAAT1 (GLAST), EAAT2 (GLT), EAAT3 (EAAC), EAAT4 and EAAT5. GLT and GLAST are responsible for most of the glutamate uptake activity. GLT is responsible for >90% of total glutamate uptake and it is the quantitatively dominating glutamate transporter in all regions of the mammalian CNS except the cerebellum, the inner ear and the retina, where GLAST is the major transporter (22, 23). The level of GLT is four times higher than GLAST in the hippocampus



and six times lower in the cerebellum, while the amount of GLAST is ten times higher than that of EAAT4 (24). GLT and GLAST proteins are only found in astroglial cells that indicates a major role of glia in glutamate removal. EAAC and EAAT4 are found in postsynaptic nerve endings. EAAC is distributed widely in the brain, whereas EAAT4 localizes specifically to the cerebellum. EAAT5 is a photoreceptor and bipolar cell glutamate transporter that is selectively expressed in the retina.

Glutamate transporters play a major role in the glutamine-glutamate cycle as well as in maintaining the nervous system at a physiological balance. If glutamate is not used for protein synthesis or energy metabolism, in the nerve cell it is transported into synaptic vesicles by a vesicular glutamate transporter and then, released during exocytosis. In astrocytes, glutamate taken up from the extracellular fluid is converted to glutamine by glutamine synthetase and is released to the extracellular fluid. It is then taken up by neurons and reconverted to glutamate intracellularly by glutaminase (Fig. 1.3). This circulation of glutamate and glutamine between astrocytes and neurons is considered to be a major pathway of glutamate recycling (25, 26). Glutamine present in the extracellular fluid does not influence neurotransmission because glutamine, in contrast to glutamate, does not activate glutamate receptors.

Figure 1.4 schematically represents the location of principal glutamate transporters.

At glutamatergic synapses, glutamate transporters can be found at five possible locations: in glial cell membrane, in the plasma membrane of postsynaptic dendritic spines, at presynaptic glutamatergic nerve terminals, at the membrane of synaptic vesicles.

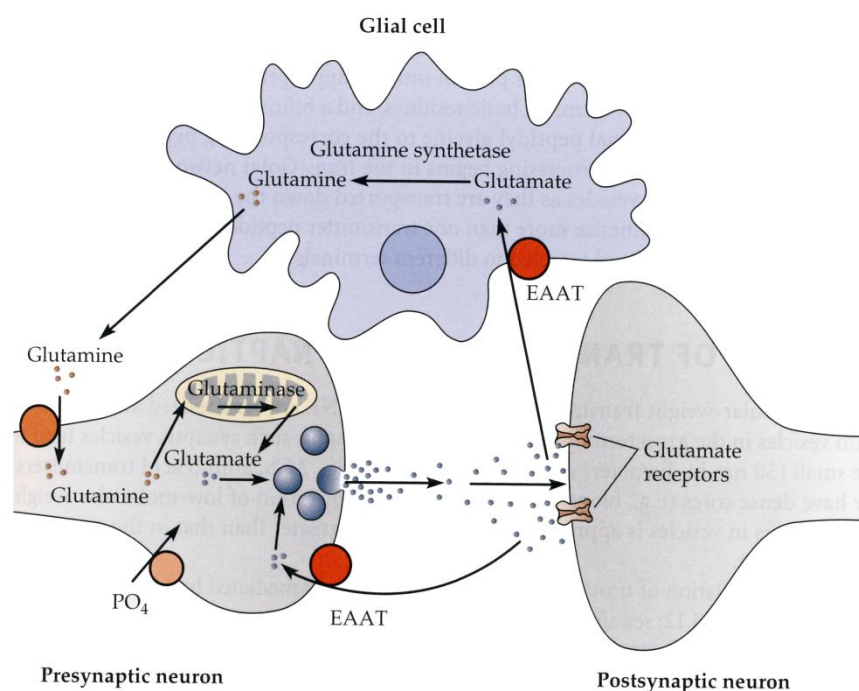


**Figure 1.3. The glutamine-glutamate cycle:** Glutamate is released from nerve terminal via exocytosis and is taken up by glutamate transporters into glial, post- and presynaptic neurons. In glial cells, glutamate is converted into glutamine, released into extracellular fluid and taken up by glutamine transporters into presynaptic neurons (adapted from (27)).

I. Glutamate transporters in glial cell plasma membranes, GLT (glutamate transporter) and GLAST (glutamate-aspartate transporter) as well as some EAAC (excitatory amino acid

carrier), remove glutamate from the extracellular fluid after it has escaped from the synaptic cleft. GLT and EAAC pump one glutamate molecule with three Na<sup>+</sup> and one H<sup>+</sup> into the cell in the exchange of one K<sup>+</sup> ion released into the extracellular space.

II. Glutamate transporters are found postsynaptically in the plasma membranes of dendritic spines. They include EAAT4 and EAAC. These transporters also exchange 1 glutamate, 3Na<sup>+</sup> and 1H<sup>+</sup> for 1K<sup>+</sup>.

III. The glutamate transporter in glutamatergic nerve terminals has still not been molecularly identified and the exact stoichiometry of the transport cycle is not known.

IV. Synaptic vesicles are filled with glutamate from cytosol via glutamate transporters located in the membrane of synaptic vesicles. Glutamate is pumped into vesicle in exchange to H<sup>+</sup>. Constant low pH in a vesicle is maintained by action of a Mg<sup>2+</sup>-dependent ATPase in the membrane pumping H<sup>+</sup> into the vesicles.

V. Glutamate is transported also via cystine-glutamate exchangers situated in glial cell membrane. Cystine is implicated in the synthesis of the antioxidant glutathione, so that the physiological role of this transporter is to carry cystine into the cell in exchange for internal glutamate in 1:1 proportion. If the extracellular concentration of glutamate is high, the cystine-glutamate carrier can reverse its functioning and release cystine while taking up glutamate inside the cell. This is considered pathological as reduced cysteine uptake may result in oxidative stress and cell death.

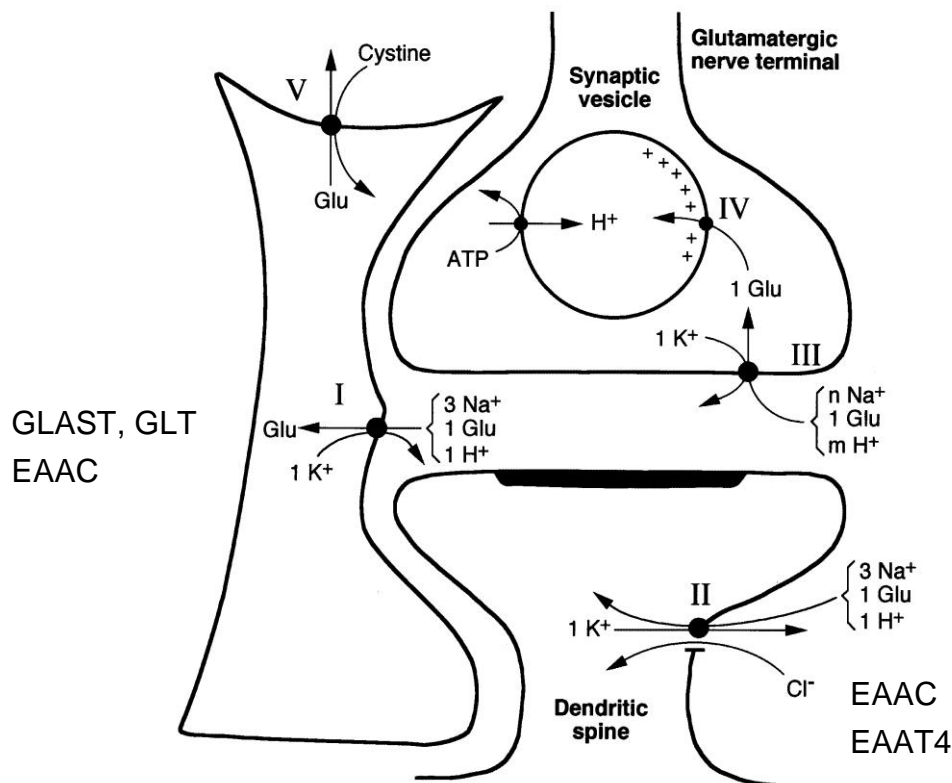


**Figure 1.4. Glutamate transporters:** I. at glial cell plasma membrane; II. at the plasma membrane of postsynaptic dendritic spines; III. at presynaptic glutamatergic nerve terminals; IV. at the membrane of synaptic vesicles; V. cystine-glutamate antiporter (adapted from (11))

Important roles of EAATs have been elucidated by genetic approaches consisting in knocking out the genes encoding for specific transporter subtypes. However, such genetic manipulations do not provide information on the dynamics of glutamate homeostasis. As a

result, the origin and role of the ambient extracellular glutamate remains poorly understood. Additionally, the estimated glutamate basal concentration differs significantly with the analytical methods that are applied. Some estimates of the glutamate resting concentration in the intact brain using biosensors have been proposed up to 35  $\mu\text{M}$  (28). However, such concentrations are problematic because they can provoke neuronal degeneration in cell culture studies (19). Thus, improving the detection methods capable of monitoring glutamate extracellular concentrations quantitatively in the brain, and coupling these techniques to pharmacological or genetic alteration of specific transporter systems, is essential approach to understanding the origin and regulation of glutamate in the extracellular fluid.

The criteria for determining the neuronal origin of glutamate release are founded on general properties of neurons:

1. Sensitivity to potassium ( $\text{K}^+$ )-evoked depolarization. When the membrane potential is depolarized to a critical or threshold level the cell responds actively with the opening of voltage-gated ion channels and fires action potentials that produces neurotransmitters release.

2. Sodium ( $\text{Na}^+$ )-channel blockage induced by tetrodotoxin (TTX). Blockage of voltage-gated  $\text{Na}^+$  channels blocks action potential generation and propagation and stops action-potential dependent vesicular release of glutamate.

3. Sensitivity to calcium ( $\text{Ca}^{2+}$ ) omission. Action potentials stimulate  $\text{Ca}^{2+}$  entry into presynaptic terminal through ion channels located in the plasma membrane. This causes the fusion of synaptic vesicles containing neurotransmitters with the plasma membrane and release of the neurotransmitter into the synaptic cleft. (29, 30).

4. Depletion of presynaptic vesicles by local administration of the selective neurotoxin  $\alpha$ -latrotoxin (massive neurotransmitter release), or blockade of vesicle fusion into the plasma membrane by tetanus of botulinum toxins.

In addition, transporter blockers can further refine the molecular dissection of the mechanisms of glutamate regulation:

$\text{DL}$ -threo- $\beta$ -benzyloxyaspartate ( $\text{DL}$ -TBOA or TBOA) is non-transportable reuptake inhibitor, which is a blocker of the glutamate transporters EAAT1-3.

Homocysteic acid (HCA) and (S)-4-carboxyphenylglycine (CPG) are inhibitors of cystine-glutamate exchange. They block both cystine uptake and glutamate release.

These pharmacological tools are available to neurochemists to validate their *in vivo* detection methods and understand the neuronal vs glial origin of the glutamate signal they detect. This question is essential to *in vivo* detection of neurotransmitters in general. Implanting a probe in the brain can produce cellular lesions, microglia proliferation, astrogliosis and the formation of a scar that prevents the probe from detecting the "true" physiological neurotransmitter pool. Such cellular injury mechanisms are still poorly understood. In general, a high neuronal dependence of the signal detected by the probe is considered a proof for accurate *in vivo* detection with minimal damage, and high glial dependence is considered indicative of a glial scar surrounding the probe.



## 2. Metabolites

*In this section I discuss the implication of metabolites in brain functioning and why it is interesting to monitor them in the brain.*

Glucose is one of the main sources of energy in our organism and about 50% of all glucose consumption is due to brain activity. For years, glucose has been considered as the main if not the unique source of energy in the brain and particularly, the main source of energy to maintain neuronal activity. According to classical models (Fig.1.5), in physiological conditions when oxygen and glucose are available in sufficient quantities, glucose enters both neuronal cells and astrocytes, and is transformed into pyruvate by glycolysis with reduction of NADH dehydrogenase. Then pyruvate undergoes oxidative conversion at the mitochondria through the Krebs's cycle with CO<sub>2</sub> production that is evacuated from the cell by diffusion. Some pyruvate is converted to lactate by lactate dehydrogenase and released into the extracellular space via monocarboxylate transporters. As long as oxygen concentration is non-limiting, NADH is constantly transformed into NAD<sup>+</sup> and the cycle repeats. In pathological conditions, for example during ischemia, a lack of oxygen leads to an altered redox state with accumulation of NADH. In such conditions, pyruvate is mainly transformed into lactate implicating NADH oxidation. Consequently, a typical example observed during severe ischemic/hypoxic episode in the brain is a marked increase of lactate/pyruvate ratio in combination with low level of glucose (31).

However, recent studies demonstrate that the neurons do not massively use glucose (32, 33). Moreover, when given the choice between glucose and lactate, neurons appear to preferentially use lactate for energy supply (34). These findings support idea that glucose may be preferentially taken up by glial cells. In fact, one principal energy consuming process of the CNS is the biosynthesis and transport of ions and neurotransmitters, especially glutamate. Glutamate is continuously removed from the extracellular fluid (ECF) by astrocytes and is recycled by conversion to glutamine, which is an important energy-consuming process triggering enhanced use of glucose by astrocytes (34). Importantly, astrocytes do not oxidize glucose entirely, but transform it into lactate that is then released into the extracellular space. Neurons can in turn use this source of lactate for energy supply. In fact, the studies on isolated cultured cell populations provided evidence that at least 75% of oxidative metabolism in neurons is supported by lactate (35, 36). The cycle of neuron energy supply is known as the astrocytes-neuron lactate shuttle hypothesis (ANLSH) (37), represented in Figure 1.6.

There are however different opinions that support or contradict the ANLSH hypothesis. Some studies report that neurons do not show considerable import of lactate, or that the shuttle works in opposite direction (neurons to astrocytes) (38, 39). Additionally, the idea that brain cells may switch between classical and ANLSH models depending on the energy requirement of the neuron has been proposed (40).

Further understanding of brain energy metabolism and specific regulations occurring in different physiological or pathological conditions is therefore required. In fact, several neurodegenerative diseases exhibit metabolic changes prior to the first clinical symptoms (for example in Alzheimer's disease) and thus the possibility to detect these first changes would permit improved diagnosis and earlier treatment.

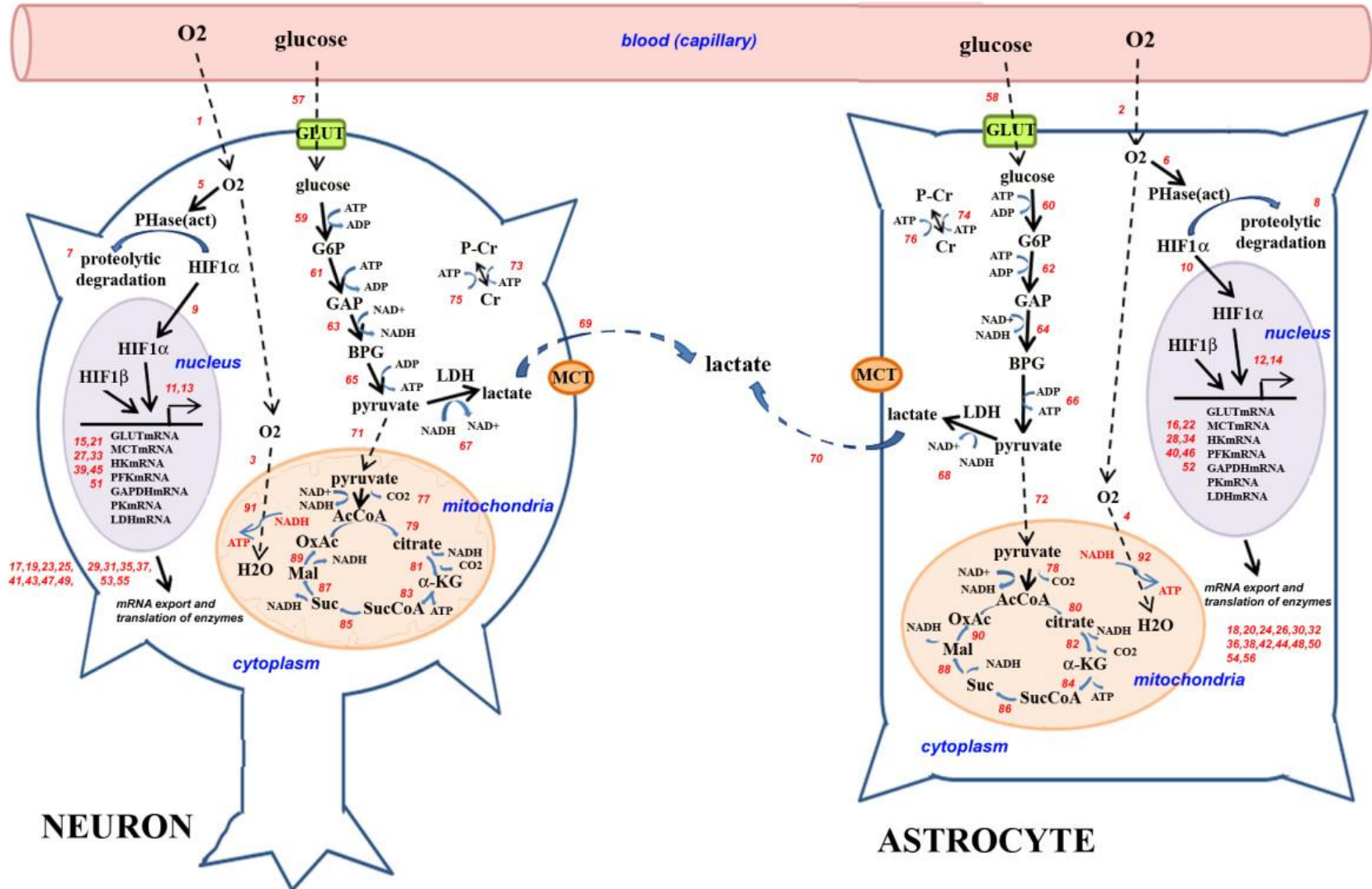


**Figure 1.5. Glucose metabolism in the brain, the classical model:** Glucose is taken up by both neurons and astrocytes, and is mainly converted into pyruvate that undergoes Krebs's cycle transformation. Only some of pyruvate is transformed in lactate and released in the extracellular space.

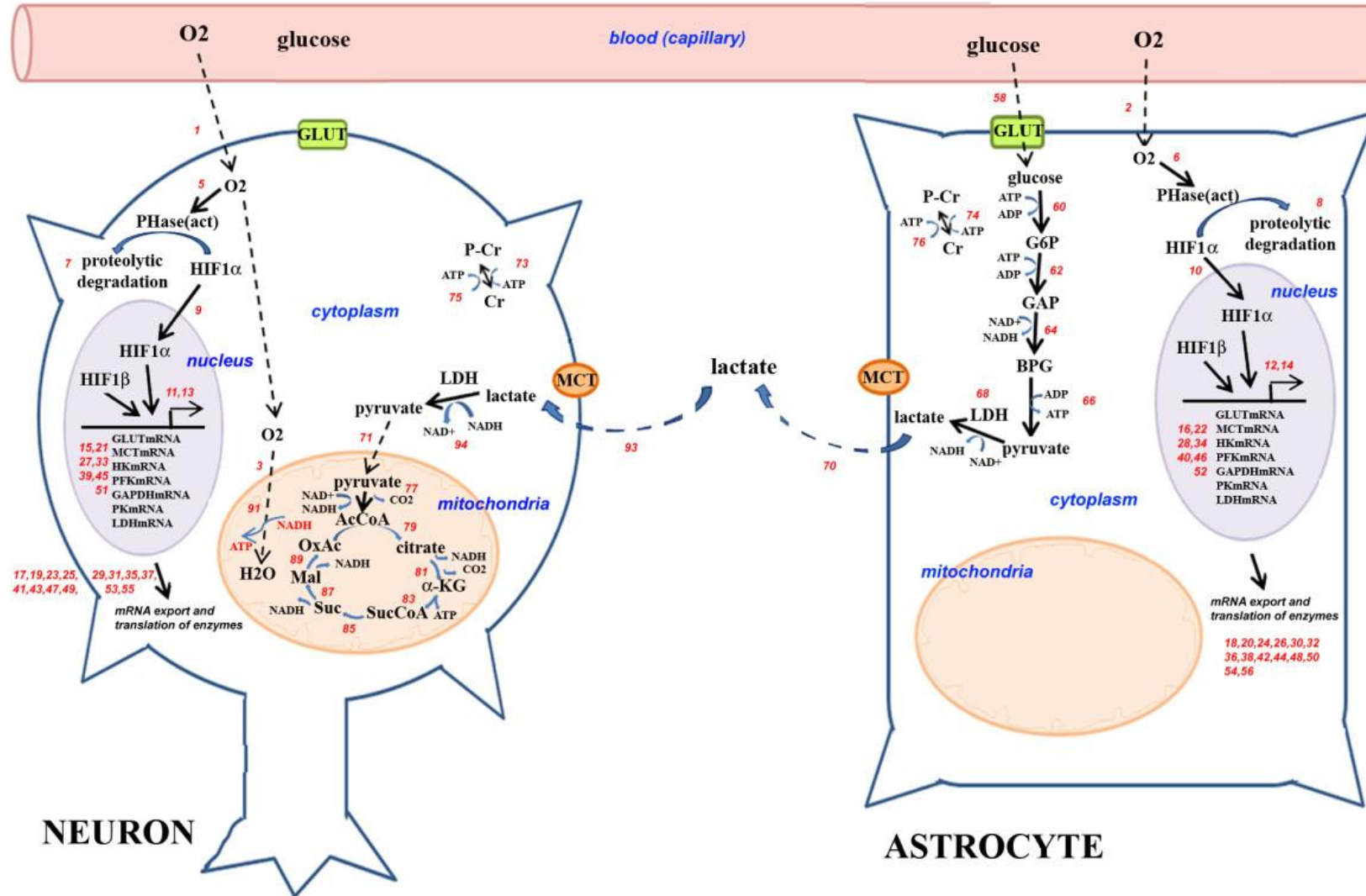


**Figure 1.6.** Glucose metabolism in the brain, the astrocyte-neuron lactate shuttle hypothesis (ANLSH): Glucose is mainly utilized by the astrocytes resulting in anaerobic conversion into lactate (40, 41). It is then taken up by neurons, converted into pyruvate and enters in aerobic conversion within mitochondria.

Unlike neurotransmitters that must be detected in the extracellular space in order to understand their signaling function, the interest of detecting glucose or lactate in the interstitial medium using invasive microprobes is arguable. For example, lactate can be detected non-invasively in the human brain using magnetic resonance imaging (MRI). Understanding the metabolic shuttle between neurons and glial cells transiting through the extracellular space is certainly one major reason for developing lactate and glucose detection with microprobes. In addition, some neurological disorders require constant monitoring of glucose, lactate or small molecule biomarkers in the brain that could be achieved by implanting probes in the brain parenchyma.

### **3. Small molecules monitoring in the brain for diagnostics of neurological disorders: example of subarachnoid hemorrhage and traumatic brain injury.**

*In this section I discuss a practical aspect of in vivo molecules monitoring in clinical settings.*

Clinical studies have provided evidence that brain monitoring is a useful approach for detecting potentially dangerous neurochemical conditions involving hypoxia/ischemia or seizure activity in pathologies like subarachnoid hemorrhage (SAH) or traumatic brain injury (TBI). In poor grade SAH or TBI, patients are often kept in neurosurgical intensive care units in a comatose state, and the secondary neurological deterioration following TBI and SAH are difficult to diagnose. In particular, TBI and SAH are often followed by delayed cerebral ischemia related to cerebral vasospasm, a reduction in the diameter of major cerebral arteries consecutive to the presence of blood in the brain parenchyma or ventricles. This blood vessel narrowing reduces the blood supply in glucose and oxygen, sometimes leading to ischemia and death. Such neurological complications can be revealed by changes in composition of the interstitial fluid, by analyzing the concentration of biomarkers in the cerebrospinal fluid or in the extracellular medium of the brain parenchyma. For example, clinical studies have shown a relationship between the neurological outcome and the concentration of biological markers comprising energy metabolites (glucose, lactate, pyruvate) and their ratio (lactate/pyruvate), excitatory amino acids (glutamate) and glycerol (a marker of cell membrane damage). In addition, changes in the ratio of glucose and lactate concentrations, or pyruvate/lactate can reveal changes in energy metabolism and energy failure indicative of neurological complications in these patients.

Enblad et al. (42) conducted a validation study in an animal primate model of cerebral ischemia. They showed that severe ischemia was associated with marked increase in lactate/pyruvate ratio (>90), and this ratio was decreased under reperfusion to 40-50 level. If the analysis is performed within the zone with moderate ischemia, the lactate/pyruvate ratio increases to 50 and returns to baseline level (<25) during reperfusion. Clinical studies of ischemic/hypoxic episodes during neurovascular surgery confirmed these results. The general conclusion was that glucose, lactate and pyruvate appear to be sensitive markers for intra-operative episodes of brain hypoxia/ischemia. Interestingly, it was found that only extended episodes of oxygen lowering leads to significant metabolic changes (31). Several descriptive studies have reported elevated levels of glutamate and aspartate in association with episodes of secondary hypoxia/ischemia. Increased concentrations of these amino acids were associated with an unfavorable clinical course of SAH patients. The quantitative data were also reported. The level of glutamate within the first days of SAH was found to be of 25.5 $\mu$ M in patients with severe disabilities compared to 4.5 $\mu$ M in good recovery cases. Another study observed a poor outcome of patients with glutamate levels of 50-60 $\mu$ M

compared to below 10 $\mu$ M for good outcome cases (31). Thus, increases in glutamate correlated with ischemic deterioration in patients suffering from SAH.

Recent studies performed by Timofeev et al. (43) demonstrated a relationship between cerebral extracellular biochemical markers such as glucose, lactate, glycerol and their ratio (lactate/pyruvate, lactate/glucose) and neurological outcome following TBI based on cohort of 223 patients. The most consistent finding of this study was the significant association of higher lactate/pyruvate ratio with increased mortality and unfavorable outcomes after TBI. These studies lead to the definition of a physiological threshold of lactate/pyruvate ratio at about 25 as a discriminator of poor vs favorable outcome in TBI and SAH patients (44, 45). They also suggested that within the first 72 h after the injury, the changes in lactate/pyruvate ratio, glycerol, glucose, glutamate can differentiate between survival categories. The feasibility of monitoring glutamate for several days following TBI has also been demonstrated. Different studies show that following TBI, a prolonged elevation of glutamate occurs and the outcome is correlated with degree of glutamate elevation. Richards et al. (46) identified glutamine as an important marker as well as the extracellular glutamine/glutamate ratio for predicting TBI outcome.

The need for continuous chemical monitoring in poor-outcome SAH and TBI patients illustrates the possible clinical applications that *in vivo* analytical techniques can have once their clinical safety and efficacy has been demonstrated.

## II. Techniques for monitoring the brain extracellular fluid: microdialysis and microelectrode biosensors

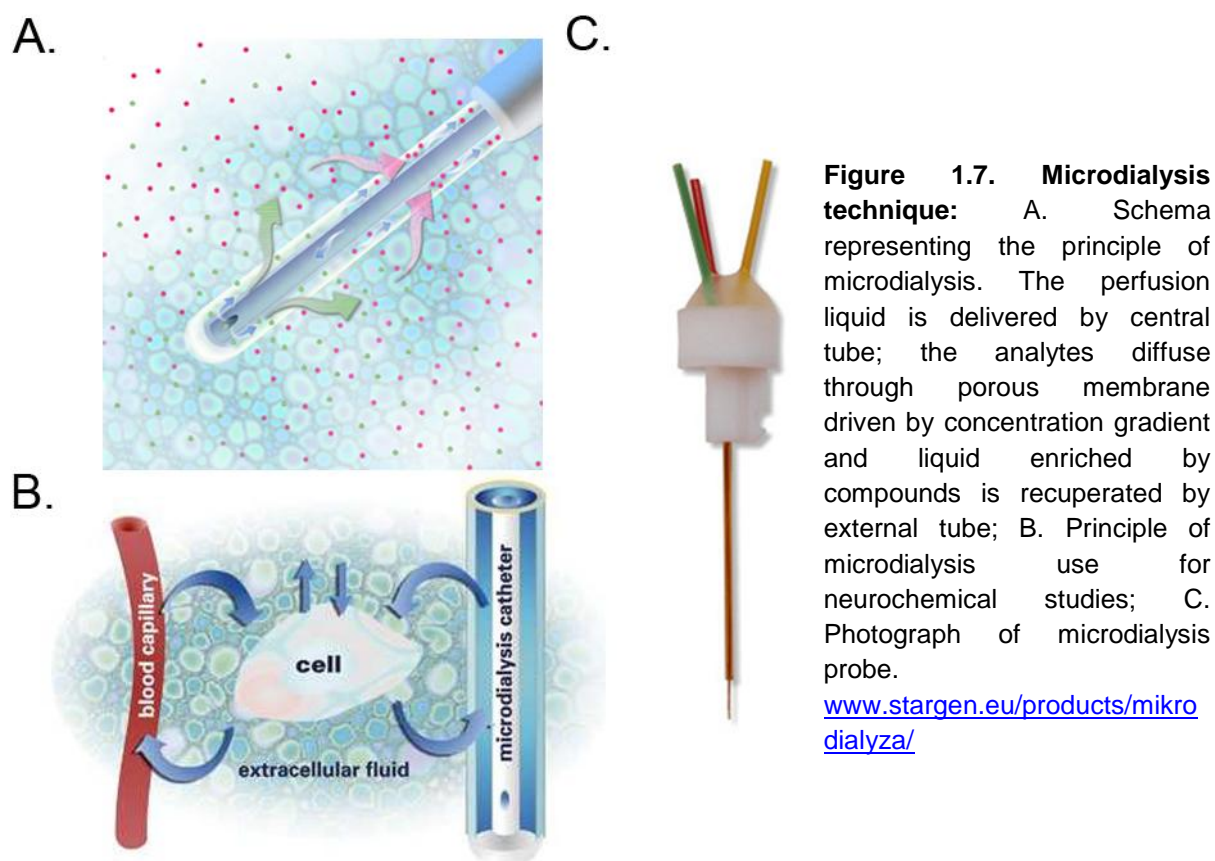
Two major methods are currently applied for small molecules monitoring in the CNS of laboratory animals: direct monitoring by chemical sensors and brain solution sampling by microdialysis followed with analysis by appropriate techniques.

### 1. Microdialysis

Intracerebral microdialysis was introduced in the 1980s and has become a powerful research tool to neurochemistry studies of the brain functioning in laboratory animals. In neurochemistry research, microdialysis is widely used to measure neurotransmitters (dopamine, serotonin, acetylcholine, glutamate, GABA), metabolites (glucose, lactate, pyruvate) and small amino acids (glycine, cysteine). It is also used for drug discovery and development of pharmacological treatments.

The principle of this technique is relatively simple. It consists in implanting a small chamber equipped with a porous dialysis membrane allowing the exchange of small molecules into the brain parenchyma. This chamber is perfused with a liquid of an ionic composition close to that of the surrounding interstitial fluid. This liquid usually does not contain the molecules of interest and thus, the concentration gradient causes the flow of analyte into the perfusion solution. The scheme of microdialysis and the photograph of dialysis probe are shown in Figure 1.7 A, C. The tool comprises two tubes closely attached one to another, one serving to deliver the artificial fluid to the area of interest in the brain and another one to collect the liquid enriched by compounds present in the extracellular milieu.





Up to now, microdialysis is a reference technique that allows continuous and simultaneous monitoring of drugs, neurotransmitters or metabolites in the extracellular fluid of the brain. Additionally, it is currently applied in clinical studies for monitoring poor-grade SAH and TBI patients. Microdialysis is extensively used in the CNS of laboratory animals. However, it is only a sampling technique and requires an appropriate separation technique and detection method to analyze the chemical contents of the fluid collected from the probe. To achieve chemical selectivity, low detection limits and high sensitivity, high performance liquid chromatography (HPLC) or capillary electrophoresis (CE) separation techniques in combination with sensitive detectors are used. The semipermeable membrane prevents cellular debris and proteins from entering into the dialysate and thus, there is no need for sample purification prior to analysis by HPLC or relative methods.

## 1.1 Methods for biomolecules analysis: High-performance analytical techniques

Biological samples obtained by microdialysis represent a complex mixture of endogenous molecules (amino acids, sugars, fatty acids, coenzymes, hormones, neurotransmitters, salts, waste products from the cells etc.) and compounds that may have been infused for the purpose of the experiment (drugs, pharmaceuticals). They require an appropriate separation procedure and detection method to permit an accurate analysis. High performance liquid chromatography (HPLC) or capillary electrophoresis (CE), coupled with high sensitive detectors (e.g. amperometry, fluorimetry, mass spectrometry etc.) are most commonly used to achieve the chemical selectivity, low detection limits and high sensitivity in analysis.

### 1.1.1 Liquid chromatography (LC)

HPLC is a type of chromatographic methods used to separate a mixture of compounds with the purpose of identifying, quantifying and purifying the individual components of the mixture. In usual chromatographic analysis, the sample to be separated and analyzed is introduced, in a discrete small volume (typically, in the order of a few  $\mu\text{L}$ ), via an injection system into the stream of a mobile phase passing through the column. The components of the sample move through the column at different rates depending on specific physical or chemical interactions with the stationary phase leading to separation. The velocity of each component depends on its chemical nature, on the properties of the stationary phase (column) and on the composition of the mobile phase. The time at which an analyte elutes from the column is called the retention time. The retention time is measured under particular conditions and is considered as an identifying characteristic signature of a given analyte. Eluting from the column the analyte is sent to a detector where it generates quantified signal. The result of the analysis is represented by a chromatogram in which the intensity of the signal is represented across time. Each separated compound generates a peak at the appropriate retention time.

Proteins, peptides, carbohydrates, lipids, amino acids, vitamins, coenzymes, and nucleic acids are the common biomolecules present in collected and analyzed biological samples. The commonly encountered chromatographic separation modes are reversed phase and ion-exchange.

*Reversed Phase Chromatography (RP-HPLC)* is widely used for separation of large and small biomolecules. The term 'reversed' means that a non-polar stationary phase and a polar eluent are employed unlike the classical HPLC. The column properties such as particle size and porosity, column length and chemical nature of stationary phase, as well as the properties of mobile phase, flow rate and eluting mode influence greatly the separation quality and resolution. These parameters determine the retention time of a given compound and its separation from other components of the sample. Retention of proteins and peptides usually occurs through a combination of adsorption/desorption and a partitioning type mechanism, compared to small molecules which usually separate strictly by a partitioning type mechanism. Adsorption/desorption mechanism includes a temporal reversible adsorption of hydrophobic part of the protein to the bonded stationary phase. Partitioning process is the distribution of the sample between the mobile and stationary phases (47).

RP-HPLC separation of proteins is usually performed on wide-pore (>30nm) silica bonded with alkyl chains. Preferably, short alkyl chains are used to reduce the possibility of protein denaturation or irreversible binding that can occur with longer alkyl chains. Most RP-HPLC phases interact with analytes via weak van der Waals forces between the analyte and bonded stationary phase. The phases that comprise unmodified alkyl chains, such as C18, C8, and C4, interact solely via this mechanism. The length of the bonded phase alkyl chain can have a dramatic effect on elution patterns, and can even produce the reversal of peak order. Porous graphitic carbon (PGC) is an alternative to modified silica for protein and peptide separation. PGC has two distinct differences compared to silica-based particles for biomolecule separations. Firstly, it is composed entirely of carbon and according to its chemical properties it is not susceptible to acidic or basic hydrolysis. It can therefore be used over a large pH range without degradation. By contrast, silica-based phases can lose bonded alkyl groups under acidic conditions, and silica can dissolve under basic conditions. Secondly, carbon particles exhibit longer retention of polar compounds that are difficult to retain using silica-based RP-HPLC phases. Many biomolecules (including oligosaccharides,

nucleosides, nucleotides, amino acids, vitamins) are too polar to be retained on C18 silica particles. However, they are retained and resolved by a PGC column. Most polar compounds require derivatization to increase their hydrophobicity in order to be retained by silica-based RP-HPLC phases.

The column efficiency is higher with smaller or porous particles that increase the surface over which sample separation could occur. Retention is generally proportional to column length. The longer a column, the longer it takes to elute the entire sample, leading to longer analysis time. However, if a longer column is used, a better resolution (degree of separation between consecutive analytes emerging from the column) is achieved due to the higher number of desorption/adsorption cycles.

*Mobile phase.* RP-HPLC mobile phases for protein and peptide separations are usually gradients of organic modifiers in water with ionic additives that control the pH and ionization state or act as an ion pair agent. The most common RP-HPLC organic mobile phase modifiers are acetonitrile or methanol. The organic modifier counteracts to the stationary phase/analyte interaction and causes sample separation and elution from the column. The higher the organic concentration, the shorter is the retention time.

Ionic additives serve to adjust or control the pH, the ionization of the analyte, and enhance retention by forming ion pairs. They reduce interactions between the analyte and the silica surface, and maintain the analyte's solubility or biological activity, or a combination of these functions. The ionic additive most commonly used is trifluoroacetic acid (TFA). It acts as an ion pair agent, which associates with positively charged functional groups on peptides and proteins, increasing reversed phase retention. TFA ensures that any residual silanol group on the silica stays protonated, thus eliminating any possible ion exchange interaction with basic solutes.

In HPLC separation, there are two possible elution modes: isocratic and gradient ones. Isocratic elution is typically effective in the separation of sample components that are not very dissimilar in their affinity for the stationary phase. In gradient elution the composition of the mobile phase is varied typically from low to high eluting strength (organic modifier content). In gradient elution, analyte molecules remain associated with the bonded phase until the concentration of organic modifier in the mobile phase reaches a point where they are released.

In *Ion Exchange Chromatography*, the adsorption of the molecules to the stationary phase is driven by the ionic interaction between the opposite charges between the ionic groups in the sample molecule and in the functional ligand on the stationary phase. The strength of the interaction is determined by the number and location of the charges on the molecule and on the functional group. Ion-exchange phase is usually classified as cation and anion exchanger. Cation exchangers are used to separate the positively-charged biomolecules and thus contain acidic groups such as  $-\text{SO}_3$ ,  $-\text{COOH}$ ,  $-\text{PO}(\text{OH})_2$ . Anion exchangers contain basic groups: secondary ( $-\text{NH}-\text{R}$ ), tertiary ( $-\text{NR}_2$ ), or quaternary amines ( $-\text{NR}_3^+$ ), and are used to separate negatively-charged compounds.

By increasing the salt concentration, generally by using a linear salt gradient, the molecules with the weakest ionic interactions start to elute from the column first. Molecules that have a stronger ionic interaction require a higher salt concentration and elute later in the gradient. Mobile phase ions compete with the analyte ions of the same charge for adsorption with ionic groups in the stationary phase. The more ions in the mobile phase (the higher the ionic strength), the shorter is the retention time of the analyte. The competition between analyte and salt for the ion exchange site also largely depends on the concentration, the nature and the charge of the salt ions and on the pH of the mobile phase.



Because all proteins and peptides have numerous functional groups that can have both positive and negative charges, the ion exchange chromatography method is largely used for protein and peptide characterization.

### 1.1.2 Capillary electrophoresis (CE)

Modern CE has demonstrated tremendous potential for a wide range of applications, from small molecules that include inorganic ions, organic acids, amino acids, peptides, drugs, nucleosides, nucleotides, vitamins, steroids, and carbohydrates, to larger molecules, such as hormones, proteins, nucleic acids, and even living cells. CE analyses are usually very fast, use little sample and reagents, and cost much less than chromatography. CE sample volumes are some of the smallest of any chromatographic method. Sample volumes for HPLC are routinely 20 $\mu$ L, but CE ones are in the order of a few nL .

Capillary electrophoresis instrumentation is relatively simple (Fig.1.8). The basic instrumental set-up consists of a sample vial, source and destination vials, a fused silica capillary, electrodes, a high-voltage power supply and on-column detector. The source vial, destination vial and capillary are filled with an electrolyte such as an aqueous buffer solution. To introduce the sample, the capillary inlet is placed into a vial containing the sample. Sample can be introduced into the capillary (1) via gravity injection, where a difference in height position of sample and buffer vials causes sample to flow into capillary, (2) pressure injection (application of pressure difference between the two ends of a capillary) or (3) electrokinetic injection, by simple turning on the voltage in the sample vial for a certain period of time. After injection, the capillary inlet is returned to the source vial. The migration of the analytes is then initiated by an electric field that is applied between the source and destination vials and is supplied to the electrodes by the high-voltage power supply.

The capillary column is a key element of the CE separation. Fused silica is the most common material used to produce capillaries for CE. The interior wall of an uncoated fused silica capillary is covered by silanol (Si-OH) groups that are negatively charged (Si-O<sup>-</sup>) at pH>3. Attracted to the negatively charged silanol groups, the positively charged cations of the buffer solution form two inner layers of cations on the capillary wall. The first layer is held tightly to the silanol groups. The outer layer (mobile layer) being farther from the silanol groups is pulled in the direction of the negatively charged cathode when an electric field is applied. Since these cations are solvated, the bulk buffer solution migrates with the mobile layer, causing an electroosmotic flow (EOF) of the buffer solution as well as the analyte. The separation of compounds by capillary electrophoresis is dependent on the differential migration of analytes in an applied electric field. Obviously, the small ions bearing one or multiple positive charges migrate easily to the negatively charged electrode, while anions are retained longer and are the last ones to emerge from the capillary.

EOF is the principal phenomenon allowing the separation of cations, anions, and neutral solutes in a single run. EOF is affected by many parameters, including buffer pH, buffer concentration, temperature, viscosity, capillary surface, field strength, organic modifiers and surfactants. However, in most cases, selectivity and resolution are improved by varying of the pH of the buffer and by using additives in order to change the mobility of the analytes.

Electrophoretic separation of biomolecules can be achieved as a result of differences in (1) electrophoretic mobility (separation by capillary zone electrophoresis and isotachopheresis), (2) size (separation in sieving media such as gels and entangled polymeric networks), (3) charge (separation by isoelectric focusing), (4) hydrophobicity (separation by micellar electrokinetic chromatography), and (5) specific interaction(s) with other biomolecules (separation by bioaffinity electrophoresis with molecular pseudophases,

e.g., cyclodextrins) (48).

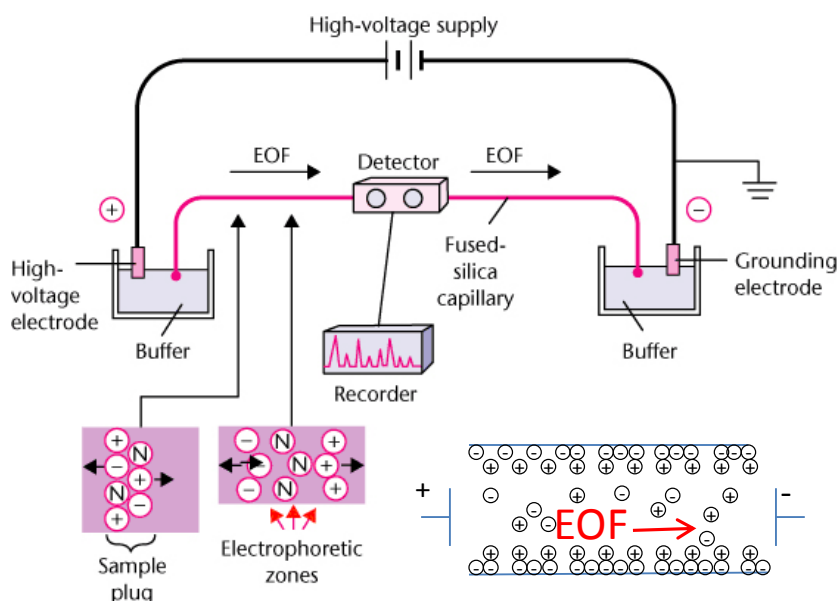


**Figure 1.8. Capillary electrophoresis technique** (adopted from (49)).

The analytes of interest are often available in very small amounts. Therefore, pre-concentration of the sample or derivatization, to improve the detection properties – fluorescence, absorbance etc., is usually required.

Adsorption of proteins to capillary walls is a serious problem in CE, resulting in changes in EOF, peak broadening, and loss of separation efficiency. Models for analyte adsorption allow mathematical correction of migration times and changes in EOF. Usually, dynamic or static wall coatings are also applied to minimize protein adsorption. For dynamic wall coatings different chemicals are added to the analyzed solution to modulate the interaction of biomolecules with the capillary wall. For example, certain molecules form a positively charged layer at the fused-silica surface, which reverses electroosmosis and leads to electrostatic repulsion of the positively charged analytes. The surfactants, cetyltrimethylammonium bromide or sodium dodecyl sulfate are also used to modify the surface charge of analytes. Permanent static inner wall coatings generally eliminate analyte interaction more effectively and are even more stable than dynamic wall coating. Nevertheless, they are more difficult to produce. Static wall coatings require a chemical modification of the fused silica capillary surface, which is usually performed by small bifunctional molecules that can attach a desired functionality to the capillary wall.

### 1.1.3 HPLC and EC detection systems

After separation the analytes elute from the column or capillary in the order determined by their retention times and are sent to the detector. Traditional detectors for liquid chromatography and capillary electrophoresis include refractive index, electrochemical, fluorescence, and ultraviolet-visible (UV-Vis) detectors.

UV absorption is the most common detection technique, but also the least sensitive one. The limit of detection is usually about  $10^{-7}$ – $10^{-6}$  mol/L. The analyte concentration is proportional to the absorbed light intensity. The advantage of UV absorption is that no sample pretreatment is necessary.

Laser-induced fluorescence (LIF) detection is often the method of choice for the analysis of low concentrations because of its high sensitivity with LOD about  $10^{-13}$ – $10^{-11}$  mol/L. However, it requires sample derivatization.

Electrochemical detectors are suitable for the detection of electroactive components (for example biogenic amines) giving low detection limits, about  $10^{-8}$ – $10^{-7}$  mol/L.

Generally, detectors generate two-dimensional data, representing signal strength as a function of time. Some detectors, including fluorescence and diode-array UV-Vis detectors, generate three-dimensional data that include not only signal strength but spectral data at each point of time. Mass spectrometers generate three-dimensional data as well. In addition to signal strength, they generate mass spectra that can provide valuable information about the molecular weight, structure, identity, quantity, and purity of a sample. Mass spectral data add specificity that increases confidence in the results of both qualitative and quantitative analyses.

An important advantage of mass-spectrometer detectors is that they can analyze compounds that lack a suitable chromophore or co-elute in unresolved peaks, reducing the need for perfect separation. Mass spectral data complements data from other detectors: two compounds may have resembling UV spectra or similar mass spectra, but it is uncommon for them to have both. The two sets of data can be used to confidently identify, confirm, and quantify compounds.

The use of mass spectrometers as detectors for CE (CE/MS) and LC (LC/MS) has increasingly gained acceptance, complementing or replacing UV absorbance, electrochemical or LIF detectors.

Mass analysis is performed first, by ionizing molecules, then by sorting and identifying the ions according to their mass-to-charge ( $m/z$ ) ratio. Two key components in this process are the ion source, which generates the ions, and the mass analyzer, which sorts the ions. Current biomolecule analysis by CE/MS or LC/MS uses electrospray ionization (ESI) because it is more amenable to polar compounds such as amines, peptides, and proteins. The ESI mode transfers ions in solution into a gas phase. It can be used in positive or negative ion polarity mode to analyze any polar compound. The eluate from the LC or EC flows through a narrow bore stainless steel tubing which is maintained at high voltage. Under the electric field, small electrically-charged droplets form and leave the tube tip when the forces of electrostatic repulsion exceed the surface tension. A high velocity gas flow supports the aerosol formation. Evaporation of the solvent on the way to the vacuum inlet by a heated gas decreases the droplet size, thereby increasing the charge density at the droplet surface. This leads to rupture of the droplet and evaporation of ions from the droplet surface into the surrounding gas when the electric field at the droplet surface becomes high enough. The desolvated ions travel through an orifice into the vacuum chamber of the mass spectrometer where they are separated according to their mass-to-charge ratio and analyzed.

Separation techniques may also be coupled with tandem mass-spectrometry detection where two consecutive mass-detection experiments are performed. The first mass spectrum represents the totality of fragment and ion mass. Then, the first mass spectrometer is used to select a single mass that is characteristic of a given analyte in a mixture. The mass selected ions undergo fragmentation, separation and analysis in the second mass-spectrometer. This technique is used for analysis of chosen components without chemical background and other components of the mixture.

Coupled high-performance separation and MS-detection techniques have found wide applications in pharmaceutical analysis: for example (1) drug metabolism studies involving the analysis and identification of impurities and degradation products in pharmaceuticals or (2) isolation and characterization of potential drug substances from natural or synthetic

sources (50). LC/MS or, CE/MS methods are currently applied for the characterization of synthetic mixtures of peptides and proteins. In traditional proteomic methods, the isolation of individual proteins by two-dimensional gel electrophoresis is generally required. The combination of capillary LC/MS/MS with intelligent, data-dependent acquisition and probability-based database searching makes it possible to rapidly identify as many as 100 proteins in a single analysis, making the analysis much more rapid and efficient. LC/ES-MS/MS appears to be a useful, sensitive and specific method for the simultaneous quantification of neurotransmitters and metabolites from the brain tissue (51).

High-performance analytical techniques now allow an efficient separation of complex biological samples and thus high selectivity in compounds identification and low detection limits. However, these techniques may require sample preparation – derivatization, pre-concentration etc, depending on analyte. These preparation steps can be time consuming and may require complex protocols. In intensive-care units, rapid analysis of biological samples may have a vital importance, as microdialysis results may indicate life-threatening emergencies. Additionally, microdialysis monitoring of the interstitial composition in patients or in animal experiments may last for hours or days and thus, generate a large quantity of samples to be analyzed. Therefore, a wide variety of miniaturized devices have been recently developed to answer the requirements of rapid analysis with efficient separation and selective detection in complex media for near real time monitoring (52). We will now review different ex-vivo analysis techniques that can be used for the rapid analysis of brain samples, especially microdialysates.

## 1.2 Methods for biomolecules analysis: Point of care units (Ex-vivo biosensors)

Modern alternative to classical analytical techniques designed to separate and quantify biomolecules in biological fluids are *ex-vivo* biosensor systems or point-of-care (POC) devices.

The term “**biosensor**” has been widely adopted to describe analytical systems where the recognition of an analyte is performed using elements of biological origin, like antibodies, antigens, nucleic acids, enzymes or mimicking biological activity like molecularly imprinted polymers or aptamers. The molecular recognition between the analyte and the biological element is then transduced into a quantitative signal using physicochemical detector components. Current progress in genetics, biochemistry, physicochemical technologies has resulted in wide range of analytical systems that may be defined as “biosensors”. For instance, Q.-T. Nguyen et al. reported an unusual biosensor for *in vivo* detection of acetylcholine (ACh) release and receptor activity (53). They used cultured cells engineered to express a specific receptor coupled to a  $\text{Ca}^{2+}$  signaling cascade together with a genetically encoded fluorescent  $\text{Ca}^{2+}$  sensor. Activation of the receptor by ACh release (or any biological molecule possessing membrane receptors coupled to  $\text{Ca}^{2+}$ ) increases cytosolic calcium in cultured cells. The subsequent binding of calcium to the indicator induces a conformational change resulting in an increase in fluorescence that is detected by two-photon laser-scanning microscopy.

Regarding the large diversity of existing analytical systems, this current review is limited to more traditional biosensor systems, where the recognition element is immobilized on a detector or near the surface of the detector surface; and that are widely utilized around the world.

POC devices do not involve the use of laboratory staff and facilities to provide the result. They can be used as “near-patient” tests, at the bedside in a hospital or doctor’s office, could be involved in health monitoring at home to manage disease or therapy. Such devices are also widely used outside the field of health and disease, for example, environment (water safety) or food industry (quality control). These tests are designed to work with complex biological media containing femtomolar to millimolar concentrations of analytes in small volume with little or no pre-preparation and provide a result in seconds to hours (54). Such devices should be inexpensive chips or cartridges and often include microfluidic features to provide or control sample preparation. Integrated microfluidic channels can control, for example, flow rate, mixing with reagents, reaction time associated with binding events, filtration of nonanalytical components of the sample, separation of interfering agents and of multiple analytes, and an effective measurement capability (54).

The analytical samples aimed to be analyzed comprise blood, saliva, urine, cerebrospinal fluid and other body fluids (for example microdialysates). There are numerous biological targets and diagnostic applications of POC devices. The best known examples of these assays are pregnancy tests and glucose monitoring strips for diabetic patients.

Proteins, enzymes, antibodies, hormones are common targets for POC diagnostics. Modern POC devices utilize immunoassay technology of antigen-antibody binding to target disease-specific protein markers such as glycated hemoglobin (HbA1c) for diabetics, C-reactive protein (CRP) for inflammation and risk of cardiovascular disease, D-dimer for early thrombosis, troponin subtypes for cardiac damage, prostate-specific antigen (PSA) for prostate cancer, and bacterial and viral infection-related markers such as human immunodeficiency virus (HIV) and hepatitis.

The small molecules most often targeted by POC diagnostics include glucose, lactate, ammonia, urea, cholesterol, triglyceride and creatinine. Regular and systematic glucose concentration control in diabetic patients is necessary to avoid the risk of hypoglycemia and hyperglycemia, and can drastically reduce the devastating complications of diabetes. Efficient control is possible only when the diabetic patient individually monitors his/her glucose concentration on a regular timeframe throughout the day(55). Cholesterol, triglycerides, and other plasma lipids are important biomarkers for diagnostics of cardiovascular disease. Stroke and diabetes are also linked to high cholesterol, bolstering its importance as a POC diagnostic target. Creatinine is a byproduct of muscle action. It is produced at a rather constant rate in the body and is filtered out of the blood by the kidneys. During kidney deficiency, this filtering is deficient and creatinine blood levels rise. Therefore, creatinine levels in blood and urine may be used to calculate the kinetics of creatinine clearance, which reflects the glomerular filtration rate and renal function. Lactate measurements are often performed in the emergency room to provide valuable information about tissue perfusion and the presence of ischemia or hypoxia.

The POC units have found wide applications in nucleic acid analysis, providing an alternative to PCR techniques. The identification of specific human cells is a promising field in POC diagnostics, for example in cancer research. Microbes, viruses and parasites are also important POC targets particularly those that cause infectious diseases. Finally, multianalyte analysis with a single POC is challenging task. However, some systems for blood chemistry and for cardiac damage markers are already available on market (i-STAT, Biosite Triage system, [www.abbottpointofcare.com/](http://www.abbottpointofcare.com/)).

The design and construction of such highly integrated small lab-on-chip devices has become possible with the progress in micro systems technologies or microelectromechanical systems (MEMS). Microfluidics is a significant component of POC devices. Micropumps and

microvalves constructed involving microfabrication technologies enable precise control of sample, buffer and reagent flow and delivery. They are indispensable for POC devices that provide sample preparation, complex assays that include incubation, mixing, or separation steps and more quantitative outputs. Separation methods integrated to POC devices include capillary electrophoresis, isoelectric focusing, various types of liquid (electro)chromatography including micellar electrokinetic chromatography (MEC), magnetic motivation and capture, acoustic waves and fields, size-based filtration (using filters, nanostructures, and microstructures), and various combinations of flow, diffusion, and sedimentation-based phenomena (54). Separation is based on charge, polarizability/dielectric properties or optical frequencies, pK/pH of minimum charge, mass, size, magnetic properties, and physical/chemical/immune-binding interactions. To detect selectively the molecule of interest one or several recognition elements are used to bind or degrade it: enzymes, DNA, aptamers, antibodies, cells. Two major detecting approaches are largely used in POC devices: electrochemical methods including amperometry, impedance spectroscopy, potentiometry, and optical methods including fluorescence, luminescence, absorbance, surface-plasmon resonance (SPR). To these classical analytical techniques some modern alternatives based on mass detection have been reported for POC detection. They include micro- and nanocantilevers, quartz-crystal microbalance, among others.

### 1.2.1 MEMS technology

Microelectromechanical systems are a major technology for construction of miniaturized analytical devices. There are three major aspects in MEMS technology that include patterning, deposition processes (physical and chemical deposition), and dry or wet etching.

#### *Patterning*

In MEMS technology, patterning refers to the structuring of a desired motif on a surface. Patterning is usually associated with photolithography process. It uses the property of photosensitive polymer materials (photoresist) that undergo polymerization under light exposition allowing the transfer of a desired pattern from a template to the photoresist.

A classical photolithography cycle consists of several steps. Firstly, an appropriate cleaning procedure is applied to the substrate to decrease the influence of contaminations on subsequent steps. Cleaning is followed by heating to a sufficient temperature to drive off any moisture that may be present on the wafer surface. Depending on the properties of the photoresist, a promoter may need to be spin-coated prior to the photoresist. Such promoter improves the adhesion of the photoresist in case the hydrophilic properties of the wafer and photoresist are opposite. The wafer is then covered with photoresist by spin-coating, i.e. a viscous, liquid solution of photoresist is dispensed onto the wafer, and it is spun rapidly to produce a uniform layer with controlled thickness. The coated wafer is then prebaked on a hotplate to remove the excess of solvent. After prebaking, the photoresist is exposed to intense light, usually ultraviolet (UV), under a lithography mask. This mask is a glass template with a desired motif made of chromium. With positive photoresist types, the exposed part of the resist becomes soluble in developer and unexposed, screened by mask remains insoluble and stays on the wafer surface. In case of negative types, exposition activates the photoresist. During post-exposition bake, the UV-activated resist polymerizes and becomes insoluble in developer while unexposed part selectively dissolves. A combined type of photoresist can be used in both positive and negative modes. For the positive mode, the procedure is similar the one described above. For the negative mode, two exposition

steps are required: the first one involving exposure to light with a mask, then a reverse bake is required followed by the second flood exposition without mask. In such configuration, the resist protected by the mask during the first light exposition becomes soluble in the developer. In some cases the post-bake is required to make the photoresist more resistive to reactive environment.

Electron beam lithography uses beam of electrons to pattern the photoresist and to create nanotechnological architectures.

Photolithographic patterning opens two different possibilities: (1) material deposition and patterning by lift-off, and (2) substrate etching under photoresist protection. Lift-off is a method for patterning thin layers of material deposited on the wafer surface. Lift-off is required when direct etching of the deposited material is impossible, difficult or leads to undesirable secondary effects. It consists in a first standard lithographic process with a negative photoresist resulting in an inverted motif i.e. the dark zones on the mask will translate into openings on the resist. Next, the deposition of the desired material all over the wafer is performed. The material reaches directly the wafer surface through the openings in the photoresist and stays on top of the resist everywhere else. When the photoresist is washed away, the material on the top is also evacuated or "lifted-off". After lift-off, the target material remains only in the regions where it had a direct contact with the substrate and repeats the features of the mask.

### *Deposition*

The possibility to deposit thin films of material is important in micromachining process. Deposition techniques are classified as physical and chemical vapor deposition methods. Physical vapor deposition consists in removing a material from a target and depositing it on a sample surface. These methods include sputtering and evaporation.

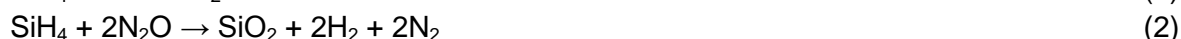
*The sputtering process* starts by creating the gaseous, often argon plasma in the deposition chamber. Then positively charged argon ions are accelerated into some source material (target), the source material is bombarded by the arriving ions and emits material particles - either individual atoms, clusters of atoms or molecules. As these particles are ejected they travel chaotically in a chamber until they come into contact with other particles or a nearby surface. If a Si wafer is placed in the path of these ejected particles it will be coated by a thin film of the source material ([www.ajaint.com/whatis.htm](http://www.ajaint.com/whatis.htm)).

*Evaporation* involves two basic processes: a material evaporation and condensation on the substrate. Evaporation takes place in vacuum, where ambient gases are almost entirely removed. In high vacuum, evaporated particles can travel directly to the deposition target without colliding with the background gas. To produce these vapors, the source material is placed in a crucible, where it is heated by an electric filament. The purity of the deposited film depends on the quality of the vacuum, and on the purity of the source material.

When comparing these two physical vapor deposition techniques, an important advantage of the sputtering process is that materials with very high melting points are easily sputtered while evaporation of these materials is problematic. Sputter deposited films have a composition close to that of the source material. They are usually smooth without pinholes. Sputtered films typically have a better adhesion on the substrate than evaporated films. Sputtering sources do not contain hot parts and thus are compatible with reactive gases such as oxygen or temperature sensitive substrates. Deposition by sputtering in contrast to evaporation has better step coverage that may be an advantage or disadvantage, depending on the desired result. If the whole wafer surface covering by protection layer is required,

sputtering is preferred. However, it is not compatible with the lift-off process for structuring the deposited film. In sputter deposition, the atoms attach the wafer surface in a rather chaotic manner resulting in isotropic deposition, whereas evaporation deposition occurs perpendicularly to the wafer surface and leaves tilted walls uncovered. In addition, sputtering tends to deposit material more slowly than evaporation. Finally, sputtering uses plasma, which produces many high-speed atoms that bombard the substrate and may damage it. Evaporated atoms possess less energy and cause less damage.

In *chemical vapour deposition* (CVD), the wafer is exposed to one or more volatile precursors, which react or decompose on the substrate surface to produce the desired deposit. Frequently, volatile secondary products are also produced, which are removed by gas flow through the reaction chamber. CVD methods are developed in large variations depending on the activation process and process conditions. Decomposition of source gases is induced either by temperature (thermal CVD) or by plasma (plasma-enhanced CVD, PECVD). The most commonly mentioned methods in research publications are low-pressure CVD (LPCVD) and PECVD. Thermal CVD occurs at high temperature in the range 300 to 900°C and is much dependent on the source gas. The PECVD takes places at lower temperatures 100-400°C, typically at 300°C. CVD reaction rates obey Arrhenius behavior – they are exponentially temperature-dependent (56). Typically silicon, silicon dioxide or silicon nitride are deposited by CVD method. The following reactions are typically used to obtain these materials from silane:



CVD is not limited to simple compounds: films can be doped during deposition. For example, silicon dioxide can be doped by phosphorus oxide by adding phosphine to the source gas flow resulting in phosphorus doped silica glass.

Metals are rarely deposited by chemical vapor deposition, and physical vapor deposition methods are usually preferred. However, CVD processes for molybdenum, tantalum, titanium, nickel, and tungsten have been developed. Most often, Mo, Ta and Ti are deposited by LPCVD from their pentachlorides. Ni, Mo, and W can be deposited at low temperatures from their carbonyl precursors. The usual source for tungsten is tungsten hexafluoride. In general, high rate of deposition is achieved with hydrogen reduction.

In comparison to physical vapour deposition, CVD may yield faster deposition rates. However, it is important to note that silicon nitride deposited by CVD is not a purely stoichiometric compound. It always contains a certain amount of hydrogen bonded to silicon or nitrogen, so that instead of  $\text{Si}_3\text{N}_4$ , it is noted as  $\text{Si}_x\text{N}_y\text{H}_a$ . Silicon dioxide films may also be contaminated with carbon, if tetraethoxysilane is used as precursor, and hydrogen as silanol group, and thus can be unstable in air or humid milieu.

### Etching

In MEMS technology, two etching processes are possible: dry plasma etching and wet etching. Both techniques may be applied to metal and insulator patterning. Etching occurs only if the process fulfils three conditions: transport of etchant to surface, surface reaction and removal of product species. Wet etching process is rather simple in theory, but difficult in practice. It must be considered that the reaction products may affect the etching reaction. For



example, silicon etching by KOH produces hydrogen bubbles that can prevent the etchant from reaching the surface. Moreover, the etching reaction is sensitive to stirring or mass convection. If the reaction is exothermic, the temperature rises during etching and the rate of reaction is not constant. So, it is difficult to predict when the process must be stopped. In addition, evaporation leads to changes in concentration during etching which again, influence the reaction rate. Consequently, for every substrate and chemical etching method, the conditions must be optimized to obtain homogeneous etching with moderate rates.

The etching process is characterized by two profiles – isotropic and anisotropic. The isotropic profile is the most frequent. Most wet etchants give a spherical-wave etch front and result in an isotropic profile (which sometimes happens in plasma etching). The material is etched isotropically when the rate of reaction is equal in all directions. If a mask is used to protect underlying wafer, isotropic etching leads to undercutting. In wet etching the resist is usually not consumed by the etchant, but it could be affected by a loss of adhesion due to the etchant reacting with the substrate under the resist. This depends on priming, feature size, or the thickness and chemical properties of the resist. The photoresist is an effective mask for room or low temperature etches, but it does not tolerate etching in hot corrosive solutions. Instead, hard masks are widely used for this purpose. For example, to etch silicon nitride, silicon dioxide is firstly deposited on its surface, then it is patterned by photoresist and HF wet etch. After resist stripping, the oxide acts as hard mask. In silicon etch by KOH, silicon oxide or silicon nitride are classically used as hard masks (56).

Electrochemical etching is a subtype of wet etching. It permits silicon etching in HF which, in usual conditions, does not occur. If silicon is placed as the anode of an electrochemical set-up, the etch rate could reach  $1\mu\text{m}/\text{min}$ . Depending on the current density, silicon can be etched in two ways: pore formation and electropolishing. Electropolishing corresponds to classical etching with complete surface removal, while in pore formation, etching occurs locally in the depth of silicon wafer leaving the initial substrate dimensions untouched but with 80% of empty space in the Si-Si structure. Such porous silicon obtained through this process has found a wide range of applications (57-59).

Anisotropic processes are spatially directional. They can be obtained with both wet and plasma etches. Potassium hydroxide and tetramethyl ammonium hydroxide are anisotropic wet etchants for silicon. With these compounds, anisotropy is attained because the rates of etching in different crystal planes differ significantly (orientation dependent etching). Unlike wet anisotropic etching, anisotropic plasma etching is usually associated with vertical sidewalls. Anisotropy results from directional ion bombardment in the plasma reactor. Vertical walls and highly accurate reproduction of photoresist dimensions permit the production of high packing density of devices on one wafer.

Plasma etching is done in a vacuum chamber by reactive gases excited by radio-frequency (RF) field. In gas plasma two kinds of active agents are formed: excited neutral molecules and ionized species. Both are important for plasma etching. Excited molecules are chemically reactive performing the chemical etching. Accelerated by RF field, ionic species bombard the surface of the substrate thus, allowing anisotropic directional etch. Plasma etching is conditioned by the volatility of the reaction products, which often requires fine optimization of the chemical conditions and bombarding parameters. If the reactions are thermodynamically favorable only soft bombarding is used to induce directionality. For example, silicon is easily etched by halogens producing highly volatile compounds  $\text{SiHal}_4$ . Therefore, no ion bombardment is needed for etching. Aluminum is also spontaneously etched by chlorine, but the surface is protected by native aluminum oxide that is insensitive to chlorine. Therefore, etching can start only after aluminum oxide removal and the conditions of ion bombardment are essential for this step. Bombardment supplies energy to

horizontal surfaces, which experience ion-induced desorption, damage and ion-activated chemical reactions. In some cases the etchant gases form a film on the sidewalls, which prevent lateral etching. Sidewalls do not experience ion bombardment, and, therefore, the etching rate is different in the longitudinal and lateral directions. Deep reactive ion etching (DRIE) largely exploits this principle to ensure high etching rates with excellent directional resolution. The Bosch process is the most widely used process for DRIE. To achieve nearly vertical structures two steps are repeated alternatively: (1) nearly isotropic plasma etching, for example using sulfur hexafluoride ( $\text{SF}_6$  for silicon), and (2) deposition of a chemically inert passivation layer, for example octafluorocyclobutane ( $\text{C}_4\text{F}_8$ ) that yields a material similar to Teflon. Each phase lasts for several seconds. The passivation layer protects the entire substrate from further chemical attack. However, during the etching phase, the directional ions that bombard the substrate attack the passivation layer at the bottom of the trench and not along the sides, thereby exposing the substrate to the chemical etchant. Consequently, etching takes place mostly at the bottom of the pits.

The development of anisotropic plasma etching methods has been a great progress for MEMS technologies. They permit a highly dense manufacturing of microdevices with high resolution in the contours. Unlike wet etching, DRIE can be done in the order of minutes and not hours. However, wet etching is still widely used. It is convenient for etching thin layers with short etching duration that do not produce significant undercut (silicon oxide etching by buffered HF solution under photoresist protection), for silicon surface cleaning (Piranha-HF cycle), for metal etching, in particular noble metals, as well as shot silicon etch by KOH. The wet etch is preferential in certain cases as it uses less expensive tools and materials. Numerous studies report conditions for plasma and wet etching of different materials (60).

Designing small multifunctional devices are one of the major challenges of the MEMS technology. In our specific context of brain monitoring, MEMS technology is used for the construction of less architecturally complex structures. Chapter 5 will discuss the application of microfabrication technology to the construction of multibiosensor probes for brain implantation and biomolecules continuous monitoring. Another example of MEMS technology application for tools development for neurobiology research was recently reported by Frey et al. (61). They demonstrated a microinjector array fabricated by a three-layer SU-8 (photosensitive polymer) process for the local delivery of specific substances into brain tissue. These injectors are designed to be assembled with implantable biosensor microprobes introduced by the same group (62). Indeed, it is common procedure in neurobiological studies to inject bioactive molecules in the vicinity of the electrode to modulate functioning of neuronal cell, transporters, receptors, ion channel etc. and record their effect on brain chemistry. Commonly, a pulled glass pipette is used as injector. However, it necessitates accurate manipulation with stereotaxic system for precise implantation at defined distance from the electrode. The microinjectors fabricated by MEMS technology and adjustable on the electrode microprobe with respect to the experimental design permits to facilitate this task. Moreover, the same group has developed a silicon multielectrode shank with microfluidic channels inside it, and openings near the recording sites to provide local delivery of drugs (63). This configuration is even more beneficial as there is only one implanted object and therefore, less brain tissue damage.

### 1.2.2 Biosensing part of analytical devices

Accurate analysis of complex biological fluid is possible only if the detector is selective to the target molecule. The selectivity is usually attained by integrating in the device a component

with sufficient specificity to the molecule of interest. Nature offers a large library of such components capable of specific recognition of target molecules: proteins (enzymes and antibodies), nucleic acids (DNA, RNA and their synthetic fragments –aptamers) and even whole cells are widely used in analytical biodevices.

An *Enzyme* is a natural catalyst. Almost all chemical reactions in biological cells need enzymes in order to occur at sufficient rates to sustain life. Enzymes are sometimes highly specific for their substrate, and accelerate one or several chemical reactions. The specificity of an enzyme is obtained through special geometric arrangement of the enzyme active center within the amino acid sequence, involving specific distribution and orientation of functional groups. Only complementary molecule with correspondent size, form, charge etc. will bind to the enzyme active center to be transformed into a product. Enzymes are classified into six groups depending on the chemical reaction that they catalyze. So far, only the class of oxidoreductases that catalyze the transfer of electron from one molecule to another has been exploited for biosensing applications with electrochemical detection system.

An *Antibody*, also known as an immunoglobulin, is a large Y-shaped protein that is used by the immune system to identify and neutralize foreign objects such as bacteria and viruses. Antibodies recognize a unique part of the target (antigen) by a similar mechanism that enzymes use to recognize their substrate, allowing these two structures to bind together with precision. Enormous diversity of antibodies allows the immune system to recognize virtually any foreign molecule or antigens. Detection of particular antibodies is a very common form of medical diagnostics. The presence of certain antibodies in the blood or biological fluid is a good signature for the presence of a pathogen (bacteria, virus, etc.) in a patient's body. Specific antibodies for a target antigen are generated by injecting the antigen into a mammal, such as a mouse, rat or rabbit. Blood isolated from these animals contains the antibody that is then separated and purified. The antibody-antigen affinity is widely used in research and clinical medicine to detect molecules of interest in biological media. The most common detection methods for such complexes are optical methods. However antibody-antigen binding does not follow well-defined kinetics and therefore, antibody-based detection is rarely quantitative.

*Nucleic acids (DNA and RNA)*. Detection of viruses, pathogenic microorganisms, mutations causing human genetic disorders, cancer, hypertension, and other diseases widely rely on genetic testing usually performed with DNA probes. For the purpose of rapid, simple and economical testing of genetic and infectious diseases small portable devices have been developed. DNA-based devices are made by immobilizing single stranded DNA (ssDNA) probes with indicators to measure the hybridization between DNA probes and their complementary DNA strands. The DNA probe is labeled with enzyme, radioactive material, chemiluminophore or ligands for optical and electrochemical detection as the nucleic acid itself is not able to provide any signal. DNA applications can be classified into three broad categories: sequencing, mutation detection, and matching detection. The analysis of gene sequences and the study of gene polymorphisms play a fundamental role in rapid detection of genetic mutations, offering the possibility of performing reliable diagnosis even before any symptoms of a disease appear.

*Aptamers* are artificial, chemically synthesized single-stranded DNA or RNA sequences that fold into secondary and tertiary structures allowing them to bind to certain targets with extremely high specificity. The high affinity of an aptamer to its target molecule (small molecules, proteins, and even entire cells) is thought to resemble chemical antibodies. However, aptamers have a number of unique features which make them a more effective choice than antibodies. First, an aptamer that is selective to a particular target (from small

inorganic ions to intact cells) is isolated from a synthetic library of aptamers via an *in vitro* process, unlike the *in vivo* process of antibody production. Aptamers, once selected, can undergo subsequent amplification through polymerase chain reaction (PCR) to produce a large quantity with high purity. The simple chemical structure of aptamers makes them easily modifiable with functional groups according to different purposes. Finally, aptamers are much more stable than antibodies, making them suitable in applications requiring harsh conditions. The application of aptamers for biosensing devices is similar to those described above for antibodies or nucleic acids (64).

### 1.2.3 Optical detection of biomolecules

Optical methods are based on the measurement of absorbance, reflectance or fluorescence emission that occurs in the ultraviolet, visible or near-infrared light spectrum. Optical methods are performed with a transducer that responds to an analyte by undergoing a change in its optical properties. Signal changes are recorded by a photodetector and then transformed into an electrical signal.

Enzymes can be used as biological recognition centers in combination with optical detection methods. In the case of oxidases, the optical sensing approach can be configured to detect the amount of oxygen consumed, the concentration of hydrogen peroxide produced or the change in pH in the medium. However, pH changes as analytical signals are rarely used. The detection of changes in oxygen concentration is possible using its property to quench the luminescence of certain indicator dyes, for example pyrenebutyric acid, pphenylanthracene, ruthenium (II) complexes, platinum (II) or palladium (II) porphyrins. Fiber-optic sensors can readily detect such optical changes *in situ*. They comprise an optical fiber with a polymer matrix incorporating the enzyme and light sensitive dye covalently attached to the fiber. In fluorescence studies, the optic fiber excites the dye layer with emitted light, and provokes its fluorescence in a shifted wavelength that travels back through the fiber and is detected by a spectrofluorimeter. When the analyte of interest is present in the solution, the oxidase transforms it with consumption of oxygen. The local decrease in oxygen concentration then produces an increase in fluorescence. The substrate concentration is thus translated into an increased light intensity emitted by dye layer that can be measured quantitatively.

Optical sensing approaches that exploit chemi- and bioluminescent reactions are simpler because no excitation light is required. In this configuration, the chemical species generated during enzymatic reaction participate in subsequent processes that result in change of optical properties. For example,  $H_2O_2$  produced by an oxidase-based enzymatic reaction catalyzes oxidation of luminol followed by light emission. The intensity of luminescence is proportional to the concentration of peroxide and consequently to analyte.

Optical transducers are most often used for detection of antigen-antibody interactions and in DNA-based devices (65). There are five configurations of heterogeneous optical immunosensors. 1. Direct immunosensors: an unlabeled antigen binds to an unlabeled antibody. The change in refractive index acts as an analytical signal. However, this approach has a low sensitivity and thus has been demonstrated for only small number of analytes (for example, for detection of anti h-IgG (66)). 2. Competitive immunosensors: an unlabeled antigen (the analyte) and its labeled form (intern standard) compete for a limited number of binding sites of the immobilized antibody. Fluorescence intensity is inversely proportional to the amount of the analyte concentration. 3. Sandwich immunosensors are widely used and require the antigen to have at least two specific sites for binding to one immobilized antibody and a second labeled antibody. Fluorescence intensity is proportional to the concentration of

the fluorescently labeled antibody attached to the first immobilized layer, which in turn is related to the concentration of the antigen in the solution. 4. Displacement immunosensors require initial saturation of immobilized antibody binding sites with a fluorescently labeled antigen. After introduction of the unlabeled analyte antigen, displacement of the labeled antigen occurs and is measured as a decrease in fluorescence intensity. 5. Immunosensors based on binding inhibition. Such sensors require the immobilization of an unlabeled analyte derivative on the support. In the absence of antigen, the labeled antibody can bind to the surface. Binding is inhibited, however, in the presence of the analyte because it blocks the binding sites of the antibody (65).

Despite the fact that binding between an antibody and an antigen is reversible and non-covalent, most immunoreactions are irreversible in practice because of high association constants and slow dissociation rates. As a result, practically all immune “sensors” are limited to a single measurement.

DNA based devices with an optical transduction element are usually constructed in two possible sensing configurations. In the first one, the single standing strand of capture DNA is attached on the support or optic fiber. Fluorescein-labeled target DNA interacts with immobilized chain in complementary manner by hybridization, and thereby the concentration of nucleotide is proportional to fluorescence intensity. Regeneration of the biosensor is possible by washing at the temperature from 65 to 80 °C, resulting in complete dissociation of the bound duplex. Another approach consists in the formation of molecular beacons (MB). MBs are single-stranded types of oligonucleotide probes that possess a stem and a loop structure. This single strand is immobilized on the waveguide preserving the loop conformation. A fluorophore attached to one end of the stem and a quencher attached to the other end, are thus in close proximity, and little or no fluorescence is observed. The stem is formed when two complementary chains of target and capture DNA (oligonucleotides with specific sequence, RNA, aptamer) are bound. Hybridization of a matching oligonucleotide to the loop results in a conformational reorganization that brings the stem apart so that fluorescence is enhanced. This technique does not require labeling of the species of interest. Moreover, DNA-based devices with optical transduction have exceptional stability, possess very low limits of detection, are highly specific, and are relatively tolerant to large temperature variations. They have a very wide applicability, since they can bind a large variety of molecular targets, especially using aptamers that can be engineered in vitro to recognize virtually any type of analyte (65, 67).

Surface plasmon resonance (SPR) has received growing interest in biomolecules sensing application in the last twenty years. SPR phenomenon can be described as the resonant, collective oscillation of valence electrons in a solid stimulated by incident light. When a photon gets on a noble metal surface (typically gold or silver) it can couple with and excite the electrons in the metal, causing them to move as a single electrical entity known as a plasmon which propagates as a surface electromagnetic wave parallel to the metal/dielectric interface. As the plasmon oscillates it generates an electric field that extends about 300 nm out from the metal surface. At a particular angle where the energy transfer from the photon to the plasmon is well matched a resonance occurs, significantly increasing energy transfer from the photon to the plasmon and causing a corresponding decrease in light reflectance from the metal surface. The resonance condition is established when the wavelength of photons matches the natural frequency of surface electrons oscillating against the restoring force of positive nuclei. If the plane of the metal surface is fixed, the resonance wavelength can be identified by scanning through a range of angles of incidence for the photon and determining the resonance angle (68).

Typical SPR optical biosensors comprise a gold-coated glass (prism) slide with chemically-modified gold surface to assure selective analyte binding to the surface (antigen-antibody couple etc.). A light wave passing through the optic prism to the gold surface is totally reflected at the interface between a prism coupler and a thin metal layer. The reflected light is detected by a photodetector. If mass is bound to the surface within this 300 nm range then it perturbs the plasmon. There are three main detection approaches that have been demonstrated in SPR optic systems: measurement of the intensity of the reflected light wave; measurement of the resonant angle transduced as a shift in the reflected beam coordinates; measurement of the resonant wavelength of the incident light wave (69).

SPR is a quantitative method for investigating a number of surface binding interactions: small molecule adsorption, protein adsorption, antibody-antigen binding, DNA hybridization and protein-DNA interactions. It provides a means not only for identifying these interactions and quantifying their equilibrium constants, kinetic constants and underlying energetics, but also for employing them in very sensitive, label-free biochemical assays.

#### 1.2.4 Electrochemical detection of biomolecules

Electrochemical detection methods use preferentially enzymes, because of their high substrate specificity and the possibility of directly monitoring enzymatic activity without intermediate molecular architectures. However, many electrochemical detection setups are possible in principle. Immunosensors use antibodies, antibody fragments or antigens to monitor binding. DNA sensors classically use the process of hybridization with complementary DNA strands. Typically in bioelectrochemistry, the binding events generate a measurable current changes (amperometric), a potential change or charge accumulation (potentiometric), an alteration in the conductive properties of a medium (conductometric) or a change in resistance (impedance) changes (impedimetric) (70-72).

*Amperometric methods* consist in a continuous current measurement that results at least in part from the oxidation or reduction of electrochemical biomolecules or electroactive species related to analyte. The most commonly used amperometric techniques are amperometry, cyclic voltammetry and chronoamperometry. In amperometry, the current is measured at a constant potential. An example of amperometric device is the glucose sensitive enzymatic biosensor, which is based on the amperometric detection of hydrogen peroxide produced by glucose oxidase (73). Amperometry may also be applied for immunosensors and immunoassays working in sandwich configuration, in which secondary antibodies are labeled by an enzyme. The amount of bound secondary antibody and consequently, of antigen, correlates with the oxidation current produced by the enzymatic reaction (74). In cyclic voltammetry, a current is measured while a cyclic triangular potential wave is applied to the electrode. The peak value of the current measured over a linear potential range is proportional to the bulk concentration of the analyte or corresponding electroactive species. Using this method, it is possible to obtain information about the redox potential and electrochemical reaction rates. The scan rate is a critical factor, since the duration of scan must provide sufficient time to allow the chemical reaction to occur. Cyclic voltammetry is used, for example, to monitor DNA hybridization. Erdem et al. (75) demonstrated the detection of DNA hybridization using Methylene Blue (MB). This indicator dye presents reversible electroactivity and strongly associates with the single-strand DNA. In the absence of analyte, this association leads to MB voltammetric signals due to the interaction of MB with oligonucleotide guanine bases. When hybridization occurs, the magnitude of the voltammetric indicator peak decreases, thus, reflecting the extent of the hybrid formation.

*Potentiometry* measures the accumulation of charge at the working electrode compared to a reference electrode in an electrochemical cell when zero or no significant current flows between them. For potentiometric measurements, the relationship between the potential and the concentration is defined by the Nernst equation. An example of potentiometric biosensor was demonstrated by Shishkanova et al. (76). They modified a potentiometric electrode with an oligonucleotide and used it as sensor to monitor the redistribution of ion concentration within the electrode/solution interface induced by the hybridization process.

*Conductometry* measures the ability of an analyte to conduct an electrical current between electrodes. Initially, conductometry has been associated with enzymes that produce charged species into the solution in response to enzymatic activity, thus changing the conductivity of the solution. However, the ionic background of complex biological samples and the small conductivity changes that are usually associated with biological events limit this detection approach for biological sensing. Another more promising approach is to monitor the changes in electrode conductance as a result of a binding event. The changes in conductance and capacitance of the analyte solution may also be measured by such impedimetric techniques, now called *electrochemical impedance spectroscopy* (EIS) (77). EIS measures the impedance of a system over a range of frequencies. It is based on the interaction of an external field with the electric dipole moment of the sample. Data obtained by EIS is expressed graphically in a Nyquist plot. The impedance spectra include a semicircle part at high frequencies, corresponding to the electron transfer limited process and a linear part at lower frequencies, resulting from the diffusion-limiting step of the electrochemical process. The semicircle diameter represents the electron transfer resistance. If the electron transfer occurs easily, the Nyquist plot appears as a straight line. By contrast, if the surface is non-conducting the plot will have a semicircle shape with a large diameter. For electrochemical sensing, impedance techniques are useful to monitor changes in electrical properties arising from biorecognition events at the surface of a modified electrode. For example, changes in the conductance of the electrode can be measured as a result of protein immobilization and antibody-antigen reactions on the electrode surface. Interestingly, impedimetric sensing can also be used to detect the binding state of DNA. Ensafi et al. (78) reported an impedance biosensor for detection of cancer, chronic lymphocytic leukemia, based on gold nanoparticles/gold modified electrode. They demonstrated that the Nyquist spectrum obtained at Au<sub>nano</sub>/Au electrode showed an almost straight line, indicating a diffusion limiting nature of the process. However, the self-assembled ssDNA on the electrode acts as an insulating layer, which obstruct the interfacial electron transfer. A semicircle was then observed after grafting the gold electrode with ssDNA. After hybridization of the complementary DNA of interest, the interfacial electron transfer was further inhibited, leading to an increase in the electron transfer resistance. This phenomenon is due to the generation of an insulating layer on the Au nanoparticle surface, which results in a higher electron transfer resistance, and significantly enlarges the diameter of the semicircle. Authors reported a DNA detection limit of about 1.0 pM.

### 1.2.5 Mass sensitive detection systems

The development of systems that can detect mass with a detection limit down to the molecular and atomic level is of particular interest in biological and biomedical fields. In mass sensors, the detection of mass changes can be determined by changes in deflection, resonance frequency, or electrical resistance of the operating element. Two most commonly

explored techniques for mass sensing are quartz crystal microbalances (QCM) and cantilevers.

A *Cantilever* is a micro- or nanomechanical system, appearing as beam attached from one side. Cantilevers are generally operated in either static deflection mode or dynamic, resonant mode. In deflection type sensors, binding on one side of a cantilever causes unbalanced surface stress resulting in a measurable beam deflection. The most common way of measuring this deflection is to use optical reflection. A laser is focused on the cantilever suspended side and reflects onto a position-sensitive detector. Cantilever deflection is then determined through displacement of the reflected laser beam. The dynamic or resonant sensing technique is based on the resonance frequency of the cantilever under specific excitation, e.g. thermal, electrostatic, magnetic, piezoelectric or optical excitation. ),. This resonance frequency depends on the mass of the cantilever. If a target molecule binds to the cantilever surface, it increases its mass and decreases its resonance frequency. By measuring this difference in frequency, slight differences in mass can be computed, revealing the quantity of bound analyte. Piezoelectric layer incorporation onto the cantilever surface permits to simplify signal detection. In response to cantilever bending, the piezoelectric layer produces an electrical signal that can be monitored directly (79).

*Quartz crystal microbalances (QCMs)*. A QCM consists of electrodes plated onto a thin disk of quartz. Quartz is a piezoelectric material, i.e. when an oscillating electric field is applied across the surface, an acoustic wave is induced perpendicularly to the crystal. If an analyte is adsorbed on the surface, a change in the frequency of oscillation occurs, that is related to the amount of bound analyte. QCM can detect subnanogram changes in mass and can detect biomolecules when a receptor protein is immobilized onto its surface. Cantilevers are supposed to be more sensitive in the vacuum, whereas QCMs are more effective in air or liquid.

Cantilevers and QCMs are usually coated with layers specific to a particular analyte. Immunoassays can be performed by coating these devices with an antibody and detecting its antigen from solution, or vice versa. Tethering single-stranded DNA to the surface can serve as a sensor for hybridization with the complementary strand of DNA (79).

The multifunctional small devices have obviously found their niche among modern analytical instruments. Point-of-care testing is now largely integrated in people's life and in clinical practice. They often perform a whole analytical cycle from sample preparation via separation to selective target detection, thus taking functions of whole laboratory, whence their name 'lab on a chip'. These devices represent a marvelous combination of physics, mathematics, chemistry, biochemistry, biology and medicine. In the future, they should facilitate clinical procedures and discharge hospital laboratories and personnel from routine analysis, thereby lowering analysis cost.

Regarding our overall objective of brain monitoring in animals and humans (and especially, monitoring of the chemical composition of brain interstitial fluid), all the biosensors techniques developed above are potentially compatible with microdialysis. Microdialysis is essentially a sampling technique that delivers minute amount of cerebrospinal fluid samples (typically in the order of a few 100 nL per minute). These samples are typically analyzed by separation techniques like HPLC, CE-LIF, or LC-MS that are expensive and time-consuming. However, microdialysate samples can also be analyzed online by adapting a biosensor system downstream of the microdialysis setup. Boutelle et al. (52) developed an electrochemical enzyme-based system for the on-line measurement of glucose, glutamate, and lactate in brain microdialysate. The dialysate stream is sampled into a valve with sampling time of few (2-3) minutes, where it is then mixed with buffer. The stream is then



connected to enzyme reactors containing a cellulose ester membrane where the appropriate oxidase enzyme and horseradish peroxidase (HRP) are absorbed. The enzyme recognizes its substrate and transforms it with producing  $H_2O_2$  that is selectively degraded by HRP. Ferrocene(II), containing in buffer acts as a mediator to reduce the HRP enzyme and transforms in the ferricinium ions. The system is coupled to working glassy carbon electrode held at a potential of -100 mV (Ag/AgCl). The ferricinium ions are reduced on the surface of the electrode, resulting in a current peak. Current peaks are then converted to concentration based on pre-, intra- and post-monitoring calibrations with standard solutions (80, 81). Numerous designs of the enzyme-based electrochemical systems for continuous molecules monitoring in microdialysate samples have also been reported, for example by Pasini group for glucose detection (82), by Nishino group for simultaneous glucose, lactate and pyruvate monitoring (83) or glutamate detection (84). The fabrication of an enzyme sensor by thin film technology with integrated microdialysis sampling system for continuous sampling and on-line monitoring of glucose has also been reported (85).

Nevertheless, despite tremendous progress in the analysis of small aqueous samples delivered by microdialysis, this strategy suffers from a number of problems. Microdialysis has a low temporal resolution. The time usually required to collect sufficient sample volume is about 10-30min with perfusion rate of 0.2  $\mu$ L/min. Even the most rapid microdialysis sampling rates published in the literature require at least few minutes to get sufficient volume. Diffusion of the molecule of interest from the brain interstitial fluid to the microdialysis probe is also a slow process that may take a few seconds *in vitro*, but that is significantly slowed down after brain implantation. Additionally, microdialysis probes usually have a diameter of about 200-300 $\mu$ m and thus, cause tissue damage upon insertion with lesions extending up to 1.4 mm from the implantation site after 30h (86). Consequently, this technique requires longer recovery time, may provoke inflammatory responses, changes of interstitial chemical composition and overall physiological functioning of the brain. To overcome these constraints implantable microelectrode biosensors have been developed and introduced in neurochemical studies as an alternative method to microdialysis. Among different detection methods and recognition elements used in "lab on a chip" devices, only amperometric sensors with enzyme recognition element have been employed so far for continuous monitoring neurotransmitters and metabolites in the CNS.

## 2. Implantable enzymatic microbiosensors (In vivo biosensors)

Enzyme amperometric biosensors are the dominant *in vivo* format for implantable biosensors capable of monitoring biochemical analytes in vivo (87). Essential methodological aspects of enzymatic microbiosensors include their geometrical configuration, microelectrode material, substrate of interest, and consequently, the choice of the enzyme, the method for enzyme immobilization and finally, the approaches to suppress of non-specific electrochemical signals present *in vivo*.

### 2.1 Microelectrodes: configuration and materials

#### *Microelectrode configuration*

In neurobiological studies two major designs of microelectrodes are used: cylindrical glass-capillary based electrodes and needle-shaped silicon-, glass- or ceramic-based microprobes.

The cylindrical glass-capillary based microelectrodes were the first implantable

microelectrodes to be designed in the early 1950s and still remain the most widely used in this domain. Their structure has hardly changed in the last years. The typical glass-capillary microelectrode is presented in Figure 1.9. A microwire with a diameter of 15-50  $\mu\text{m}$  made of carbon, platinum, iridium, gold or of other conductive material is inserted into a pulled glass capillary and the tip of the pipette is cut so that the wire extends from the glass by 100 to 500  $\mu\text{m}$ . The junction between the microwire and the pipette tip is sealed by locally melting the glass or by gluing (88-90).

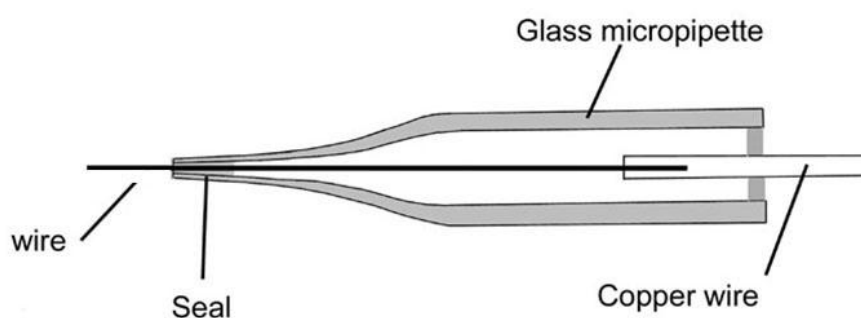


**Figure 1.9. Cylindrical glass-capillary microelectrode:**

electroconductive wire is placed into the glass capillary expanding to a distance defining electrode size. The rest of the wire is isolated by sealing the glass.

These electrodes are very simple in fabrication and handling, their size permits to access to the deepest brain structures with minimal tissue damage. However, their fabrication procedure is manual and thus time-consuming and expensive. Moreover, hand-made fabrication leads to poor reproducibility of the electrode tip surface. Additionally, simultaneous monitoring of different molecules or the same molecule in the different structures of the brain is of great interest for understanding the dynamics of metabolism and cell signaling, but is difficult using this electrode design. Such multiple simultaneous recordings would require implantation of multiple microelectrodes, which is technically challenging and leads to increase in brain damage and data misinterpretation. These multiple recordings became possible with the introduction of microprobes incorporating multiple microelectrodes.

Wise's group was the first one to use microelectromechanical systems (MEMS) technology to realize multi-electrode microprobes (91-94). Generally, the fabrication process consists of metal deposition on a support surface (silicon, glass or ceramic) and its patterning by "lift-off" to define electrode shape, number and relative placement on the microprobe; then the needle shape of probe must be formed and the desired thickness must be obtained. To ensure minimum tissue damage, the thickness of the probe should not exceed 50-100  $\mu\text{m}$ . The last but not the least important step is the isolation of the whole microprobe surface excepting recording sites and contact pads.

Silicon is the most widely used support material for microprobe construction by MEMS technology. However glass and ceramic supports utilization have also been reported. Ceramic-based materials show increased strength and electrical inertness. They are widely used as substrate by Gerhardt's group (95, 96). However, ceramic is rather inert and the DRIE or KOH-etch cannot be applied to shape the microprobe into a needle or to cut it out from the bulk material. The thickness of the shaft is defined by the thickness of the initial ceramic support and single microprobes must be cut out by either a diamond blade or an

industrial laser. As alternative to silicon and ceramic materials, Lin et al. (97) reported fabrication of microprobe arrays for neural recording using glass support.

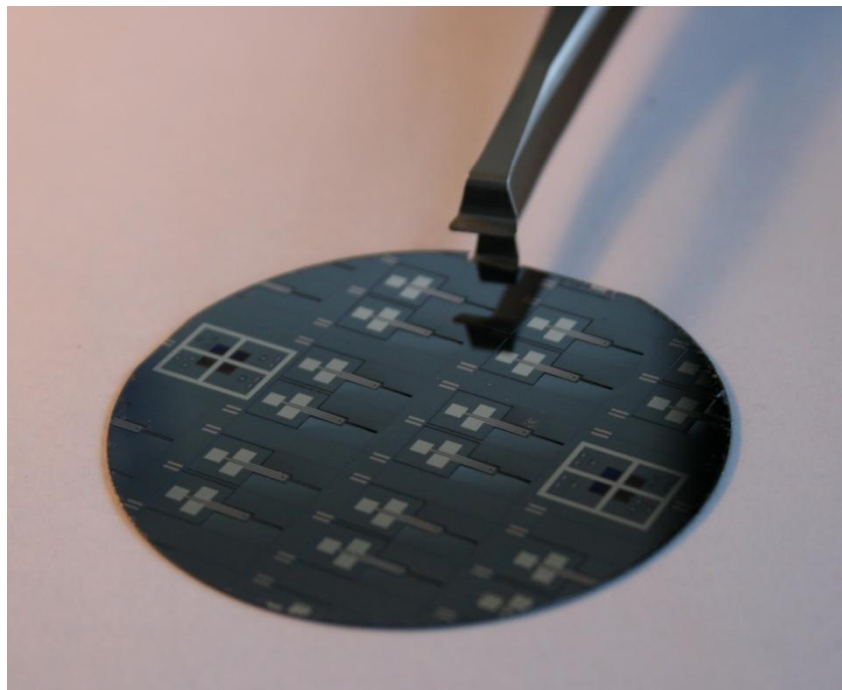


**Figure 1.10. Processed wafer:** silicon wafer of 2inch bears 12 suspended shafts with 3 microelectrodes on each.

A top passivation layer is an indispensable element of the microdevice. It isolates the conducting lines leaving only the recording sites and contact pads to be exposed. Silicon nitride is commonly used as top passivation layer, because of its excellent insulating properties. It is superior to silicon dioxide as it creates an improved diffusion barrier against water molecules and sodium ions, and does not swell in aqueous solutions. It is usually deposited on the whole substrate, followed by reactive ion etching on the recording sites and contact pads. However, the thickness of silicon nitride is limited by the growth time, approximately 200-300nm per hour, making the process time-consuming and costly. Parylene and polyimide materials are used as an alternative to silicon nitride. They can form passivation layers of micrometric thickness (subsequent etch is also required to expose the recording sites and contact pads). The emergence of photostructurable epoxy resins, SU8 photoresists, has opened new possibilities in microfabrication processes by providing excellent top insulator layers for microprobes. SU8 is a photosensitive polymer, highly transparent and allowing fabrication of structures with different thicknesses ranging from one to hundreds of micrometers. SU8 therefore greatly facilitates probe design: its highly cross-linked structure assures stability to different chemicals and possesses biocompatible properties, making it an excellent material for implantable microprobes (98, 99).

*In vivo* implantation requires the microelectrode array to have limited thickness, preferably not exceeding 50  $\mu\text{m}$ . To achieve selective silicon etching to decrease the needle thickness, boron-etch stop technique has been initially used. Firstly, silicon is covered by a boron source, followed by a deep boron diffusion process with controlled penetration thickness. After all the fabrication steps performed to obtain a final design of microprobe, KOH etch removes undoped and unprotected silicon to release a silicon needle. However, this method is time-consuming and costly penetration thickness is limited to 15 $\mu\text{m}$  (100, 101).

Progress in dry etching techniques, especially the development of deep reactive ion etching (DRIE) has facilitated the overall fabrication protocol. DRIE can perform a deep anisotropic etch within minutes instead of hours, resulting in microprobes with well defined contours that respect the initial design (62, 102-104). Figure 1.10 represents an example of silicon wafer with 12 final microprobes each bearing three microelectrodes. Thus, unlike the hand-made microelectrode presented above, MEMS technology allows the mass fabrication of numerous microprobes in one parallel process.

Overall, there are several major advantages of microfabrication over handmade electrodes. First, the technique allows highly reproducible production of small electrodes. Second, numerous microelectrodes are patterned onto a single substrate resulting in increased probe yield at a decreased cost. Third, microfabrication methods allow manufacturing numerous microelectrode designs with multiple recording sites in well-defined, highly reproducible geometrical configurations. This is ideal for designing a microprobe that can be easily and precisely positioned within a single or even multiple brain structures simultaneously with the aid of stereotaxic surgery equipment.

### *Microelectrode materials*

Numerous electrode materials for biosensor construction are reported in the literature. Gold (103, 105, 106), platinum, platinum/iridium, Pd (90, 107-110), carbon fiber (88, 89, 111, 112) and carbon covered by noble metals (73) are the most frequently used materials.

The general principle underlying enzymatic biosensor detection lies in the detection of hydrogen peroxide, the product of oxidase-based enzymatic reactions. The oxidation of peroxide is known to be electrocatalyzed. Platinum, platinum/iridium, Pd (and other noble metals) electrodes are the most widely used materials for amperometric enzymatic biosensors construction because they possess catalytic properties suitable for peroxide ( $H_2O_2$ ) oxidation. For example, platinum oxides  $Pt(OH)_2$  formed on the surface of Pt or Pt/Ir alloys can catalyze  $H_2O_2$  oxidation(113). The oxidation of peroxide may be presented as follows (114, 115):



where the first step is the formation of a complex between peroxide and oxidized platinum sites (1); then, electron transfer occurs involving Pt reduction and peroxide oxidation (2), followed by the restoration of  $Pt^{2+}$  sites on the electrode at +500mV working potential (3). Hence, it follows that the electrode surface must be electrically treated to insure its best catalytic properties. A common method to prepare the platinum surface is to cycle the electrode with a potential wave ranging from low negative to high positive value, typically -1÷1V in 1M  $H_2SO_4$  (62). This procedure cleans the surface at low negative potentials and oxidizes it at high positive currents.

The catalytic nature of hydrogen peroxide oxidation explains the lower effectiveness and lower sensitivity of gold microelectrode biosensors that have no catalytic properties unlike the platinum.

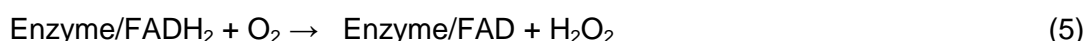
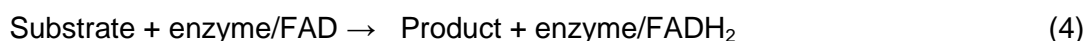
Carbon is another electrode material that is largely used in brain neurochemical studies, mostly for biogenic amine detection. Even if carbon microelectrodes were used for *in*

*in vivo* experiments they are less suitable for H<sub>2</sub>O<sub>2</sub> detection than platinum electrodes. The oxidation of peroxide on the carbon fiber requires a higher holding potential compared to Pt, (+500 mV vs. +850 mV for carbon). A higher holding potential will lead to higher interference signals from other endogenous electroactive molecules present *in vivo*. High holding potentials can also damage living tissues. However, carbon fibers can be easily modified by chemical etching, permitting to obtain implantable electrode with very small dimensions that are favorable for *in vivo* brain experiments. Such etched carbon fiber is then covered by a noble metal (most commonly ruthenium or platinum) by electrodeposition or by sputtering. The resulting electrodes will thus combine the advantages of carbon fiber size and electrochemical properties of noble metals (116). Additionally, this approach has demonstrated an increased sensitivity to hydrogen peroxide (117). Therefore, it is potentially interesting for *in vivo* microelectrode implantation.

## 2.2 Biosensing part – enzyme

Oxidoreductases and particularly, oxidases are the principle class of enzymes used for biosensor construction. An oxidase is an enzyme that catalyzes an oxidation reaction that involves molecular oxygen (O<sub>2</sub>) as the electron acceptor and reduces it into hydrogen peroxide (H<sub>2</sub>O<sub>2</sub>) or water. Example of such electrodes based on oxidase enzymes are glucose, lactate, choline, glutamate, D-serine biosensors (55, 73, 90, 111). Figure 1.11 represents a typical cylindrical glass-capillary based microbiosensor and the principle of glucose detection. Glucose oxidase mediates the conversion of glucose into gluconolactone with production of H<sub>2</sub>O<sub>2</sub>. H<sub>2</sub>O<sub>2</sub>, in turn, reaches the Pt surface, and is oxidized into oxygen with the transfer of two electrons and release of two protons into solution. These two electrons give a rise to an amperometric current recorded by the electrode that is proportional to the concentration of glucose in the solution.

To transform their substrate, oxidases use cofactors that act as electron acceptors to assist the electron transfer from substrate to oxygen or alternative electron acceptors. Cofactors are non-protein compounds bound to the protein and could be either of organic or inorganic origin. Organic cofactors comprise numerous vitamins or their derivatives. Inorganic cofactors usually include iron, magnesium, manganese, cobalt, copper, zinc, selenium, and molybdenum ions (118). Most oxidases utilize flavin adenine dinucleotide (FAD) as cofactor. Thus glutamate-, choline-, glucose-, D-amino acid oxidases are FAD-dependent enzymes. L-Lactate oxidase uses flavin mononucleotide (FMN) cofactor (<http://www.brenda-enzymes.info/>). Substrate oxidation by FAD-dependent enzymes and subsequent detection on a biosensor can be presented as follows:



Molecular oxygen acts as an electron acceptor, transporting electrons from the enzyme active site to the electrode surface under its reduced form H<sub>2</sub>O<sub>2</sub>. Therefore, the response of an oxidase-based sensor can depend on ambient oxygen. In physiological conditions, the concentration of oxygen in the extracellular fluid is not limiting for molecule detection at low μM concentration. If a high concentration of the substrate is expected, like for glucose or lactate that are present in the extracellular fluid at 10<sup>-4</sup> – 10<sup>-3</sup> M, different

approaches are employed to preserve the linear response of the biosensor. The first method is to create a diffusion barrier near electrode and enzyme that is highly permeable to small molecules, e.g. oxygen,  $\text{H}_2\text{O}_2$ , but highly reduces the flux of the substrate, like glucose. Thus, despite a high concentration in bulk solution, glucose diffuses at much lower concentrations near enzyme surface. Nafion, cellulose or polyurethane are usually used for this purpose (111, 119).

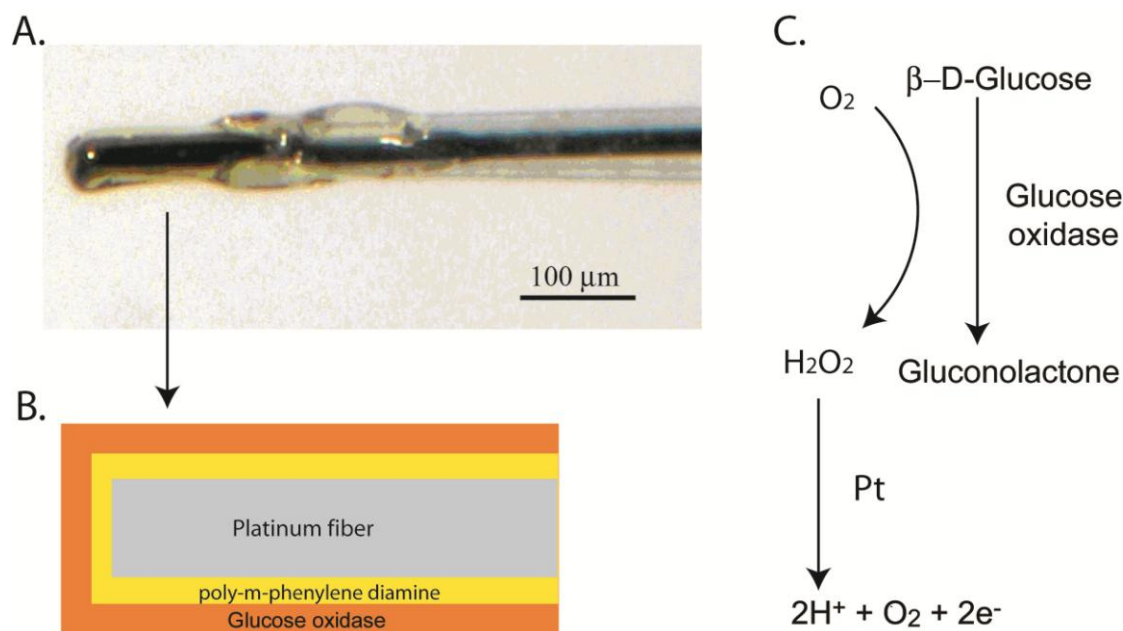


**Figure 1.11. Glucose biosensor:** A. photography of the microelectrode tip; B. schematic representation of microelectrode tip where thin layer of glucose oxidase is deposited; C. glucose oxidase catalyzes glucose transformation in gluconolactone with production of hydrogen peroxide.

The second approach consists in the use of an alternative electron acceptor that would be more effective in such conditions. However, such mediator should not react with endogenous molecules such as ascorbic acid, dopamine, serotonin etc. Importantly, the mediator must effectively compete with oxygen in accepting electrons because no  $\text{H}_2\text{O}_2$  will be detected under such low potentials. Additionally, it must be reliably immobilized together with enzyme and it should be nontoxic. Redox hydrogel-based electrochemical biosensors developed by Heller's group are good representatives of such approach (120). Redox polymer is a polyvinylpyridine polymer partially modified with bromoethylamine and containing  $\text{Os}^{2+/3+}$  complexed groups which enables the electron transport. This polymer together with the enzyme glucose oxidase was immobilized on the surface of Pt a wire to construct a biosensor operating at  $-100\text{mV}$ . Another example of a mediator suitable for biosensors is Prussian blue which is a selective electrocatalyst for hydrogen peroxide reduction in the presence of oxygen, allowing biosensor functioning at 0 or  $-50\text{mV}$  potentials (121).

Oxidases may be used together with other enzymes for biosensor construction. This approach is very promising as it enables the detection of a wider range of biomolecules. Llaudet et al. (122) reported on an enzymatic biosensor sensitive to Adenosine-5'-triphosphate (ATP), recognized as an important extracellular signaling agent. They immobilized two enzymes: glycerol kinase (GK) and glycerol-3-phosphate oxidase (G3POx) (Fig. 1.12, A). Glycerol kinase catalyzes the transfer of a phosphate group from ATP to

glycerol thus forming glycerol phosphate that is then degraded by G3Pox to  $\text{H}_2\text{O}_2$  and glycerone phosphate.

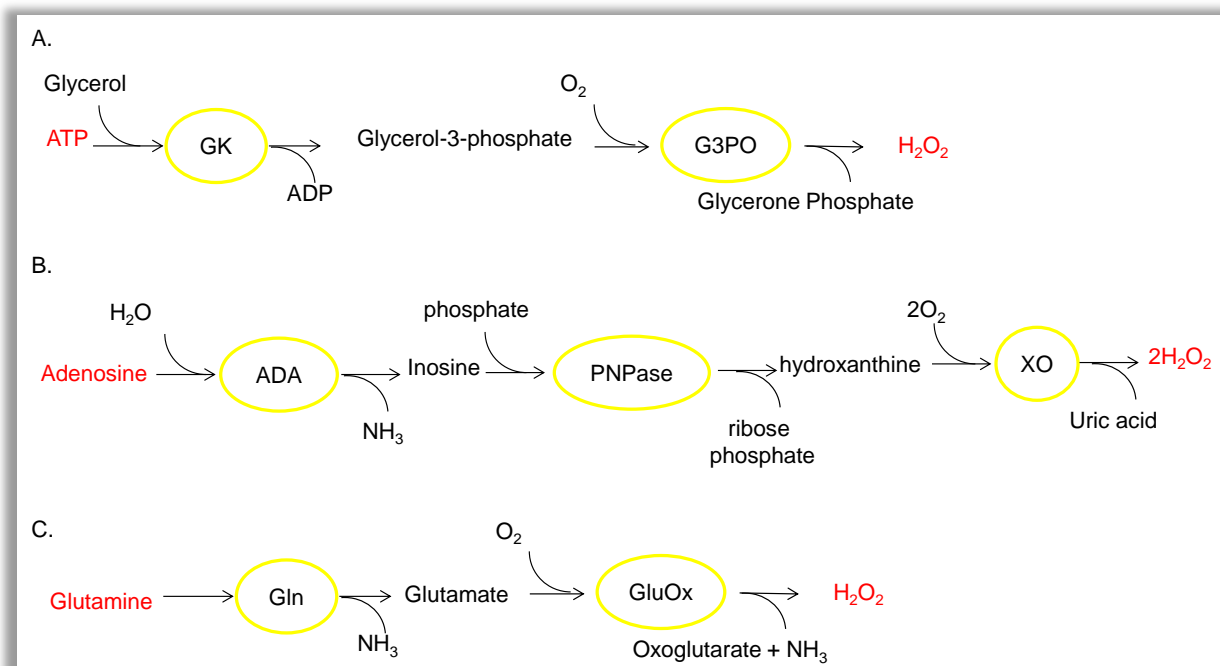


**Figure 1.12. Multienzymatic biosensor design:** A. ATP biosensor – bienzymatic ATP degradation scheme; B. Adenosine biosensor – three-enzymatic adenosine conversion; C. Bienzymatic glutamine biosensor. ATP (Adenosine-5'-triphosphate), GK (glycerol kinase), G3Pox (glycerol-3-phosphate oxidase), ADA (adenosine deaminase), PNPase (nucleoside phosphorylase), XO (xantine oxidase), GLn (glutaminase).

The same group developed a three enzyme biosensor for detecting purine, and in particular adenosine, in the CNS (109). They combined adenosine deaminase (ADA), nucleoside phosphorylase (PNPase) and xantine oxidase (XO) in the same enzymatic layer on the electrode. Adenosine is converted by ADA into inosine, which is then transformed into hypoxanthine by PNPase and finally it was degraded into uric acid and hydrogen peroxide (Fig. 1.12, B). A glutamine biosensor has also been reported (108). Glutamine is transformed into glutamate by glutaminase (Gln) and then glutamate is transformed to oxoglutarate and hydrogen peroxide by glutamate oxidase (Fig. 1.12, C).

However, in the case of biosensors constructed with multiple enzymes, great attention must be paid to data analysis. Especially, it must be verified that the signal detected by the biosensor depends only on the substrate of the first enzyme, and not on the ones of intermediate enzymes. For example, in the case of glutamine/glutamate biosensors for *in-vivo* glutamine monitoring, a second biosensor sensitive to glutamate only must be employed in order to verify that the signals that are detected depend on glutamine. To calculate the glutamine basal concentration the difference in currents between biosensors for glutamine/glutamate and glutamate-only have to be computed (and not the usual difference between oxidase-biosensor and BSA or control biosensor).

#### *Kinetics of enzymatic reaction*

The simplest and the best known model of enzymatic kinetics is the Michaelis–Menten

model. It describes the enzymatic reaction by following equation:



In this model, the substrate S combines with the enzyme E to form an intermediate complex ES. This step is reversible and is characterized by a formation constant  $k_1$  and a dissociation constant  $k_{-1}$ . If enzymatic conversion occurs, the complex breaks down into product P and releases enzyme E. This step is characterized by constant  $k_2$ . The overall rate of enzymatic reaction can be described by differential equation:

$$\frac{d[ES]}{dt} = k_1[E][S] - k_{-1}[ES] - k_2[ES] \quad (8)$$

Under the assumption of constant concentration of enzyme-substrate complex (quasi-steady-state approximation) and taking into consideration that the rate of reaction of product formation is expressed as  $V=k_2*[ES]$ , the final equation of reaction rate can be derived:

$$V = \frac{k_1 k_2 [E]^o [S]}{k_1 [S] + k_{-1} + k_2} \quad \text{or} \quad V = \frac{k_2 [E]^o [S]}{K_M + [S]}, \quad \text{where} \quad K_M = \frac{k_{-1} + k_2}{k_1} \quad (9)$$

V represents the rate of enzymatic reaction as a function of the substrate concentration [S] (Fig. 1.13).  $K_M$  is usually termed Michaelis–Menten constant. It is a kinetic constant measured in concentration units and it shows the concentration of substrate for which the velocity of the enzymatic reaction is equivalent to a half of its maximum value. It also indicates the substrate concentration range within which effective catalysis occurs.

$k_2$  is generally represented as  $k_{cat}$ . The units of  $k_{cat}$  are seconds<sup>-1</sup>.  $k_{cat}$  measures the number of substrate molecules turned over per enzyme molecule per second. Thus,  $k_{cat}$  is sometimes called the turnover number. It gives a direct measure of the catalytic production of product under optimum conditions (saturated enzyme).

$k_{cat}/K_M$  - is often thought of as a measure of enzyme efficiency. If  $[S] \ll K_M$ , equation (6) becomes:

$$V = \frac{k_{cat}}{K_M} [E]^o [S] \quad (10)$$

a large value of  $k_{cat}$  (rapid turnover) or a small value of  $K_M$  (high affinity for substrate) results in a large  $k_{cat}/K_M$  value. The  $k_{cat}/K_M$  ratio allows for direct comparison of the effectiveness of an enzyme toward different substrates. When an enzyme has a choice between two substrates, A or B, present at equal, dilute concentrations the simple comparison of their  $k_{cat}/K_M$  ratios could estimate the efficiency of enzyme toward the substrates.

$$\frac{V_A}{V_B} = \frac{(k_{cat}/K_M)_A [E][A]}{(k_{cat}/K_M)_B [E][B]} = \frac{(k_{cat}/K_M)_A}{(k_{cat}/K_M)_B}, \quad (\text{if } [A]=[B]) \quad (11)$$



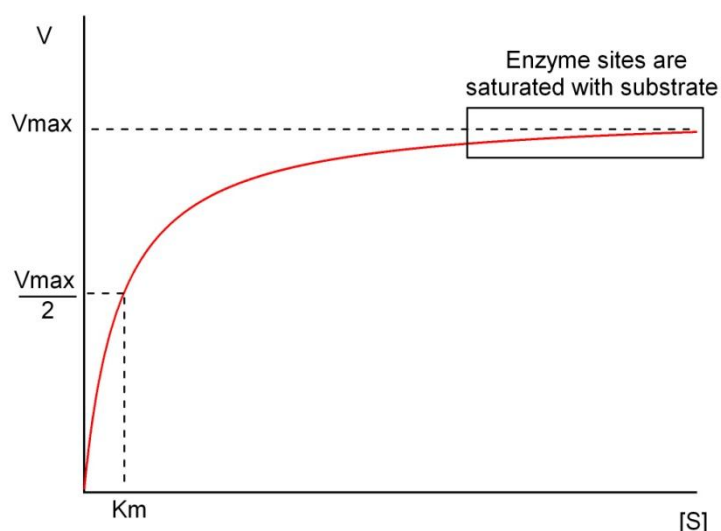


**Figure 1.13. Michaelis–Menten kinetics:** the velocity of enzymatic reaction is dependent on substrate concentration. The rate of enzymatic reaction is the highest when all enzyme sites are saturated with enzyme (under optimum pH and T, °C).

If  $[S] \gg K_M$ , the equation 6 transforms in  $V = k_{cat} * [E^o]$  i.e. the velocity of reaction becomes independent of substrate and reaches its maximum value (in conditions of optimal pH and temperature). Thus, the general equation representing Michaelis–Menten model is following:

$$V = \frac{V_{max}[S]}{K_M + [S]} \quad (12)$$

In turn, the current-concentration relationship that characterizes a biosensor can be approximated by the modified equation:

$$I(C) = \frac{I_{max} * [S]}{K_m^{App} + [S]} \quad (13)$$

where  $I_{max}$  is the maximum current recorded by the biosensor and  $K_m^{App}$  is the apparent Michaelis-Menten constant for the biosensor.  $K_m^{App}$  is related to the  $K_m$  of the enzyme immobilized on the electrode, but also depends on other parameters, such as the diffusion rates of the substrate,  $O_2$ , and peroxide within the enzyme layer. Because of this, the  $K_m^{App}$  of a biosensor is often very different from the  $K_m$  of its free enzyme.

#### *Enzyme immobilization on the electrode surface*

To construct enzymatic biosensors, enzyme must be deposited onto the electrode surface and immobilized by an appropriate method that prevents its leaking in aqueous solution. The review of existing immobilization methods, their advantages and disadvantages is given in Chapter 3. Enzymes are characterized by high specificity toward their substrates, leading to suppose the same level of selectivity of biosensors. However, the influence of immobilization procedure on enzyme properties and overall final biosensor performances is still poorly understood and remains largely empirical. The influence of enzyme immobilization on its overall properties is reviewed and discussed in the Chapters 3, 4.

## 2.3 Non-specific interaction suppression

Analysis of complex biological fluids with biosensors requires an excellent selectivity. The problem, usually, does not lie in the enzymatic reaction itself, which is exquisitely selective, but in the electrochemical detection of resulting peroxide. Optimal peroxide oxidation takes place at potentials, for which red/ox reactions of other endogenous electroactive molecules, like serotonin, dopamine, ascorbic acid, uric acid etc. can occur. These molecules are usually present in high concentrations in the brain, and cause important interference in the final biosensor response, leading to an overestimation of the concentration of the molecule of interest. To avoid this problem, different interference removal approaches have been proposed.

*Exclusion layer.* Such layers are designed to block or minimize the diffusion of undesirable compounds to the electrode surface. One of the most widely used materials to create a perm-selective layer is Nafion®, an anionic Teflon® derivative. The negatively charged sulfonic acid groups scattered over the polymer matrix of Nafion repel anions from the electrode surfaces. In contrary, these negatively charged sulfonic acid groups concentrate cationic species such as DA, NE and 5-HT. However, the hydrophobic properties of a certain negatively charged species can compete with anionic charge rejection. Thus, Nafion does not efficiently reject 5-HIAA (5-Hydroxyindoleacetic acid metabolite of serotonin). Nevertheless, Nafion® films provide very satisfactory anion exclusion (112, 123).

Because Nafion can concentrate biogenic amines and has a low capacity to repel hydrophobic molecules like 5-HIAA, other more effective screening layer materials have been used. For example, polyphenylenediamine or PPD is a polymer obtained from the meta-, orto- or para-phenylenediamine monomer by electropolymerization on the electrode surface. Schuvailo et al. (73) provided evidence that meta-PPD layer provides more effective screening properties than its isomers. The selectivity of mPPD is achieved by forming a size exclusion layer that prevents larger molecules such as ascorbic acid, dopamine, serotonin, DOPAC etc. from reaching the recording surface. Smaller molecules, such as nitric oxide and H<sub>2</sub>O<sub>2</sub>, can diffuse through the matrix to the electrode surface.

*Differential method.* The mPPD layer lets non-specific small molecules through the membrane, potentially impacting the final biosensor signal. To eliminate this non-specific current a second electrode is placed close to the biosensor of interest. It has the same size and construction, and is coated with an inactive protein membrane instead of the enzyme (control electrode) (90, 96, 119). Subtraction of current detected by the control electrode from that of the biosensor gives the specific current corresponding only to the molecule of interest (enzyme substrate).

*Additional enzyme integration.* Ascorbic acid is present in the extracellular fluid at especially high concentrations (100-500µM), so that Nafion layer may not be sufficiently efficient to repel it. The co-immobilization of ascorbic acid oxidase (AAOx) as a complement approach to Nafion perm-selective layer is used. The benefit of AAOx is that it converts the ascorbic acid to dehydroascorbate releasing not H<sub>2</sub>O<sub>2</sub>, but a molecule of water, which does not interfere with electrochemical detection (112).

*Mediators.* An additional way to decrease the influence of interfering molecules on the biosensor signal is to integrate a mediator into enzyme containing matrix. In the previous section it was noted that mediators could act as electron acceptors, thus taking oxygen function, and that they operate at lower potentials than those required for H<sub>2</sub>O<sub>2</sub> oxidation. In general, biosensors containing a mediator in their construction operate at 0mV or -100mV. At these low potentials, oxidation of interfering molecules does not occur.

## 2.4 Requirements for implantable microbiosensors

Enzymatic biosensors must fulfill several criteria to be used *in vivo* and in particular in Neuroscience.

- Biosensor *dimensions* greatly influence the accuracy of data collection. Small biosensors cause less tissue lesion, provoke fewer physiological perturbations. Additionally, smaller biosensors have higher spatial resolution, permitting local measurements in discrete brain regions. Currently, the smallest dimensions of microelectrode biosensors are in the order of 10-40  $\mu\text{M}$  in diameter and 100-200  $\mu\text{m}$  long (90, 119, 124). The effects of probe implantation on brain inflammation, microglial proliferation and scar formation are still poorly understood. .
- Optimal *sensitivity* is required. It must be sufficiently high to enable detection of low basal concentrations and small changes in concentration. Moreover, the response must remain linear within the range of target concentrations. To detect low concentrations a high signal-to-noise ratio is favorable to give low limit of detection (LOF). Usually, microelectrode biosensors yield detection limits in the order of 200 nM (125).
- The biosensor must possess high *selectivity* towards a molecule of interest. It must have high specificity towards the analyte or its secondary substrates must not be present in the measuring environment. For example glucose oxidase readily detects 2-DG, but this molecule is not present in vivo. In addition, the possible interference by endogenous electroactive molecules is usually eliminated by appropriate screening layers la Nafion or PPD.
- The *response time* defines the temporal resolution of the biosensor. Fast response time is required to monitor biological events. It is especially useful for the real-time monitoring of neurotransmitters release and re-uptake that can occur within milliseconds. However, the kinetics of oxidase-based enzymatic reactions do not permit faster response times than 2-3 s (90, 119).
- The *stability* or *life time* of the biosensor in operating conditions and during the storage must also be optimized. The stability of biosensor signal must be ensured throughout the duration of the experiment. For this purpose, biosensor calibration prior and after experiment is indispensable. In our hands, experiments in which the biosensor lost more than 25% of its sensitivity must be regarded inconclusive and discarded. Longer storage life is favorable for optimal exploitation of enzyme, which could be expensive. Current microelectrode biosensors are stable during a typical in vivo experiment of up to 5 hours and can be stored safely at 4°C for a few days (90, 119).
- *Biocompatibility* of all biosensor components is necessary to avoid alterations in the functional properties of brain tissues and to avoid tissue reactions as inflammation, gliosis etc.
- In case of multisensing probe, “*cross-talk communication*” between adjacent electrodes must be minimized (see following section).

- Enzyme *immobilization* considerably influences biosensor characteristics and the immobilization process should fulfill the following demands:
  - provide reliable attachment of enzyme on the electrode surface
  - avoid toxic organic fixative agents in respect to biocompatibility
  - preserve enzyme activity and selectivity
  - preferably low-cost and fast

## 2.5 Implantable multisensing microprobes in Neuroscience

Glass-capillary enzymatic biosensors are largely used in neuroscience for detection of metabolites (glucose, lactate, glycerol) and neurotransmitters monitoring (choline, acetylcholine, glutamate, D-serine). However, neuroscientists have an interest in monitoring several biomolecules simultaneously. Although MEMS protocols and fabrication facilities first became available a long time ago, the fabrication of needle-like multisensing microprobes bearing multiple biosensors is still in its early stages of development. In 1990s pioneer publications reported on the fabrication of needle-like multielectrode probes of small dimensions, appropriate for *in vivo* implantation (100, 101, 126). Such probes, however, were designed to record neuronal electrical signals such as local field potentials, but not for biosensing.

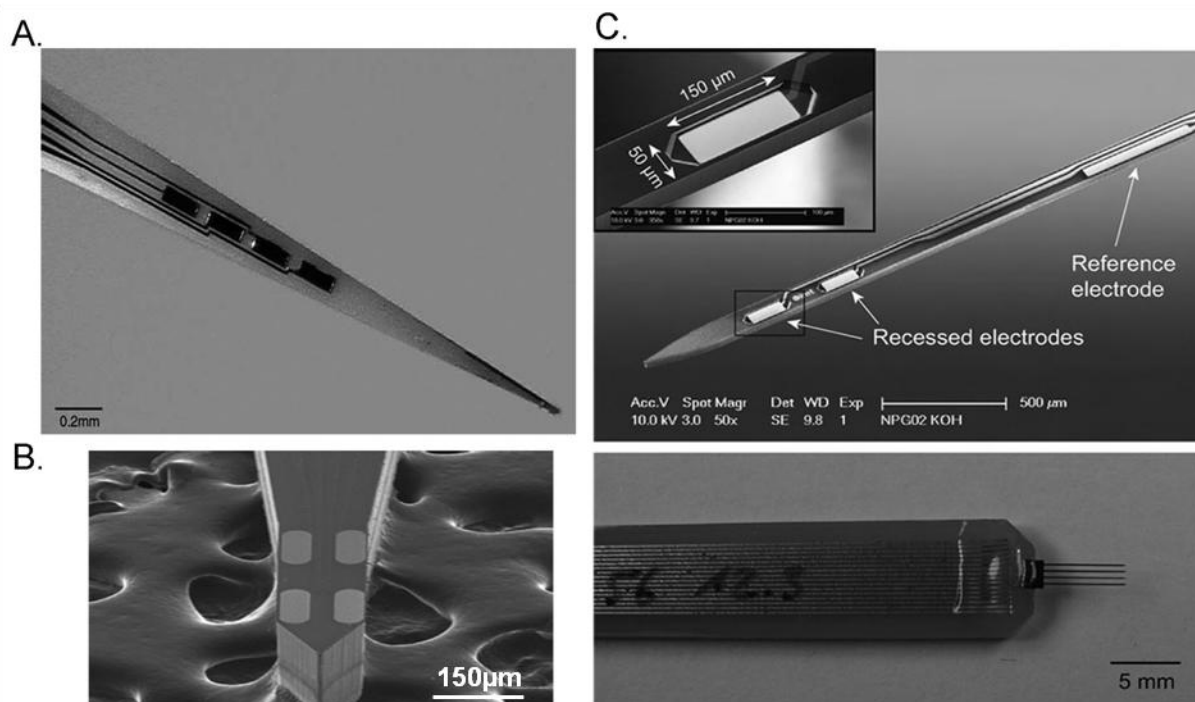


**Figure 1.14. Multisensing microprobes:** A. Microprobe on ceramic substrate with 4 patterned microelectrodes designed by G. Gerhard's group (127); B. Silicon wafer-based microelectrode array designed by N. Maidment's group (102); C. Silicon microprobe with two working and reference electrodes designed by M. Koudelka-Hep's group (62).

Gerhardt et al. were the first to develop needle-shaped microprobes with multiple electrodes modified by an enzyme, and apply them for *in vivo* studies (95, 123). One of their designs of multielectrode probe is presented in the Figure 1.14, A. The microarray is fabricated on ceramic substrate of 130µm thickness. Initial attempts were made to use

thinner, 25-50  $\mu\text{m}$  thick ceramic substrates. However, the resulting substrates were very fragile. The multiprobe (Fig. 1.14A) is composed of four 50x150  $\mu\text{m}^2$  Pt recording sites with Pt connecting lines and bonding pads. To improve the attachment of Pt (150nm) to ceramic an adhesion layer of titanium (50nm) was deposited previously on platinum. The recording sites are positioned 1 mm from the tip of the microprobe with 50 $\mu\text{m}$  spacing between sites. To insulate the conducting lines the microelectrode array was coated with polyimide except on the recording sites and contact pads (1-10 $\mu\text{m}$ ). The needle was cut out of the bulk ceramic wafer using a diamond saw (95, 96, 123, 127).

Maidment's group also proposed a distinct design of implantable microprobe (Fig. 1.14, B). They used 150  $\mu\text{m}$  thin silicon substrate with double-side thermally grown silicon dioxide to isolate the substrate from the electrodes. Platinum (100nm) was used to produce the working electrodes with chromium (20nm) for adhesion layer. Silicon dioxide (1 $\mu\text{m}$ ) was deposited by plasma enhanced chemical vapor to provide top isolation layer, where contact pads and electrode sites were opened by reactive ion etching (RIE). RIE was then used to etch through the top and bottom silicon dioxide layers to define needle contours and subsequent DRIE was performed to etch through the silicon substrate. This technological design gives probe shafts of 150 $\mu\text{m}$  thickness and 120 $\mu\text{m}$  wide. The electrode sites are oval in shape, with a width of 40 $\mu\text{m}$  and a length of 100 $\mu\text{m}$ , horizontally separated by 40 $\mu\text{m}$  and 100  $\mu\text{m}$  vertical separation (102).

A third group found to have successfully reported on implantable microprobes is lead by M.Koudelka-Hep. They manufactured a multisensing probe with two working electrodes and one reference electrode (Fig.1.14, C). The fabrication sequence starts with a 300 $\mu\text{m}$  silicon wafer. A recess of 10 $\mu\text{m}$  is firstly etched in silicon by KOH. Then, silicon oxide and silicon nitride (200nm/200nm) are deposited as bottom passivation. Metallization (20nm of Ta and 130nm of Pt) is patterned using a combination of thick photoresist to reliably cover the edges of the recesses. A second set of silicon nitride and silicon oxide layers (200/200nm) is used as top passivation and opened at the recording sites and contact pads by RIE. The microprobes are formed by a first thinning from the backside by DRIE toward the intended shaft thickness and a second DRIE etch from the front side to shape a needle contour resulting in 100 $\mu\text{m}$  width and 80 $\mu\text{m}$  thickness. Small joints retain the microprobes in the remaining wafer grid (62). To produce a reference electrode, first a silver layer of 4-5 $\mu\text{m}$  is galvanostatically grown on the Pt surface using a depositing bath, then, about 1  $\mu\text{m}$  of the surface is electrochemically transformed into AgCl.

Other similar designs can be found in the literature that are quite similar to the ones already described (100). After the different microtechnological fabrication steps, each single probe is attached to a printed circuit board. Bonding pads and bonding wires are encapsulated by inert polymer or epoxy glue to protect them mechanically and provide electrical isolation between the connections. Then, the Pt surface must be cleaned, to obtain optimal sensitivity toward  $\text{H}_2\text{O}_2$ . Typically, the microprobes are washed with acetone, ethanol and water, but chemically stronger mixtures can also be used, like hot phosphoric acid or Piranha mixture (1:4  $\text{H}_2\text{O}_2$ : $\text{H}_2\text{SO}_4$ ) depending on the materials that were used during fabrication. To pre-treat the Pt surface, cyclic voltammetry scanning is commonly used. The electrodes are placed in 1M  $\text{H}_2\text{SO}_4$  and the potential is scanned over a range of -1 to +1V at 100mV/sec till the signal remains stable.

A variety of enzyme deposition methods have been reported including drop-on (73, 90, 107, 111) and electropolymerization techniques (128-131), lift-off techniques and photolithography i.e. the use of photosensitive polymers carrying enzyme molecules for patterned polymerization (132, 133). However, most of these methods have considerable

limitations when applying to the multisensing probes with micrometric dimensions. The drop-on technique that consists in applying a droplet of enzyme solution onto each microelectrode site, which is the most common and simple method of enzyme deposition method, becomes difficult as droplets of a few picoliters are required to fill the small electrode cavities while avoiding cross-contamination of adjacent electrodes. Electrochemical deposition of an electropolymerizable matrix with enzyme entrapment usually leads to increased chemical cross-talk and, additionally, to poor sensitivity. The lift-off and photolithographic techniques requires covering the whole substrate by the enzyme solution prior to patterning, thus leading to significant waste of expensive enzyme material. In addition, UV-exposition is normally required for photosensitive layer structuring. This procedure, however, may provoke the formation of free radicals and damage the fragile enzyme structure leading to enzyme inactivation or loss of selectivity. Finally, covering the entire surface by an enzyme layer may lead to cross-contamination of neighboring electrodes or enzyme mixing during the multiple steps of the method.

A large choice of immobilization methods is currently available for enzyme attachment onto the electrode surface. However, only a few of them are used in glass capillary microbiosensors and even fewer in microprobe architecture. The most commonly used technique is immobilization by cross-linking with Glutaraldehyde. To our knowledge, it is the sole method used for fabrication of multisensing probes that have been subsequently validated *in vivo*. There are two possibilities of enzyme application: manual and electroassisted. In the manual method, a solution containing 1-2% of enzyme, 1-2% of BSA and 0.125% glutaraldehyde is prepared. A small drop of enzyme solution is then suspended at the tip of the microsyringe needle and it is used to coat the recording site manually under a stereomicroscope, and with the help of a micromanipulator. The recording sites have tiny dimensions and enzyme deposition even with microscope, microsyringe and micromanipulators is a challenging task. Thereby, the enzyme is often deposited onto two recording sites and neutral space between them. In their microprobe architecture, Frey et al. (62) have used an alternative method for surface functionalisation that consists in electrochemically aided adsorption (EAA) (134) of oxidase onto electrode surface and cross-linking with glutaraldehyde. The advantage of this procedure is that it is spatially controlled and allows highly parallel deposition on multiple sites of different enzymes at different locations on the same microprobe. The *in vitro* characterization of four simultaneously modified electrodes with choline or glutamate oxidases yielded biosensors with good reproducibility and sensitivity. Authors have also tested two parallel biosensors sensitive to choline and glutamate. Their method did not produce cross-contamination with unspecific adsorption during serial enzyme deposition, or cross-talk between two electrodes separated by 200µm. However, the authors only tested low substrate concentrations and their conclusions are valid only for these conditions. In the case of glucose or lactate that are abundant in the CNS, cross-influencing signals may be larger.

#### *Enzymatic cross-talk*

A cross-talk phenomenon appears on enzyme modified electrodes placed in close proximity, when their diffusion layers overlap. When hydrogen peroxide is produced and detected on one electrode, it can also diffuse to the neighboring electrodes (Fig.1.15). The degree of cross-talk depends on the distance between adjacent electrodes and the intensity of the cross-talk signal depends on the concentration of H<sub>2</sub>O<sub>2</sub> diffusing out of the enzyme layer to distant recording sites, which depends linearly on the concentration of enzyme substrate in the solution. Cross-talk is smaller in the presence low µM concentration of the

molecule of interest that produces a non-significant flux of  $\text{H}_2\text{O}_2$ . This is a case for glutamate, choline, D-serine monitoring under physiological conditions, but not for glucose or, lactate monitoring. This problem has been discussed in several studies, mainly in flow-type integrated sensor probes (108, 135-137).

As an example, let's imagine a multisensing microprobe in which a glutamate microelectrode lies adjacent to a glucose microelectrode. If the glucose concentration in the brain is  $500 \mu\text{M}$ , the enzyme present on the microelectrode will produce  $500 \mu\text{M}$  of  $\text{H}_2\text{O}_2$  at steady state. If the glucose biosensor response lies in its linear range with a sensitivity of  $10\text{pA}/\mu\text{M}$  of glucose, and half of the enzymatically produced  $\text{H}_2\text{O}_2$  diffuses out of the enzyme layer without reaching the electrode, it will detect about  $2500 \text{ pA}$  of current. On the other hand, if the glutamate biosensor is sensitive to glutamate at about  $10\text{pA}/\mu\text{M}$  with an extracellular glutamate concentration in the brain  $2\mu\text{M}$ , the detected signal will be about  $20\text{pA}$ . If 5 % of the  $\text{H}_2\text{O}_2$  leaking out of the glucose electrode reaches the glutamate electrode, the cross-talk current detected by glutamate biosensor will be  $125 \text{ pA}$  and final current at  $145 \text{ pA}$ , more than 7 times the true signal from glutamate. Therefore, in this configuration, a modest cross-talk of 5% can cause a considerable error in glutamate detection.

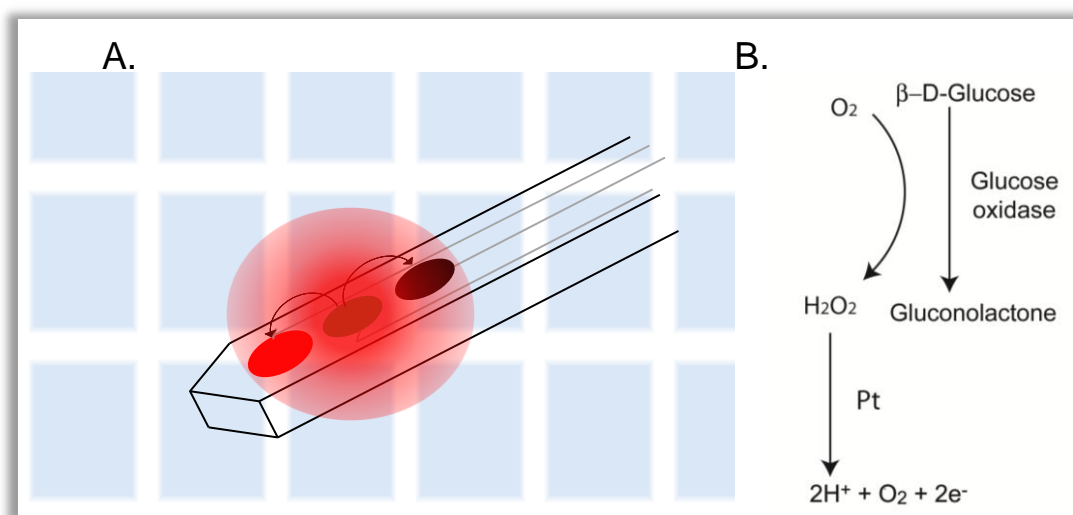


**Figure 1.15. Schema of cross-talk effect:** on the working electrode  $\text{Glucose oxidase}$  converts glucose into gluconolactone and hydrogen peroxide. Part of  $\text{H}_2\text{O}_2$  diffuses to the  $\text{Pt}$  surface, to be oxidized and gives rise to the oxidation current. The second part of  $\text{H}_2\text{O}_2$  diffuses to bulk solution and it may rich the surface of adjacent electrodes giving rise of the current on them, and thus causing cross-talk.

Yu et al. (138) provided evidence that cross-talk is a general phenomenon and is not necessarily related to enzyme biosensors. In a similar experiment configuration, two electrodes placed at a distance of  $10 \mu\text{m}$  were exposed to a  $\text{Fe}(\text{CN})_6^{4-}$  solution and  $-0.3 \text{ V}$  is applied for both electrodes (vs.  $\text{Ag}/\text{AgCl}$ ). After stabilization, the potential on the first electrode was switched to  $+0.3 \text{ V}$  while maintaining the negative potential on the second electrode. At  $+0.3 \text{ V}$  the  $\text{Fe}(\text{CN})_6^{4-}$  oxidized to  $\text{Fe}(\text{CN})_6^{3-}$  at one electrode, diffused to the bulk solution, and reached the second electrode to generate a reduction current at  $-0.3\text{V}$ . This current was evidence for cross-talk between the two electrodes, and the intensity of the cross-talk current was dependent on the distance between two electrodes.

Cross-talk effects on needle-type multisensing microelectrode design have also been described by Quinto et al. (135). They performed measurements on an array of four Pt microelectrodes 25µm wide and spaced 25µm apart. The glucose oxidase was deposited onto the first electrode by electroassisted coagulation and immobilization with glutaraldehyde. After substrate injection the oxidation current was registered on all electrodes. The response on the closest non-modified electrode at distance of 25µm ranged within 50-70% of that obtained at the modified one. The signal on the fourth electrode distant by 125µm from the first electrode was found to be about 25%. They evaluated the influence of non-specific enzyme adsorption on the electrode site. The array was produced in similar manner with the exception that no current was applied and thus there was no electroassisted precipitation on the first electrode. There was a remaining sensitivity to glucose of about 4-8% of that found when glucose oxidase electrodeposited, indicating non specific enzyme adsorption. The authors proposed three ways to eliminate cross-talk using catalase –a very active enzyme catalyzing decomposition of H<sub>2</sub>O<sub>2</sub> to water and oxygen. The first approach consisted in immersion of the device in catalase solution. However, authors did not succeed in obtaining a stable catalase layer, and cross-talk suppression was not satisfactory. The second method consisted in depositing a catalase layer over an enzyme-modified electrode to prevent H<sub>2</sub>O<sub>2</sub> diffusion into the bulk solution. This method decreased the cross-talk between adjacent electrodes, but it also dramatically decreased the sensitivity of the sensor to glucose. The third method consisted in depositing a catalase layer on the electrode adjacent to the enzyme-modified one. In this case, the sensitivity of the enzymatic electrode decreased by 25%, and no signal was observed on catalase modified electrode. Interestingly, the response on the third and fourth electrodes decreased by 93% and 80%. The final cross-talk on the third and fourth electrodes was about 3%. The idea of using catalase had already been described to decrease cross-talk in a flow-system for glucose and lactate analysis (139, 140). It is probably a promising method to cross-talk between enzyme electrodes. Finally, Suzuki et al. (137) studied the effects of enzymatic activity, membrane density and thickness on the degree of cross-talk between electrodes. They concluded that larger cross-talk was observed in dense and thick enzyme membranes with high activity, in which most of the H<sub>2</sub>O<sub>2</sub> is produced at the surface of the enzyme-immobilized membrane. These results suggest that cross-talk could be decreased in biosensors prepared with thinner enzyme layers.

#### *Multisensing array applications for in vivo studies*

Despite a great interest to microfabrication technologies and their wide application in construction of analytical microdevices potentially suitable for in vivo studies, examples of successful in vivo recordings using such devices are rather limited. Wassum et al. (102) demonstrated the ability of their silicon microelectrode array (MEA) glutamate biosensors to detect cortically-evoked glutamate release in the nucleus accumbens of anesthetized rats. They have also applied their biosensing probes to monitor extracellular glutamate in the basolateral amygdala (BLA) during a behavioral task involving seeking actions with sucrose (141).

Frey et al. (62) reported on the fabrication of a silicon microprobe array with integrated choline or glutamate biosensors, control sensor and reference electrode. To demonstrate the proper functioning of their device, the authors implanted this multisensor in the cortex of anesthetized rats for glutamate or acetylcholine detection. Acetylcholine release was then triggered pharmacologically. To demonstrate the ability of choline biosensor to



monitor endogenous choline concentrations two experiments with chemical stimulations were performed. Firstly, KCl-induced acetylcholine release was measured by detection of choline (because acetylcholine is degraded to choline by acetylcholinesterase within a few ms). In a second set of experiments, acetylcholine release was evoked by nicotine administration. When neostigmine was infused previously to nicotine no current increase could be detected on the choline biosensor indicating specific choline detection (Neostigmine is an inhibitor of acetylcholinesterase). These experiments demonstrate the feasibility of developed microdevice for *in vivo* biomolecules monitoring.

In addition, ceramic-based multielectrode microprobes have been validated by Gerhardt's group. Their devices are also used in configuration of one biosensor and one control electrode. However, Burmeister et al. (142) reported on a microprobe for simultaneous detection of choline and acetylcholine. In this work they adapted the self-referencing method for acetylcholine detection, in which the electrode modified with acetylcholinesterase and choline oxidase corresponded to working electrode and the electrode modified with choline oxidase only was the "control" electrode. The experiments with KCl-stimulated acetylcholine release *in vivo* were performed to validate the dual biosensor array. Ceramic-based glutamate biosensor with control-BSA electrode were largely used in studies aimed at quantifying basal physiological glutamate concentration and its variations under chemical stimulations, blockage of neuronal activity (using the voltage-activated Na<sup>+</sup> channel blocker tetrodotoxin) or inhibition of glutamate reuptake (with TBOA) in freely-moving or anesthetized rodents (28, 107, 127). This biosensor configuration was also used to measure tonic and phasic glutamate neurotransmission in the putamen of unanesthetized non-human primates (143). In this work the authors evaluated the influence of the sterilization procedure on biosensor sensitivity and concluded that it was acceptably stable. Validation in primate is an important step toward MEA clinical applications. It demonstrates that multielectrode microarrays can be used as a supplemental diagnostic to provide neurosurgeons with a real-time measurement of extracellular glutamate, which is markedly elevated in epileptogenic brain regions and during epileptic seizures. Such measurements may provide important indicators of the clinical course following brain injury. In addition, detection glucose, lactate, O<sub>2</sub> and other possible biomarkers may be an important diagnostic tool for detection neurological deterioration in patients suffering from subarachnoid hemorrhage.

Enzymatic microelectrode biosensors are still a field in development. However, they have already found important applications for *in vivo* neurological studies in laboratory animals. They are a promising alternative to microdialysis. However, important improvements are still required for biosensor application in clinical practice. It is important to increase the mechanical strength of the biosensors to avoid breakage upon implantation in the patient's brain; preventing biofouling of the enzyme layer and decreasing tissue reaction at the implantation site are also important fields of development to increase the long-term signal stability of the biosensors in the living brain; developing sterilization procedures compatible with preserved enzyme activity will also determine their application in clinical practice. However, the number of molecules that it is possible to detect by biosensors is limited by the choice of available enzymes. In this respect, many important bioactive molecules in the brain can only be detected by microdialysis coupled to HPLC or CE-LIF. Consequently, microsensors and microdialysis techniques remain complementary for neurochemical analysis of the brain.

### III. Experimental strategy

When I arrived in the host laboratory, my thesis project was aimed at developing silicon-based microfabricated multifunctional biosensors for simultaneous detection of several molecules (glucose, lactate, glutamate, D-serine) in animal models of brain diseases. When the thesis project started, the team was already studying glutamate release in brain slices and cell cultures using biosensors with Glutamate oxidase immobilized by glutaraldehyde. Cell culture media are usually made of salts (calcium, sodium, magnesium, potassium, phosphate, etc.), amino acids and glucose. In particular, the usual Dulbecco/Vogt modified Eagle's minimal essential medium (DMEM) contains about 4 mM of L-glutamine. To our surprise, the glutamate oxidase-based biosensors estimated glutamate levels in these culture media to be around 500  $\mu$ M, which was incompatible with cell survival and was contradicted by measurements based on capillary electrophoresis. The biosensors were then characterized for the selectivity to all proteinogenic amino acids and a large decrease in enzyme substrate specificity was detected. This puzzling finding motivated us to study the effect of enzyme immobilization on enzyme specificity and biosensor performance in general and prompted us to develop a new immobilization method that would preserve the enzyme kinetic parameters.

The experimental strategy is summarized in following steps:

1. Development of simple, robust and chemically mild immobilization method with enhanced biocompatible properties and preserving natural enzyme specificity (chemical protocol optimization; biosensors *in vitro* characterization; *in vivo* validation).

2. Comparative study of five enzyme immobilization methods used in biosensor construction for neurochemical studies: optimization of chemical protocols; comparative study of biosensor performances (response time, sensitivity, enzymatic kinetics, stability).

3. The study of immobilization effect on enzyme substrate-specificity and on glutamate detection *in vivo*: evaluation of enzyme activity toward the secondary substrates; estimation of glucose and glutamate concentration in biological samples using biosensors and HPLC or CE; *in vivo* glutamate detection.

4. Development of multisensing microprobes for simultaneous monitoring of glucose, lactate and nonspecific current variations in the CNS of the anesthetized rat: development of MEMS-fabrication protocol; enzyme local deposition and immobilization; the cross-talk evaluation; *in vitro* and *in vivo* validation.



# Chapter 2:

## **Covalent enzyme immobilization by poly(ethylene glycol) diglycidyl ether (PEGDE) for microelectrode biosensors preparation**

This chapter describes a new method of enzyme immobilization that provides a simple, low cost and non-toxic alternative for the preparation of in vivo microelectrode biosensors. The chapter reproduces the original paper published on May 2011 in the International journal Biosensors and Bioelectronics:

Vasylieva, N., Barnych, B., Meiller, A., Maucler, C., Pollegioni, L., Lin, J. S., Barbier, D., and Marinesco, S. (2011) Covalent enzyme immobilization by poly(ethylene glycol) diglycidyl ether (PEGDE) for microelectrode biosensor preparation, Biosens Bioelectron 26, 3993-4000.



## COVALENT ENZYME IMMOBILIZATION BY POLY(ETHYLENE GLYCOL) DIGLYCIDYL ETHER (PEGDE) FOR MICROELECTRODE BIOSENSOR PREPARATION

*Natalia VASYLIEVA<sup>1,2</sup>, Bogdan BARNYCH<sup>3</sup>, Anne MEILLER<sup>4</sup>, Caroline MAUCLER<sup>1</sup>, Loredano POLLEGIONI<sup>5</sup>, Jian-Sheng LIN<sup>1</sup>, Daniel BARBIER<sup>2</sup> and Stéphane MARINESCO<sup>1,4</sup>*

<sup>1</sup>INSERM U1028, CNRS UMR5292, Lyon Neuroscience Research Center, Integrated Physiology of the Waking State, Lyon, F-69000, France, Université Claude Bernard Lyon I, 69373 Lyon Cedex 08, FRANCE.

<sup>2</sup>Institut de nanotechnologie de Lyon, CNRS UMR-5270, INSA de Lyon, FRANCE.

<sup>3</sup>Institut de Chimie et Biochimie Moléculaires et Supramoléculaires (ICBMS), UMR 5246 CNRS, Université Lyon 1, 69622 Villeurbanne Cedex, FRANCE.

<sup>4</sup>Plate-forme technologique Neurochem, Université Claude-Bernard-Lyon I, 69373 Lyon Cedex 08, FRANCE.

<sup>5</sup>The Protein Factory, Centro Interuniversitario di Biotecnologie Proteiche, Politecnico di Milano and Università degli Studi dell'Insubria, Varese, ITALY.

\* corresponding author: Stéphane Marinesco, INSERM U1028, CNRS UMR5292, Centre de Recherche en Neurosciences de Lyon, Faculté de médecine, 8 avenue Rockefeller, 69373 Lyon Cedex 08, France. Tel : +33 (0)4 78777041, Fax : +33 (0)4 78777150, Email : [stephane.marinesco@univ-lyon1.fr](mailto:stephane.marinesco@univ-lyon1.fr)

## ABSTRACT

Poly(ethylene glycol) diglycidyl ether (PEGDE) is widely used as an additive for cross-linking polymers bearing amine, hydroxyl, or carboxyl groups. However, the idea of using PEGDE alone for immobilizing proteins on biosensors has never been thoroughly explored. We report the successful fabrication of microelectrode biosensors based on glucose oxidase, D-amino acid oxidase, and glutamate oxidase immobilized using PEGDE. We found that biosensors made with PEGDE exhibited high sensitivity and a response time on the order of seconds, which is sufficient for observing biological processes *in vivo*. The enzymatic activity on these biosensors was highly stable over several months when they were stored at 4 °C, and over at least 3 d at 37 °C. Glucose microelectrode biosensors implanted in the central nervous system of anesthetized rats reliably monitored changes in brain glucose levels induced by sequential administration of insulin and glucose. PEGDE provides a simple, low cost, non-toxic alternative for the preparation of *in vivo* microelectrode biosensors.

Keywords: amperometry, enzymatic electrode, glucose, D-serine, glutamate, *in vivo* monitoring.

## 1. Introduction

Implantable enzymatic biosensors are widely used for *in vivo* monitoring applications (144, 145). For instance, they have been used in neuroscience research to detect neurotransmitters and metabolites with outstanding temporal resolution. Enzymatic biosensors are typically constructed according to a common basic design in which an enzymatic layer is immobilized on a platinum (Pt) electrode. A variety of immobilization techniques are currently available. Enzyme cross-linking using glutaraldehyde, which is probably the oldest method, remains a reference procedure for simple, stable, and reproducible covalent enzyme immobilization (146), (95), (88). Enzyme entrapment in a poly-o-phenylenediamine (PPD) layer has been reported (147), but the resultant material is generally less stable and less sensitive than that produced with glutaraldehyde fixation. Enzymes have also been immobilized in sol-gels (148) and polypyrrole matrices (149). However, both of these methods involve toxic components that limit their potential use in clinical applications.

One elegant procedure involves binding enzyme molecules to a redox hydrogel composed of water soluble poly(1-vinylimidazole) (150) or poly(4-vinylpyridine) (120, 151) and  $[\text{Os}(\text{bpy})_2\text{Cl}]^+$ . Several enzymes, including glucose oxidase and glutamate oxidase, have been immobilized successfully using this technique (152), (153). Additionally, glucose biosensors based on this or similar principles have been approved for glucose monitoring in diabetic patients ((55); (154)). However, the components of such redox hydrogels are expensive and the process requires several synthetic steps. Thus, there is a need for the development of simple, clean, and low-cost enzyme immobilization methods that can be easily reproduced in non-expert laboratories.

In this study, we investigated the potentially interesting process of enzyme immobilization using poly(ethylene glycol) diglycidyl ether (PEGDE) for biosensor preparation. PEGDE is an essential component of redox hydrogels used for glucose biosensors and is widely used in commercial devices such as the implantable Freestyle Navigator system (Abbott laboratories, review in (55)). However, its ability to immobilize enzymes on its own has never been thoroughly characterized. Recently, Zigah et al. ((155)) successfully immobilized glucose oxidase on an amino-modified silicon substrate using PEGDE, suggesting that biosensor fabrication using PEGDE alone is indeed possible. Here, we examined the feasibility of immobilizing several enzymes, including glucose oxidase, D-amino acid oxidase, and glutamate oxidase, on Pt microelectrodes using PEGDE alone. The *in vitro* and *in vivo* stability, sensitivity, and response time of biosensors produced using this method were measured and compared to respective reference values obtained for biosensors prepared using glutaraldehyde fixation.

## 2. Materials and Methods

### 2.1. Enzyme preparation

Glucose oxidase (EC 1.4.3.11) from *Aspergillus niger* was purchased in powder form from Sigma-Aldrich (100–250 U/mg, Saint Quentin Fallavier, France). The final enzyme solution used for biosensor preparation contained 60 mg/mL glucose oxidase, 30 mg/mL bovine



serum albumin (BSA, Sigma), and 1% glycerol in phosphate buffered saline solution (PBS 0.01 M, pH 7.4).

Recombinant *R. gracilis* D-amino acid oxidase (RgDAAO, EC 1.4.3.3.) was overexpressed in *E. coli* and purified as reported by Molla et al. ((156)). The final solution contained 58 mg/mL of the protein, 25 mg/mL BSA, and 1% glycerol in PBS (0.01 M, pH 7.4).

L-Glutamate oxidase (EC 1.4.3.11) from *Streptomyces sp. X119-6* was purchased from Yamasa Corporation (Choshi, Chiba, Japan). The working solution contained 57 mg/mL of the protein, 81 mg/mL BSA, and 1% glycerol in PBS (0.01 M, pH 7.4). Poly(ethylene glycol) diglycidyl ether, average MW 526 (Sigma-Aldrich) was added to the enzyme aliquot prior to biosensor preparation.

## 2.2. Microelectrode biosensor preparation

Biosensors were constructed using a 25  $\mu\text{m}$  diameter 90% Pt/10% Ir wire (Goodfellow, Huntington, U.K.) glued to a copper wire using conductive silver paint (Radiospares, Beauvais, France). The sensor wire was inserted into a pulled glass capillary (Harvard Apparatus, Edenbridge, U.K.), and the tip of the pipette was cut so the Pt wire extended from the glass approximately 100  $\mu\text{m}$ . The junction between the Pt and the pipette tip was sealed by locally melting the glass. The junction between the copper wire and the glass was sealed with epoxy resin (Araldite, Bostik, Paris, France). The electrodes were washed for 30 min in ethanol. For *in vivo* experiments, a poly-m-phenylenediamine screening layer was deposited by electropolymerization for 20 min in 100 mM m-phenylenediamine (Sigma-Aldrich) solution in 0.01 M PBS at pH 7.4 under a constant potential of +700 mV versus a Ag/AgCl reference electrode. The enzyme layer was deposited by dipping the Pt tip of the electrode in the enzyme solution. Control sensors were treated using a bovine serum albumin solution consisting of 400 mg/mL BSA, 10 mg/mL PEGDE, and 1% glycerol in 0.01 M PBS, pH 7.4. The electrodes were placed in an oven at 55 °C for 2 h, then stored at 4 °C for short-term storage and at -20 °C for long-term storage. In a few experiments, the enzyme was immobilized by exposure to saturated glutaraldehyde vapors for 2.5 to 3 min, as reported by Pernot et al. ((90)).

Before the experiments all sensors were tested for detection of serotonin (5-HT, 20  $\mu\text{M}$  in PBS), enzyme substrate (glucose, D-serine, or glutamate, 1  $\mu\text{M}$  in PBS), and  $\text{H}_2\text{O}_2$  (1  $\mu\text{M}$  in PBS). Only those electrodes with an effective PPD screening layer and exhibiting less than 1.2  $\mu\text{A}\cdot\text{mM}^{-1}\text{cm}^{-2}$  response for 5-HT were included in the study.

Glucose microelectrode biosensors for *in vivo* experiments were covered with an additional polyurethane membrane to increase their dynamic range and to protect the enzyme layer from biofouling in the brain. The tip of the electrode was dipped four times in a 5% solution of polyurethane in THF (Sigma) with 10 min intervals between dips at room temperature to dry the layer. After this treatment, the glucose biosensors displayed a linear relationship between oxidation current and glucose concentration up to 3 mM.

## 2.3. Recordings

All recordings were obtained using a VA-10 electrochemistry amplifier (NPI Electronics, Tamm, Germany) equipped with a two-electrode potentiostat. Data acquisition was performed using a 16-bit USB-6221 acquisition board (National Instruments, Nanterre, France) controlled by homemade software based on Igor Pro 6.4 procedures (Wavemetrics, Eugene, OR). The oxidation current was recorded at 1 kHz and averaged over 1000 data points, yielding a final sampling frequency of 1 Hz (except for response time analyses, in

which the signal was averaged over 100 data points, or 10 Hz).

*In vitro* calibrations were performed in standard PBS (0.01 M, pH 7.4) solutions. The reference electrode was a chloride-treated silver wire (Ag/AgCl) placed directly in the recording chamber. Recordings were obtained using constant potential amperometry at +500 mV versus the Ag/AgCl reference electrode, which was determined by cyclic voltamperometry to be the optimal for H<sub>2</sub>O<sub>2</sub>, as product of enzymatic reaction, oxidation. For *in vivo* studies, the biosensors were calibrated before and after the experiments to ensure the sensitivity remained stable.

#### 2.4. *In vivo* experiments

All experiments were performed under isoflurane anesthesia, and the animals were treated according to European regulations. The experimental procedure was validated by the local committee on animals in research of Université Claude Bernard Lyon I. Adult, male Wistar rats weighing 300–500 g were placed in a stereotaxic apparatus (Stoelting, Dublin, Ireland). Their body temperature was maintained at 37 °C using a homeothermic blanket (Leticia, Barcelona, Spain). A glucose microbiosensor was implanted in the frontal cortex (1.5 mm ventral to the dura) adjacent to a control biosensor covered with BSA. Recordings were started at least 1 h after implantation to ensure stabilization of the baseline electrochemical currents. Insulin (25 U/kg of body weight) was injected after an additional 30 min period of control recording, and 1 h later an injection of glucose (3 g/kg of body weight) was administered.

To achieve selective detection *in vivo*, all microelectrodes were coated with a layer of PPD and polyurethane. The PPD polymer creates a screening layer that prevents oxidation of endogenous molecules present in the brain such as serotonin, dopamine, ascorbate, and cysteine ((90)) (Figure S 2.5). The sensors were also prepared using an additional layer of polyurethane (see above). Glucose biosensors were implanted in combination with a control biosensor (BSA-PEGDE) on the contralateral side of the brain to control for nonspecific variations in oxidation current. Quantitative assessments of brain glucose concentrations were obtained by subtracting the non-specific current of the control biosensor from the output of the glucose biosensor.

#### 2.5. Statistics

Data are presented as means ± standard deviations (SDs), except for data from *in vivo* measurements, where means ± standard errors of the mean are reported. Comparisons between two data groups were performed using the Student's *t*-test for equal, unequal, or paired variances as indicated by the F-test for equal variance (significance level,  $p < 0.05$ ). The analyses were performed using the analysis tool-pack of Excel (Microsoft Office 2007) and SPSS 12.0 for Windows. The sample size ( $n$ ) was equal to the number of biosensors constructed under the same protocol, or the number of animals used in the *in vivo* experiments (where a new biosensor was used in every experiment).

### 3. Results

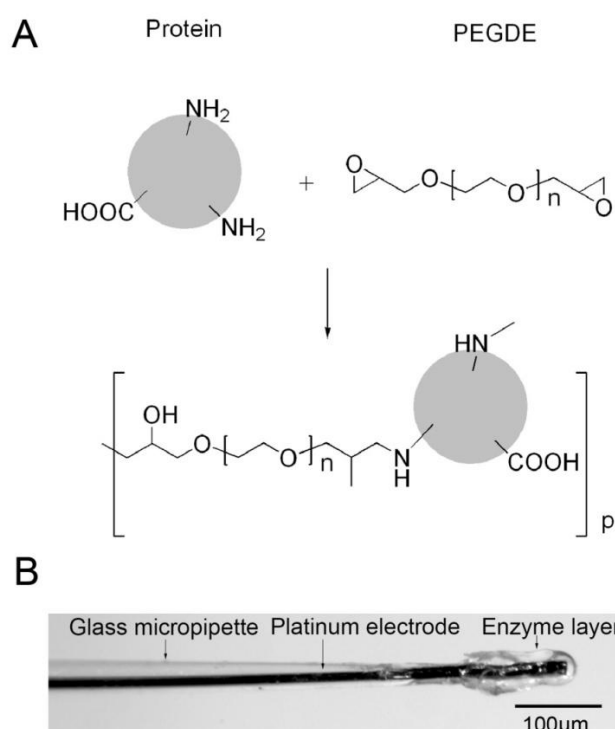
#### 3.1. Principles of enzyme immobilization on electrodes

PEGDE contains two epoxy groups that can react with amino, hydroxyl, and carboxyl groups. Reaction with the amine functional groups present in proteins creates an enzymatic matrix on

the electrode surface (scheme 2.1A). The reaction between the diepoxide and proteins is slow at room temperature (~48 h), but can be accelerated considerably by increasing the temperature ((151)). In the case of enzymatic biosensor preparation, the reaction is limited to conditions that preserve enzymatic activity. We therefore set the temperature at 55 °C, which is low enough to preserve the activity of all oxidase enzymes we tested. At this temperature, a 2-h incubation of the enzyme/PEGDE mixture was sufficient to achieve immobilization in a stable membrane. Therefore, this incubation time was used throughout the study.

### 3.2. Optimization of PEGDE concentration

We first tested the PEGDE enzyme immobilization process by preparing glucose oxidase-based biosensors. We studied the dependence of biosensor sensitivity on the amount of PEGDE added to the enzyme (Fig. 2.1), and normalized the response using the ratio of glucose sensitivity (pA/μM) to H<sub>2</sub>O<sub>2</sub> sensitivity (pA/μM) to eliminate variability in the electrode surface and H<sub>2</sub>O<sub>2</sub> sensitivity. The PEGDE concentration in the enzyme solution was varied from 4 to 100 mg/mL while the glucose oxidase concentration was fixed at 60 mg/mL, BSA at 30 mg/mL, and glycerol at 1% in 0.01 M PBS (pH = 7.4). This solution was viscous enough to be deposited on the microelectrode surface and then fixed for 2 h at 55 °C. The sensitivity of the biosensors followed a bell-shaped curve. At the minimum PEGDE concentration of 4 mg/mL, only 36.4% (n = 11) of the biosensors exhibited stable enzyme immobilization and the sensitivity ratio was low (0.18 ± 0.04). The biosensor sensitivity increased at higher concentrations, reaching a maximum of 0.37 ± 0.05 at 20 mg/mL. At concentrations of 100 mg/mL or greater, the biosensors displayed a very low sensitivity ratio (≈0.01). At these high PEGDE concentrations, the enzymatic membrane was stably immobilized on the electrode surface but the glucose activity was quite low, probably due to enzyme deactivation from excessive cross-linking. At the optimal PEGDE concentration of 20 mg/mL, enzyme immobilization was reproducible with a coefficient of variation of approximately 12% in the sensitivity ratio between microelectrodes.



**Scheme 2.1.** A. General reaction scheme of protein with poly(ethylene glycol) diglycidyl ether. All protein molecules (enzyme, bovine serum albumin, etc.) contain amino- and carboxyl groups that may react with the 2 epoxides of PEGDE, resulting in immobilization. B. Photomicrograph of glucose biosensor tip.

Similar experiments were performed with other enzymes, including D-amino acid oxidase (DAAO) and glutamate oxidase, which also exhibited a bell-shaped dependence of biosensor sensitivity on PEGDE concentration (data not shown). The optimal PEGDE concentrations for DAAO and glutamate oxidase were 5.9 mg/mL and 78 mg/mL, respectively.

The enzyme membrane appeared as a transparent light-yellow film (Scheme 2.1B). The membrane was insoluble in water, but swelled slightly with increasing water content.

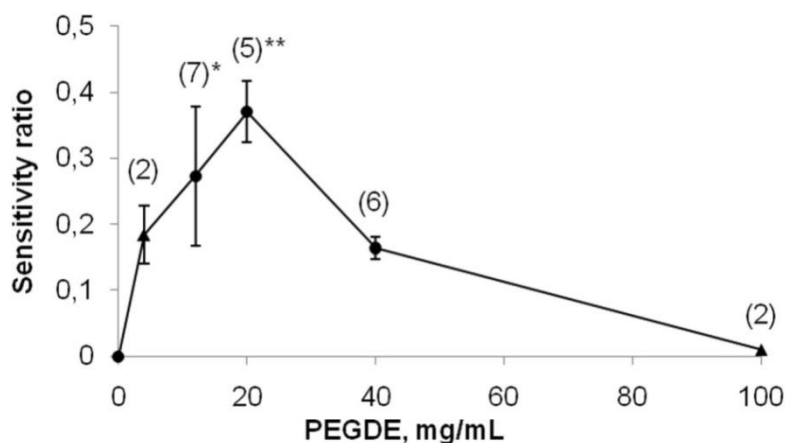


**Figure 2.1:** Dependence of glucose biosensor sensitivity ratio (ratio of glucose sensitivity (pA/ $\mu$ M) to  $H_2O_2$  sensitivity (pA/ $\mu$ M)) on PEGDE concentration in the enzyme solution. PEGDE concentration is expressed in mg/mL of 0.01 M PBS containing glucose oxidase (60 mg/mL), BSA (30 mg/mL), and glycerol (1%). The relationship between biosensor sensitivity and PEGDE concentration was a bell-shaped curve with a maximum near 20 mg/mL. Concentrations of 4 and 100 mg/mL resulted in unreliable biosensors with unstable enzyme immobilization ( $\blacktriangleright$ ). \*\* Significant difference from all other concentrations, \* significant difference from 40 mg/mL. The numbers of biosensors constructed using each protocol are presented above the data points.

### 3.3 Characteristics of glucose biosensors

To further characterize the performance of the glucose biosensors, we determined their response time, linear range, and apparent Michaelis-Menten constant ( $K_m^{App}$ ). For response time analysis, the biosensors were transferred rapidly between PBS and a 20  $\mu$ M glucose solution, generating a step increase in the amperometric signal. The response time, defined as the time required to reach 90% of the plateau response, was equal to  $3.1 \pm 1.2$  s ( $n = 12$ , Fig. 2.2A).

We then constructed a calibration plot for glucose concentrations in the range of 0–1 mM. A linear dependence of oxidation current on glucose concentration was observed up to 400  $\mu$ M, with a sensitivity of  $12.3 \pm 3.8$  pA/ $\mu$ M ( $n = 35$ ). The electrical noise level was approximately 4 fA (RMS), yielding a theoretical *in vitro* detection limit of  $\sim 1$  nM ( $3\times$  noise).

The apparent Michaelis-Menten constant  $K_m^{App}$  was estimated by fitting the calibration curve between 0 and 1 mM to the following equation:

$$I(C) = \frac{(I_{max} * C)}{(K_m^{App} + C)}$$

in which  $I(C)$  is the oxidation current as a function of glucose concentration ( $C$ ) and  $I_{\max}$  is the maximum oxidation current recorded by the biosensor.  $I_{\max}$  was equal to  $12.8 \pm 6.6$  nA and  $K_m^{\text{App}}$  was  $1.4 \pm 0.3$  mM ( $n = 6$ ). The  $K_m^{\text{App}}$  of the biosensor was substantially lower than the  $K_m$  of the free enzyme, ranging between 26 mM ((157); (158)) and 30 mM ((159); (160)). This effect, which has been described previously ((161); (90)), could be a result of substrate and product pre-concentration in the membrane layer.

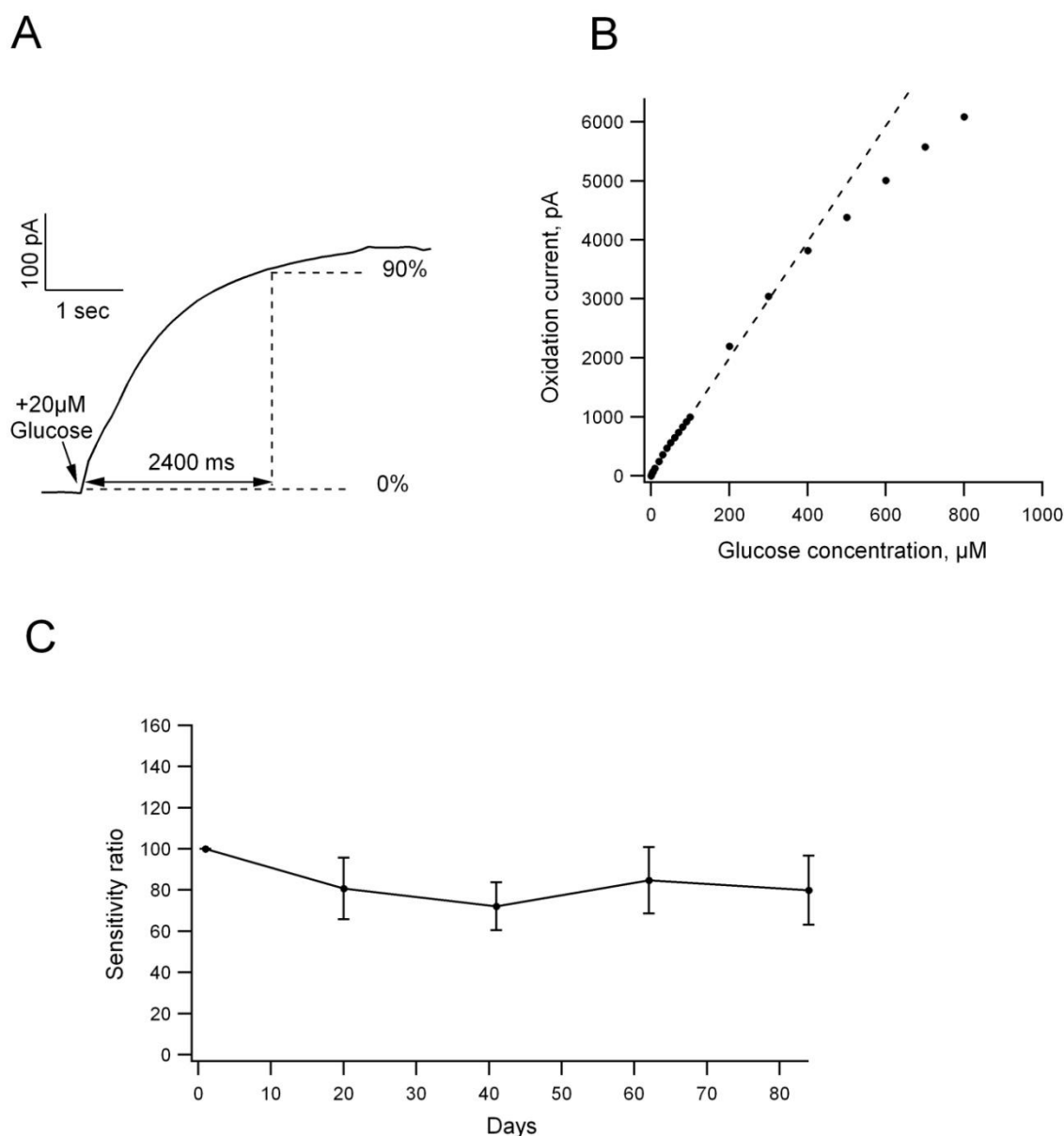


**Figure 2.2. Glucose biosensors:** (A) Response of biosensor to changes in glucose concentration (0–20 μM). Biosensor response time was calculated as the time between 0 and 90% of the current step. (B) Calibration curve between 0 and 1 mM for computing Michaelis-Menten kinetic parameters. The linear range was 0–400 μM.  $I(\text{pA}) = 9.80 * C(\mu\text{M}) + 42.08$ ,  $R = 0.998$ . (C) Long-term storage stability of glucose microbiosensors at 4 °C ( $n = 6$ ).

Finally, we assessed the stability of our biosensors in both operating (i.e. exposed to glucose) and storage conditions. Glucose biosensors could be used repeatedly for *in vitro* and *in vivo* experiments lasting 4–5 h (see section 3.6). We also tested their stability following a 3-d immersion in PBS at 37 °C. When glucose oxidase was immobilized directly on Pt microelectrodes, the sensitivity of the biosensors decreased by 40% after 2 d ( $n = 5$ ),

indicating poor stability of the enzyme layer. However, when the Pt surface was covered with an electropolymerized PPD layer, the enzyme was much more stable. This effect could have been the result of more efficient enzyme cross-linking as the PEGDE reacted with amino groups present on the PPD layer and improvements in enzyme grafting on the microelectrode surface. With this additional PPD layer, the sensitivity of the biosensors actually increased by  $23 \pm 17\%$  after 3 d at  $37\text{ }^{\circ}\text{C}$  ( $n = 3$ ). This slight increase could be the result of a reorganization of the PPD structure that increased  $\text{H}_2\text{O}_2$  permeability over time.

Long term stability during dry storage at  $4\text{ }^{\circ}\text{C}$  over 3 mos. was also determined using biosensors containing an additional PPD layer. To determine the biosensor sensitivity 4 calibration concentrations were tested for each electrode. The sensitivity of the biosensors decreased slightly after the first 20 d, but remained stable for the next 2 mos. (Fig. 2.2C). Overall, the enzyme layer was stable over time when immobilization was performed on PPD.

### 3.4 D-serine and glutamate biosensors

The same kinetic parameters reported for glucose biosensors above were also determined for D-serine (DAAO) and glutamate (glutamate oxidase) biosensors. The response times for serine biosensors ( $n = 6$ ) and glutamate biosensors ( $n = 4$ ) were found to be  $3.7 \pm 0.9\text{ s}$  and  $3.6 \pm 0.5\text{ s}$ , respectively (Fig. 2.3A, C). For the D-serine biosensors, the linear range was  $0\text{--}200\text{ }\mu\text{M}$ , with a sensitivity of  $15.3 \pm 4.0\text{ pA}/\mu\text{M}$  ( $n = 19$ ) and an *in vitro* detection limit of approximately  $0.8\text{ nM}$ . The Michaelis-Menten parameters  $I_{\text{max}}$  and  $K_m^{\text{App}}$  were  $19.2 \pm 5.5\text{ nA}$  and  $1.3 \pm 0.4\text{ mM}$  ( $n = 4$ , Fig. 2.3B). For the glutamate biosensors, the linear range was  $0\text{--}100\text{ }\mu\text{M}$ , with a sensitivity of  $14.4 \pm 5.2\text{ pA}/\mu\text{M}$  ( $n = 12$ ) and an *in vitro* detection limit of approximately  $0.8\text{ nM}$ .  $I_{\text{max}}$  and  $K_m^{\text{App}}$  were  $10.2 \pm 1.3\text{ nA}$  and  $0.79 \pm 0.17\text{ mM}$  ( $n = 4$ , Fig. 2.3D). The apparent Michaelis-Menten constant of the D-serine biosensor was significantly lower than the  $K_m$  of the free enzyme in solution ( $13.75\text{ mM}$ , (162)), an effect that was presumably related to the immobilization procedure itself as reported previously ((163)). On the contrary, the glutamate biosensors had a higher  $K_m^{\text{App}}$  than the free enzyme ( $0.2\text{ mM}$  Yamasa Corporation, Choshi, Chiba, Japan). It should be noted, however, that  $K_m^{\text{App}}$  values reported for glutamate biosensors are highly dependent on the immobilization method, ranging from  $3\text{ mM}$  (redox hydrogel immobilization, (164)) and  $2.8\text{ mM}$  (immobilization in Nafion®, (165)), to  $0.78\text{ mM}$  (immobilization in a sol-gel layer, (148)). Thus, the  $K_m^{\text{App}}$  of glutamate oxidase immobilized with PEGDE observed in our experiment is within the range of values obtained with other methods.

The DAAO biosensors were used repeatedly in *in vivo* experiments lasting 4 to 5 h without losing activity (data not shown). The glutamate biosensors were stored in dry conditions at  $4\text{ }^{\circ}\text{C}$  for at least 1 wk without losing enzymatic activity. Overall, these results indicate that enzyme immobilization with PEGDE yields stable, reproducible and sensitive biosensors for at least three different oxidase enzymes.

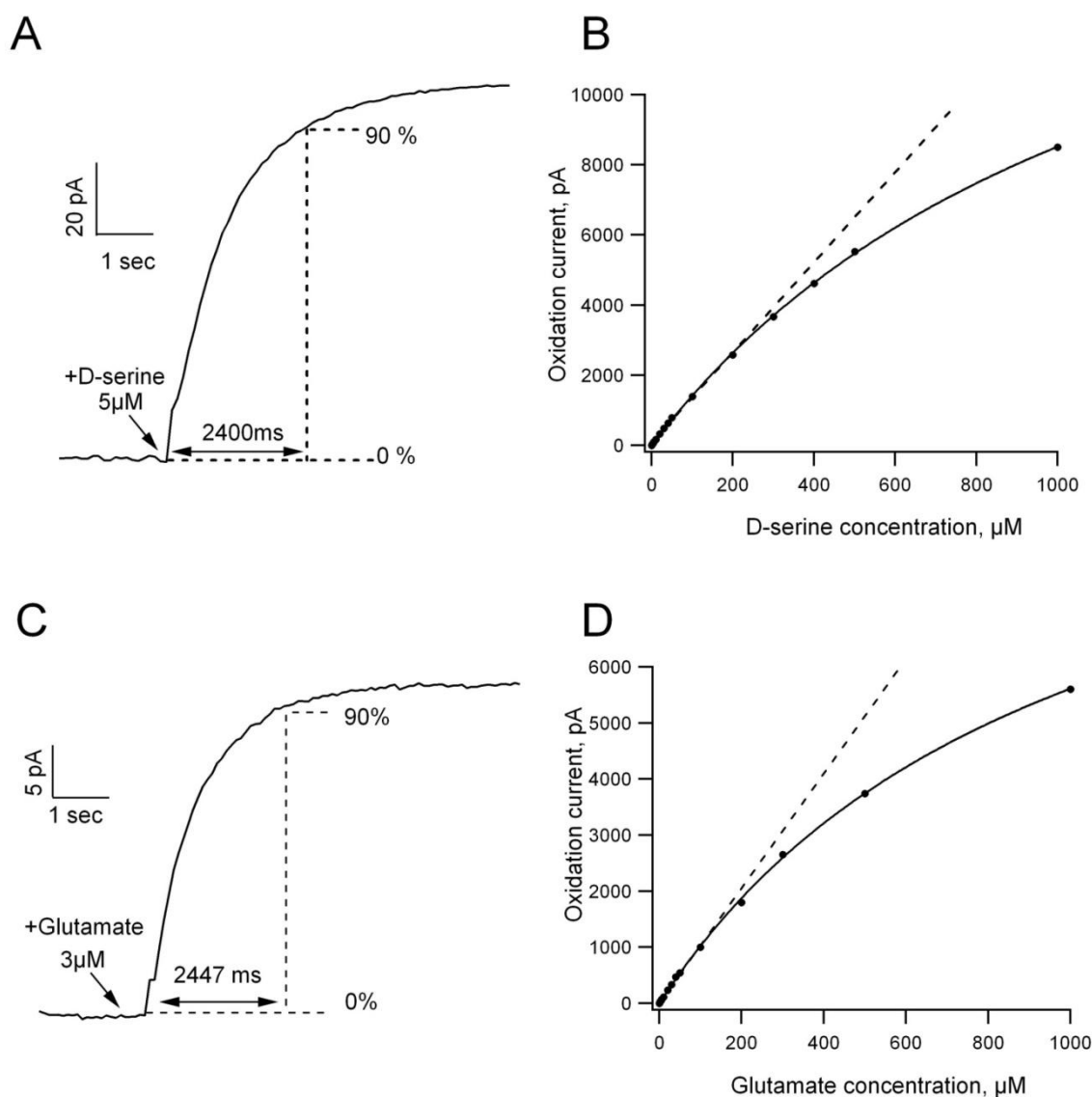


**Figure 2.3.:** D-Serine biosensors (top) and glutamate biosensors (bottom). (A), (C) Response of biosensor to changes in D-serine (0–5 μM) and glutamate (0–3 μM) concentration and response time estimation (see Fig. 2.2). (B), (D) Calibration curve for 0–1 mM D-serine and 0–1 mM glutamate for the computation of Michaelis-Menten kinetic parameters. Linear regression equation for D-serine biosensor:  $I(\text{pA}) = 13.0 * C(\mu\text{M}) + 48.7$ ,  $R = 0.998$ . Linear regression equation for glutamate biosensors:  $I(\text{pA}) = 10.2 * C(\mu\text{M}) + 16.2$ ,  $R = 0.998$ .

### 3.5. Comparison with glutaraldehyde fixation

We systematically compared the characteristics of our biosensors with those obtained after fixation with glutaraldehyde, one of the most widely used fixative reagents for enzymatic biosensor fabrication (Table 2.1). The response times of the PEGDE biosensors were similar to those obtained using glutaraldehyde (except for glutamate oxidase, for which PEGDE yielded a higher value). The  $K_m^{\text{App}}$  values were generally similar between the two methods (except for DAAO, for which PEGDE yielded a lower value). The PEGDE biosensor sensitivities were generally higher than those observed with glutaraldehyde fixation, except for the glutamate sensor, for which the sensitivity was similar. The kinetic behavior of the biosensors is summarized in Table 2.1A.

### 3.6 *In vivo* validation

We tested the utility of the PEGDE biosensors in applications requiring *in vivo* brain implantation. In initial experiments, we implanted glucose biosensors in the frontal cortex of anesthetized rats. Basal brain glucose concentrations were  $0.68 \pm 0.15$  mM ( $n = 8$ ), which is consistent with findings from other studies of *in vivo* brain glucose monitoring with biosensors ((111); (166)). Injection of insulin (25 U/kg body weight intraperitoneally) induced a steady decrease in oxidation current from the glucose microbiosensor, but not from the control electrode. Injection of glucose (3 g/kg) 1 h after insulin administration quickly raised the brain glucose signal above its original value (Fig. 2.4A). The extracellular brain glucose concentration 1 h after insulin injection was  $0.19 \pm 0.05$  mM, and the concentration rose to  $1.1 \pm 0.2$  mM after glucose injection (Fig. 4B). Calibration experiments performed after electrode removal from the brain revealed that our biosensors were still functional after *in vivo* implantation, with some even displaying a slight increase in sensitivity (Fig. 2.4C, Table 2.1B, probable explanation section 3.3). The effects of insulin and subsequent glucose administration are well documented ((111)). The fact that we could detect them with our glucose oxidase/PEGDE biosensors therefore indicates that our method is well suited for *in vivo* brain glucose monitoring.

In a second set of experiments, we compared the *in vivo* performance of PEGDE-immobilized D-serine biosensors to that of glutaraldehyde-based electrodes. We implanted PEGDE or glutaraldehyde-immobilized D-serine biosensors in the frontal cortex of anesthetized rats, the D-serine baseline current was found to be  $0.34 \pm 0.08$   $\mu\text{A}\cdot\text{cm}^{-2}$  for PEGDE based sensors and  $0.31 \pm 0.06$   $\mu\text{A}\cdot\text{cm}^{-2}$  for glutaraldehyde-fixed sensors. The corresponding baseline D-serine concentration was approximately 2–2.5  $\mu\text{M}$  based on the two methods.

A stable PPD layer is essential to maintaining the selectivity of the electrochemical recordings throughout the experiments. We assessed the PPD stability in two independent sets of experiments, using serotonin as a typical example of an oxidizable neurotransmitter present *in vivo* whose detection must be avoided for selective enzymatic measurements. Following storage of the biosensors in PBS at 37 °C for 3 d, a 20- $\mu\text{M}$  concentration of serotonin was undetectable using freshly prepared biosensors and was detected at only  $0.2 \pm 0.3$   $\mu\text{A}\cdot\text{mM}^{-1}\text{cm}^{-2}$  after 3 d ( $n = 3$ ) when the sensors were fabricated using PEGDE, compared to  $1.8 \pm 0.9$   $\mu\text{A}\cdot\text{mM}^{-1}\text{cm}^{-2}$  when glutaraldehyde fixation was used ( $n = 4$ , Table 2.1B). The same comparison was performed after a 5-h implantation *in vivo*, revealing that PPD retained better performance as a screening layer with PEGDE fixation than with glutaraldehyde (Table 2.1B). For *in vivo* experiments, a sensitivity to serotonin of less than  $1.2$   $\mu\text{A}\cdot\text{mM}^{-1}\text{cm}^{-2}$  (i.e. <1% of the glucose, D-serine, or glutamate signal) is required both before and after implantation to ensure optimum selectivity. Therefore, more than half of the biosensors prepared with glutaraldehyde fixation did not fulfill this criterion at the end of a 5 h *in vivo* experiment. In this regard, the increased PPD stability observed in PEGDE-immobilized sensors is a useful property for *in vivo* applications. Overall, these experiments demonstrate that biosensors prepared using PEGDE immobilized enzymes are fully functional *in vivo*, and display better performance for recording *in vivo* signals than those prepared with glutaraldehyde fixation.



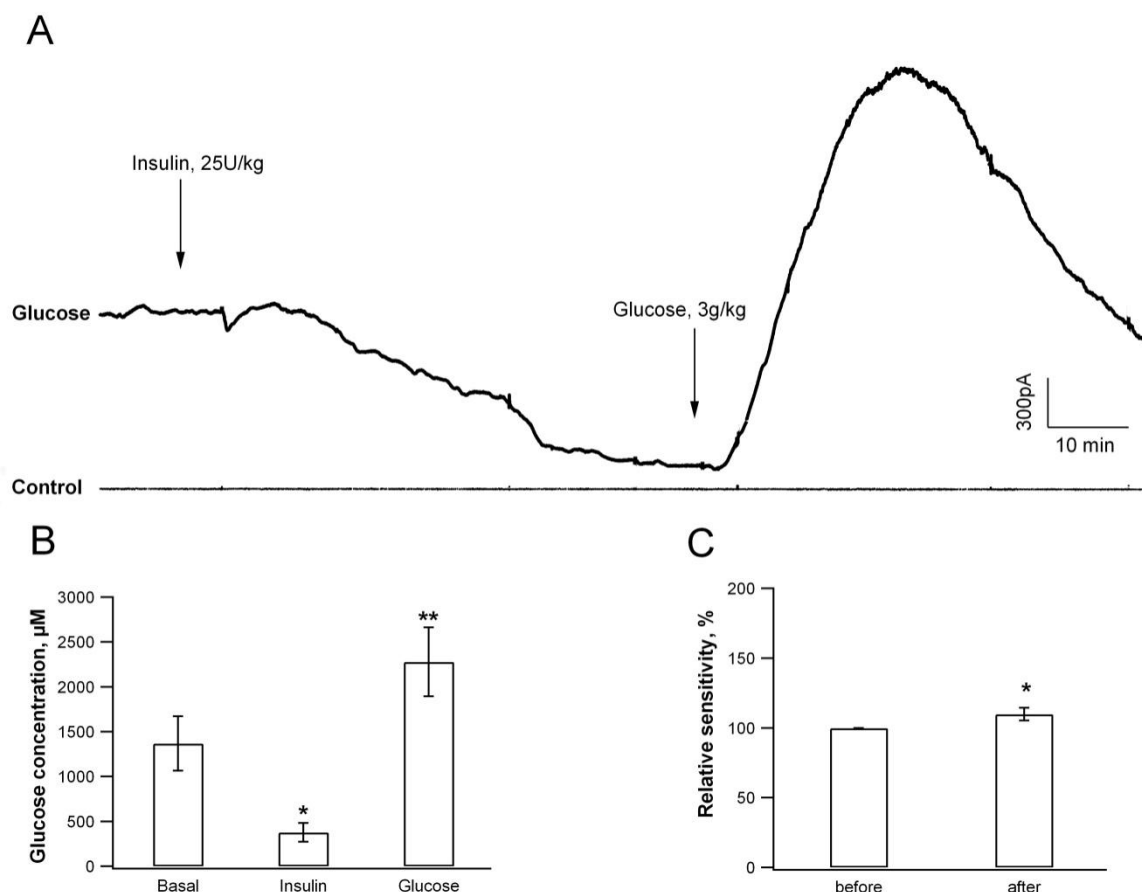


**Figure 2.4.** Examples of biosensor recordings *in vivo*. (A) Glucose monitoring using a PEGDE/glucose oxidase biosensor implanted in the frontal cortex of an anesthetized rat. Brain glucose levels decreased following an intraperitoneal injection of insulin (25 U/kg body weight) and then increased following a subsequent glucose injection (3 g/kg body weight). For quantitative estimation of *in vivo* glucose concentrations, the signal detected by a glucose microbiosensor (bold line) was compared to that recorded by a control (BSA) biosensor implanted on the contralateral side of the brain (thin line). (B) Glucose concentrations estimated before and 1 h after insulin administration and at the peak of the rebound in glucose concentration. (C) Sensitivity to glucose before and after implantation revealing the stability of the biosensors *in vivo* (n = 6).

#### 4. Discussion

In the present study, a matrix based on covalent binding between enzymes, BSA, and PEGDE was employed for biosensor preparation. PEGDE preserved enzymatic activity and yielded biosensors with similar or better sensitivity and response time than biosensors produced with glutaraldehyde fixation, a classical method for enzyme immobilization on biosensors. When microelectrode biosensors fabricated using PEGDE were implanted in the brain of anesthetized rats, they produced reliable *in vivo* measurements for at least 4–5 h. The method was validated for three different enzymes: glucose oxidase, D-amino acid oxidase, and glutamate oxidase. These experimental results demonstrate that PEGDE may be used to fabricate stable, fast-responding, and sensitive biosensors designed for *in vivo* implantation.

PEGDE is an essential component of redox hydrogels used for biosensors to monitor

blood glucose levels in diabetic patients ((120, 151); (150); (55)). In those hydrogels, PEGDE is used as a cross-linking agent to bind enzymes to complexes of water soluble poly(1-vinylimidazole) and  $[\text{Os}(\text{bpy})_2\text{Cl}]^+$ , thereby producing efficient electron diffusion between the enzymatic redox centers and the electrode ((150)). This principle has also been applied successfully to microelectrode biosensors designed for brain implantation ((152); (153)). Our study demonstrates that reliable biosensors may be obtained using PEGDE alone. In this case, enzymatic activity is monitored through the oxidation of  $\text{H}_2\text{O}_2$  on the Pt surface. For *in vivo* applications, an additional PPD screening layer designed to avoid the detection of endogenous oxidizable molecules such as ascorbic acid, uric acid, dopamine, and serotonin is deposited on the Pt electrode ((73); (167)). PEGDE therefore provides a simple, minimal setup for enzyme immobilization on electrode surfaces without the need for preliminary synthetic steps. Interestingly, omitting the redox mediator in the hydrogel yielded response times that were approximately 10 times faster than those obtained using  $[\text{Os}(\text{bpy})_2\text{Cl}]^+$  ((168)), which can be an important advantage for *in vivo* detection of neurotransmitters such as glutamate.

In conclusion, the present experiments showed PEGDE to be a feasible option for covalent enzyme immobilization in biosensor preparation. Several methods currently in use, such as glutaraldehyde fixation ((95); (88)) and enzyme entrapment in a sol-gel ((148)) or functionalized polypyrrole matrix ((149)), require the use of toxic components that exclude potentially important clinical applications. Thus it is noteworthy that PEGDE offers a clean, non-toxic alternative to these methods. Together with its low cost and ease of use, these advantageous properties should make PEGDE a promising method for future biosensor applications.

### Acknowledgements

This study was supported by Inserm U628 and Université Claude Bernard Lyon I, and by grants from Agence Nationale pour la Recherche (ANR-09-BLAN-0063 Neurosense) and Institut Fédératif des Neurosciences de Lyon (Projet structurant IFNL 2008). NV, BB, and CM are recipients of PhD fellowships from Ministère de la Recherche. LP thanks the financial support of Regione Lombardia “Accordi per la Cooperazione Internazionale – Progetto Istantensor: 15764, Rif. SAL-35”. Estelle Enriquez provided valuable technical assistance in electrode preparation and validation. We are grateful to Alexander Kuhn, Florence Lagarde and Eric Codner for helpful discussions on an earlier version of the manuscript.

Table 2.1. Comparison of biosensor characteristics with proteins immobilized by glutaraldehyde versus PEGDE.

**A. Kinetic parameters**

	Glucose oxidase		D-aminoacid oxidase		Glutamate oxidase	
	PEGDE	Glutaraldehyde	PEGDE	Glutaraldehyde	PEGDE	Glutaraldehyde
sensitivity, $\mu\text{A.mM}^{-1}\text{cm}^{-2}$	$147 \pm 45$ (n = 35)*	$106 \pm 29$ (n = 10)	$212 \pm 119$ (n = 19)*	$87 \pm 27$ (n = 18)	$173 \pm 63$ (n = 12)	$178 \pm 99$ (n = 44)
response time, s	$3.1 \pm 1.2$ (n = 12)	$2.4 \pm 0.8$ (n = 6)	$3.7 \pm 0.9$ (n = 6)	$3.2 \pm 0.5$ (n = 4)	$3.6 \pm 0.5$ (n = 4)	$2.1 \pm 1$ (n = 6)*
$K_M^{app}$ , mM	$1.4 \pm 0.3$ (n = 6)	$1.1 \pm 0.2$ (n = 6)	$1.3 \pm 0.4$ (n = 4)*	$3.6 \pm 0.4$ (n = 4)	$0.79 \pm 0.17$ (n = 4)	$0.93 \pm 0.48$ (n = 4)

**B. PPD layer stability**

	<i>In vivo</i> condition**		<i>In vitro</i> 37 °C	
	PEGDE	Glutaraldehyde	PEGDE	Glutaraldehyde
Sensitivity to serotonin ( $\mu\text{A.mM}^{-1}\text{cm}^{-2}$ )				
Before	$0.3 \pm 0.2$ (n = 13)	$0.1 \pm 0.1$ (n = 9)	0	0
After	$0.9 \pm 0.8$ (n = 13)	$1.5 \pm 2.0$ (n = 9)*	$0.2 \pm 0.3$ (n = 3)	$1.8 \pm 0.9$ (n = 4)*

\* significant difference

\*\* criterion for *in vivo* experiments is serotonin  $<1.2 \mu\text{A.mM}^{-1}\text{cm}^{-2}$

### Supporting information

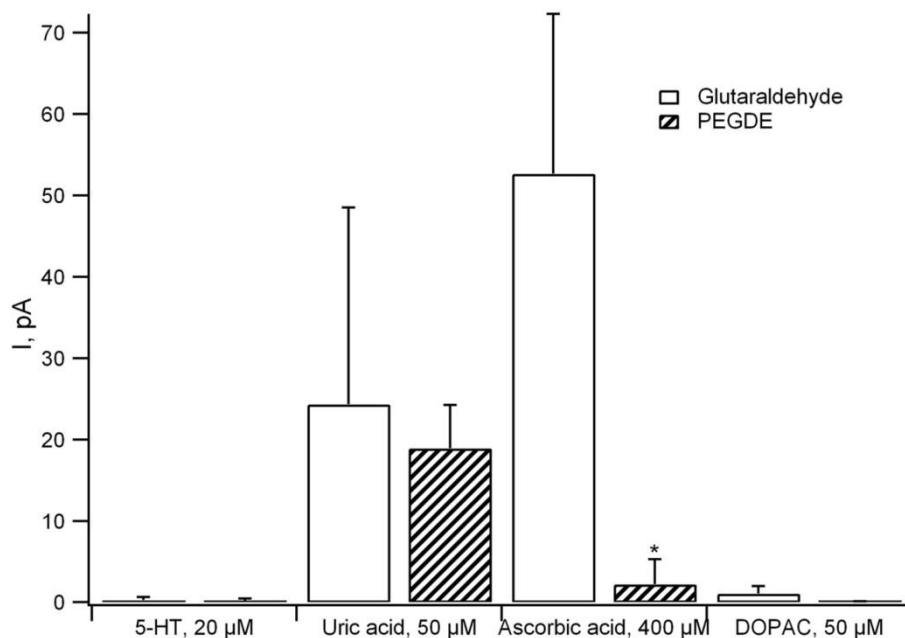


**Figure S2.5:** Biosensor sensitivity towards the endogenous electroactive molecules in physiological concentrations. The glutaraldehyde-based biosensors are more sensible to interfering molecules than PEGDE-based ones.



# Chapter 3:

## Comparative study of immobilization methods for biosensor construction

This chapter reviews the most widely used enzyme immobilization methods for implantable microbiosensor construction. The advantages and constraints of these methods are discussed and relative experimental protocols are described. Operational parameters of Glucose biosensors constructed using glutaraldehyde, PEGDE, sol-gel, hydrogel and derived polypyrrole matrix are compared in terms of sensitivity, response time, linear range, apparent Michaelis-Menten constant, and stability.

This chapter will appear as a book section in MICROELECTRODE BIOSENSORS (*Humana Press*, S. Marinesco and N. Dale Ed).



## ENZYME IMMOBILIZATION ON MICROELECTRODE BIOSENSORS

*Natalia Vasylieva<sup>1,2</sup> and Stéphane Marinesco<sup>1,3</sup>*

<sup>1</sup>INSERM U1028, CNRS UMR5292, Lyon Neuroscience Research Center, Integrated Physiology of the Waking State, Lyon, F-69000, France, Université Claude Bernard Lyon I, 69373 Lyon Cedex 08, FRANCE.

<sup>2</sup>Institut de nanotechnologie de Lyon, CNRS UMR-5270, INSA de Lyon, France.

<sup>3</sup>Plate-forme technologique Neurochem, Université Claude-Bernard-Lyon I, 69373 Lyon Cedex 08, FRANCE.

\* Corresponding author: Natalia Vasylieva, INSERM U1028, CNRS UMR5292, Centre de Recherche en Neurosciences de Lyon, Faculté de médecine, 8 avenue Rockefeller, 69373 Lyon Cedex 08, France.

Tel: +33 (0)4 78777041, Fax: +33 (0)4 78777150,

Email: natalia.vasylieva@insa-lyon.fr



## ABSTRACT

Protein immobilization is a key step in biosensor preparation that impacts on the overall performance. Among the wide variety of immobilization techniques currently available, only a few have been reliably applied *in vivo*. In this chapter, we discuss five different enzyme immobilization procedures, namely covalent immobilization by cross-linking using glutaraldehyde, poly(ethyleneglycol) diglycidyl ether (PEGDE), or a hydrogel matrix and enzyme entrapment in a sol-gel or polypyrrole-derived matrices. We describe in detail experimental protocols for each method as applied to glucose oxidase and glutamate oxidase-based biosensors. Enzymatic microelectrodes prepared using these five different procedures were then compared in terms of sensitivity, response time, linear range, apparent Michaelis-Menten constant, and stability. An optimal method would ideally be non-toxic, simple and cheap and display high sensitivity, a large linear range, and relatively fast response time. Although there is no current consensus on an ideal immobilization method, PEGDE and sol-gel techniques are potentially promising procedures for *in vivo* laboratory studies.

KEYWORDS: enzyme electrode, Glucose, Glutamate, immobilization techniques.

## 1. Introduction

Enzymatic biosensors are now widely used for monitoring concentrations of molecules *in vivo* (144). For instance, they have been used in medical practice to monitor glycemia in diabetic patients (55), (154). They are also used in animals to detect neurotransmitters or metabolites with excellent temporal resolution in the central nervous system (145).

Such biosensors usually rely on the same basic design of an enzymatic layer immobilized on a platinum electrode. In fact, enzyme immobilization on the electrode surface is a critical step in assembling amperometric biosensors. The immobilized enzyme should be stable over time, especially *in vivo* at 37°C, and retain significant activity to provide optimal sensitivity. Enzyme immobilization can also impact the final operating parameters of the biosensor, such as response time, linear range, or selectivity. Finally, in the context of *in vivo* implantation, the biocompatibility and overall toxicity of the biosensor can be affected by the presence of chemicals used during immobilization.

A wide variety of immobilization techniques are now available. They can be divided into three major groups: cross-linking (146), (95), (88), (134), (62), entrapment in polymer matrices (147), (148), (149), (109), and adsorption through physical or electrostatic interactions, e.g. the Langmuir-Blodgett film technique (169), (170). For biological applications, cross-linking and enzyme entrapment are the most widely used methods, because of their reliability and stability. Adsorption techniques often result in less stable immobilization and have not been validated *in vivo* to our knowledge.

In this chapter, we describe the influence of the immobilization method used for biosensor construction on its final operating parameters. We have chosen several methods that have been previously used in neuroscience research, namely cross-linking by glutaraldehyde or PEGDE, chemical binding to a polymer with or without redox centers, and entrapment in a sol-gel or in an electrochemically generated polypyrrole-derived matrix. Based on data from the literature and on our own experience, we compare these methods in terms of simplicity, ease-of-use, toxicity, and overall final biosensor performance.

## 2. Immobilization methods and protocols

### 2.1 Cross-linking

Cross-linking is the process of covalently binding two or more molecules. Proteins are natural polymers with a variety of functional groups and can be readily bound together by many cross-linking agents. This property has been widely applied to biosensor fabrication, in which stable binding of proteins to the electrode surface is required. The two main chemical functions in a protein that can react with a cross-linker are the amine (-NH<sub>2</sub>) and carboxyl (-COOH) groups. All proteins possess at least one amino group at their N-terminal end and one on every lysine residue. Similarly, carboxyl groups are present at the C-terminal end and on glutamic acid and aspartic acid residues. Because they are charged at physiological pH, amino and carboxyl groups tend to be exposed on the outer surface of the protein, which makes them primary candidates for reacting with a cross-linking agent.

When choosing an appropriate cross-linker, an important parameter is the length of

the spacer arm, i.e. the distance between the reactive groups. This length will determine, in part, the flexibility of the protein matrix and the degrees of freedom that the proteins retain once immobilized. The cross-linker that has been used for the longest time for biosensor preparation is glutaraldehyde and this is still the reference. In our laboratory, we are now using poly(ethylene glycol) diglycidyl ether (PEGDE) with very positive results.

### 2.1.1 Glutaraldehyde

Glutaraldehyde (pentane-1,5-dial) is a small molecule (MW 100) bearing two aldehyde groups that can react with proteins (Fig. 3.1). Each free aldehyde group reacts with a different protein molecule, thus creating a ramified network (Fig. 3.1). Unbound aldehyde groups usually oxidize over time under normal storage conditions.

This method requires minimal equipment and the reaction can be accomplished in a few minutes. Its simplicity has made it the reference method. It should be noted that glutaraldehyde is very toxic and should be manipulated with caution (fume hood, gloves, and goggles). Thus, even though glutaraldehyde is still widely used in scientific groups worldwide (143), (62), (171), its possible clinical applications are limited.

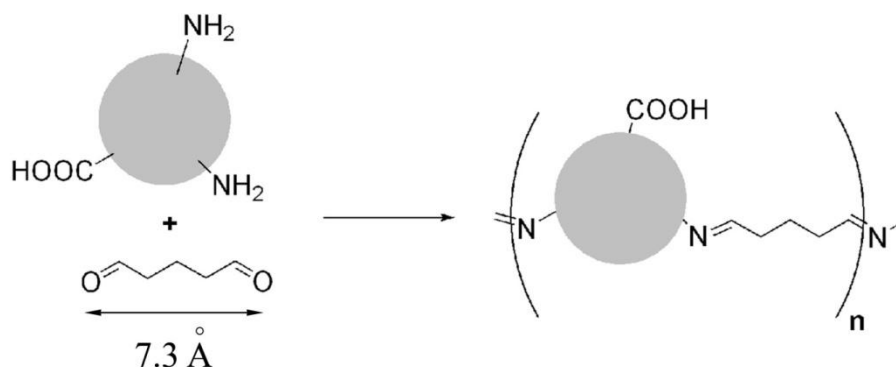


**Figure 3.1: Glutaraldehyde method.** Reaction scheme for protein cross-linking by glutaraldehyde. Aldehyde groups react preferentially with amino groups present within the protein to produce covalent bonds between proteins.

Glutaraldehyde cross-linking can be performed in at least two ways, by adding glutaraldehyde to the enzyme mixture or by exposing the enzyme to saturated vapor. Below, we present different procedures for immobilizing glucose oxidase and glutamate oxidase on a biosensor using glutaraldehyde. Unless specified otherwise, the glucose oxidase (EC 1.4.3.11) used was from *Aspergillus niger* and was purchased from Sigma-Aldrich (100-250 U/mg, Saint Quentin Fallavier, France), while the L-glutamate oxidase (EC 1.4.3.11) used was from *Streptomyces sp.X119-6* and was purchased from Yamasa Corporation (Choshi, Chiba, Japan, also distributed by Seikagaku Inc. and Associated of Cape Cod Inc.).

#### Fixation in saturated vapor

*To prepare a glucose biosensor, the working solution contains 60 mg/mL of glucose oxidase, 30 mg/mL of bovine serum albumin (BSA, Sigma), and 1% glycerol in 0.01 M phosphate-buffered saline (PBS), pH 7.4, while that for a glutamate biosensor contains 125*

mg/mL of the enzyme, 60 mg/mL of BSA, and 1% glycerol in 0.01 M PBS, pH 7.4. The enzyme layer is deposited on the electrode surface by dipping the electrode in the enzyme solution. As the solution evaporates, it becomes thicker and an enzyme layer is deposited on the electrode. At this stage, however, the enzyme would quickly dissolve if the electrode was dipped into an aqueous solution. For immobilization, 5 mL of 25% glutaraldehyde (Sigma-Aldrich) is placed at the bottom of a closed dish. After approximately 2 min, the chamber is filled with near-saturating glutaraldehyde vapor, then the electrodes with their enzyme layer are placed in the vapor for about 3 min. The biosensors are then thoroughly washed and kept at 4°C for short-term storage and at -20°C for long-term storage (90)).

#### Fixation in liquid phase

Enzyme immobilization using glutaraldehyde in solution has been thoroughly described by Greg A. Gerhardt's group ((172)) and is described in detail in Chapter 1.2. For glutamate biosensors, glutamate oxidase (~0.2 mg) is dissolved in 10  $\mu$ L of a solution containing 2% BSA and 0.13% glutaraldehyde, then one drop (~0.5  $\mu$ L) of this mixture is deposited onto one of the microelectrode sites on a silicon microprobe and allowed to dry. The microprobe is stored at -5 °C before use and in 0.1 M PBS between measurements.

#### 2.1.2 PEGDE matrix

Another bifunctional molecule used for enzyme binding is PEGDE, a non-toxic chemical reagent that contains two epoxy groups able to react with amino-, hydroxyl-, and carboxyl groups. Under mild conditions of temperature, PEGDE reacts preferentially with amine functions present in proteins and creates a matrix for enzyme immobilization on the electrode surface very similar to those obtained using glutaraldehyde (Fig. 3.2). However, in contrast to glutaraldehyde, the kinetics of the reaction between proteins and epoxy groups at room temperature is rather slow (about 48 hours), but can be considerably accelerated by a temperature increase (151). In the specific case of enzymatic biosensor preparation, this reaction must occur under conditions that preserve enzymatic activity. PEGDE is a non-toxic, barely irritant molecule and can be used by non-qualified staff.

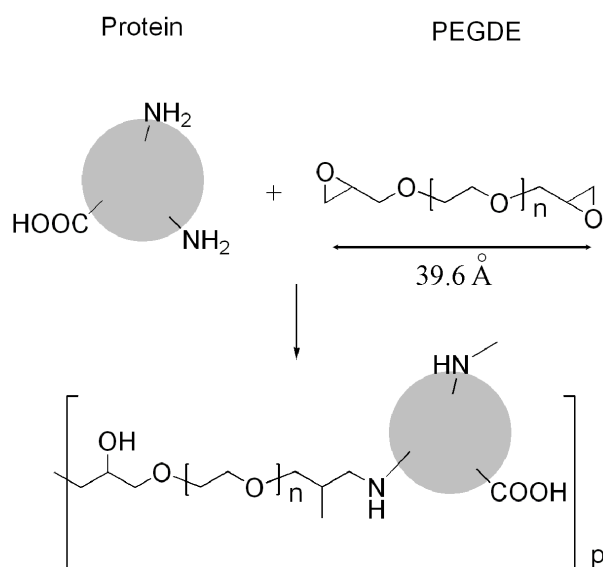


**Figure 3.2: Poly(ethylene glycol) diglycidyl ether (PEGDE) method.** General reaction scheme of a protein with PEGDE. Amino-groups present within proteins can react with the two epoxy rings of the PEGDE molecule, resulting in covalent immobilization.

This method is very sensitive to heating conditions. If the curing temperature is too low, reliable enzyme immobilization does not occur, whereas too high a temperature can cause enzyme denaturation or inactivation. The amount of PEGDE added to the enzyme solution is also critical, as low amounts of PEGDE do not result in stable immobilization, whereas excess PEGDE leads to enzyme inactivation and low biosensor sensitivity. We now present two examples of the preparation of glucose and glutamate biosensors (173).

#### *Enzyme immobilization*

*To prepare a glucose biosensor, the working solution contains 60 mg/mL of glucose oxidase, 30 mg/mL of BSA (Sigma), 1% glycerol, and 20 mg/mL of PEGDE (average MW 526, Sigma-Aldrich) in 0.01 M PBS, pH 7.4, while, for the glutamate biosensor, the working solution contains 57 mg/mL of L-glutamate oxidase, 80 mg/mL of BSA, 1% glycerol, and 80 mg/mL of PEGDE in 0.01 M PBS, pH 7.4. To prepare control microbiosensors, the oxidase is replaced by BSA (Sigma) and the working solution consists of 400 mg/mL BSA, 10 mg/mL of PEGDE, and 1% glycerol in 0.01 M PBS, pH 7.4. In all cases, the solution containing all components except PEGDE is stored as frozen aliquots and the PEGDE is added just before biosensor preparation. Like for glutaraldehyde fixation, the enzyme layer is deposited by dipping the electrode in a thick enzyme solution, which results in a membrane that is still unstable and soluble in water. Immobilization occurs when the electrode is placed in a 55°C oven for 2 h. Biosensors are then kept at 4°C for short-term storage and at -20°C for long-term storage.*

For the two oxidases, the enzymatic membrane has a transparent light yellow appearance, is insoluble in water, and swells as it increased its water content.

### **2.1.3 Redox hydrogel**

Redox hydrogels are electron-conducting matrices created by cross-linking of water-soluble redox polymers that provide an electrical connection between the redox centers of enzyme molecules and the electrode. In such hydrogels, the polymer is usually a polyvinylpyridine and the redox functions, tethered to the polymer backbones, are metal-organic complexes of  $\text{Os}^{2+/3+}$  with substituted and unsubstituted pyridine (174). PEGDE is used as a cross-linking agent for binding enzymes to complexes of redox polymer, thereby producing efficient electron diffusion between the enzymatic redox centers and the electrode (120, 151), (150). The enzyme immobilization reaction is illustrated in Figure 3.3A.

An electron mediator is immobilized in the matrix, together with the enzyme, and lowers the potential at which peroxide, released by the enzyme, is detected. Figure 3.3B shows the electron transfer pathway of the redox hydrogel-based biosensor (152), (164).

Both the redox polymer and PEGDE are highly water-soluble, but the membrane resulting from the reaction is insoluble and has a swollen gel-like polymer structure. When the electrode is placed in a solution, the membrane increases its water content, which minimizes the diffusion constraints and provides easy permeation of the film by enzyme substrates and product molecules.

Several enzymes, including glucose oxidase or glutamate oxidase, have been successfully immobilized on biosensors using this technique (120), (152), (153). Moreover, glucose biosensors based on this or similar principles have been validated for glucose monitoring in diabetic patients (55), (154). However, the components of such redox hydrogels, when available commercially, are expensive, or require several steps of organic

synthesis. This method is therefore more difficult to implement in a non-expert laboratory than those using only glutaraldehyde or PEGDE. Below, we present an experimental protocol designed by Adam Heller's laboratory and validated in neuroscience research by Adrian C. Michael's and Ben Westerink's groups (151), (153), (168), (175).

### 2.1.3.1. Redox polymer synthesis

0.494g (0.864 mmol) of *cis-bis* (2,2'-bipyridine-*N,N'*)dichloroosmium (II) (Colonial Metals, Inc. or Johnson Matthey) and 0.430 g (4.09 mequiv) of poly(4-vinylpyridine) are heated under nitrogen in 18 mL of ethylene glycol for 2 h. After the solution is cooled to room temperature, 30 mL of dimethyl formamide and 1.5 g (7.3 mmol) of 2-bromoethylamine hydrobromide are added, and the solution stirred at 45°C overnight, then the crude polymer is precipitated by pouring the solution into rapidly stirred acetone. The hygroscopic precipitate is collected, dissolved in H<sub>2</sub>O, filtered, and precipitated as a PF<sub>6</sub><sup>-</sup> salt by addition of a solution of NH<sub>4</sub>PF<sub>6</sub>. The dry PF<sub>6</sub><sup>-</sup> salt (0.49 g) is dissolved in 20 mL of acetonitrile, diluted with 50 mL of H<sub>2</sub>O, and stirred for 2 h over 5.2 g of anion exchange beads (Bio-Rad AG1-X4, chloride form, TRISKEM), then the mixture is filtered and the filtrate evaporated under vacuum to ca. 10 mL. Concentrated HCl is then added to bring the pH to 2 and the solution is dripped into rapidly stirred acetonitrile. The precipitate formed is then filtered and dried in a vacuum desiccator (151).

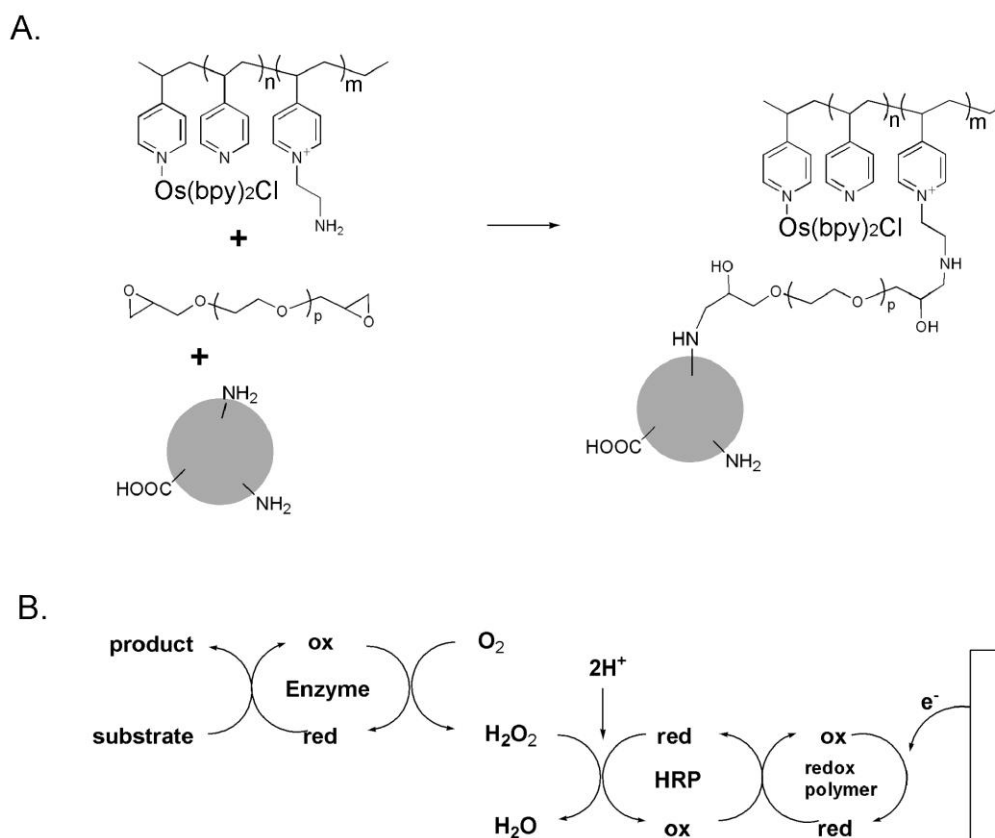


**Figure 3.3: Redox hydrogel matrix method.** A. Schematic illustration of enzyme immobilization in a hydrogel phase. The PEGDE cross-linker attaches the enzyme by its amine groups to the redox polymer backbone (polyvinylpyridine grafted with Os<sup>2+/3+</sup> complexes). B. Electron transfer between the enzyme and the electrode by polymer redox centers.

### 2.1.3.2. Biosensor construction

*Unless stated otherwise, all reagents are dissolved in HEPES buffer, pH 8.*

#### *Glucose sensor*

*The aqueous mixture of redox polymer and enzyme is composed of 20  $\mu\text{L}$  of redox polymer (1 mg/ml in water), 4  $\mu\text{L}$  of PEGDE (3 mg/mL in water), 20  $\mu\text{L}$  of ascorbate oxidase (AAOx) (EC 1.10.3.3; from *Curcubita* sp) (10 mg/mL), 10  $\mu\text{L}$  of horseradish peroxidase (2 mg/mL), and 10  $\mu\text{L}$  of glucose oxidase (50  $\mu\text{g/mL}$ ). A 10  $\mu\text{L}$  aliquot of the mixture is suspended on the end of a pipette and painted onto an electrode for 10 min. The sensor is then dried at 37°C for 1 h, soaked in water for 15 min, and dried in ambient air for 1 h (175).*

#### *Glutamate biosensor*

*The aqueous mixture of redox polymer and enzyme is composed of 20  $\mu\text{L}$  of redox polymer (1 mg/mL), 4  $\mu\text{L}$  of PEGDE (3 mg/mL), 10  $\mu\text{L}$  of HRP (0.474 U/ $\mu\text{L}$ , 3 mg/mL), 10  $\mu\text{L}$  of AAOx (1.4 U/ $\mu\text{L}$ , 10 mg/mL), and 10  $\mu\text{L}$  of glutamate oxidase (0.0242 U/ $\mu\text{L}$ , 2 mg/mL). Coating is performed by a 10 min manual dipping procedure. After coating, the sensors are cured for 1 h at 37°C, followed by a 10 min rinse in pure water and drying in ambient air for 2 h (153).*

In our hands, omitting the electron mediator from the hydrogel yields response times that are about 10 times faster than those using  $[\text{Os}(\text{bpy})_2\text{Cl}]^+$  (168), a critical factor for the *in vivo* detection of neurotransmitters, such as glutamate. We have therefore modified the synthesis of redox hydrogels to obtain hydrogels without metal-organic complexes, as described below.

### 2.1.3.3 Hydrogel without metal-organic complexes

#### Polymer synthesis

*A solution containing 0.430 g (4.09 mequiv) of poly(4-vinylpyridine), 30 mL of DMF, and 1.5 g (7.3 mmol) of 2-bromoethylamine hydrobromide is prepared and stirred at 45°C overnight, then the crude polymer is precipitated by pouring the solution into rapidly stirred acetone. The hygroscopic precipitate is collected and dissolved in a minimal volume of  $\text{H}_2\text{O}$  and the solution filtered and the filtrate again poured into rapidly stirred acetone, the precipitate collected and dissolved in a minimal volume of  $\text{H}_2\text{O}$ , and the solution filtered and evaporated under vacuum.*

#### Biosensor construction

*All reagents are dissolved in 0.01 M PBS, pH 7.4*

*For glucose biosensors, 5  $\mu\text{L}$  of the polymer (6 mg/ml), 10  $\mu\text{L}$  of 6 mM SDS, 4  $\mu\text{L}$  of PEGDE (80 mg/mL), and 5  $\mu\text{L}$  of a mixture of 60 mg/mL (12600U/mL) of glucose oxidase and 30 mg/mL of BSA are mixed thoroughly. The enzyme layer is then deposited by dipping the tip of the electrode in the enzyme solution and the sensor dried at 45°C for 1 h and soaked in water.*

*For glutamate biosensors, the aqueous mixture of polymer and enzyme is prepared using 25  $\mu\text{L}$  of polymer (15 mg/mL), 5  $\mu\text{L}$  of PEGDE (45 mg/mL), and 7  $\mu\text{L}$  of glutamate oxidase (0.64 U/ $\mu\text{L}$ , 100 mg/mL). The resulting solution is rather liquid and difficult to deposit on a microelectrode and it is usually necessary to concentrate it under vacuum at room temperature until viscous. The enzyme layer is deposited by dipping the tip of the electrode in the enzyme solution, then the sensor is dried at 45°C for 2 h and soaked in water.*

Several alternatives to enzyme immobilization by cross-linking procedures are now

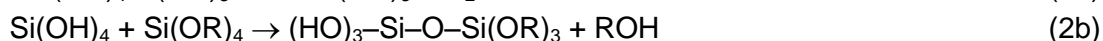
available. A very promising approach involves enzyme entrapment in a matrix.

## 2.2. Enzyme entrapment

The basic principle of enzyme entrapment consists in creating a polymer layer on the surface of the electrode. The enzyme to be immobilized on the biosensor is added to the monomer solution, and, during synthesis of the polymer, enzyme molecules are mechanically or electrostatically entrapped in the matrix created by the polymer or adsorbed in the layer. Because there are no strong chemical bonds between the enzyme and the polymer (mainly physical constraints), it is presumed that such procedures result in better preservation of enzyme activity. In particular, biosensors prepared using these methods could, in principle, display enhanced sensitivity and selectivity. We will now describe the two main methods for enzyme entrapment, sol-gel matrices and polypyrrole (and polyphenylenediamine) electropolymerization.

### 2.2.1 Sol-gel matrix

The sol-gel method is widely used in materials science, as well as in the biosensor domain and creates a porous matrix containing molecules or substrates of interest on the electrode surface. The method consists of the hydrolysis of precursors (Reaction 1), usually alkoxy silanes ( $\text{Si}(\text{OR})_4$ ), followed by polymerization of the products (Reaction 2a,b). The process can be described by the following reactions (176), (177):



The rate of the first reaction is strongly dependent on the pH of the solution. It is very slow at pH 7 and is increased in strong alkaline or acidic media. In contrast, the rates of reactions 2a and 2b are highest at a slightly alkaline pH ((178), (177)). To prepare a silica matrix containing an enzyme on the surface of an electrode surface, electrochemically-induced pH changes are often used. For example, the electrochemical reduction of nitrate and  $\text{H}^+$  ions added to the precursor solution causes a localized increase in pH through reactions 3 and 4:



A gel is generated only where a negative potential is applied and the local pH increased (179), (178), (148) (Fig. 3.4). This procedure is especially interesting when using micro-fabricated probes with multiple electrodes etched on the surface; in this case, a given enzyme can be specifically immobilized on selected sensing spots by controlling the applied potential. Moreover, by adjusting the time during which the potential is applied to the electrode, the thickness of the matrix can be controlled. Additionally, sol-gel-derived silica-based materials are well-suited for enzyme entrapment because they are chemically inert and have a three-dimensional structure that allows some level of mobility for encapsulated biomolecules, thus preserving optimal catalytic activity (180). However, sol-gel matrices also



have some disadvantages. For example, the precursors for sol-gel formation are toxic, which can limit potential clinical applications; in particular, tetramethoxysilane (TMOS) is toxic by inhalation. Other types of silanes can probably be chosen for the sol-gel procedure in order to decrease toxicity. In our hands, the sol-gel approach proved to be delicate to set up in the lab, especially because many different sol-gel protocols have been presented in the literature (e.g. (180), (148), (181)). Moreover, biosensors based on sol-gel procedures tend to display a significant initial decrease in sensitivity, probably due to a loss of biological material (180).

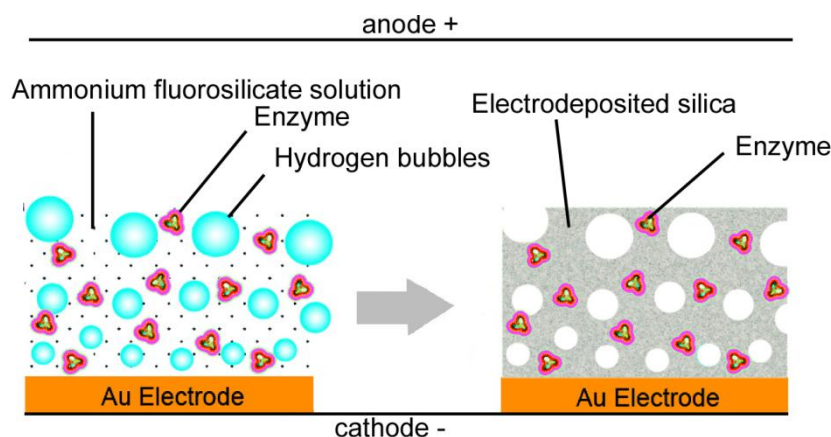


**Figure 3. 4 : Sol-gel method.** Illustration of electrochemical deposition of a porous silica matrix on the electrode surface. The process of matrix (gel) formation is triggered by an electrochemically-induced change in the pH in the initial solution (sol). Such pH changes are accompanied by the release of hydrogen bubbles that are important for the formation of the porous matrix structure.

We propose two protocols for sol-gel matrix deposition on the surface of the electrode.

*Method 1: Example of oxidase enzyme entrapment (182)*

Two acidic solutions of hydrolyzed silanes are prepared containing, respectively, TMOS (Sigma-Aldrich) or (3-aminopropyl) trimethoxysilane (APTEOS, Sigma-Aldrich). The acidified TMOS solution is prepared from 7.39 mL of TMOS, 1.69 mL of distilled H<sub>2</sub>O, and 0.11 mL of 0.04 M HCl, and is sonicated on ice for 20 min, then can be stored on ice for several days. The APTEOS solution is prepared from 5.55 mL of APTEOS and 5 mL of H<sub>2</sub>O, then the pH is adjusted to 3 with concentrated HCl and the solution sonicated on ice for 20 min prior to storing on ice. The sol solution is then prepared for electrochemical deposition. The mixture contains 1 part acidified TMOS solution, 1 part APTEOS solution, 2 parts 1 M glycerol, 1 part PEG 400 average MW, 4 parts 50 mM Tris pH 6.3, and 2 parts 0.4 M KNO<sub>3</sub>. To prepare glutamate or ATP sensors, respectively, one unit of L-glutamate oxidase (148) or 5 units of glycerol kinase plus 5 units of glycerol-3-phosphate oxidase (122) are dissolved in 10  $\mu$ L of sol mix just before use and transferred into a small capillary. The working and reference Ag/AgCl electrodes are introduced from opposite ends and a potential between -0.9 and -1.2 V is applied for 10-40 sec and a transparent, smooth, and robust gel layer is formed. The PEG and glycerol are added to stabilize the mixture of sol-gel and enzyme, while the nitrate is added to allow the formation of hydroxide ions and the subsequent pH increase on application of a negative potential. The biosensors produced are stored in PBS, pH 7.4.

*Method 2: Example of hemoglobin entrapment (180)*

A sol is prepared by mixing 2.125 g of TEOS with 2 mL of water and 2.5 mL of 0.01 M

*HCl for 12 h on a magnetic stirrer, then 0.07 M phosphate buffer, pH 6.0, is added to the silica sol to neutralize it and a one-tenth volume of 0.5 mM hemoglobin solution (Hb, MW 64000, Sigma) is added to the hydrolyzed sol. The electrode is then dipped into this mixture and a constant potential of -1.2 V is applied for 7 sec, triggering electro-assisted deposition of the sol-gel layer. The electrode is then washed, dried for 60 min in air, and stored at 4°C. The stability of the deposited layer and the performance of the bioelectrode are improved by addition of 0.02 M cetyltrimethylammonium bromide, a cationic surfactant, to the starting solution.*

For good reproducibility and a high quality silica layer, the working electrode must be thoroughly cleaned and dried for at least 1 h at 90°C before electrodeposition. Moreover, the authors noted that the addition of Au nanoparticles can improve biosensor performance (180).

An alternative entrapment method utilizing a biomimetic silification method has also been presented recently. Briefly, a silica gel layer is grown on the surface of the electrode after functionalization by poly-L-lysine. Like the sol-gel procedure, this method uses silane precursors for matrix formation and enzyme entrapment. Various enzymes can be immobilized under mild conditions using this procedure (183).

### **2.2.2 Polypyrrole-derived matrix**

Electrochemical polymerization is a simple and attractive method for biosensor construction. Enzymes are entrapped either during the growth of a polymer generated by electrooxidation of a monomer contained in the enzyme solution (131) or in an adsorbed enzyme/monomer layer (184). Pyrrole and pyrrole-derived monomers are the most widely used components because they are one of the few families of conductive polymers that are stable at ambient temperature and that can be easily used with different electrolytes, including aqueous solutions. During polymerization, the applied potential generates reactive pyrrole-cation radicals that react with neighboring monomer molecules, thereby producing a polymer layer on the electrode surface (131) (Fig. 3.5B). As in sol-gel procedures, it is easy to control the thickness or the position of the layer on specific sensing spots by adjusting the electrooxidation time or applying the voltage to specific places on a multi-electrode microprobe. Additionally, the relatively low potential (+700 mV relative to the Ag/AgCl) required for electropolymerization provides sufficiently mild conditions to avoid enzyme denaturation (149). However, in our hands, polypyrrole entrapment proved to be one of the most difficult methods to implement in the laboratory. In fact, optimal results are obtained not with pyrrole itself, but with modified monomers in which a carbon chain is added to the pyrrole moiety. Such monomers are not commercially available and require multiphase organic synthesis (185), with even simplified synthetic schemes consisting of at least 5 steps (109). The pyrrole-derived monomer used in our studies was kindly supplied by Serge Cosnier's laboratory. We have tested the following method for electropolymerization of an adsorbed pyrrole-enzyme layer (184), (149).

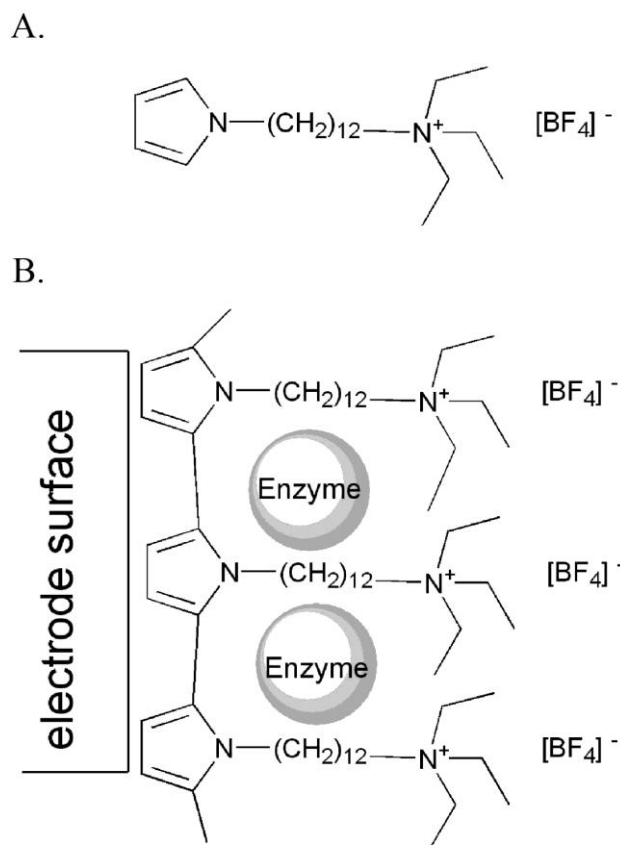


**Figure 3.5: Polypyrrole method.** A. Chemical structure of the monomer of (12-pyrrol-1-yl)dodecyltriethylammonium tetrafluoroborate. B. Schematic illustration of enzyme entrapment in the electrodeposited matrix.

#### *Enzyme entrapment*

The glucose oxidase solution used for biosensor preparation contains 60 mg/mL of glucose oxidase, 30 mg/mL of BSA (Sigma), and 1% glycerol in 0.01 M PBS, pH 7.4. An aliquot of this solution (5  $\mu$ L) is dried in vacuum at room temperature and the pyrrole-derived monomer (300 mM), previously sonicated in water for 15 min, is added and carefully mixed to give a final concentration of 8.3 mM of monomer and 2.5 mg/mL of protein (124). The enzyme layer is deposited on the electrode surface by dip-coating and left in vacuum for dehydration.

Polymerization is carried out in a two-electrode configuration system. The adsorbed enzyme-pyrrole-derived layer is polymerized in PBS at 800 mV constant potential versus an Ag/AgCl reference electrode for 10 min.

Data from the literature suggest that biosensors prepared using this procedure have a rather short life-time. Electrodes stored at 4°C for 50 days lose about 50% of their sensitivity (186), whereas implantation in a biological preparation often causes partial or complete loss of sensitivity (109), (124).

In our list of possible enzyme entrapment methods, we should also mention polyphenylenediamine (PPD) polymers. Unlike polypyrrole, PPD is not electrically conductive, so the polymer layer cannot grow into such thick layers as those obtained with sol-gel or polypyrrole procedures. We have not tested this method in our laboratory. Instead,

we invite the reader to refer to section 1.2, which is entirely devoted to this procedure.

### 3. Quantitative comparison of different immobilization methods

We tested the different immobilization procedures described above on glucose and glutamate biosensors. When testing hydrogels, we focused exclusively on the method without redox centers, which results in more rapid response times and appears more suitable for monitoring fast changes in neurotransmitter levels. The sol-gel procedure used was method 1 (p. 70). Using polypyrrole, biosensors were prepared successfully using glucose oxidase, but the method proved very unreliable with other enzymes, those prepared with choline oxidase having a very low sensitivity and D-amino acid oxidase could not be immobilized at all. For this reason, we abandoned this method and did not perform further tests with glutamate oxidase. To compare the influence of the immobilization method on the major biosensor parameters, we determined their sensitivity, response time, linear range, the apparent Michaelis-Menten constant, and stability.

#### 3.1. Apparent Michaelis – Menten constant and linear range

Enzymatic biosensors convert a specific substrate to its product while producing electrochemically detectable peroxide. The activity of most enzymes can be described by the Michaelis-Menten equation:

$$V(C) = \frac{V_{max} \times C}{K_m + C} \quad (6)$$

In turn, the current-concentration relationship that characterizes a biosensor can be approximated by the modified equation:

$$I(C) = \frac{I_{max} \times C}{K_m^{App} + C} \quad (7)$$

where  $I_{max}$  is the maximum current recorded by the biosensor and  $K_m^{App}$  is the apparent Michaelis-Menten constant for the biosensor.  $K_m^{App}$  is related to the  $K_m$  of the enzyme immobilized on the electrode, but also depends on other parameters, such as the diffusion rates of the substrate,  $O_2$ , and peroxide within the enzyme layer. Because of this, the  $K_m^{App}$  of a biosensor is often very different from the  $K_m$  of its free enzyme.

To determine the relationship between the current detected by the biosensor and the substrate concentration experimentally, we measured the current steps produced by addition of increasing amounts of enzyme substrate to the recording medium. Plotting the value of the oxidation current against the substrate concentration gives a curve that can be fitted to the modified Michaelis-Menten equation to yield the approximate value of  $K_m^{App}$ .

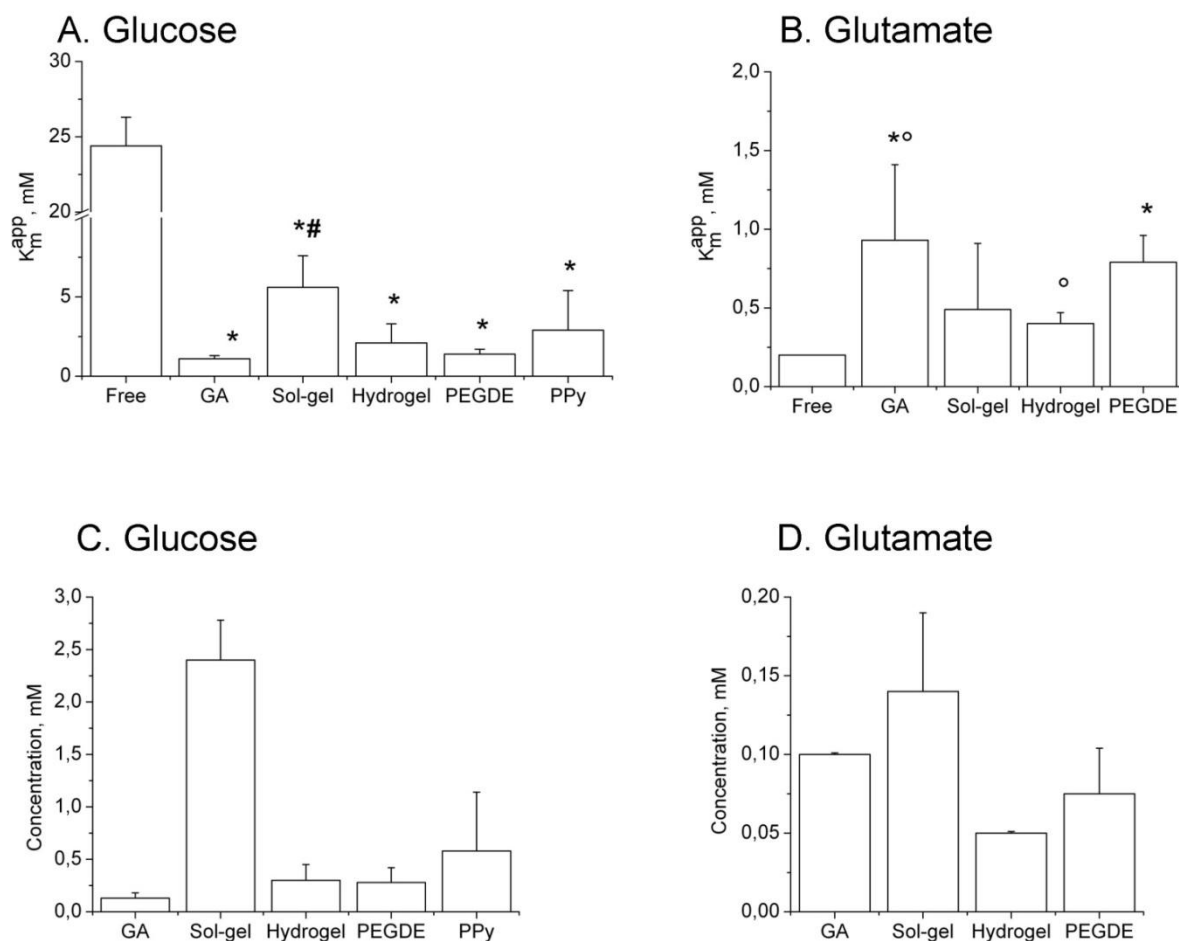


**Figure 3.6 : Apparent Michaelis-Menten constant and linear range.** Influence of the enzyme immobilization method on the apparent Michaelis-Menten constant of biosensors with immobilized glucose oxidase (A) or glutamate oxidase (B). Biosensor linear response range for detection of glucose (C) or glutamate (D) ( $R^2=0.998$ ). The data are in good agreement with theoretical Michaelis-Menten kinetics, predicting linearity up to concentrations around  $K_m^{App}/10$ . Only biosensors prepared with the sol-gel method displayed larger linear ranges than those predicted by Michaelis-Menten kinetics. The data are presented as the mean  $\pm$  standard deviation (SD). The experiment sample size,  $n$ , was the number of biosensors constructed using the same protocol (4-6 electrodes). \* Significantly different from the free enzyme, # significantly different from all other immobilization methods, ° significant difference between the two indicated methods. Statistical comparisons were performed using ANOVA, followed by a LSD post-hoc test ( $p<0.05$ ). GA, glutaraldehyde; Ppy, polypyrrole.

The  $K_m^{App}$  values of the glucose biosensors were very variable, ranging from  $1.1\pm 0.2$  mM with glutaraldehyde fixation to  $5.6\pm 2$  mM with sol-gel entrapment (Fig. 3.6A). Thus, the  $K_m^{App}$  was substantially lower than the  $K_m$  of the free enzyme, which is between 26 mM (157), (158) and 30 mM (159), (160). The  $K_m^{App}$  of glutamate biosensors were also very variable, ranging from  $0.4\pm 0.1$  mM for the hydrogel method to  $0.9\pm 0.5$  mM for glutaraldehyde fixation (Fig. 3.6B). In contrast, the glutamate biosensors had a  $K_m^{App}$  higher than the  $K_m$  of the free enzyme (0.2 mM, (187), (188)). These effects could result, in part, from substrate pre-concentration or exclusion from the membrane layer. In fact, substrate pre-concentration would decrease the  $K_m^{App}$ , whereas substrate exclusion from the membrane would increase it. Such apparent concentration effects have been described in the literature (161),(90).

To determine the linear range of our biosensors, we plotted the experimental current values obtained using the lowest concentrations that we tested and performed a linear fit. The linear range was defined as the highest concentration for which a successful fit at  $R^2 = 0.998$  was still possible. For glucose and glutamate biosensors prepared with cross-linking methods (glutaraldehyde, hydrogel, or PEGDE) or with polypyrrole, the linear range was between 0 and 100-300  $\mu\text{M}$  glucose ( $n=6$ ) and between 0 and 75  $\mu\text{M}$  glutamate ( $n=4-6$ ). These results are in agreement with theoretical calculations predicting that the linear range should extend up to concentrations around  $K_m^{\text{App}}/10$ . Only biosensors prepared with a sol-gel matrix did not follow this rule, as their linear range extended up to 2.5 mM glucose ( $n=6$ ,  $R^2=0.998$ ) and 140  $\mu\text{M}$  glutamate ( $n=4$ ,  $R^2=0.998$ ). These results suggest that biosensors with enzyme entrapped in a sol-gel matrix may not follow the theoretical kinetics of the Michaelis-Menten model.

### 3.2. Biosensor sensitivity

Because biosensors are mostly used in their linear (or dynamic) range, the sensitivity of the sensor is defined as the initial slope of the current-concentration curve (the biosensor equivalent of  $K_m/V_{\text{max}}$  for the free enzyme) and is expressed in  $\text{pA}/\mu\text{M}$  of substrate or, more accurately, in  $\mu\text{A}\cdot\text{mM}^{-1}\text{cm}^{-2}$  of electrode surface (in our studies, the microelectrode surface was about  $8300 \mu\text{m}^2$ ).

For glucose biosensors, the sensitivity varied from  $12.2 \pm 3.7 \text{ pA}/\mu\text{M}$  ( $n=35$ ) for a PEGDE matrix to  $1 \pm 0.1 \text{ pA}/\mu\text{M}$  ( $n=7$ ) for a sol-gel matrix (Fig. 3.7A). For glutamate biosensors, the glutaraldehyde, PEGDE, and hydrogel methods gave sensitivities between  $21.6 \pm 3.1$  and  $14.4 \pm 8.2 \text{ pA}/\mu\text{M}$ , with only sol-gel entrapment giving a significant lower value of  $7.8 \pm 3.5 \text{ pA}/\mu\text{M}$  (Fig. 3.7B). It should be noted that sol-gel-based biosensors display excellent sensitivity with fresh-prepared electrodes, then the sensitivity rapidly decreases during the first hour of use, finally reaching a stable value.

Overall, our tests with glucose oxidase and glutamate oxidase indicate that covalent immobilization methods using protein cross-linking (glutaraldehyde, PEGDE, and hydrogel) yield more sensitive biosensors than methods based on enzyme entrapment (sol-gel and polypyrrole).

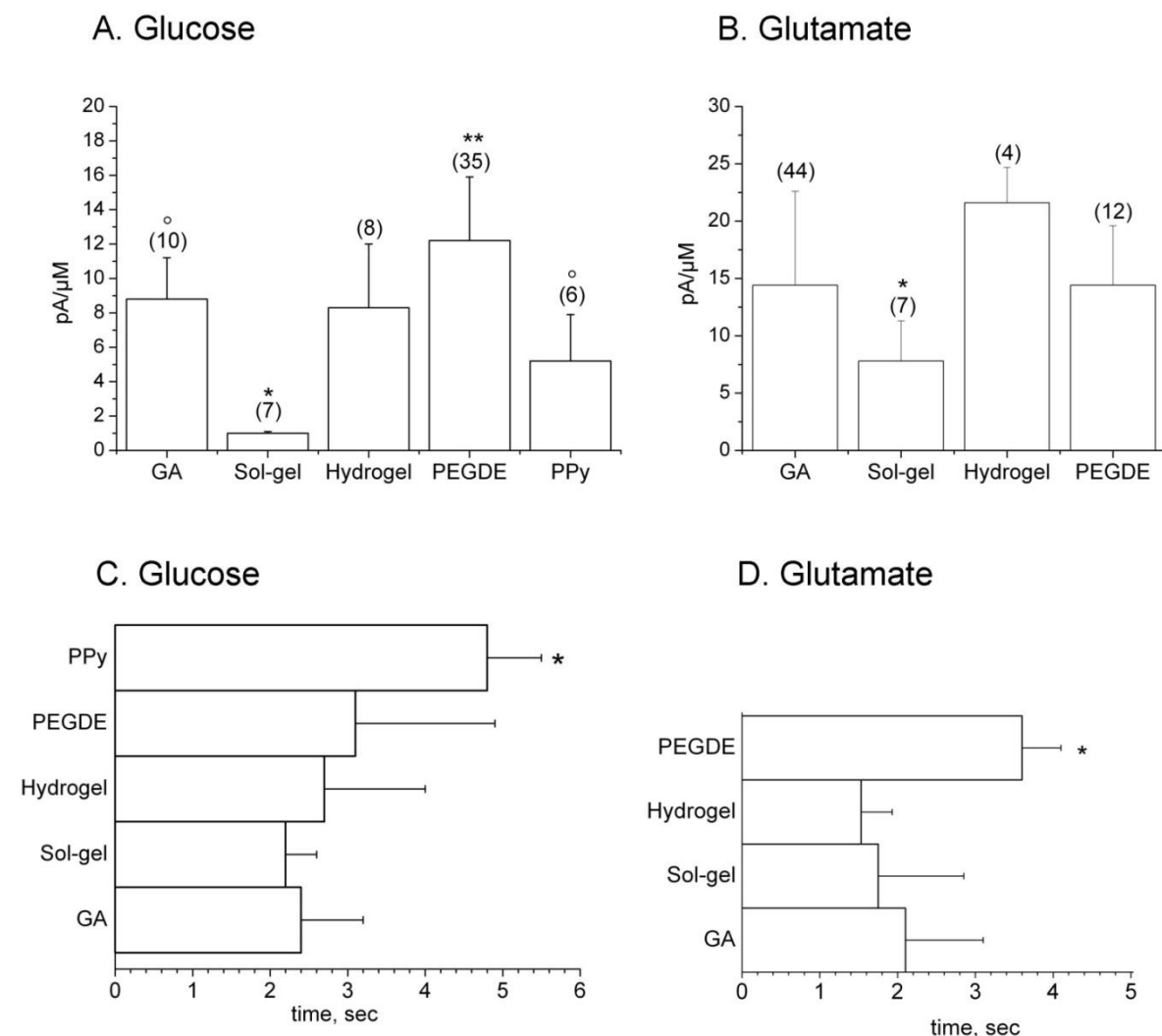


**Figure 3.7: Biosensor sensitivity and response time.** A and B: Dependence of biosensor sensitivity to glucose (A) or glutamate (B) on the method used for enzyme immobilization. Biosensors with enzyme entrapped in a sol-gel matrix showed the lowest sensitivity. \* and \*\* reflect, respectively, a significantly lower or higher sensitivity compared to all other methods, ° significant difference between the indicated methods. C and D: Response time of glucose (C) and glutamate (D) biosensors as a function of the immobilization method. \* Significant difference from all other methods, n=4-6.

### 3.3 Response time

Microelectrode biosensors designed for neuroscience research should detect neurotransmitters or metabolites with a high temporal resolution. Unlike the direct oxidation of biogenic amines on carbon-fiber electrodes, which allows the subsecond detection of dopamine or serotonin (189), enzymatic biosensors are limited by the kinetics of the enzymatic reaction and usually display response times of the order of a few seconds. To determine the response time, biosensors are rapidly transferred from PBS to a solution containing a known concentration of the enzyme substrate, which generates a step of

oxidation current at the biosensor. The response time is typically defined as the time required to reach 90% of the plateau response.

When testing the different types of biosensors, we found that the immobilization method significantly influenced the response time of the electrode (Fig 3.8). For glucose biosensors, the response time was in the range of 2 to 3 seconds, except for a significantly slower response of polypyrrole-based biosensors ( $4.8 \pm 0.7$  sec,  $n=6$  Figure 3.8A.). For glutamate biosensors, the response time was in the range of 1.5 to 2.1 seconds ( $n=4$ ), except for the significantly slower PEGDE-based biosensors ( $3.6 \pm 0.5$  sec,  $n=12$ , Figure 3.8B.). Thus, both PEGDE and polypyrrole tended to yield biosensors with slightly slower response times.

### 3.4 Stability

For reliable *in vivo* experiments, in which biosensors are implanted in the brain for several hours or even days, the stability of the enzyme layer is a crucial parameter. An important aspect of biosensor stability is its interaction with the biological milieu and its susceptibility to biofouling processes taking place in the living brain. In this regard, a minimal tip size is advisable to decrease inflammation and/or hemorrhage during implantation. The biocompatibility of the materials used for electrode construction and the method of enzyme immobilization can have a significant impact on the life-time of the biosensor *in vivo*. If the enzyme matrix is poorly compatible with brain tissue, membrane biofouling will lead to enzyme inactivation (190). For example, bringing biosensors with a enzyme-containing polypyrrole-derived or sol-gel matrix into contact with biological tissues frequently causes partial or complete loss of sensitivity (109), (124), (191).

We first tested the stability of the biosensors when left in PBS at 37°C. Biosensors formed by cross-linking by glutaraldehyde, hydrogel, or PEGDE and by polypyrrole-derived matrix methods showed remarkable stability when left for 2-3 hours at 37°C. Biosensors prepared using PEGDE immobilization were stable for up to 3d at 37°C (173). In contrast, the sensitivity of sol-gel electrodes decreased within the first 2-3 hours until a constant value was reached, then remained stable for several days or weeks.

In a second set of experiments on stability, we implanted biosensors *in vivo*. We only tried the three cross-linking methods using glutaraldehyde, hydrogel, or PEGDE. We were able to detect D-serine for up to 5 h in the frontal cortex of anesthetized rats using D-amino acid oxidase biosensors and compared their sensitivity before and after implantation and found no significant change. Sol-gel based biosensors have also been used *in vivo* for purine detection (192).

Thus, the methods that we chose to compare are indeed well-suited for *in vivo* experiments, except possibly in the case of some polypyrrole-based biosensors, which might be better adapted to *in vitro* (slice) experiments.

## 4. Conclusions

In reviewing these five major immobilization procedures available in the field of implantable microelectrode biosensors, one of our goals was to provide detailed experimental protocols that would allow the reader to set up these methods in his/her laboratory. Another goal was to identify the most efficient methods and to select them for future studies. In this regard, of the methods tested, PEGDE displayed promising properties:



- PEGDE is non-toxic, can be manipulated by non-experts, and potential clinical applications can be considered;
- The PEGDE method is simple and cheap: the reagent is commercially available and enzyme immobilization involves only one reagent, without any requirement for custom chemical synthesis;
- Enzyme immobilization using PEGDE results in a very physically and enzymatically stable product (2-3 months at 4°C or 3 days at 37°C).

These advantages should make the PEGDE approach a valuable method for future biosensor applications. However, considering the operational parameters of all the biosensors that we tested, it is difficult to identify a single specific immobilization procedure with optimal overall biosensor performance. For example, PEGDE tends to give higher sensitivities that are mitigated by slightly slower response times. Additionally, PEGDE lacks the electrochemical control over membrane growth that is available with sol-gel or polypyrrole methods. In this regard, sol-gel procedures and their latest developments should attract great interest in the future.

We believe that more efforts should be made to come up with a consensual method for enzyme immobilization that would satisfy all the criteria of low toxicity, simplicity, stability, sensitivity, fast kinetic parameters, and fine control of membrane deposition. As biosensor technologies continue to develop and to spread to different laboratories, we have no doubt that such a consensus will emerge in the near future.

**Acknowledgements:** This study was supported by Inserm U628 and Université Claude Bernard Lyon I and by grants from the Agence Nationale pour la Recherche (ANR-09-BLAN-0063 Neurosense) and Institut Fédératif des Neurosciences de Lyon (Projet structurant IFNL 2008). NV received a PhD fellowship from the Ministère de la Recherche. Estelle Enriquez, Anne Meiller, and Caroline Maucler provided valuable technical assistance. We are grateful to Thomas Barkas for helpful comments on an earlier version of the manuscript.

# Chapter 4:

## **Effect of enzyme immobilization on biosensors substrate-specificity: consequences for glutamate detection in the central nervous system**

This chapter raises a question of the effect of enzyme immobilization on the apparent substrate-specificity of the biosensor that is extremely important for obtaining specific measurements *in vivo*. The microelectrode glucose biosensors designed for *in vivo* brain implantation in rats were constructed using five enzyme immobilization methods. The selectivity of corresponding glucose biosensors was assessed *in vitro*. PEGDE and glutaraldehyde covalent immobilization methods were also compared using glutamate oxidase. The corresponding glutamate biosensors were tested in brain homogenates and dialysates, and the accuracy of biosensor measurements was controlled by HPLC and CE-LIF methods. Glutamate biosensors were used to detect changes of glutamate extracellular concentration in the cortex of anesthetized and awake rats, in response to electrical and pharmacological stimulations.



**An immobilization method for biosensors with preserved enzyme specificity:  
consequences for glutamate detection in the central nervous system**

*Natalia VASYLIEVA<sup>1,2,3</sup>, Caroline MAUCLER<sup>1,2</sup>, Anne MEILLER<sup>1,2</sup>, Henry VISCOGLIOSI<sup>4</sup>,  
Thomas LIEUTAUD<sup>1,2</sup>, Daniel BARBIER<sup>3</sup> and Stéphane MARINESCO<sup>1,2</sup>*

<sup>1</sup>INSERM U1028, CNRS UMR5292, Lyon Neuroscience Research Center, Plate-forme technologique AniRA-Neurochem, team WAKE, F-69000 Lyon, FRANCE.

<sup>2</sup>University Claude Bernard Lyon 1, Lyon, F-69000, France

<sup>3</sup>Institut de nanotechnologie de Lyon, CNRS UMR-5270, INSA de Lyon, FRANCE.

<sup>4</sup>Service Central d'Analyse, UMR-5280 – Echangeur de Solaize, SOLAIZE, FRANCE

\* corresponding author: Stéphane Marinesco, INSERM U1028, CNRS UMR5292, Centre de Recherche en Neurosciences de Lyon, Team WAKE, Faculté de médecine, 8 avenue Rockefeller, 69373 Lyon Cedex 08, France. Tel : +33 (0)4 78777041, Fax : +33 (0)4 78777150, Email : [stephane.marinesco@univ-lyon1.fr](mailto:stephane.marinesco@univ-lyon1.fr)

## ABSTRACT

Enzymatic biosensors are widely used in neurobiology for *in vivo* monitoring of metabolites and neurotransmitters. These devices achieve selective detection through the excellent specificity of natural enzymes immobilized on a microelectrode. However, the effect of immobilization on substrate-specificity is still poorly understood. This is a potentially crucial issue for detecting neurotransmitters like glutamate that are present at low concentration in the brain interstitial fluid. In this study, we prepared microelectrode biosensors for *in vivo* brain monitoring using five different immobilization methods. We focused on two covalent methods using either glutaraldehyde, or a diepoxyde with longer spacer arm, poly(ethylene glycol) diglycidyl ether (PEGDE). We found that glutaraldehyde significantly decreased enzyme substrate specificity. Glutamate- and glucose-oxidase immobilized with glutaraldehyde were more active towards secondary substrates like glutamine and asparagine or 2-deoxy-D-glucose and D-mannose. By contrast, PEGDE preserved enzyme substrate specificity. This effect had a dramatic impact on glutamate detection in the brain. Using PEGDE-based biosensors, glutamate basal concentration *in vivo* was about 1.2  $\mu\text{M}$  and partially depended on neuronal activity, whereas it was estimated around 16  $\mu\text{M}$  with glutaraldehyde-based biosensors. Moreover, glutaraldehyde biosensors detected an apparent glutamate spillover following neuronal stimulation, which was not confirmed using PEGDE biosensors, and probably reflected changes in other amino acid concentrations. We conclude that enzyme immobilization can significantly affect the specificity of enzymatic reactions used for biosensor detection. PEGDE can be used to immobilize a wide variety of oxidase enzymes for preparing stable and sensitive biosensors with preserved substrate-specificity.

## 1. Introduction

Enzymatic biosensors are widely used for detecting and monitoring molecules *in vivo* and in biological samples (144). For instance, they are used in medical practice to monitor glycemia in diabetic patients (55, 154). They are also used in central nervous system of laboratory animals to detect metabolites (glucose, lactate) or transmitters (glutamate, acetylcholine, D-serine etc.) (90, 119) and study the mechanisms of cell-to-cell communication, as well as the processes of physiological or pathological brain functioning (141, 192, 193).

To achieve selective detection of a single molecule in complex media, biosensors rely on the excellent specificity of natural enzymes immobilized on the surface of an electrode. One of the most useful consequences of immobilization is an improvement of enzyme stability (194). A wide variety of methods providing stable immobilization is currently available: for example covalent attachment to the matrix of redox polymers (195), cross-linking with bifunctional agents like glutaraldehyde (196), immobilization into porous support materials such as agarose, porous glasses etc. (197, 198). Immobilization can also impact enzyme substrate-specificity. Such effects have been described in the field of enzymatic catalysis, although they remain largely empirical and unpredictable (194, 199, 200). For example, lipases or penicillin G acylase can change their enantioselectivity after glutaraldehyde immobilization (194, 200).  $\alpha$ -D-galactosidase also changes its selectivity once cross-linked with glutaraldehyde (201). However, such effects on enzyme substrate-specificity have never been thoroughly investigated in the field of biosensor fabrication. Because biosensor selectivity relies on the substrate-specificity of the immobilized enzyme, it can be hypothesized that mild immobilization techniques would be most likely to preserve original catalytic parameters. Possible effects on enzyme-substrate specificity could be a crucial point for detecting neurotransmitters like glutamate that are present in low micromolar concentrations in the brain interstitial fluid. Recently, we successfully fabricated stable and sensitive microelectrode biosensors by immobilizing oxidase enzymes on the surface a platinum microelectrode under especially mild conditions, using the diepoxide poly(ethylene glycol) diglycidyl ether (PEGDE) (119). PEGDE immobilization is therefore a potential candidate for obtaining biosensors with preserved substrate specificity.

In this study, we tested five types of microelectrode biosensors designed for *in vivo* brain implantation in rats, that differed only by the enzyme immobilization method. We compared crosslinking by glutaraldehyde and PEGDE, entrapment into sol-gel and derived polypyrrole matrices, and attachment to a hydrogel matrix. These methods were tested on glucose oxidase and the selectivity of corresponding glucose biosensor was then assessed *in vitro*. PEGDE and glutaraldehyde covalent immobilization methods were also compared using glutamate oxidase. The corresponding glutamate biosensors were tested in brain homogenates and dialysates, and the accuracy of biosensor concentration estimates was controlled by HPLC and CE-LIF methods. Finally, both types of glutamate biosensors were used to detect changes of glutamate extracellular concentration in the cortex of anesthetized and awake rats, in response to electrical and pharmacological stimulations.

## 2. Materials and Methods

### 1. Enzyme preparation

Glucose oxidase (EC 1.4.3.11) from *Aspergillus niger* was purchased in powder form from Sigma-Aldrich (100–250 U/mg, Saint Quentin Fallavier, France). The final enzyme solution used for biosensor preparation contained 60 mg/mL glucose oxidase, 30 mg/mL bovine serum albumin (BSA, Sigma), 1% glycerol in phosphate buffered saline solution (PBS 0.01 M, pH 7.4).

L-Glutamate oxidase 7U/mg (EC 1.4.3.11) from *Streptomyces* sp. was purchased from Yamasa Corporation (Choshi, Chiba, Japan). The working solution contained 100 mg/mL of the protein, 150 mg/mL BSA, 1% glycerol in PBS (0.01 M, pH 7.4).

A bovine serum albumin solution consisting of 400 mg/mL BSA, and 1% glycerol in 0.01 M PBS, pH 7.4 was used for fabricating control biosensors.

## 2. Free enzyme selectivity assay

The enzyme solutions were prepared to obtain a final concentration of 3.3 mg/L (0.1 U) of Glucose oxidase, and 46.2 mg/L (0.1 U) of Glutamate oxidase in PBS 0.01M, pH 7.4 at ambient temperature. Enzyme activity was estimated at room temperature, by immersing a bare Pt electrode with a constant potential of +500 mV versus an Ag/AgCl reference into enzyme solution. The enzyme substrate was then added to the enzyme solution at a final concentration of 10 mM. After adding the substrate, the oxidation current recorded by the Pt microelectrode increased linearly, representing peroxide accumulation over time. The initial slope of the oxidation current was corrected by the sensitivity of the microelectrode to peroxide to estimate the speed of peroxide production, and hence, enzymatic activity for the substrate of interest. Enzymatic activity for secondary substrates was expressed as a percentage of the activity for the primary substrate (glucose for glucose oxidase and glutamate for glutamate oxidase).

## 3. Microelectrode preparation

Microelectrodes were constructed according to the protocol described by Pernot et al. (90) and Vasylyeva et al. (119). Briefly, 25  $\mu$ m 90% Pt/10% Ir wire was glued to a copper wire using conductive silver paint. The sensor wire was inserted into a pulled glass capillary so that Pt wire extended from the glass approximately 100  $\mu$ m. The junction between the Pt and the pipette was sealed by locally melting the glass. For *in vivo* experiments, a poly-m-phenylenediamine (PPD) screening layer was deposited by electropolymerization at +700 mV (vs Ag/AgCl) in a 100 mM m-phenylenediamine solution in PBS 0.01M pH 7.4. The PPD polymer creates a screening layer that prevents oxidation of the endogenous molecules present in the brain, such as serotonin, dopamine, ascorbate, and cysteine (90).

## 4. Enzyme deposition and immobilization

In case of immobilization by PEGDE, Glutaraldehyde or in hydrogel matrix, the enzyme layer was deposited by dipping the tip of the Pt microelectrode into the enzyme solution.

*PEGDE*. Prior to biosensor preparation, poly(ethylene glycol) diglycidyl ether, average MW 526 (Sigma-Aldrich, St Quentin Fallavier, France) was added to the BSA, Glucose or Glutamate oxidase aliquots at concentrations of 10 mg/mL, 20mg/mL or 100mg/mL respectively. The electrodes with Glucose oxidase or BSA were placed in an oven at 55 °C for 2 h and the ones with Glutamate oxidase were placed in oven at 48°C for 1h30min (119).

*Glutaraldehyde*. 5 mL of 25% glutaraldehyde (Sigma-Aldrich,) was placed at the bottom of a closed dish. After approximately 2 min, the chamber was filled with near-saturating glutaraldehyde vapor; the electrodes with their enzyme layer were placed in the

vapor for about 3 min and then thoroughly washed in water. (90)

*Hydrogel polymer matrix.* Polymer synthesis: A solution containing 0.430 g (4.09 mequiv) of poly(4-vinylpyridine), 30 mL of dimethyl formamide (DMF), and 1.5 g (7.3 mmol) of 2-bromoethylamine hydrobromide is prepared and stirred at 45°C overnight, then the crude polymer is precipitated by pouring the solution into rapidly stirred acetone. The hygroscopic precipitate is collected and dissolved in a minimal volume of H<sub>2</sub>O. The solution is then filtered and the filtrate poured again into rapidly stirred acetone. The precipitate is then collected, dissolved in a minimal volume of H<sub>2</sub>O, filtered again and evaporated under vacuum (adapted from (151)).

For glucose biosensors, 5 µL of the polymer (6 mg/ml), 10 µL of 6 mM sodium dodecyl sulfate (SDS), 4 µL of PEGDE (80 mg/mL), and 5 µL (0.3 mg) of glucose oxidase aliquot (60mg/mL) were mixed thoroughly. The electrodes with enzyme layer were dried at 45°C for 1 h and soaked in water.

*Sol-gel.* Two acidic solutions of hydrolyzed silanes were prepared containing, respectively, TMOS (Sigma-Aldrich) or (3-aminopropyl) trimethoxysilane (APTEOS, Sigma-Aldrich). The acidified TMOS solution was prepared from 7.39 mL of TMOS, 1.69 mL of distilled H<sub>2</sub>O, and 0.11 mL of 0.04 M HCl, and was sonicated on ice for 20 min. The APTEOS solution was prepared from 5.55 mL of APTEOS and 5 mL of H<sub>2</sub>O, then pH was adjusted to 3 with concentrated HCl and the solution was sonicated on ice for 20 min. The sol solution is then prepared with 1 part acidified TMOS solution, 1 part APTEOS solution, 2 parts 1 M glycerol, 1 part PEG 400 average MW, 4 parts 50 mM Tris pH 6.3, and 2 parts 0.4 M KNO<sub>3</sub>. Just before use, Glucose oxidase was dissolved into the sol mix at 20mg/mL. It was then transferred into an electrochemical cell, in which the working and reference Ag/AgCl electrodes were immersed. Potential between -0.9 and -1.2 V was applied for 10-40 sec and a transparent and smooth gel layer was formed on the working electrode (adapted from (182)).

*Polypyrrole-derived matrix.* Pyrrole-derived monomer was supplied by S. Cosnier (Université Joseph Fourier, Grenoble). The pyrrole-derived monomer was sonicated in water for 15 min and then added to an aliquot of glucose oxidase, previously dried in vacuum at room temperature. The solution was carefully mixed with final proportion of 3.32 monomer mM per 1 mg/mL of protein (124). The enzyme layer was firstly deposited on the electrode surface by dip-coating and left in vacuum for dehydration. The adsorbed enzyme-pyrrole-derived layer was polymerized in PBS at 800 mV constant potential versus an Ag/AgCl reference electrode for 10 min (adapted from (124)).

The biosensors were stored at 4 °C for short-term storage and at -20 °C for long-term storage. Before the experiments all sensors were tested for detection of the enzyme substrate (glucose or glutamate, 1 µM in PBS), and H<sub>2</sub>O<sub>2</sub> (1 µM in PBS). In addition the effectiveness of the PPD layer for achieving selectivity against endogenous oxidizable molecules was tested with serotonin (5-HT, 20 µM in PBS).

## 5. Recordings

All recordings were obtained using a VA-10 amperometry amplifier (NPI Electronics, Tamm, Germany) equipped with a two-electrode potentiostat. Data acquisition was performed using a 16-bit USB-6221 acquisition board (National Instruments, Nanterre, France) controlled by homemade software based on Igor Pro 6.4 procedures (Wavemetrics, Eugene, OR). The oxidation current was recorded at 1 kHz and averaged over 1000 data points, yielding a final sampling frequency of 1 Hz.

*In vitro* calibrations were performed in PBS (0.01 M, pH 7.4) solutions. The reference



electrode was a chloride-treated silver wire (Ag/AgCl) placed directly into the recording chamber. Recordings were obtained using constant potential amperometry at +500 mV versus the Ag/AgCl reference electrode. For *in vivo* studies, the biosensors were calibrated before and after implantation into the brain to ensure that the sensitivity remained stable over the course of the experiment.

## **6. *In vivo* experiments**

The experiments were performed under isoflurane or urethane anesthesia. The animals were treated in accordance with European directive 86/609/CEE. The experimental procedure was validated by the local committee on animals in research of Université Claude Bernard Lyon I (n° BH2010-19). Male Wistar rats weighing 300–500 g were placed in a stereotaxic apparatus (Stoelting, Dublin, Ireland). Their body temperature was maintained at 37 °C using a homeothermic blanket (Letica, Barcelona, Spain). The skull and dura were removed to expose the surface of the brain. Biosensors and microdialysis probes were inserted in the following coordinate range: AP: 2-3 mm anterior from bregma, ML: 2-4 mm, DV: 1mm).

### *Biosensor recordings in anesthetized rats*

Glutaraldehyde- and PEGDE-based biosensors were implanted in the frontal cortex (1 mm ventral to the pia) adjacent to a biosensor covered with BSA to control for nonspecific variations in oxidation current. An Ag/AgCl reference electrode was placed on the surface of the skull and wetted regularly with saline to ensure optimal electrical contact. Recordings were started at least 1 h after implantation to ensure stabilization of the baseline electrochemical currents, after which glutamate basal concentrations were estimated during an additional 30 min period of recording. Tetrodotoxin (TTX, 20µL, 100µM) was injected next to glutamate and control biosensors with a pressure injection device (Pneumatic picopump PV 820, WPI, Hertfordshire, UK). (3S)-3-[[3-[[4-(Trifluoromethyl)benzoyl]amino]phenyl]methoxy]-L-aspartic acid (TFB-TBOA, 5mM solution in 5% DMSO) was applied on the brain surface near glutamate and control biosensors inserted 0.3 mm under the pia. Quantitative assessments of brain glutamate concentrations were obtained by subtracting the non-specific current of the control biosensor from the glutamate biosensor current.

Stimulation of neuronal axons in the perforant path was performed using a concentric bipolar electrode (FHC, Bowdoin, ME). Coordinates: stimulation electrode: AP:-8.0mm, ML: 4.4mm, and recording electrode: -3.5mm, ML: 2.2 mm).

### *Biosensor recordings in awake freely-moving animals*

Two micromanipulators were surgically implanted (M2E, Eaubonne, France) on the surface of the skull using dental cement (Paladur resin, Henry Schein, France) under isoflurane anesthesia. A reference Ag/AgCl electrode was also implanted in contact with dura. The animal was then placed in an individual cage for one week to recover from surgery. During this time period, two mock biosensors were inserted into the cortex, 0.5 mm dorsal from the desired recording site, and manipulated every day. On the day of the *in vivo* recording, one glutamate biosensor and one control (BSA) biosensor were implanted through each micromanipulator 1 mm under the pia. Recordings were started 1 h after biosensor insertion to ensure stabilization of the baseline electrochemical currents.

### *Preparation of brain dialysate samples*

Microdialysis probes CMA 12 Elite (polyarylethersulfone membrane, 0.5mm; cut off 20 kDa, PHYMEP, France) were inserted in the frontal cortex 1.5 mm below the pia. The probes were perfused with Ringer lactate (Na<sup>+</sup> 130mM, K<sup>+</sup> 5.4 mM, Ca<sup>2+</sup> 1.8 mM, Lactate 27.7 mM, Laboratoires Chaix et Du Marais Lavoisier, France) at a flow rate of 1 µl/min using a

microinjection pump (Harvard Apparatus, Les Ulis, France). The dialysates were collected every hour into vials and immediately frozen at  $-80^{\circ}\text{C}$  to prevent glutamine conversion into glutamate (202).

**7. Preparation of brain and blood samples.** Male Wistar rats were decapitated under pentobarbital anesthesia and the head was immediately frozen by submersion in liquid nitrogen. The brain was removed and homogenized in 5 mL of 5% trichloroacetic acid (TCA) to precipitate macromolecules. After 20 sec sonication the homogenate was then centrifuged at 8 000 g for 10 min. TCA was extracted six times from supernatant using diethyl ether before storage at  $-80^{\circ}\text{C}$ .

Immediately after decapitation, 1mL of trunk blood was collected and centrifuged 15 min at 2 000 g. The serum was then collected and processed like brain homogenates (protein precipitation with TCA, centrifugation, extraction with ether) before storage at  $-80^{\circ}\text{C}$ .

## 8. HPLC and capillary electrophoresis

*Sugars* in brain homogenates and serum were analyzed by ion chromatography with amperometric detection on gold electrode using a Dionex HPLC system consisting of an automatic injector AS50, quaternary gradient pump GP50 equipped with integrated amperometric detector ED40 and driven by Chromeleon® Dionex chromatography software. Separation was carried out on a Dionex carbopac PA1 pre-column (50mmx4mm), followed by a Dionex carbopac PA1 column (250mmx4mm). Injected volume was 100 $\mu\text{L}$  and detection was performed on gold working electrode with Ag/AgCl reference electrode. The sugars were eluted by step-gradient NaOH ranging from 15mM to 135 mM in 1 h.

*Amino acids* in brain homogenates and dialysates were derivatized with 20  $\mu\text{L}$  6-aminoquinolyl-N-hydroxysuccinimidyl carbamate (10 $\mu\text{L}$  sample, 70  $\mu\text{L}$  borate buffer, 55  $^{\circ}\text{C}$ , 10 min) and analyzed by reversed phase chromatography. An HPLC Waters 2695 Alliance system was equipped with a fluorimetric detector Waters 474 (cuvette cell of 5 $\mu\text{L}$ ) and AccQ-Tag Waters column (150mmx3.9mm) containing C18 modified silica phase (particle size 6  $\mu\text{m}$ ) driven by Waters Empower software. Amino acids were eluted using a triple gradient: buffer (sodium acetate at 140mM, triethylamine 17mM, pH 5.05), acetonitrile and ultra-pure water with flow rate 1mL/min, column temperature 37 $^{\circ}\text{C}$  and volume injection 10 $\mu\text{L}$ .

Glutamate analysis by capillary electrophoresis coupled to laser-induced fluorescence (CE-LIF) was performed by the Technological Platform AniRA-Neurochem France (203).

## 9. Statistics

Data are presented as mean  $\pm$  standard deviation (SD) for *in vitro* measurements in standard solutions and as means  $\pm$  standard errors of the mean (SEM) for *ex-vivo/ in vivo* measurements. Comparisons between two data groups were performed using a paired or unpaired Student's *t*-test for equal or unequal variance as indicated by the F-test for equal variance (significance level,  $p < 0.05$ ). Comparisons between three or more data groups were performed using an ANOVA followed by a Fisher LSD post-hoc analysis. Statistical analyses were performed using the Excell analysis tool-pack (Microsoft Office 2007) and SPSS 12.0 for Windows. The sample size (*n*) was equal to the number of biosensors constructed under the same protocol, or the number of animals used in the *in vivo* experiments (where a new biosensor was used in every experiment).

### 3. Results

#### Effect of enzyme immobilization on glucose oxidase substrate specificity

Glucose oxidase is commonly used to monitor glycemia in diabetic patients or glucose intracerebral concentrations in animals (193, 204). In addition to glucose, Glucose oxidase exhibits significant activity to other sugars like 2-Deoxy-D-Glucose (2-DG), D-Galactose, D-Mannose and D-Xylose. It is weakly active to D-Lactose and is insensitive to D-Fructose (205, 206). We determined the effect of enzyme immobilization on Glucose oxidase substrate specificity by testing five immobilization procedures: covalent immobilization with glutaraldehyde (90), PEGDE (119) or hydrogel (153, 175), or entrapment in sol-gel (148, 182) or derived polypyrrole matrices (149, 184). In many studies, hydrogel matrices have been prepared with an electron mediator such as  $[\text{Os}(\text{bpy})_2\text{Cl}]^+$ . However, such mediators have been shown to slow down the biosensor response and were avoided in this study (168). We have therefore simplified the synthesis of hydrogels by eliminating the metal-organic complex additives from the reactive mixture (151).

We then measured the activity of Glucose oxidase either in its free form (PBS solution), or immobilized on a biosensor by one of these five methods, for glucose, and its secondary substrates 2-DG, Galactose, Mannose, Xylose, Lactose and Fructose (Fig. 4.1). After glutaraldehyde immobilization, Glucose oxidase activity for all secondary substrates increased significantly. By contrast, PEGDE and hydrogel immobilization resulted in increased activity to 2-DG (Fig 4.1A), but not to other secondary substrates; sol-gel immobilization resulted in increased activity to 2-DG and Fructose (Fig. 4.1B-D). Finally, derived polypyrrole entrapment did not induce significant effects on Glucose oxidase activity towards any secondary substrate. To quantify these effects on enzyme specificity, we introduced a selectivity constant computed as the ratio of activity to glucose by the geometric mean of activities for secondary substrates (the geometric mean is well suited for averaging data in different numeric ranges, as is the case for 2-DG and fructose activities for example, Fig. 4.1E). There was a significant effect of the enzyme immobilization method on glucose oxidase substrate specificity ( $F(5,29)=12.8$ ,  $p<0.01$ ). We obtained a selectivity constant of  $455 \pm 33$  for the free enzyme that was not significantly different from those computed after enzyme immobilization by PEGDE ( $335 \pm 219$ ,  $n=6$ ), hydrogel ( $405 \pm 123$ ,  $n=6$ ) or sol-gel ( $286 \pm 111$ ). However, glutaraldehyde significantly decreased the selectivity constant to  $138 \pm 60$  ( $p<0.01$ ,  $n=6$ ). Surprisingly, biosensors prepared with glucose oxidase immobilized by derived polypyrrole showed an increased apparent specificity to glucose compared to the free form of glucose oxidase ( $767 \pm 205$ ,  $p<0.01$ ,  $n=6$ , Fig. 4.1E). These results show that the immobilization methods chosen for biosensor fabrication can significantly impact glucose oxidase substrate specificity.

In addition to glucose, glutamate biosensor detection *in vivo* has also been the focus of intense investigation (28, 112, 141, 152). We therefore determined the effects of immobilization on Glutamate oxidase, the enzyme that is typically used for glutamate detection.

#### Effect of enzyme immobilization on Glutamate oxidase substrate specificity

For studying Glutamate oxidase, we focused on glutaraldehyde and PEGDE immobilization methods. We could not achieve stable glutamate oxidase immobilization using derived polypyrrole. Sol-gel immobilization yielded biosensors that were stable only for a few hours at room temperature, which was insufficient to complete our selectivity studies. In addition, hydrogel and PEGDE immobilization appeared very similar because (1) PEGDE is a

component used for hydrogel preparation and is responsible for enzyme covalent immobilization in the hydrogel mixture, and (2) we did not detect any significant difference between the two methods with Glucose oxidase.

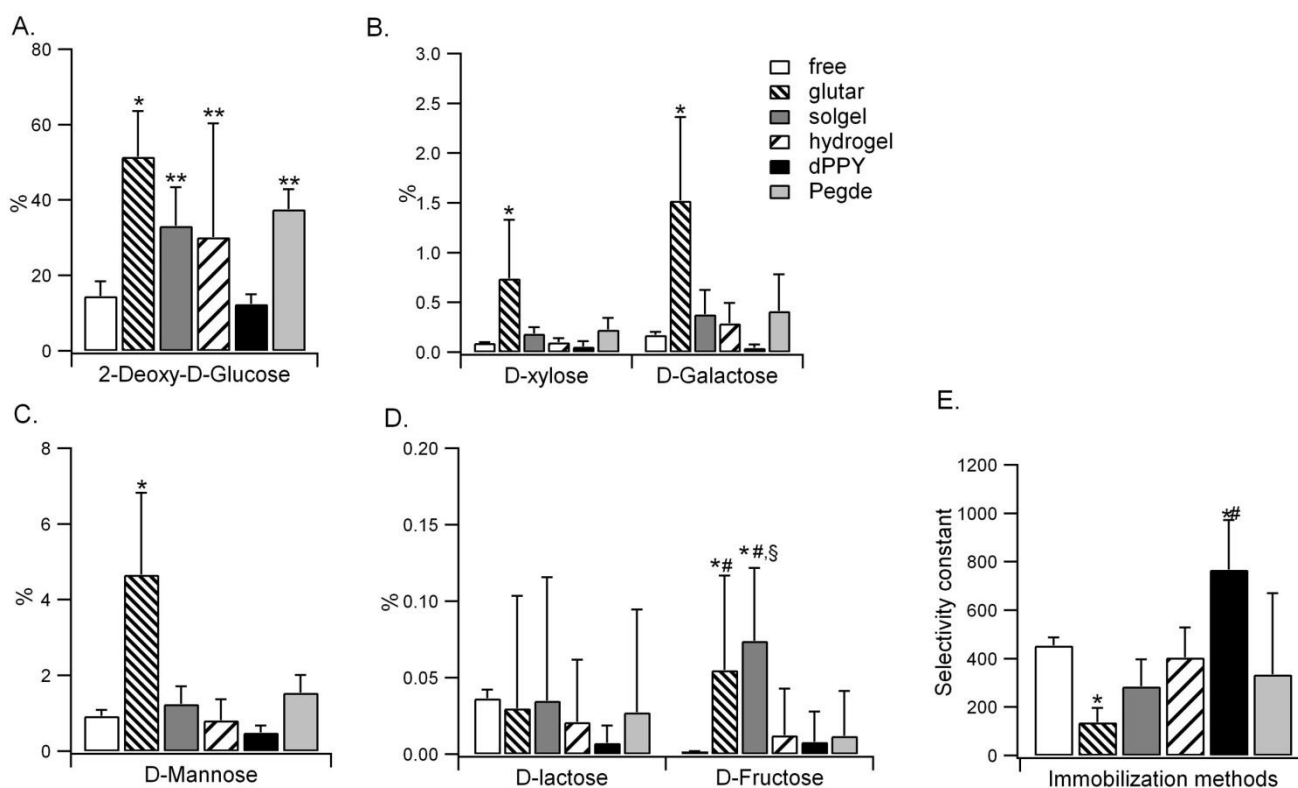


**Figure 4.1: Effect of enzyme immobilization method on glucose oxidase substrate-specificity.**

Enzymatic activity was tested on D-sugars other than glucose: A. Deoxy-D-Glucose, B. Xylose and Galactose, C. Mannose, D. Lactose and Fructose. Glucose oxidase was tested in its free form (free), or after immobilization by glutaraldehyde (glutar), sol-gel, hydrogel, derived polypyrrole (dPPy) or poly(ethylene glycol) diglycidyl ether (PEGDE). The least selective biosensors were obtained using Glutar and the most selective ones were based on dPPy. \* Significantly different from the free enzyme, \*\* significantly different from the free enzyme and Glutar, # significantly different from dPPy, § significantly different from PEGDE, n=6. E. Selectivity constant representing the impact of immobilization technique on enzyme selectivity, \* significantly different from free enzyme, # significantly different from other methods.

We tested Glutamate oxidase activity on four potential secondary substrates present *in vivo*: glutamine, asparagine, aspartate and histidine (100-500  $\mu$ M). Glutamate oxidase in its free form (PBS solution, pH 7.4) is extremely specific to glutamate. There was no detectable activity to the four amino acids that we tested (Fig. 4.2). Very little activity to these secondary substrates could be detected when glutamate oxidase was immobilized by PEGDE (0.03 to 0.3 % of glutamate activity, Fig. 4.2). This loss of enzyme specificity was exacerbated when immobilization was performed using glutaraldehyde, with a secondary activity to asparagine up to 15% of the activity to glutamate (Fig. 4.2). A selectivity ratio could not be defined for the free form of Glutamate oxidase (it would be infinite), but was  $1494 \pm 648$  after PEGDE immobilization and  $22 \pm 14$  after glutaraldehyde immobilization ( $p < 0.01$ ,  $n = 12$ ). Therefore Glutamate oxidase lost its substrate specificity after immobilization, especially when glutaraldehyde was used as the cross-linker.

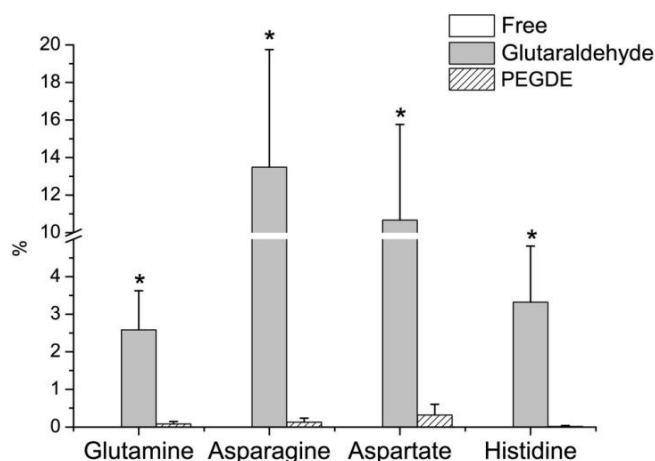


**Figure 4.2: Effect of enzyme immobilization method on glutamate oxidase substrate-specificity.** Enzymatic activity was tested on interfering amino acids glutamine, asparagine, aspartate and histidine. Free Glutamate oxidase appeared completely specific to glutamate –no signal was observed in presence of other amino acids. Specificity was dramatically altered after glutaraldehyde immobilization, resulting in detection of glutamine, asparagine, aspartic acid and histidine. By contrast, immobilization with PEGDE preserved enzyme specificity. \* Significantly different from the free enzyme,  $n \geq 12$ .

### Glucose and glutamate detection in biological media

Biological media such as serum, cerebrospinal fluid, brain homogenates or microdialysates are complex mixtures containing probably several hundred different molecules. The loss of enzyme specificity following immobilization on a biosensor could therefore profoundly impact analyte detection and quantification, especially when measurements are performed *in vivo*. To evaluate the potential impact of this loss of specificity, we quantified the concentrations of potential secondary substrates of Glucose oxidase and Glutamate oxidase in serum, brain homogenates and microdialysates obtained from rats.

We used HPLC coupled to amperometric detection to measure D-glucose, D-mannose and D-galactose in rat serum and brain homogenates (Fig. S 4.6). 2-DG is a specific glycolysis blocker that is not present in biological media under physiological conditions (207). D-galactose was undetectable in serum and present only at very low levels in brain homogenates ( $0.61 \pm 0.11 \mu\text{g/g}$  wet tissue, Table 4.1). Significant D-mannose concentrations were detected in serum ( $0.03 \pm 0.01 \text{ mM}$ ) and brain homogenates ( $24.42 \pm 6.19 \mu\text{g/g}$  wet tissue, Table 4.1). However, D-glucose was by far the most concentrated sugar in our biological media ( $11 \pm 2 \text{ mM}$  in serum,  $97.37 \pm 10.37 \mu\text{g/g}$  wet tissue in brain homogenates, Table 4.1). Because potential secondary substrates of Glucose oxidase were detected in comparatively lower amounts than glucose, we expected that the changes in enzyme specificity induced by immobilization would not impact biosensor glucose detection significantly.

We next used HPLC coupled to fluorimetric detection to detect amino acids in rat brain homogenates and microdialysates. We measured the concentrations of 20 proteinogenic amino acids (excepting hydroxy-proline, example chromatograms in supplementary Fig. S4.7). In brain homogenates, glutamate was the most concentrated amino acid ( $1981 \pm 434 \mu\text{g/g}$  wet tissue) followed by glutamine ( $1044 \pm 245 \mu\text{g/g}$  wet tissue) and aspartate ( $427 \pm 100 \mu\text{g/g}$  wet tissue, Table 4.2). By contrast, in brain microdialysates (a good representation of the brain interstitial fluid), glutamate was present at low concentrations ( $4 \pm 1 \mu\text{M}$ ) compared to glutamine ( $41 \pm 15 \mu\text{M}$ ), proline ( $12 \pm 8 \mu\text{M}$ ) and lysine ( $9 \pm 2 \mu\text{M}$ , Table 4.2). This comparatively low glutamate concentration compared to potential secondary substrates of Glutamate oxidase suggested that unlike glucose, glutamate biosensor detection in the CNS could be significantly impacted by the loss of substrate specificity induced by enzyme immobilization.

**Table 4.1. HPLC identification of sugars in serum and brain homogenates**

Sugar	Serum	Brain homogenate
	Concentration (mM)	Concentration ( $\mu\text{g/g}$ )
Galactose	< 0.00055	0.61 $\pm$ 0.11
Glucose	10.86 $\pm$ 1.93	97.37 $\pm$ 10.37
Mannose	0.0333 $\pm$ 0.0144	24.42 $\pm$ 6.19

To verify the validity of our biosensor measurements, we estimated glucose and glutamate concentrations in the same biological samples using biosensors prepared with glutaraldehyde or PEGDE immobilization, and compared them to HPLC or CE-LIF data (because of the small volumes of brain microdialysates, glutamate concentrations were estimated using CE-LIF). As expected, HPLC and biosensors prepared with Glucose oxidase immobilized by glutaraldehyde or PEGDE yielded similar glucose concentrations confirming that glucose biosensor detection was not impacted by potential secondary substrates of Glucose oxidase (Fig 4.3). However, glutamate detection in brain microdialysates using biosensors prepared with glutaraldehyde yielded significantly higher estimates when Glutamate oxidase was immobilized with glutaraldehyde (145.1 $\pm$ 43.0% of CE estimate,  $F(2,68)=6.20$ ,  $p<0.01$ ) than with PEGDE (108.7 $\pm$ 46.1% of CE estimate, Fig 4.3). We estimated the impact of possible interference by glutamine, asparagine, aspartate, and histidine, based on their concentrations measured in microdialysates by HPLC, and the enzymatic activity measured after glutaraldehyde immobilization. In addition to the specific electrochemical signal generated by the 4  $\mu\text{M}$  glutamate present in the microdialysates, biosensors prepared using glutaraldehyde would detect non-specific signals that would add 1  $\mu\text{M}$  (40  $\mu\text{M}$  glutamine, 2.5 % enzymatic activity), 0.18  $\mu\text{M}$  (1.5  $\mu\text{M}$  asparagine, 12% activity), 0.16  $\mu\text{M}$  (1.6  $\mu\text{M}$  aspartate, 10% activity) and 0.09  $\mu\text{M}$  (3  $\mu\text{M}$  histidine, 3% activity), therefore a total of 1.43  $\mu\text{M}$  (+ 35.8%) apparent glutamate. Therefore, non-specific detection of glutamine, asparagine, aspartate and histidine by glutamate oxidase after immobilization of glutaraldehyde accounted for most of the discrepancy between glutaraldehyde-based biosensors and PEGDE-based biosensors or CE. These results indicate that enzyme immobilization using PEGDE should be preferred for glutamate detection in the CNS.

**Table 4.2. HPLC identification of proteinogenic amino acids in brain dialysate and homogenate**

Aminoacids	Brain dialysate	Brain homogenate
	Conc., $\mu\text{M}$	Conc., $\mu\text{g/g}$
<b>Aspartic acid</b>	<b>1.58 <math>\pm</math> 0.45</b>	<b>426.8<math>\pm</math>100.1</b>
Glutamic acid	4.04 $\pm$ 0.90	1980.6 $\pm$ 434.1
Serine	4.90 $\pm$ 1.8	104.4 $\pm$ 16.6
<b>Asparagine</b>	<b>1.53 <math>\pm</math> 0.61</b>	<b>7.0<math>\pm</math>0.7</b>
Glycine	2.96 $\pm$ 0.57	48.4 $\pm$ 2.5
<b>Glutamine</b>	<b>41.44 <math>\pm</math> 15</b>	<b>1044.2<math>\pm</math>244.7</b>
<b>Histidine</b>	<b>2.89 <math>\pm</math> 0.30</b>	<b>12.2<math>\pm</math>1.8</b>
Threonine	5.01 $\pm$ 0.92	83.0 $\pm$ 18.4
Arginine	3.89 $\pm$ 0.48	14.6 $\pm$ 1.3
Alanine	6.04 $\pm$ 0.94	42.8 $\pm$ 1.3
Proline	11.85 $\pm$ 7.9	57.3 $\pm$ 5.2
Tyrosine	0.71 $\pm$ 0.20	10.0 $\pm$ 1.2
Cysteine	0.83 $\pm$ 0.00	6.6 $\pm$ 5.5
Valine	3.89 $\pm$ 0.44	6.9 $\pm$ 0.5
Methionine	0.72 $\pm$ 0.23	4.5 $\pm$ 0.4
Iso-leucine	3.07 $\pm$ 0.43	3.2 $\pm$ 0.0
Leucine	2.54 $\pm$ 0.46	8.1 $\pm$ 0.4
Lysine	8.71 $\pm$ 2.06	31.6 $\pm$ 4.8
Phenylalanine	1.48 $\pm$ 0.24	6.9 $\pm$ 1.4
Tryptophan	3.20 $\pm$ 0.75	97.9 $\pm$ 38.8

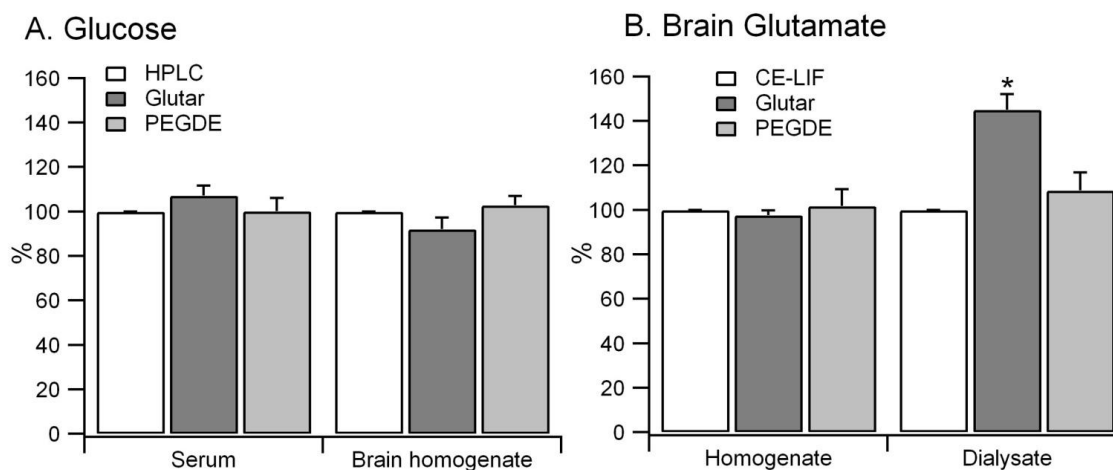


**Figure 4.3: Biosensor specificity in biological samples.** A. Glucose. The glucose concentration estimated by Glutaraldehyde- or PEGDE-based biosensors in serum or brain homogenates was not significantly different from that measured by HPLC ( $n \geq 16$ ). B. Glutamate. Glutamate concentration estimates in brain homogenates were similar for CE-LIF and biosensors prepared with glutaraldehyde or PEGDE. However, in brain microdialysates, biosensors prepared with glutaraldehyde yielded significantly higher estimates of glutamate concentration. \* Significantly different from EPC,  $n \geq 25$ .

### ***In vivo* glutamate detection**

We then implanted biosensors in which glutamate oxidase was immobilized by PEGDE or glutaraldehyde *in vivo* to determine whether more selective glutamate biosensors could change our understanding of glutamate regulation in the interstitial fluid. We first implanted our biosensors in animals anesthetized with isoflurane to determine glutamate basal concentrations in cortex. Three biosensors were implanted side by side: two glutamate biosensors using glutaraldehyde or PEGDE immobilization, and one control biosensor in which glutamate oxidase was replaced by bovine serum albumin (BSA, Fig. 4.4A). The steady-state current reflecting the basal level of glutamate was monitored after an initial 30 min stabilization period. The oxidation current detected by glutaraldehyde-based biosensor was  $118 \pm 8.5$  pA, significantly higher than that detected by PEGDE-based biosensors ( $28.2 \pm 1.2$  pA) and control biosensors ( $16.2 \pm 1.0$  pA, Fig. 4.4B,  $F(2,15)=20.69$ ,  $p < 0.01$ ). We then computed the extracellular glutamate concentrations from these oxidation currents (see methods). PEGDE-based biosensors estimated glutamate resting level in the cortex at  $1.16 \pm 0.34$   $\mu$ M, whereas glutaraldehyde-based biosensors provided much higher estimates at  $16.4 \pm 8.4$   $\mu$ M ( $n=6$ , Fig. 4.4C).

We then determined whether glutamate basal concentrations varied with the level and the type of anesthesia. We measured glutamate extracellular concentrations under isoflurane and urethane anesthesia, as well as in awake animals. However, no significant difference was observed between these three situations (Fig. 4.4D).



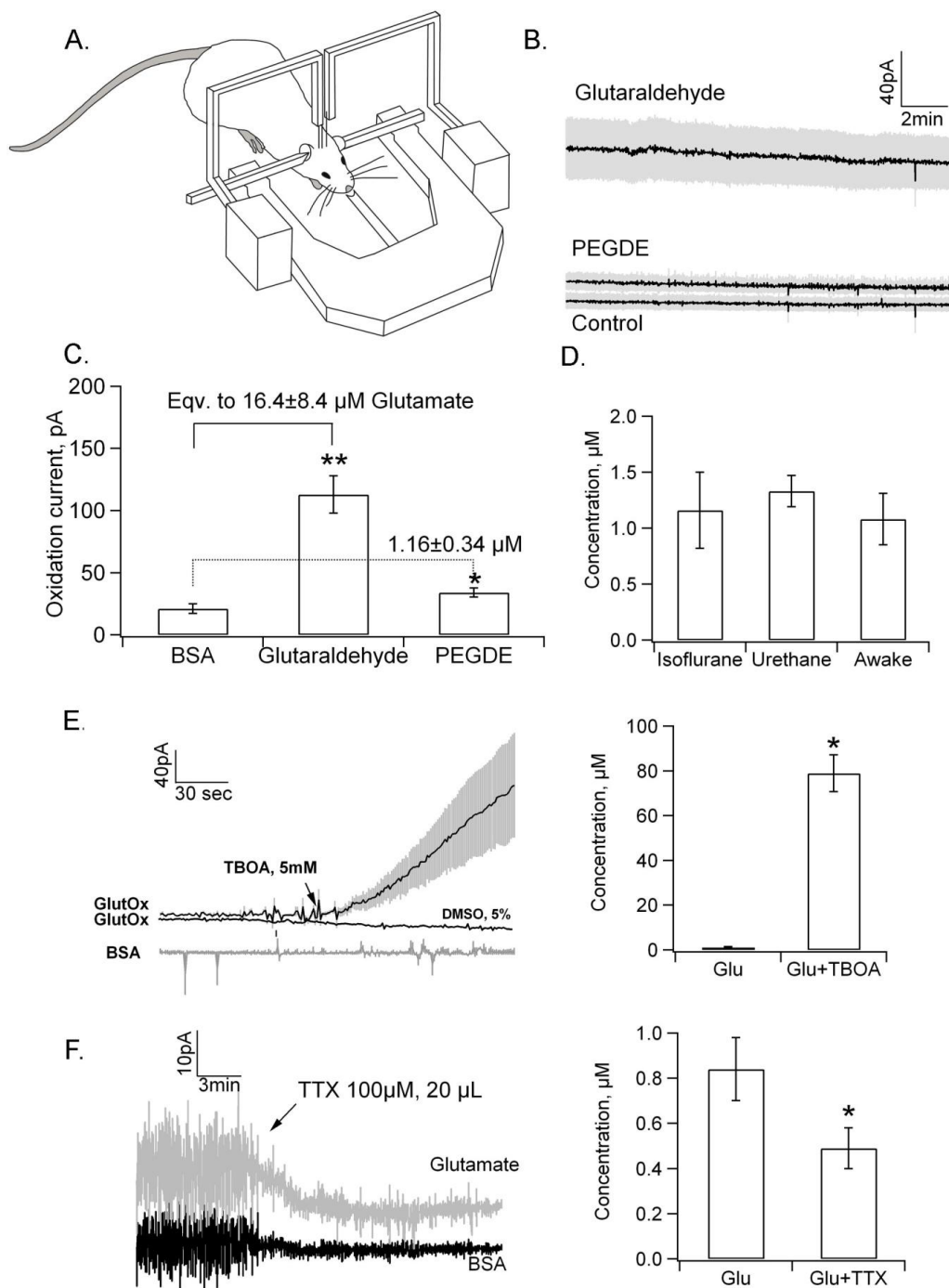


**Figure 4.4 : *In vivo* glutamate detection in the cortex.** A. Schematic representation of the rat position in the stereotaxic apparatus with respective position of working and control biosensors. B. Oxidation currents recorded in the cortex of an anesthetized rat with Glutaraldehyde and PEGDE-based biosensors, and by a control biosensor. Glutamate concentrations were computed from the difference in currents recorded by glutamate oxidase biosensors and control biosensors. C. Quantitative estimation of glutamate basal concentration in the cortex under isoflurane anesthesia. \* Significant difference from the control electrode, n=6. D. Glutamate concentration under urethane or isoflurane anesthesia compared to that in an awake animal. E. Effect of TBOA administration on glutamate extracellular concentration in the cortex (20μL, 5mM). Mean glutamate concentration after TBOA application is increased from 1.16±0.33μM to 79±8μM (right). \* Significant difference from the control electrode, n=6. F. Effect of a local TTX injection (20μL, 100μM) on Glutamate extracellular concentration. Glutamate basal concentration rapidly decreases by 34.8±9.3% after TTX application. \* Significantly different from the basal glutamate concentration, n ≥5.

We then sought to modulate glutamate extracellular levels pharmacologically using the glutamate reuptake blocker TBOA and the voltage-gated Na<sup>+</sup> channel blocker TTX. TBOA (5mM in DMSO 5%) was applied on the pia, and glutamate extracellular concentration was monitored 0.3 mm below the surface. TBOA induced a rapid increase in glutamate concentration from  $1.16 \pm 0.34 \mu\text{M}$  to  $79 \pm 8 \mu\text{M}$  ( $n=5$ ,  $p<0.01$ ), Fig. 4.4E). This increase in oxidation current was not detected at the control biosensor or in response to DMSO (5%) application alone, and confirmed that the electrochemical signal detected by PEGDE-based biosensors was dependent on extracellular glutamate. TTX (100 $\mu\text{M}$ , 20 $\mu\text{L}$ ) was injected locally near a glutamate- and control biosensor. Blockage of voltage-gated Na<sup>+</sup> channels produced a rapid silencing of neuronal firing evidenced by a drop in local field potentials detected by our biosensors (Fig. 4.4F, (208)). In response to neuronal silencing, glutamate extracellular concentration decreased by  $34.8 \pm 9.3\%$  (21.47 to 14.14 pA,  $n=6$   $p<0.01$ ). By contrast, electrochemical currents detected by the control biosensor decreased only by  $0.78 \pm 0.18$  pA (Fig. 4.4F).

Finally, we sought to detect glutamate spillover into the extrasynaptic space following neuronal stimulation. A stimulating electrode was inserted in the perforant path and a microelectrode biosensor was implanted in the dentate gyrus to monitor glutamate levels in response to stimulation (Fig. 4.5A). Field potentials evoked by perforant path stimulation were recorded from the biosensor at different depths to adjust the position of the stimulating electrode and biosensor and to place the biosensor at the current sink of the stimulation (208). Stimulation of the perforant path evoked a transient increase in oxidation current in biosensors prepared with glutaraldehyde, equivalent to  $1.46 \pm 0.19 \mu\text{M}$  glutamate during about 5s. However, this apparent glutamate spillover was not confirmed using biosensors prepared with PEGDE. There was a significant difference between the current response evoked by neuronal stimulation at glutaraldehyde-based biosensors compared to PEGDE-based biosensors ( $n=6$ ,  $p<0.01$ , Fig. 4.5B, right).

## 4. Discussion

### *Effects of immobilization techniques on enzyme substrate specificity*

One basic principle underlying enzymatic biosensor technology is to use the excellent substrate specificity of natural enzymes to recognize molecules in complex media. In this study, we found that the different immobilization methods used for preparing enzymatic biosensors can significantly alter the substrate specificity of the enzyme. For example, immobilization with glutaraldehyde significantly degraded the selectivity of Glucose oxidase, whereas alternative methods like PEGDE, hydrogel, sol-gel or derived polypyrrole entrapment preserved it. This effect was confirmed with Glutamate oxidase whose substrate specificity was preserved after immobilization with PEGDE, but not glutaraldehyde.

The precise molecular mechanisms that underlie these effects on substrate specificity are difficult to determine and remain largely empirical. Enzyme immobilization creates chemical bonds between the enzyme and the matrix that could modify its tridimensional conformation and substrate recognition (194). Moreover, immobilized enzyme molecules are surrounded by a macromolecular matrix in which different substrates must diffuse before reaching the active site. The changes in diffusion coefficients between the solution and the matrix, as well as the affinity of each substrate towards the matrix could cause them to be concentrated or excluded from the enzyme membrane, thus creating a partitioning effect (209-212). Such kinetics and diffusion effects are often difficult to distinguish.

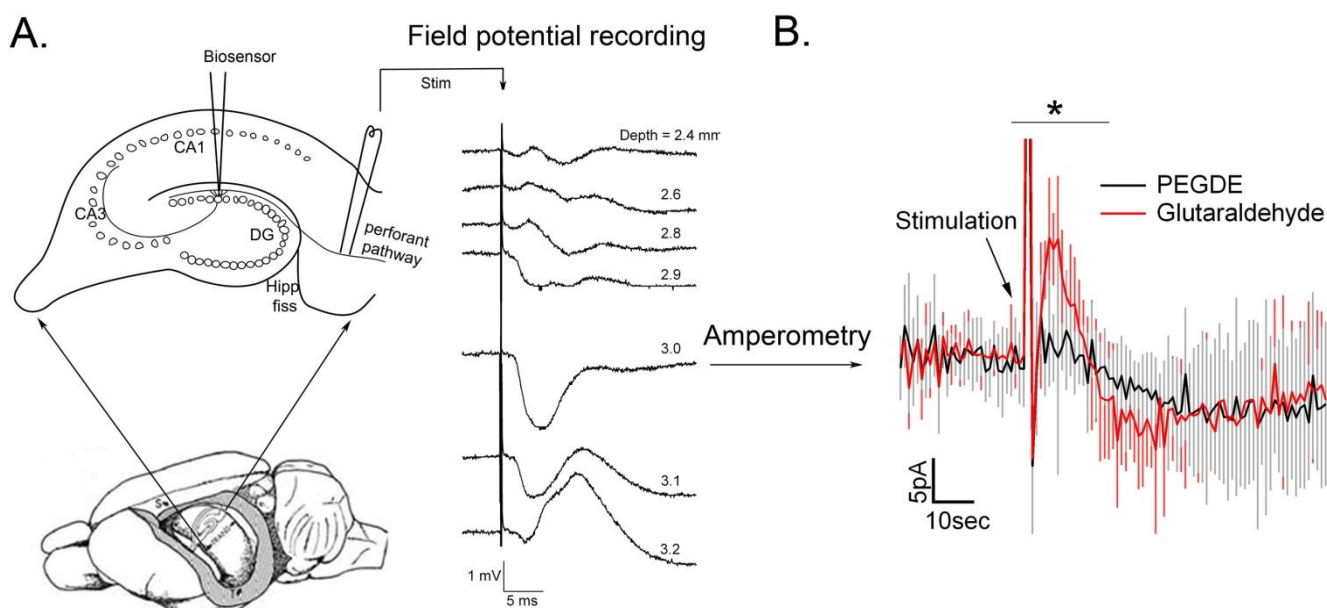


**Figure 4. 5 : Detection of Glutamate spillover in the dentate gyrus.** A. Schematic representation of the stimulation setup. A stimulating electrode and a microelectrode biosensor were inserted in the perforant path and the dentate gyrus respectively in an anesthetized rat. Field potentials evoked by perforant path stimulation are recorded from the biosensor. The stimulating electrode and biosensor positions are adjusted in order to place the biosensor at the current sink of the stimulation. B. Stimulation of the perforant path evoked an increase in oxidation current on biosensor prepared with glutaraldehyde (equivalent to  $1.46 \pm 0.19 \mu\text{M}$  Glutamate) However, this apparent glutamate spillover was not confirmed using biosensors prepared with PEGDE, suggesting that it was due to changes in the concentrations of other amino acids. \* Significant current increase.

Modification of enzyme substrate specificity by immobilization is frequently encountered. Enzyme immobilization often results in a loss of substrate specificity due to enzyme rigidification, but can also lead to improved apparent specificity (194). For example,  $\alpha$ -D-galactosidase, an enzyme with natural broad substrate specificity, becomes unable to hydrolyze large oligosaccharides once immobilized with glutaraldehyde, because of steric hindrance within the membrane matrix, resulting in improved apparent substrate specificity (201). In addition, immobilization can improve the enantioselectivity of lipases or Penicillin G acylase by blocking the large conformational changes required for catalysis of some but not all substrates (194). In our hands, enzyme entrapment in a derived polypyrrole matrix also resulted in enhanced apparent specificity compared to the free enzyme, although most of the other immobilization methods that we tested decreased it.

In biosensor preparation, specific detection of a single substrate in complex mixtures requires the use of enzymes with high substrate specificity, which must be preserved during immobilization. To prevent unwanted distortion in the enzyme active site, or limitation in its mobility, it is necessary to use mild immobilization protocols. In this regard, PEGDE immobilization is indeed particularly mild. The kinetics of the cross-linking reaction between PEGDE epoxy groups and amine groups on the enzyme surface is slow (48h at room temperature, 2h at  $55^\circ\text{C}$ , (119, 151)). Moreover, the length of the PEGDE spacer arm is about 4 nm, which is favorable to preserve the conformation of the enzyme, and allow

conformational changes during catalysis. In fact, the overall dimensions of the deglycosylated glucose oxidase dimer are  $7 \times 5.5 \times 8$  nm (213), and thus, comparable to the length of the PEGDE spacer arm. By comparison, glutaraldehyde immobilization is much faster (2-3 min at room temperature) and the spacer arm is more than five times shorter (about 0.7 nm, computed using HyperChem Software, Fig. S 4.8), resulting in protein rigidification (194).

#### Consequences for *in vivo* biosensor detection

Changes in enzyme substrate specificity due to immobilization on a microelectrode can have crucial consequences for *in vivo* biosensor detection. In this study, we determined the specificity of our biosensor measurements by comparing them to HPLC or CE-LIF analyses. We show that changes in glucose oxidase substrate specificity has no significant consequences on glucose detection in blood or brain because glucose is present *in vivo* at higher concentrations (a few mM, (111)) than those of the possible interfering molecules galactose or mannose. However, glutamate is present at much lower concentrations than glucose in the brain extracellular fluid (no more than a few  $\mu\text{M}$ , (16, 19)) and possible interfering molecules like glutamine, asparagine or aspartate can lead to significant electrochemical currents if the specificity of glutamate oxidase is not preserved during immobilization. As a result, glutamate biosensors prepared with glutaraldehyde immobilization significantly overestimated the true glutamate concentration present in rat brain microdialysates due to a loss of substrate specificity.

Glutamate is the principal excitatory neurotransmitter in the brain and is implicated in many brain diseases like stroke, epilepsy or Parkinson's disease (214). Glutamate detection in the central nervous system *in vivo* is therefore an important technical and scientific challenge. Glutamate is readily detected *in vivo* using microdialysis: its concentration in the rat cortex ranges between 0.2 and 4  $\mu\text{M}$  under anesthesia (215-217) and from 0.2 to 9  $\mu\text{M}$  in awake animals (218-220). However, this technique suffers from a low temporal resolution and local brain injuries produced upon implantation of the microdialysis probe into the brain parenchyma (221, 222). Glutamate detection *in vivo* using microelectrode biosensors has already been performed, but so far, has provided extremely variable results ranging from 1.6  $\mu\text{M}$  (glutaraldehyde) (107) to 29  $\mu\text{M}$  (hydrogel) (112, 152) under anesthesia and to 45  $\mu\text{M}$  in awake animals (glutaraldehyde) (28). In addition to their high variability, such high concentration estimates are problematic because excessive extracellular glutamate levels can cause excitotoxicity. For example, culture studies show that neurons can hardly survive for 24h in the presence of 20  $\mu\text{M}$  glutamate (19). Our study now shows that the immobilization method that is used for manufacturing microelectrode biosensors can significantly impact the quantification of glutamate concentration in the brain extracellular fluid, with glutaraldehyde immobilization leading to significant overestimation due to a loss of glutamate oxidase substrate specificity.

We have investigated the regulation of glutamate extracellular concentration *in vivo* using microelectrode biosensors that differed only by the immobilization method that was used during manufacturing (microelectrode size and impedance were the same). We have shown that glutamate extracellular concentration estimated by PEGDE-based biosensors is (1)  $1.16 \pm 0.34$   $\mu\text{M}$  at rest in the cortex, (2) not dependent upon anesthesia (as evidenced in awake animals or under isofurane or urethane anesthesia), (3) partly (35%) dependent on nerve impulse as revealed by TTX administration, and (4) not significantly impacted by spillover from synaptic stimulation in the dentate gyrus. These results are at variance with previous studies using glutaraldehyde-based biosensors suggesting that glutamate levels are

higher during wakefulness than during anesthesia (28, 107), or that glutamate could readily diffuse from the synapse to the extrasynaptic space in response to neuronal stimulation (223). In addition, TTX administration is often used to validate the neuronal origin (by blocking voltage-gated Na<sup>+</sup> channels necessary for nerve impulse) of the glutamate detected by biosensors. TTX was reported to decrease glutamate extracellular concentration by 25% (hydrogel) (152), 90% (hydrogel) (112) or even 100% (glutaraldehyde) (107). The 35% decrease in glutamate extracellular concentration detected by our PEGDE-based glutamate biosensors is consistent with the current model of extracellular glutamate regulation by the cysteine-glutamate exchanger, a Na<sup>+</sup>-dependent antiporter preferentially located on glia (8). The lack of detectable glutamate spillover following synaptic stimulation is also consistent with recent imaging studies relying on glutamate fluorescent detection, that found glutamate spillover of about 2 μM during less than 300 ms. (224). Such rapid changes in glutamate concentration would not be detectable using enzymatic biosensors with a response time of 2-3 s.

The use of more specific glutamate biosensors based on a PEGDE-based mild enzyme immobilization method therefore leads to an understanding of brain glutamate regulation that is consistent with independent data from the literature. Among the possible molecules that could interfere with glutamate detection in glutaraldehyde-based biosensors, glutamine is especially concerning because (1) it is present at much higher concentrations than glutamate in the brain extracellular fluid, (2) it is detected by glutamate-oxidase immobilized with glutaraldehyde, and (3) it is actively shuttled between neurons and glia during the process of neurotransmission (25, 26), which could give rise to fast transients resembling those associated to neurotransmitter release and spillover. However, other factors than enzyme immobilization, such as microelectrode size or placement, are probably important as well for accurate glutamate detection *in vivo*. More studies will be required in the future for determining the physiological range of glutamate extracellular concentrations. In this regard, patch-clamp studies in brain slices have estimated resting ambient glutamate concentration around 25 nM (225), which is much lower than our current biosensor estimates. This difference is clearly independent of glutamate oxidase substrate specificity and its origin will need to be further explored. Overall, the use of microelectrode biosensors prepared with mild enzyme immobilization methods like those involving PEGDE paves the way for accurate direct measurements of neurotransmitter concentrations *in vivo*, and will therefore provide valuable tools for studying the chemistry of brain cell communication.

## 5. Conclusion

PEGDE-based enzyme immobilization is an optimal method for microelectrode biosensor preparation. Because it involves covalent cross-linking between the enzyme and its surrounding matrix, this method allows stable immobilization (119) that is especially suited for *in vivo* measurements. It is simple and non-toxic, which makes it potentially biocompatible. This study now shows that PEGDE immobilization is mild enough to preserve enzyme substrate specificity, which is the basis of specific measurements *in vivo*. These advantages make PEGDE an optimal component for the immobilization not only of glucose oxidase and glutamate oxidase, but also of a wide range of other enzymes with potential interest for *in vivo* biosensor technology. This method paves the way for accurate direct measurements of neurotransmitter concentrations *in vivo*, and will therefore provide valuable tools for studying the chemistry of brain cell communication.

## **Acknowledgements**

This study was supported by Inserm U1028 and Université Claude Bernard Lyon I, and by grants from Agence Nationale pour la Recherche (ANR-09-BLAN-0063 Neurosense) and Lyon Neuroscience Research Center. NV and CM are recipients of PhD fellowships from Ministère de la Recherche. We are grateful to Sandrine Parrot for capillary electrophoresis glutamate analysis performed at AniRA-Neurochem Technological Platform. Serge Cosnier kindly provided samples of pyrrole-derived monomer. We are grateful to Bogdan Barnych for help with synthesis of hydrogel polymer.

### Supporting information

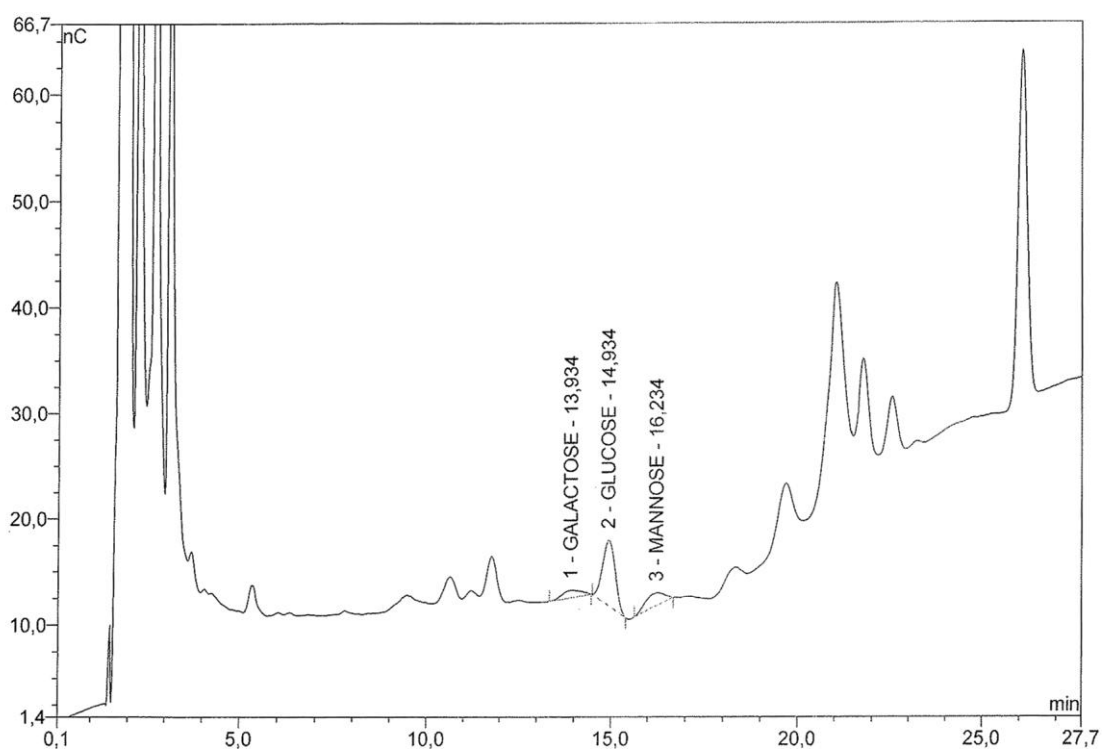


**Figure S4.6: HPLC analysis of sugars in brain homogenates.** Example chromatogram obtained from a rat brain homogenate. Galactose, glucose and mannose are detected at 13.9, 14.9 and 16.2 min retention time respectively (peaks 1, 2, 3).

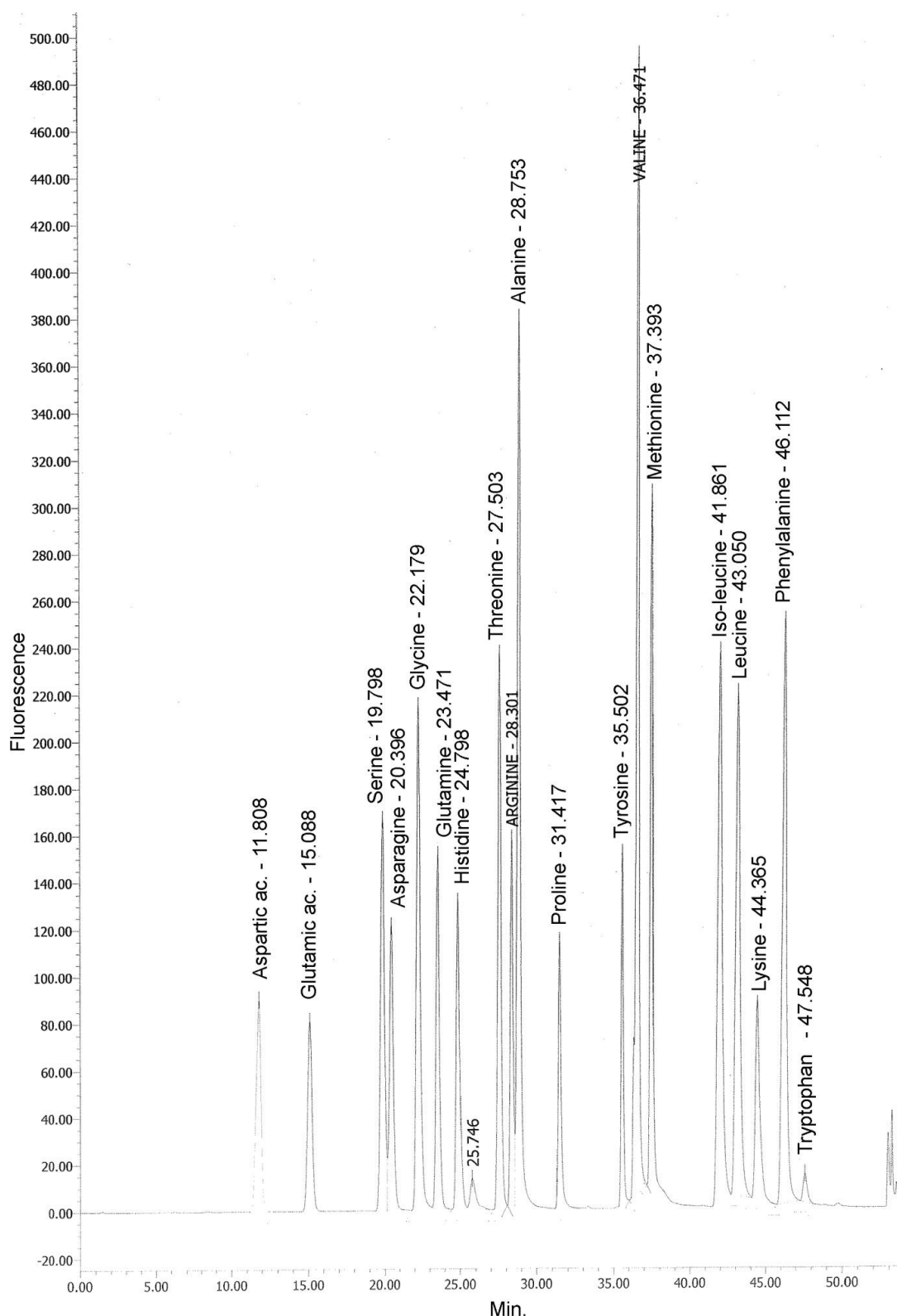


**Figure S4.7: HPLC analysis of amino acids in brain homogenate.** Example chromatogram obtained from a rat brain homogenate. Proteinogenic amino acids (excepting hydroxyl-proline) are detected peaks between 11.8 (aspartic acid) and 47.5 min (tryptophan) retention time. Fluorescence intensity is expressed in arbitrary units.



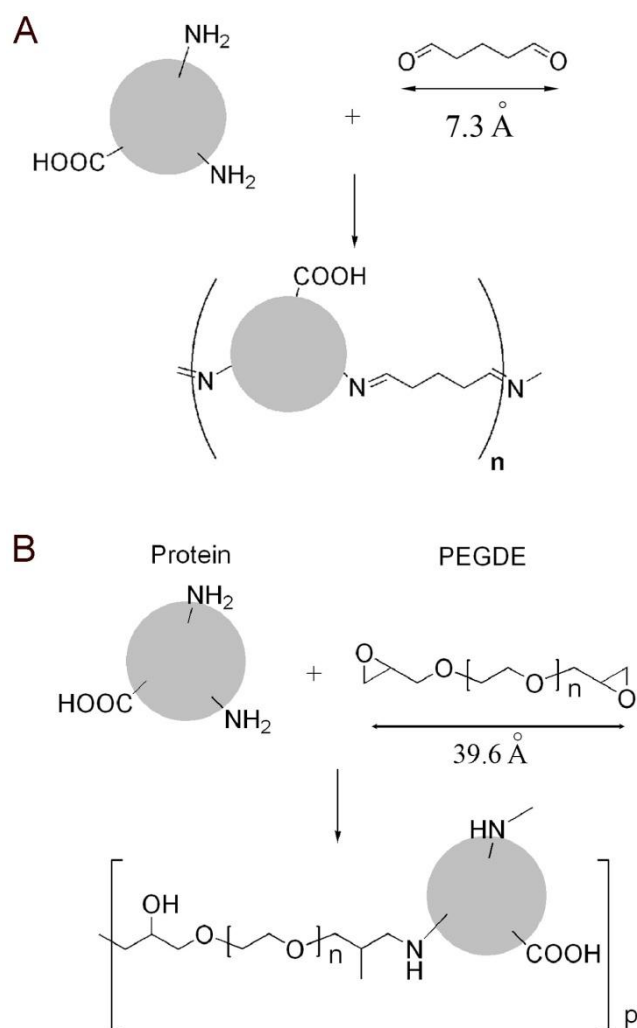


**Figure S4.8: Covalent immobilization techniques.** A. Reaction scheme for protein cross-linking by glutaraldehyde. Aldehyde groups react preferentially with amino groups present within the protein to produce covalent bonds between proteins. B. General reaction scheme of protein with poly(ethylene glycol) diglycidyl ether. Protein molecules contain amino- and carboxyl groups that may react with the 2 epoxides of PEGDE, resulting in immobilization. One major difference between PEGDE and glutaraldehyde is the length of the spacer arm. It is 4 nm for PEGDE but only 0.7 nm for glutaraldehyde (computed with the HyperChem Software).

## Chapter 5:

# Multi-sensing bioprobes on silicon

This chapter describes the development of a three-electrode microarray using microfabrication technologies on silicon. It adapts the published conference proceeding at Eurosensors XXV, September 4-7, 2011, Athens, Greece:

Vasylieva, N., Sabac, A., Marinesco, S., and Barbier, D. (2011) *Simple and non toxic enzyme immobilization onto platinum electrodes for detection of metabolic molecules in the rat brain using silicon micro-needles*, Procedia Engineering 25, 1361-1364.

The chapter presents the procedures of enzyme deposition on the electrode surface and the optimization of immobilization conditions. Studies of peroxide diffusion and enzymatic cross-talk are presented. The multi-sensing microarrays for simultaneous glucose and lactate monitoring have been validated in the cortex of anesthetized rats.



Enzymatic microelectrode biosensors are a powerful tool for *in vivo* molecules monitoring in the CNS of laboratory animals. They have a small size preserving brain integrity and high temporal resolution. These biosensors are often fabricated employing a platinum wire encased in a glass-capillary. They are very fragile and potentially dangerous for clinical application in humans. Additionally, current neurological studies attempt to understand different parallel processes occurring in brain functioning that require the monitoring of several biological markers and/or signaling molecules. This would require implanting several electrodes leading to extended brain damage and alteration in physiological brain functioning. During the last decade, increasing accessibility to “Clean-room” facilities for microelectrochemical systems development has made it possible to fabricate microdevices comprising several electrodes on silicon, ceramic or even flexible polymer supports that are more robust than glass micropipettes. These devices are now largely used for neural recordings (94, 101, 226-228). However, up to now, only a few groups have succeeded in using such multi-electrode microprobes for enzymatic biosensor construction and monitoring *in vivo*. Miniaturization of electrodes makes enzyme deposition difficult because good spatial resolution is required to limit cross-contamination of adjacent electrodes by different enzymes. In addition, biosensors have to remain high sensitivity toward their substrates despite their miniaturized planar geometry. Finally, these biosensors must keep their *in vivo* and long-term stability.

The development of such microdevices is a complex multistage process combining techniques from different disciplines. Their development starts by considering the specific requirements of their application, in the present case, *in vivo* implantation in the brain of laboratory animals. Design elaboration includes a choice of the optimal geometrical configuration and appropriate dimensions; a choice of the transducer type and detection scheme. Additionally, the fabrication procedure is desired to be flexible and easy to modify.

In addition to the principal criteria listed in the bibliography section (Chapter 1), the fabrication process of implantable microprobe arrays has to satisfy additional points to be successfully applied for neurological studies:

- the substrate material must be mechanically stable to avoid breakage during implantation in the brain parenchyma;
- isolation between electrodes and conductive parts is of crucial importance to avoid electrical cross-talk between electrodes;
- the microprobe tip has to be of optimal shape to facilitate brain tissue penetration;
- the optimal microprobe dimensions have to be sufficiently large to place numerous electrodes and their connection lines, while causing minimal tissue damage following implantation;
- biocompatibility of materials exposed to the brain tissue.

In this study, we developed a three-electrode microprobe for simultaneous glucose and lactate monitoring with reference to a control electrode. We first optimized the fabrication protocol. Our main study was then focused on cross-talk between adjacent electrodes (i.e. non-specific contamination of the lactate electrode by adjacent glucose oxidase activity and vice versa). We demonstrated the diffusive and non-enzymatic nature of the cross-talk phenomenon on a bare platinum using  $\text{Fe}^{2+}/\text{Fe}^{3+}$  redox pair of ferrocyanide/ferrocyanate solution. We then tested enzyme deposition and immobilization techniques to obtain stable glucose and lactate sensitive biosensors with minimal cross-talk between electrodes. We

optimized biosensor fabrication in order to obtain linear responses for expected *in vivo* glucose and lactate concentrations. Finally, a proof of concept was performed by implantation of the three-electrode microprobe in the cortex of the anesthetized rats with simultaneous glucose and lactate monitoring in physiological conditions and under pharmacological stimulation.

## 1. Microprobes fabrication

Microprobes were fabricated starting from 250  $\mu\text{m}$   $\langle 100 \rangle$  silicon wafer with previously grown thermal oxide (1-2  $\mu\text{m}$ ). Metallization (20nm Ti and 150nm Pt) was patterned by a lift-off process using AZ5214 photoresist to design the three-electrode probe. Negative SU8-2 photoresist was used as top passivation to give final SU8 thickness of 4 $\mu\text{m}$ . It was opened at the recording sites and bonding pads by photoresist development. A third lithography step was used to transfer a mask pattern to form the needle contour on the front wafer side and a fourth mask pattern was transferred to the back side to allow etching the silicon substrate underneath the needle. A subsequent  $\text{NH}_4^+/\text{HF}$  etch of double side oxide was performed. To determine the needle shape, the first DRIE etch was performed on the front side, followed by a second one on the back side to define the needle thickness (50 $\mu\text{m}$ ). During wet and dry etching, the Pt and SU8 surfaces were protected by SPR 220-4.5 thick photoresist. During the DRIE process, the surface of the resist is affected by bombardment and treatment of reactive chemical species, which may change its chemical properties and complicate its final removal from the electrodes. However, if the thickness of the resist is sufficient, the inferior layer will remain unchanged and its removal will eliminate the superior solidified layer. Finally, the probes were broken down manually and packed with custom-made printed circuit boards. Fabrication scheme is presented in Figure 5.1. The fabrication conditions and evolution of microprobe design are detailed in Annex 1.

To construct an implantable enzymatic microelectrode array, we used silicon as a substrate because of its strength and elasticity, and because it can be processed by different MEMS-technologies that are not available for ceramic supports. For example, silicon wafers can be etched to define the dimensions of the final needle, while ceramic probe possess a fixed thickness, usually of some hundreds of micrometers that yield thicker devices and more extensive tissue damage. Additionally, devices on ceramic substrate require an industrial saw or laser to be cut out from the bulk material that makes the fabrication process more complicated.

Our microelectrode array design includes a needle of 3 mm length with 100x50  $\mu\text{m}^2$  cross-section followed by a 3mm part of 1000x50  $\mu\text{m}^2$  cross-section. This silicon needle bears three platinum electrodes of 40x200  $\mu\text{m}^2$ , with 200 $\mu\text{m}$  spacing between them and located 300 $\mu\text{m}$  away from the needle tip. The connection lines are of 10  $\mu\text{m}$  width with 10  $\mu\text{m}$  space between them. The original base is a 250  $\mu\text{m}$  thick silicon wafer.

An SU8 photosensitive polymer was used as top passivation. The SU8 resist allows a large range of possible thickness that is practical for optimizing the micro-needle design. Additionally, the use of photosensitive resist simplifies the overall process because it permits a rapid deposition and structuring of the top layer, and avoids the slow  $\text{SiO}_2$  or  $\text{Si}_3\text{N}_4$  sputtering and subsequent dry etch steps.

In the final design, the probes are attached to the bulk material by clips that can be ruptured to release the microdevice. This approach is useful for protecting the device and allows its storage with minimal risk of breakage.

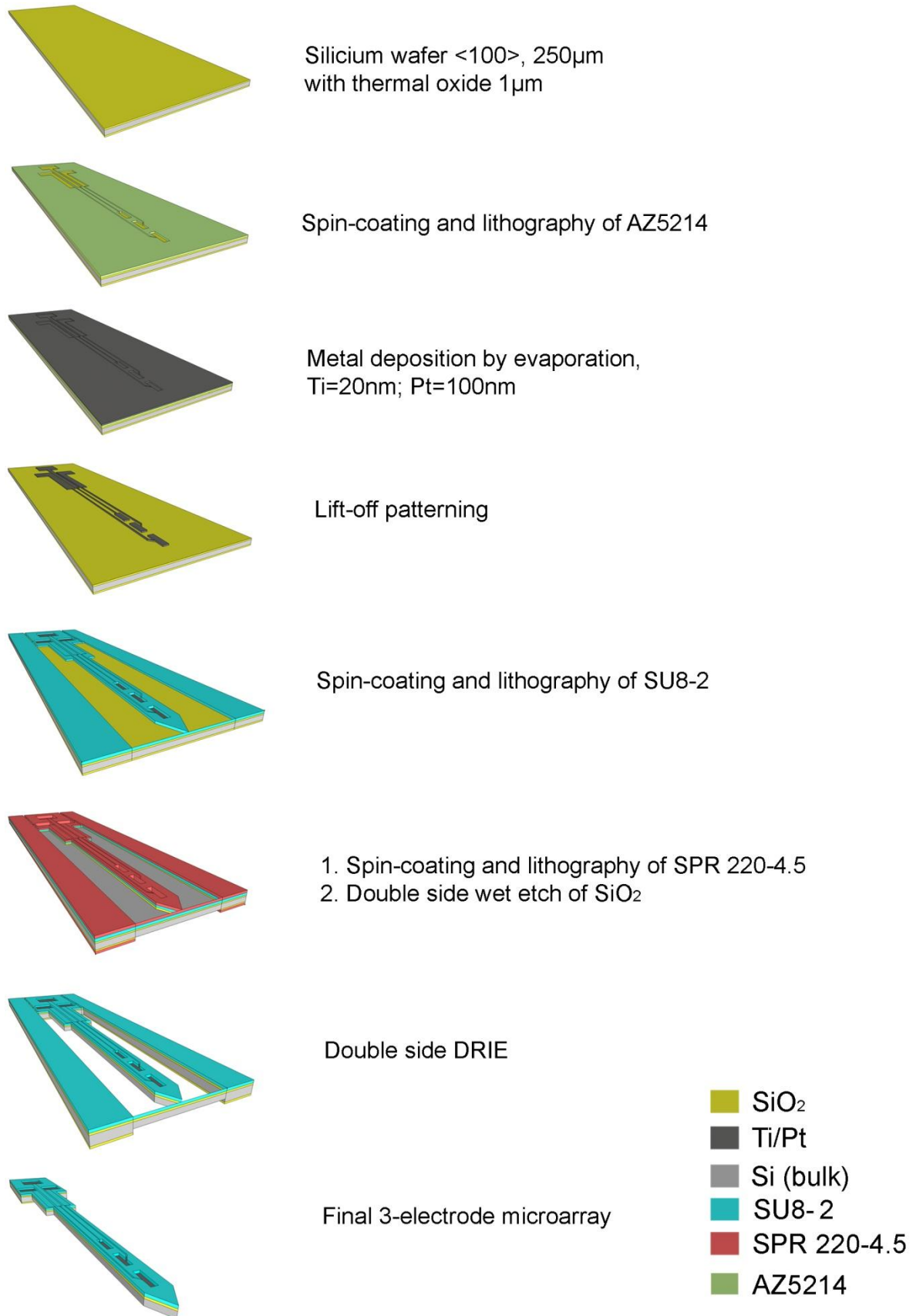
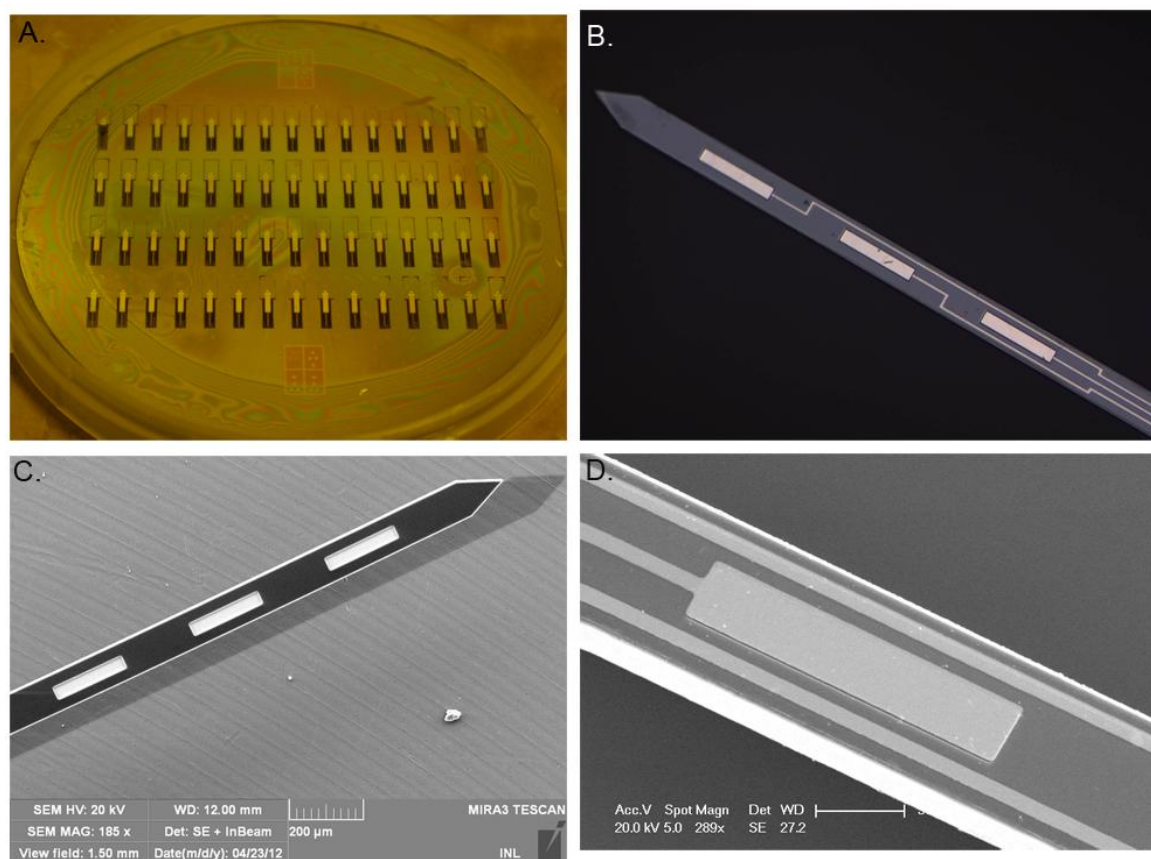


Figure 5.1. Microprobe fabrication process.



**Figure 5.2. Fabricated microelectrode array:** A. The processed wafer with 60 fabricated microarrays; B. Three-electrode micro-needle picture by optical microscope demonstrating position of electroactive sites and connection lines; C. SEM picture of the microprobe demonstrating three adjacent electrodes; D. Close view of one electrode and connection lines.

Figure 5.2 shows a picture of a processed 4-inch silicon wafer with 4 rows of 15 multielectrode arrays (Fig. 5.2A) and a picture of the microprobe tip demonstrating a position of the three electrodes and their connection lines (Fig. 2B). SEM pictures of the final microneedle (Fig. 5.2C, D) demonstrate homogeneous SU8 isolation layer without defects or breaks and reveals the existence of small wells of SU8 photoresist at the bottom of which Pt electrodes are placed;

Prior to any electrochemical experiment, electrodes were cleaned by voltammetry treatment with potential cycling in  $-1000\div 1000$  mV range in 1M  $\text{H}_2\text{SO}_4$  solution 15-25 times until a stable electrode response was obtained.

## 2. Electrochemical (diffusion) cross-talk

To obtain accurate simultaneous monitoring of different molecules, each electrode response must be independent of the neighboring ones. As discussed in Chapter 1, cross-talk in enzymatic biosensors appears when hydrogen peroxide produced by enzymatic reactions diffuses in the bulk solution. This peroxide may reach an adjacent electrode and undergo an electrochemical reaction on the platinum surface giving rise to an oxidation current – i.e. a cross-talk current. To characterize this cross-talk phenomenon on our

multielectrode microarrays, we were interested in characterizing the diffusion of chemical molecules from one electrode to an adjacent one. Enzymatic reactions are complex events that may be influenced by oxygen and substrate concentration, pH changes following substrate conversion etc. complicating the interpretation of obtained data. Therefore, we first studied inter-electrode diffusion in a ferrocyanide/ferricyanide solution on a bare platinum electrode array.

Ferrocyanide/ferricyanide is a classical electrochemical system with standard potential about +0.4 V vs. Ag/AgCl at 25°C that exhibits a nearly reversible electrode reaction. Potassium ferricyanide ( $K_3[Fe(CN)_6]$ ) is an iron compound with oxidation number +3 that can be reduced in ferrocyanide with iron oxidation number +2 at potential under +0.4 V. In this diffusion study we aimed to demonstrate that three electrodes monitor the same residual current at holding potential  $> +0.4$  V in ferricyanide solution (no redox reaction occurs in these conditions). Then, we tested whether diffusion currents would appear on neighboring electrodes when the holding potential is switched to  $< +0.4$  V on one of the electrodes (which would reduce ferricyanide into ferrocyanide).

We used a 10 mM solution of potassium ferricyanide in 0.5 M KCl at room temperature. Electrochemical experiments were performed in 2-electrode configuration versus an Ag/AgCl reference electrode. Electrode potential was maintained at +500 mV for electrodes stabilization and was rapidly switched to -500 mV to provoke redox reaction on one of the electrodes. Figure 5.3C shows experimental curves obtained in such conditions. During first 15 seconds at +500mV all electrodes demonstrated similar faint current; then current was switched to -500 mV on the back (1<sup>st</sup>) electrode as indicated in Figure 5.3A (black electrode). After a slight delay an oxidation current appeared on the adjacent (second, green) electrode, but not on the third (red) one that were both maintained at +500 mV. This oxidation current was the result of the reduction reaction occurring on the first electrode. At -500mV ferrocyanide is reduced to ferricyanide which diffuses into the bulk solution and reaches adjacent electrodes that are maintained at a holding potential sufficient to re-oxidize it back to ferricyanide giving rise to an oxidation current, showed in green in Figure 5.3C. After 115 sec, the holding potential on the first electrode was switched back to +500 mV for 200 sec to allow the current to relax to its initial values. The holding potential of electrode 2 (green) was then switched to -500 mV as indicated in Figure 5.3B. Ferrocyanide then diffused to adjacent electrodes 1 and 3, giving rise to similar oxidation currents on electrodes 1 and 3 (black and red traces, Figure 5.3C). This experiment therefore provides evidence for chemical cross-talk between adjacent electrodes due to the diffusion of molecules between electrodes placed in close proximity.

In the literature, top layers of different thickness are used for isolation. We were interested in comparing the effect of top layer on chemical cross-talk, considering that thicker layers may create wells of defined depth with the electrode placed at the bottom. Such design has the potential of increasing the diffusion path between adjacent electrodes and limiting diffusion and cross-contamination of recording sites.



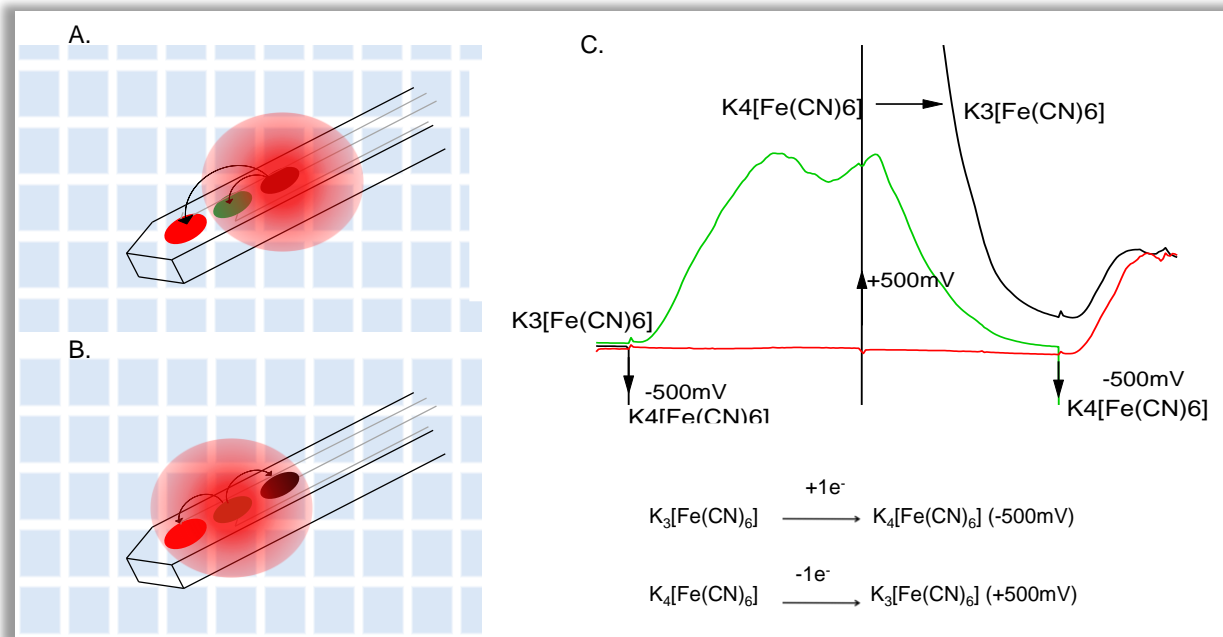


**Figure 5.3. Diffusion cross-talk:** A. Potential is switched from +500 mV to -500 mV on the first electrode to reduce  $\text{Fe}(\text{CN})_6^{3-}$  into  $\text{Fe}(\text{CN})_6^{4-}$ . Obtained species diffuse to the adjacent green electrode. B. Potential is switched from +500 mV to -500 mV on the second electrode and obtained species diffuse to the both adjacent electrodes. C. Experimental curve demonstrating diffusion nature of cross-talk.

We tested different SU8 thicknesses to optimize the final design of our microarray. A thickness of 0.8, 2 and 4, and 11  $\mu\text{m}$  was obtained using SU8 2000.5, SU8-2, SU8-2010 resists respectively. The second series of micro-needles was obtained starting from a 11 $\mu\text{m}$  SU8-2010 layer with subsequent oxygen plasma etching to obtain 3.5, 7.7 and 10 $\mu\text{m}$  SU8 isolation layers. Oxygen plasma is supposed to react with SU8 layer and tune its properties from hydrophobic to hydrophilic which could also influence the kinetics of chemical diffusion between electrodes. Microelectrode arrays constructed with different SU8 layers were tested according the protocol described above. All microdevices were constructed with the same mask design, to ensure that all electrodes had the same electroactive surface. To compare the effect of the top layer thickness on cross-talk, we plotted the value of the oxidation current at the end of the 115 sec period on the electrode adjacent to the one conditioned at -500mV.

Figure 5.4 shows the effect of top layer thickness and oxygen plasma treatment on cross-talk currents. Microarrays with top layer obtained by direct deposition of SU8 photoresist with defined final thickness (without plasma treatment), showed equal cross-talk currents independently on SU8 thickness (blue points). By contrast, microdevices with their top layer obtained by oxygen plasma thinning of an initial 11 $\mu\text{m}$  thick SU8 layer had considerably higher cross-talk currents (red points). Despite an apparent dependence of the detected current on SU8 (plasma-treated) thickness, such difference is probably caused by a change in hydrophobicity rather than the layer thickness. Indeed, to obtain a 10  $\mu\text{m}$  layer from 11  $\mu\text{m}$ , only a couple seconds of plasma etching is required. Microarrays with this conditions show values of oxidation current close to those obtained without oxygen plasma treatment. For thinning a 11 $\mu\text{m}$  layer down to 3.5  $\mu\text{m}$ , about 10 min of plasma etching is required. We hypothesize that the surface of the resist becomes more hydrophilic with increasing etching times, thus favoring chemical diffusion between electrodes and cross-talk.

In our final microprobes design, we used direct SU8 photoresist deposition with 4 $\mu\text{m}$  final thickness.

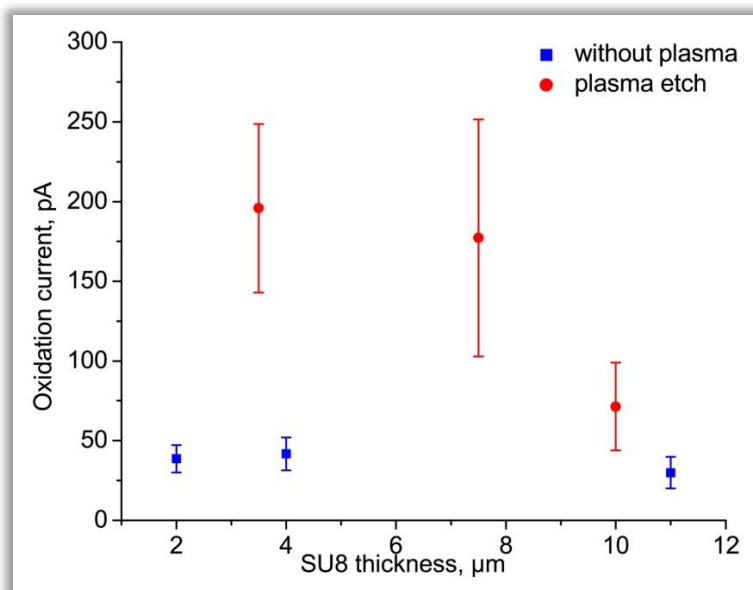


**Figure 5.4. Impact of top layer thickness on cross-talk currents:** microdevices with top layer obtained by oxygen plasma thinning of initial SU8 layer have higher cross-talk currents, then microdevices where top layer was directly deposited with final thickness.

### 3. Enzyme integration

Functionalisation of microelectrode arrays is a difficult task that requires precise local deposition of enzyme on one electrode without cross-contamination of the neighboring ones. Different approaches have been discussed in the literature to overcome this difficulty. The most simple method in is the local deposition of small drop of enzyme solution containing a fixative agent or with subsequent immobilization in glutaraldehyde vapors (123, 138). However, when the microelectrode surface is in the order of 100- 1000  $\mu\text{m}^2$ , expensive equipment is required to deposit small drops of a few nano- or picoliter volume. Another approach consists in enzyme electrodeposition or entrapment into an electrodeposited matrix. The enzyme may be deposited directly from its solution containing glutaraldehyde (as fixative component). If a holding potential opposite to the enzyme charge in solution is applied to the electrode, it will attract the enzyme to the electrode surface and concentrate it until a sufficient concentration is reached for cross-linking by glutaraldehyde to occur (62). A wide range of electroactive polymers have been described in the literature. Protein entrapment in poly-phenylenediamine matrix, polypyrrole or derived-polypyrrole matrixes, or in sol-gel layers has been widely discussed (147, 229, 230). However, almost all methods use potentially toxic monomers or result in deposition of thin enzymatic layers, leading to biosensor low sensitivity and low signal stability. We were looking for a method permitting local enzyme deposition, involving cheap and non-toxic materials, requiring simple experimental procedure and ensuring stable, preferentially covalent protein immobilization. In regard to these requirements, enzyme entrapment in chitosan matrix is of particular interest.

Chitosan is a natural polyaminosaccharide (Fig. 5.5A). It is a major component of the shells of crustaceans and thus is commercially obtained at a low cost from rich natural sources. Chitosan possesses distinct chemical and biological properties. Its linear polyglucosamine chains of high molecular weight, has reactive amino and hydroxyl groups, advantageous to chemical modifications. Chitosan is a cationic polyelectrolyte ( $\text{pK}_a \approx 6.5$ ),

that is insoluble in water but dissolves in acidic media at  $\text{pH} < 6.5$ . When dissolved, chitosan bears positive charges on  $-\text{NH}_3^+$  groups. It easily adheres to negatively charged surfaces or aggregates with polyanionic compounds. The chemical properties of chitosan make it an excellent material for gel formation. Additionally, chitosan is characterized by high biocompatibility, non-toxicity, physiological inertness, and remarkable affinity to proteins with anti-tumoral and anti-cholesteremic properties. It has already found a wide range of applications in medicine and biotechnology as bacteriostatic and fungistatic agent, for drug delivery vehicle, drug controlled release system, artificial cells, contact lenses, artificial skin, surgical sutures and for tissue engineering etc. (231, 232).

The biocompatible properties of the chitosan structure and its reported ability to entrap enzyme in its matrix (128, 129, 233-236) motivated us to adapt this method for immobilization of lactate and glucose oxidases on our multielectrode arrays. Moreover, amine functional groups present in chitosan structure would provide reliable attachment points of proteins by PEGDE to the chitosan layer, preventing enzyme leaching from the deposited membrane.

### Enzyme deposition in chitosan matrix and cross-talk studies

Chitosan was purchased in powder form at low and medium molecular weight (Sigma-Aldrich, Saint Quentin Fallavier, France). The standard solution was prepared with 0.05 M acetic acid and contained 0.5 % of chitosan each form (total 1% chitosan solution).

Glucose oxidase (EC 1.4.3.11) from *Aspergillus niger* was purchased in powder form from Sigma-Aldrich (100–250 U/mg). The final enzyme solution used for deposition contained 10mg/mL glucose oxidase, 10mg/mL PEGDE, and 0.5% chitosan in acetic acid solution 0.025 M.

Control electrodes were covered with a matrix obtained from a solution containing 10mg/mL PEGDE and 0.5% chitosan in acetic acid solution 0.025 M.

The principle of chitosan deposition is presented in Figure 5.5. Chitosan is first dissolved in acetic acid at  $\text{pH} \sim 4$ . The deposition on the electrode can occur only if the local  $\text{pH}$  is  $> 6.5$ . Such local change in  $\text{pH}$  can be obtained if a negative potential is applied to the working electrode. At sufficiently negative potential water can be reduced to hydrogen and  $\text{OH}^-$  by electrolysis with local increase of  $\text{pH}$  as showed in Figure 5.5A.

The deposition procedure was carried out with a 3-electrode configuration with an Ag/AgCl reference and a counter electrode. A micro-needle with 3 platinum electrodes was first immersed in a chitosan/PEGDE solution without enzyme; a negative potential of -1.40 V was then applied to two consecutive electrodes for 150 sec, which provoked chitosan precipitation onto the electrode surface, accompanied with PEGDE entrapment (Fig. 5.5C). After deposition, microprobes were rapidly washed in purified water and placed in an oven at  $55^\circ\text{C}$  for 2h to allow chitosan reaction with PEGDE. Next, the microprobes were placed in a glucose oxidase solution containing PEGDE and chitosan and the deposition procedure was repeated for the last electrode at -1.3 V for 100 sec, followed by 2h enzyme fixation at  $55^\circ\text{C}$ .

Figure 5.5C shows a picture of microneedle with two electrodes covered by chitosan membrane, while the third electrode remains unmodified if no potential is applied.

We then estimated the extent of chemical cross-talk on these microprobes. The first electrode was covered by a chitosan membrane containing glucose oxidase, the second and third electrodes were covered by control chitosan membrane without enzyme. The probes were systematically tested in 1 mM glucose, similar to *in vivo* glucose concentrations. Cross-talk was estimated as the ratio of current detected on the second (and third) electrode by the current on the first electrode. In cross-talk studies we used microprobes with 0.8  $\mu\text{m}$  and 4 $\mu\text{m}$

thick top isolation layer. Table 5.1 shows the obtained data, with significant cross-talk on for both 0.8  $\mu\text{m}$  or 4  $\mu\text{m}$  SU8 thickness.

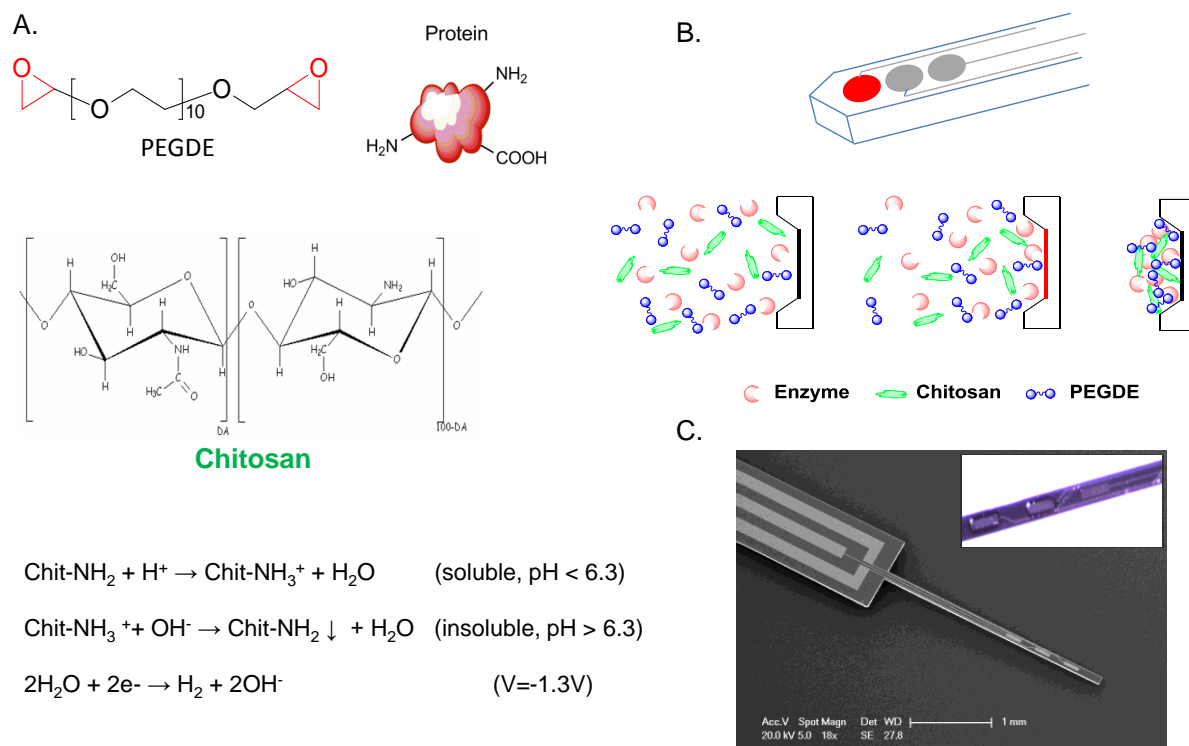


**Figure 5.5. Local enzyme deposition by entrapment in chitosan matrix:** A. Chitosan solution contains enzyme and PEGDE cross-linker. At acid pH chitosan remains soluble in aqua solution but locally precipitates when negative potential is applied. B. Schematic representation of electrode process. Chitosan precipitation is accompanied by PEGDE and enzyme entrapment. C. Microprobe picture demonstrating good spatial resolution of chitosan deposition.

In both cases a high cross-talk current was detected on adjacent electrodes. This effect is difficult to explain. We suppose that non-specific adsorption of the glucose-oxidase-chitosan solution may occur on the chitosan matrix previously deposited on control electrodes (cross-contamination) thus giving detectable oxidation currents in response to glucose.

Table 5.1. Cross-talk study on microprobes with enzyme entrapped in chitosan matrix

	Cross-talk (SU8 0.8 $\mu\text{m}$ )			Cross-talk (SU8 4 $\mu\text{m}$ )			
	1 <sup>st</sup> electrode	2 <sup>nd</sup> electrode	3 <sup>rd</sup> electrode	1 <sup>st</sup> electrode	2 <sup>nd</sup> electrode	3 <sup>rd</sup> electrode	
% (n=18)	100	15 $\pm$ 6	12 $\pm$ 6	% (n=12)	100	47.7 $\pm$ 34	39.4 $\pm$ 34

## Enzyme local drop deposition and cross-talk studies

To overcome the problem of possible cross-contamination, we attempted to apply the enzyme solution by dispensing droplets directly onto the surface of the electrodes. An automated dispensing system ('spotter') was used to apply 3 drops of enzyme solution with a total volume of about 1 nL. Figure 5.6 illustrates the excellent spatial resolution of drop deposition method. A glucose oxidase solution, containing 20 mg/mL of enzyme was deposited on the first electrode and the two others were covered with an inactive protein solution (bovine serum albumin, BSA). These protein layers were then immobilized in glutaraldehyde vapors for 3 min and microarrays were tested for cross-talk. Cross-talk currents on the two control electrodes adjacent to the glucose-sensitive electrode were faint, and amounted to  $1.44 \pm 1.72\%$  and  $0.15 \pm 0.19\%$  of the biosensor signal (Table 5.2). These values were significantly lower than those obtained with chitosan enzyme entrapment.

Despite the potentially high efficiency of such automated dispensing system for depositing nL-size droplets, such devices are not optimized for enzyme use. For example, we frequently encountered foam formation in the enzyme solution, capillary fouling, and aspiration into the dispensing control unit. In addition, such devices are costly and require trained staff for operation. Therefore, we adapted the spotter principle in our laboratory to produce controlled enzyme application.

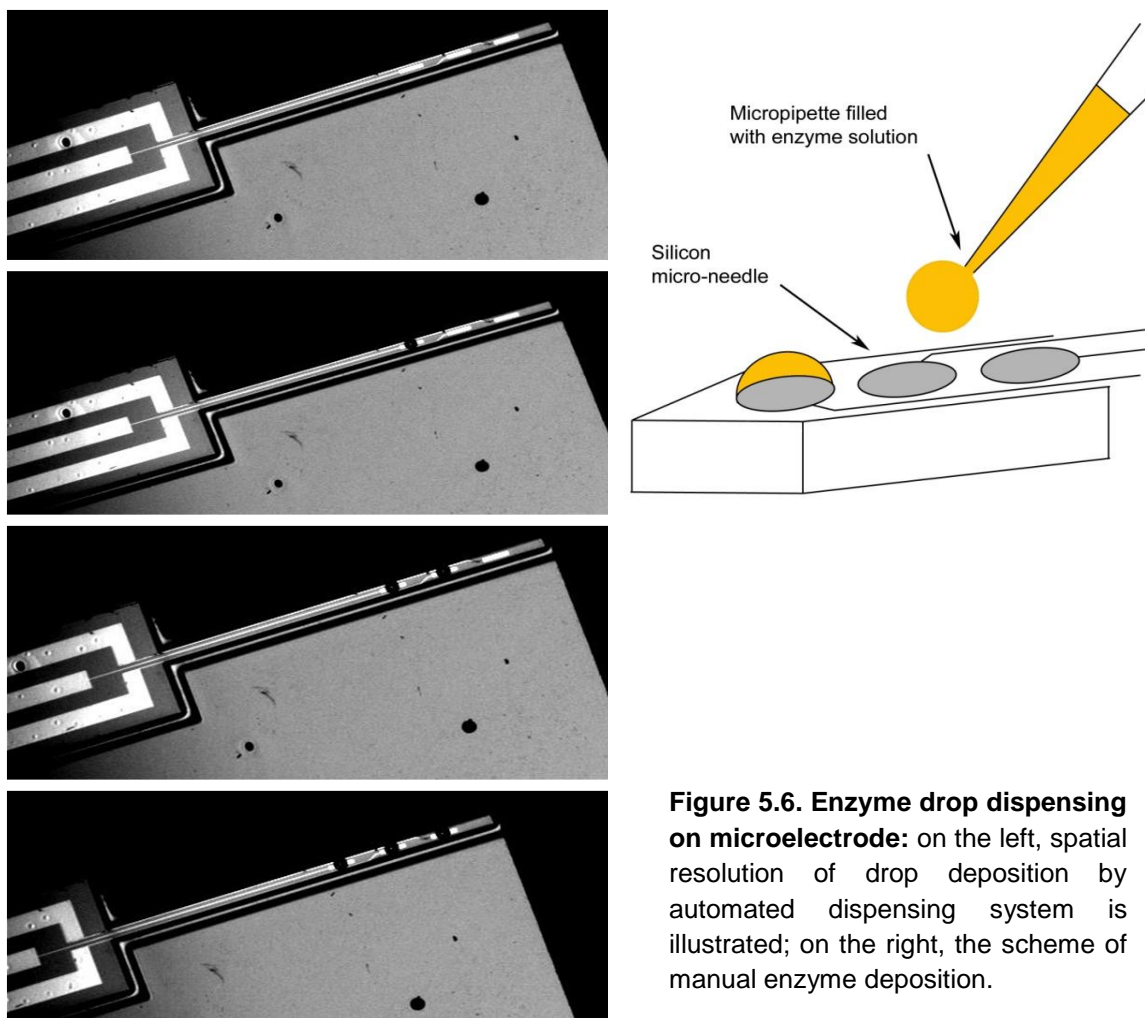


**Figure 5.6. Enzyme drop dispensing on microelectrode:** on the left, spatial resolution of drop deposition by automated dispensing system is illustrated; on the right, the scheme of manual enzyme deposition.

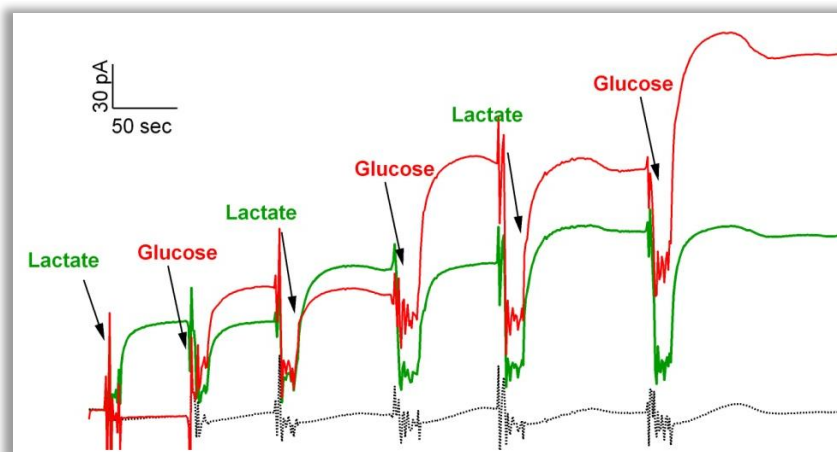
Our home-made dispensing system included a pulled glass capillary, with a tip opening of  $<40\mu\text{m}$  diameter and a pneumatic picopump (PV 820, WPI, Hertfordshire, UK). The glass capillary was filled with the enzyme solution and attached to the picopump through polyethylene tubing with tight junction. The pneumatic picopump delivered a brief pulse of nitrogen gas with controlled pressure and duration inside the capillary and ejected a controlled enzyme volume (the general scheme is illustrated in Fig. 5.6). We functionalized the first electrode with glucose oxidase and the two others were covered with a BSA layer. Proteins were then fixed in glutaraldehyde vapors or by PEGDE cross-linking. Finally, the microarrays were tested for cross-talk. Cross-talk currents on the control electrodes adjacent to the glucose-sensitive electrode were estimated at  $2.46\pm 1.43\%$  and  $0.12\pm 0.18\%$  of the biosensor signal. The cross-talk currents were not significantly different from that obtained with the commercial dispensing system and were acceptable for *in vivo* experiments (i.e.  $< 5\%$ ).

Table 5.2. Cross-talk study on microprobes with enzyme applied by drop dispensing

Cross talk (SU8 $4\mu\text{m}$ )			
%	1 <sup>st</sup> electrode	2 <sup>nd</sup> electrode	3 <sup>rd</sup> electrode
spotter (n=12)	100	$1.44\pm 1.72$	$0.15\pm 0.19$
manual (n=14)	100	$2.46\pm 1.43$	$0.12\pm 0.18$

Figure 5.7 demonstrates a simple calibration experiment of the silicon needle with three electrodes modified by Lactate oxidase, BSA and Glucose oxidase. At the beginning of the experiment, the three electrodes stabilize with the same resting current; injection of lactate ( $100\mu\text{M}$ ) leads to a step in oxidation current on the electrode modified with Lactate oxidase (green line), while the currents on the control (BSA) electrode (black line) and glucose biosensor (red line) remain unchanged. The subsequent injection of glucose increases oxidation current on the glucose biosensor and not on the control electrode or lactate biosensor. The repetitive injection of glucose and lactate solutions confirms the independence in biosensor responses and the absence of significant cross-talk between electrodes.

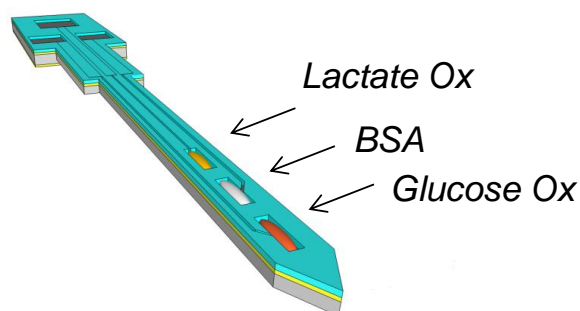




**Figure 5.7. In vitro calibration:** the consecutive injection of glucose and lactate solutions increases an oxidation current on correspondent biosensors of glucose (red line) and lactate (green line) without significant increase on the control electrode (black line).

#### 4. Microprobe biosensor validation for in vivo experiments

We then tested these microelectrode arrays for simultaneous detection of glucose and lactate in the cortex of anesthetized rats. Prior to *in vivo* experiments, microarrays have to be validated according to the following criteria:



Criteria for *in vivo* application

1. Cross-talk free
2. Enzyme activity
3. Signal stability (at 37°C)
  - Glucose oxidase
  - Lactate oxidase
4. Linearity of response for *in vivo*
  - Concentration range

In addition to allowing independent simultaneous recordings on the three electrodes, the immobilization procedure has to ensure reliable enzyme attachment to the electrode surface and preserve enzyme activity so that the biosensors possess a linear response within the *in vivo* concentration range.

Selectivity studies in Chapter 4 demonstrated that Glucose detection in the brain was not affected by Glutaraldehyde immobilization. Therefore we used this method for BSA and glucose oxidase immobilization on the microarray electrodes, because it is much more rapid than PEGDE. However, unlike the traditional biosensors prepared with glass capillaries and Pt wires, reliable and stable immobilization was achieved only after 8 minutes of fixation in glutaraldehyde vapors. In addition, Lactate oxidase (EC 1.13.12.4) was very sensitive to glutaraldehyde. Immobilization resulted either in complete enzyme deactivation or insufficient fixation so that biosensor's signal decreased with time, probably due to enzyme leaking in solution. Thus, PEGDE appeared to be a suitable method for lactate oxidase fixation. Its mild chemical procedure preserved enzyme activity; while the ease of PEGDE dosage and slow reaction kinetics allowed to adjust the immobilization conditions and obtain a stable enzymatic membrane. Optimization of the procedure consisted in (1) immobilization of

enzyme on microarray electrode using enzyme solution with varying composition; (2) measuring the sensitivity of the biosensor; (3) biosensor incubation in water bath at 37°C for 3h, to test its stability near *in vivo* conditions.

The biosensor signal was considered stable if it did not decrease more than 15% after incubation at 37°C for 3h. We tested five solutions containing the same Lactate oxidase concentration fixed at 20 mg/mL; BSA concentration varying between 20-80 mg/mL and PEGDE concentration increasing from 25 to 80 mg/mL. Figure 5.8 represents the stability of obtained biosensors. The most sensitive and stable biosensors were obtained using solution containing 20 mg/mL of Lactate oxidase, 20 mg/mL of BSA and 80mg/mL of PEGDE in PBS buffer (10mM, pH 7.4).

The sensitivity of resulting biosensors was  $44.8 \pm 37.4 \mu\text{A} \cdot \text{mM}^{-1} \text{cm}^{-2}$  (n=9) for glucose and  $140.4 \pm 113.5 \mu\text{A} \cdot \text{mM}^{-1} \text{cm}^{-2}$  (n=11) for lactate, and their sensitivity after 3h at 37°C was  $97.6 \pm 27.1\%$  of their initial sensitivity.

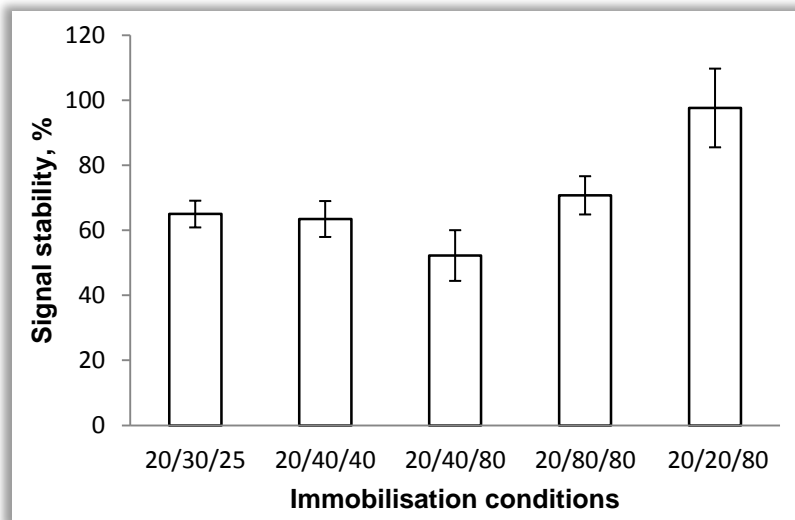


**Figure 5.8. Optimization of immobilization conditions:** stability of the biosensor response after 3h at 37°C depending on enzyme solution composition. The composition of solution is expressed in mg/mL for Lactate oxidase/BSA/PEGDE, n=2 for all solutions, n=4 for 20/20/80.

The brain basal glucose concentration is known to vary between  $0.47 \pm 0.18$  and  $2.4\text{-}3.3$  mM (111, 119, 237-239); while lactate concentration has been reported at  $0.11 \pm 0.025$  mM,  $0.346 \pm 0.021$  mM (239-241) and up to  $1.21 \pm 0.06$  mM (242, 243). Therefore, it is important to obtain biosensors with a linear range extending up to 0.5-2.5 mM lactate and glucose concentrations. However, the response of biosensor follows the Michaelis-Menten kinetics and thus, generally deviates from linearity at high substrate concentrations. To obtain a linear response of glucose and lactate biosensors in the desired concentration range, we deposited an additional top membrane of polyurethane. This membrane creates a diffusion barrier and decreases the flux of substrate to the enzyme immobilized on the biosensor surface. As a result, the concentration of substrate that effectively reaches the enzyme molecules entrapped beneath the polyurethane layer is lower than the actual bulk concentration in the bath, resulting in an extended linear range (73). In our hands 3-6 layers deposited from polyurethane solution (2-3% in THF) by dip coating was sufficient to obtain a linear range extending up to 1.5-3 mM lactate or glucose (Fig. 5.9). Figure 5.9 demonstrates the effect of additional polyurethane layer on lactate biosensor response.

Finally, we used these three electrode microarray for *in vivo* recording of glucose and lactate. Adult, male Wistar rats weighing 150–500g were placed in a stereo-taxic apparatus.



Their body temperature was maintained at 37°C using a homeothermic blanket. The microprobe with lactate-, glucose biosensors and control electrode covered by inactive protein (BSA) was implanted in the frontal cortex (2.5mm ventral to the dura). Recordings were started at least 1h after implantation to ensure stabilization of the baseline electrochemical currents. Insulin (25U/kg of body weight, intraperitoneal [i.p.] injection) was administered after an additional 30min period of control recording, and 30min later an injection of glucose (3 g/kg of body weight, i.p.) was performed.

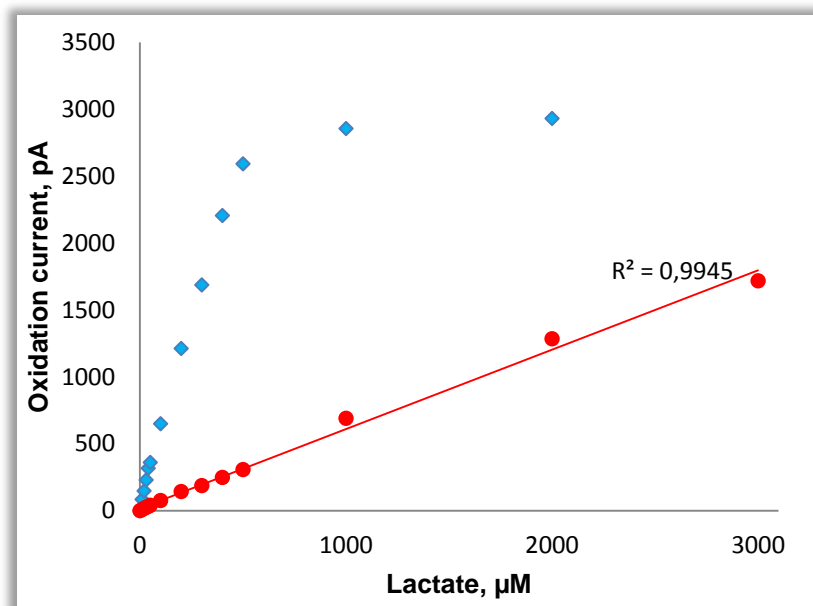


**Figure 5.9. Correction of the linearity response range:** polyurethane top membrane on biosensor limits the flux of lactate to enzyme, decreasing the sensitivity of biosensor and expanding the range of linear response.

To eliminate the influence of endogenous electroactive molecules, the electrodes were covered by PPD membrane according to the protocol described in the previous chapters.

Figure 5.10A shows a photograph of an anesthetized rat with implanted multi-sensor microprobe. Figure 5.10B illustrates an experimental recording. In the initial portion of the graph (first 30 min), the oxidation currents recorded by the glucose- and lactate biosensors were substantially higher than those recorded by the control electrode. The basal extracellular glucose and lactate concentrations were estimated at about 1.2mM and 400µM, respectively, which is consistent with previous studies.

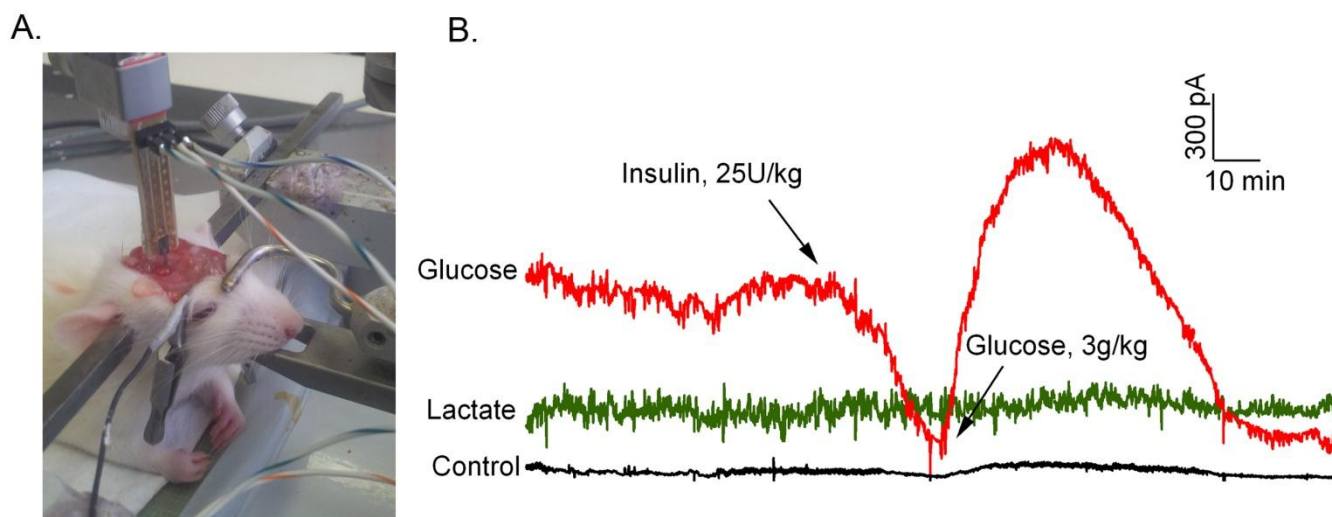


**Figure 5.10. Simultaneous *in vivo* recording of glucose and lactate -Proof of the concept:** A. The photograph representing the implantation of multi-electrode array in the frontal cortex of anesthetized rat; B. *in vivo* monitoring of glucose and lactate. Brain glucose concentration decreased after insulin injection (25U/kg of body weight); and then increased following subsequent glucose administration (3g/kg of body weight). Brain lactate concentration was not affected by glucose changes.

The injection of insulin resulted in a significant decrease of brain glucose concentration and correspondent oxidation current from the glucose biosensor (red line). Subsequent administration of a glucose solution raised the glucose signal over its initial value. This glucose monitoring profile is typical for biosensor validation and is similar to that reported in the Chapter 2. Extending previous studies, our multisensing probe allowed us to study the changes in lactate extracellular concentration simultaneously with glucose. No significant variation in lactate oxidation current was observed. Additionally, the control electrode, placed between glucose and lactate biosensors detected only slight changes in current following insulin and glucose administration, indicating only small possible cross-talk.

Therefore, through these *in vivo* experiments we confirmed the concept of independent simultaneous glucose and lactate monitoring *in vivo*. Hence, this monitoring tool can be applied for more complex neurochemical studies, aiming to understand the metabolic regulation of energy substrates in the brain.



# Conclusion and perspectives



The present thesis is devoted to *in vivo* methods for molecules monitoring in neurological studies. It focuses on microelectrode enzymatic biosensors that provide unique tools for investigating brain physiopathology in laboratory animals. This work explores the chemistry of enzyme immobilization, its influence on enzyme activity and enzymatic kinetics, and its effect on biosensor operation parameters such as response time, sensitivity and stability of biosensor response. We raised the question of the effect of enzyme immobilization on the apparent substrate-specificity of the biosensor that is extremely important for obtaining specific measurements *in vivo*.

We have developed a simple, non-toxic and cheap immobilization method employing PEGDE for cross-linking the enzyme to the electrode surface that is applicable to the majority of oxidase enzymes that we have tested. It offers a good alternative to the four major immobilization procedures available in the field of implantable microelectrode biosensors. Compared to existing methods, PEGDE displays promising properties: it is non-toxic so can be manipulated by non-experts, and potential clinical applications can be considered; it is simple and cheap: the reagent is commercially available and enzyme immobilization involves only one step, without requirement for custom chemical synthesis. Because it involves covalent cross-linking between the enzyme and its surrounding matrix, this method allows stable immobilization that is especially advantageous for *in vivo* measurements. Importantly, compared to other methods, and most particularly to glutaraldehyde, PEGDE immobilization is mild enough to preserve enzyme substrate specificity. These advantages make PEGDE an optimal component for immobilization of a wide range of enzymes with potential interest for *in vivo* biosensor technology.

This enzyme immobilization method considerably improves biosensor performance and ensures the accuracy of quantitative neurotransmitter detection *in vivo*. Overall, this method provides a valuable tool for studying the chemistry of brain cell communication.

Despite the wide acceptance of biosensors as advantageous tools for monitoring brain activity, they still require further investigations to be accepted as a reliable analytical technique. For example, it must be considered that during enzymatic catalysis there is a local change in pH around the biosensor that may influence its response. This is especially important when rapid local events are aimed to be recorded and thus such uncontrollable variations in biosensor performance may induce an error and misinterpretation of the biological event. Enzymatic biosensors aimed at monitoring molecules that are present in high concentrations (e.g. lactate or glucose) *in vivo* require an accurate characterization regarding the oxygen concentration necessary for normal biosensor functioning compared to the oxygen levels available in the brain.

This thesis has also attempted to develop multielectrode microprobes for simultaneous monitoring of important biological markers of brain metabolism and potential messengers of pathological brain functioning. We fabricated a three-electrode microprobe and characterized the main criteria required for their *in vivo* application. Although, these microarrays necessitate further improvements in terms of technological process, parallelization of enzyme deposition and miniaturization, they offer an alternative to classical monoelectrode design. First, the silicon substrate is more robust than glass capillaries, possesses better resistivity to breakage, and thus is advantageous for *in vivo* implantation; second, the multielectrode design induces less damage following implantation, preserving brain integrity. Considering the high variability of experimental data in living organisms, simultaneous molecules detection will provide more accurate comparisons between physiological or pathological conditions than experiments run in multiple animals.

These multisensing devices will be used in neurochemical studies to allow biologists improve their understanding of chemical communication between brain cells and study the mechanisms of brain regulation through monitoring of metabolites and neurotransmitters concentration. This understanding is indispensable to devise proper pharmacological strategies and efficient medical treatment of numerous neurological diseases.

As a long-term perspective, the biosensors developed during this thesis can possibly be applied to brain monitoring in human patients after traumatic brain injury or poor-grade subarachnoid hemorrhage. These patients are often kept in a minimally responsive state that is problematic for accurate diagnosis of neurological complications. Such detection technologies can therefore improve the monitoring of these patients in neurological intensive care units.

# Bibliography





1. Rice, M., and Nicholson, C. (1995) Diffusion and ion shifts in the brain extracellular microenvironment and their relevance for voltametric measurements, In *Voltammetric Methods in Brain Systems* (Boulton A, Baker G, and R, A., Eds.), Humana Press.
2. Kandel, E. R. (2006) *In Search of Memory*, 1st ed., W. W. Norton and Company, Inc., New York.
3. Greengard, P. (2001) The neurobiology of slow synaptic transmission, *Science* 294, 1024-1030.
4. Brighina, E., Bresolin, N., Pardi, G., and Rango, M. (2009) Human Fetal Brain Chemistry as Detected by Proton Magnetic Resonance Spectroscopy, *Pediatric Neurology* 40, 327-342.
5. Cetin, I., Barberis, B., Brusati, V., Brighina, E., Mandia, L., Arighi, A., Radaelli, T., Biondetti, P., Bresolin, N., Pardi, G., and Rango, M. (2011) Lactate detection in the brain of growth-restricted fetuses with magnetic resonance spectroscopy, *American Journal of Obstetrics and Gynecology* 205, 350.e351-350.e357.
6. Davie, S. N., and Grocott, H. P. (2012) Impact of extracranial contamination on regional cerebral oxygen saturation: a comparison of three cerebral oximetry technologies, *Anesthesiology* 116, 834-840.
7. Burger, P. M., Mehl, E., Cameron, P. L., Maycox, P. R., Baumert, M., Lottspeich, F., De Camilli, P., and Jahn, R. (1989) Synaptic vesicles immunisolated from rat cerebral cortex contain high levels of glutamate, *Neuron* 3, 715-720.
8. Baker, D. A., Xi, Z. X., Shen, H., Swanson, C. J., and Kalivas, P. W. (2002) The origin and neuronal function of in vivo nonsynaptic glutamate, *J Neurosci* 22, 9134-9141.
9. Pellerin, L., Bouzier-Sore, A.-K., Aubert, A., Serres, S., Merle, M., Costalat, R., and Magistretti, P. J. (2007) Activity-dependent regulation of energy metabolism by astrocytes: An update, *Glia* 55, 1251-1262.
10. Barco, A., Bailey, C. H., and Kandel, E. R. (2006) Common molecular mechanisms in explicit and implicit memory, *J Neurochem* 97, 1520-1533.
11. Danbolt, N. C. (2001) Glutamate uptake, *Progress in Neurobiology* 65, 1-105.
12. Featherstone, D. E., and Shippy, S. A. (2008) Regulation of synaptic transmission by ambient extracellular glutamate, *Neuroscientist* 14, 171-181.
13. Clements, J. D., Lester, R. A., Tong, G., Jahr, C. E., and Westbrook, G. L. (1992) The time course of glutamate in the synaptic cleft, *Science* 258, 1498-1501.
14. Ottersen, O. P., Zhang, N., and Walberg, F. (1992) Metabolic compartmentation of glutamate and glutamine: morphological evidence obtained by quantitative immunocytochemistry in rat cerebellum, *Neuroscience* 46, 519-534.
15. Bouvier, M., Szatkowski, M., Amato, A., and Attwell, D. (1992) The glial cell glutamate uptake carrier countertransports pH-changing anions, *Nature* 360, 471-474.
16. Zerangue, N., and Kavanaugh, M. P. (1996) Flux coupling in a neuronal glutamate transporter, *Nature* 383, 634-637.
17. Levy, L. M., Warr, O., and Attwell, D. (1998) Stoichiometry of the glial glutamate transporter GLT-1 expressed inducibly in a Chinese hamster ovary cell line selected for low endogenous Na<sup>+</sup>-dependent glutamate uptake, *J Neurosci* 18, 9620-9628.
18. Miele, M., Boutelle, M. G., and Fillenz, M. (1996) The source of physiologically stimulated glutamate efflux from the striatum of conscious rats, *J Physiol* 497, 745-751.
19. Cheung, N. S., Pascoe, C. J., Giardina, S. F., John, C. A., and Beart, P. M. (1998) Micromolar L-glutamate induces extensive apoptosis in an apoptotic-necrotic continuum of insult-dependent, excitotoxic injury in cultured cortical neurones, *Neuropharmacology* 37, 1419-1429.
20. Wang, Y., and Qin, Z. H. (2010) Molecular and cellular mechanisms of excitotoxic neuronal death, *Apoptosis* 15, 1382-1402.
21. Logan, W. J., and Snyder, S. H. (1972) High affinity uptake systems for glycine, glutamic and aspartic acids in synaptosomes of rat central nervous tissues, *Brain Res* 42, 413-431.
22. Maragakis, N. J., Dietrich, J., Wong, V., Xue, H., Mayer-Proschel, M., Rao, M. S., and

- Rothstein, J. D. (2004) Glutamate transporter expression and function in human glial progenitors, *Glia* 45, 133-143.
23. Kim, K., Lee, S. G., Kegelman, T. P., Su, Z. Z., Das, S. K., Dash, R., Dasgupta, S., Barral, P. M., Hedvat, M., Diaz, P., Reed, J. C., Stebbins, J. L., Pellecchia, M., Sarkar, D., and Fisher, P. B. (2010) Role of excitatory amino acid transporter-2 (EAAT2) and glutamate in neurodegeneration: Opportunities for developing novel therapeutics, *J Cell Physiol*.
  24. Lehre, K. P., and Danbolt, N. C. (1998) The number of glutamate transporter subtype molecules at glutamatergic synapses: chemical and stereological quantification in young adult rat brain, *J Neurosci* 18, 8751-8757.
  25. Vandenberg, C. J., and Garfinkel, D. (1971) A simulation study of brain compartments. Metabolism of glutamate and related substances in mouse brain, *Biochem J*. 123, 211–218.
  26. Martinez-Hernandez, A., Bell, K. P., and Norenberg, M. D. (1977) Glutamine synthetase: glial localization in brain, *Science* 195, 1356-1358.
  27. Frey, O. (2010) Biosensor Microprobe Arrays for In Vivo Monitoring of Neurotransmitters, École polytechnique fédérale de Lausanne.
  28. Rutherford, E. C., Pomerleau, F., Huettl, P., Stromberg, I., and Gerhardt, G. A. (2007) Chronic second-by-second measures of L-glutamate in the central nervous system of freely moving rats, *J Neurochem* 102, 712-722.
  29. Kish, P. E., and Ueda, T. (1991) Calcium-dependent release of accumulated glutamate from synaptic vesicles within permeabilized nerve terminals, *Neurosci Lett* 122, 179-182.
  30. Ellis-Davies, G. C. (2008) Neurobiology with caged calcium, *Chem Rev* 108, 1603-1613.
  31. Hillered, L., Vespa, P. M., and Hovda, D. A. (2005) Translational neurochemical research in acute human brain injury: the current status and potential future for cerebral microdialysis, *J Neurotrauma* 22, 3-41.
  32. Barros, L. F., Courjaret, R., Jakoby, P., Loaiza, A., Lohr, C., and Deitmer, J. W. (2009) Preferential transport and metabolism of glucose in Bergmann glia over Purkinje cells: a multiphoton study of cerebellar slices, *Glia* 57, 962-970.
  33. Herrero-Mendez, A., Almeida, A., Fernandez, E., Maestre, C., Moncada, S., and Bolanos, J. P. (2009) The bioenergetic and antioxidant status of neurons is controlled by continuous degradation of a key glycolytic enzyme by APC/C-Cdh1, *Nature cell biology* 11, 747-752.
  34. Pellerin, L. (2010) Food for thought: the importance of glucose and other energy substrates for sustaining brain function under varying levels of activity, *Diabetes & metabolism* 36 Suppl 3, S59-63.
  35. Pierre, K., and Pellerin, L. (2005) Monocarboxylate transporters in the central nervous system: distribution, regulation and function, *J Neurochem* 94, 1-14.
  36. Bouzier-Sore, A. K., Voisin, P., Bouchaud, V., Bezancon, E., Franconi, J. M., and Pellerin, L. (2006) Competition between glucose and lactate as oxidative energy substrates in both neurons and astrocytes: a comparative NMR study, *Eur J Neurosci* 24, 1687-1694.
  37. Pellerin, L. (2003) Lactate as a pivotal element in neuron–glia metabolic cooperation, *Neurochemistry International* 43, 331-338.
  38. Gjedde, A., Marrett, S., and Vafae, M. (2002) Oxidative and nonoxidative metabolism of excited neurons and astrocytes, *J Cereb Blood Flow Metab* 22, 1-14.
  39. Mangia, S., Simpson, I. A., Vannucci, S. J., and Carruthers, A. (2009) The in vivo neuron-to-astrocyte lactate shuttle in human brain: evidence from modeling of measured lactate levels during visual stimulation, *J Neurochem* 109 Suppl 1, 55-62.
  40. Genc, S., Kurnaz, I. A., and Ozilgen, M. (2011) Astrocyte-neuron lactate shuttle may boost more ATP supply to the neuron under hypoxic conditions--in silico study supported by in vitro expression data, *BMC systems biology* 5, 162.
  41. Kaelin, W. G., Jr., and Thompson, C. B. (2010) Q&A: Cancer: clues from cell metabolism, *Nature* 465, 562-564.

42. Enblad, P., Frykholm, P., Valtysson, J., Silander, H. C., Andersson, J., Fasth, K. J., Watanabe, Y., Langstrom, B., Hillered, L., and Persson, L. (2001) Middle cerebral artery occlusion and reperfusion in primates monitored by microdialysis and sequential positron emission tomography, *Stroke* 32, 1574-1580.
43. Timofeev, I., Carpenter, K. L., Nortje, J., Al-Rawi, P. G., O'Connell, M. T., Czosnyka, M., Smielewski, P., Pickard, J. D., Menon, D. K., Kirkpatrick, P. J., Gupta, A. K., and Hutchinson, P. J. (2011) Cerebral extracellular chemistry and outcome following traumatic brain injury: a microdialysis study of 223 patients, *Brain* 134, 484-494.
44. Persson, L., and Hillered, L. (1992) Chemical monitoring of neurosurgical intensive care patients using intracerebral microdialysis, *J Neurosurg* 76, 72-80.
45. Reinstrup, P., Stahl, N., Møllergaard, P., Uski, T., Ungerstedt, U., and Nordstrom, C. H. (2000) Intracerebral microdialysis in clinical practice: baseline values for chemical markers during wakefulness, anesthesia, and neurosurgery, *Neurosurgery* 47, 701-709; discussion 709-710.
46. Richards, D. A., Tolias, C. M., Sgouros, S., and Bowery, N. G. (2003) Extracellular glutamine to glutamate ratio may predict outcome in the injured brain: a clinical microdialysis study in children, *Pharmacol Res* 48, 101-109.
47. Guide, T. Successful Separations of Peptides, Proteins and Other Biomolecules, In *Technical Guide: HPLC Analysis of Biomolecules*, Thermo Electron corporation.
48. Huck, C. W., and Bonn, G. K. (2008) Analysis of proteins by capillary electrophoresis, In *Capillary Electrophoresis: Methods and Protocols* (Schmitt-Kopplin, P., Ed.) 2008 ed., pp 507-540, Humana Press.
49. Righetti, P. G. (2001) Capillary Electrophoresis, In *eLS*, John Wiley & Sons, Ltd.
50. Lim, C. K., and Lord, G. (2002) Current developments in LC-MS for pharmaceutical analysis, *Biol Pharm Bull* 25, 547-557.
51. Tareke, E., Bowyer, J. F., and Doerge, D. R. (2007) Quantification of rat brain neurotransmitters and metabolites using liquid chromatography/electrospray tandem mass spectrometry and comparison with liquid chromatography/electrochemical detection, *Rapid Commun Mass Spectrom* 21, 3898-3904.
52. Boutelle, M. G., Fellows, L. K., and Cook, C. (1992) Enzyme packed bed system for the on-line measurement of glucose, glutamate, and lactate in brain microdialysate, *Anal Chem* 64, 1790-1794.
53. Nguyen, Q. T., Schroeder, L. F., Mank, M., Muller, A., Taylor, P., Griesbeck, O., and Kleinfeld, D. (2010) An in vivo biosensor for neurotransmitter release and in situ receptor activity, *Nat Neurosci* 13, 127-132.
54. Gubala, V., Harris, L. F., Ricco, A. J., Tan, M. X., and Williams, D. E. (2012) Point of care diagnostics: status and future, *Anal Chem* 84, 487-515.
55. Heller, A., and Feldman, B. (2008) Electrochemical glucose sensors and their applications in diabetes management, *Chem Rev* 108, 2482-2505.
56. Franssila, S., (Ed.) (2004) *Introduction to Microfabrication*, John Wiley & Sons Ltd, England.
57. Lopez-Garcia, J., Martin-Palma, R. J., Manso, M., and Martinez-Duar, J. M. (2007) Porous silicon based structures for the electrical biosensing of glucose, *Sensors and Actuators B* 126, 82-85.
58. Jane, A., Dronov, R., Hodges, A., and Voelcker, N. H. (2009) Porous silicon biosensors on the advance, *Trends Biotechnol* 27, 230-239.
59. Shmigol, I. V., Alekseev, S. A., Lavrynenko, O. Y., Vasylieva, N. S., Zaitsev, V. N., Barbier, D., and Pokrovsky, V. A. (2009) Chemically modified porous silicon for laser desorption/ionization mass spectrometry of ionic dyes, *J Mass Spectrom* 44, 1234-1240.
60. Williams, K. R., Gupta, K., and Wasilik, M. (2003) Etch Rates for Micromachining Processing—Part II, *Journal of Microelectromechanical Systems* 12, 761 - 778
61. Frey, O., Holtzman, T., McNamara, R. M., Theobald, D. E. H., van der Wal, P. D., de Rooij, N. F., Dalley, J. W., and Koudelka-Hep, M. (2011) Simultaneous neurochemical stimulation and recording using an assembly of biosensor silicon microprobes and SU-8 microinjectors, *Sensors and Actuators B: Chemical* 154, 96-

- 105.
62. Frey, O., Holtzman, T., McNamara, R. M., Theobald, D. E., van der Wal, P. D., de Rooij, N. F., Dalley, J. W., and Koudelka-Hep, M. (2010) Enzyme-based choline and L-glutamate biosensor electrodes on silicon microprobe arrays, *Biosens Bioelectron* 26, 477-484.
63. Frey, O., van der Wal, P. D., Spieth, S., Brett, O., Seidl, K., Paul, O., Ruther, P., Zengerle, R., and de Rooij, N. F. (2011) Biosensor microprobes with integrated microfluidic channels for bi-directional neurochemical interaction, *J Neural Eng* 8, 066001.
64. Iliuk, A. B., Hu, L., and Tao, W. A. (2011) Aptamer in bioanalytical applications, *Anal Chem* 83, 4440-4452.
65. Borisov, S. M., and Wolfbeis, O. S. (2008) Optical biosensors, *Chem Rev* 108, 423-461.
66. Huber, W., Barner, R., Fattinger, C., Hübscher, J., Koller, H., Müller, F., Schalatter, D., and Lukosz, W. (1992) Direct optical immunosensing (sensitivity and selectivity), *Sensors and Actuators B: Chemical* 6, 122-126.
67. Li, J., Tan, W., Wang, K., Xiao, D., Yang, X., He, X., and Tang, Z. (2001) Ultrasensitive optical DNA biosensor based on surface immobilization of molecular beacon by a bridge structure, *Anal Sci* 17, 1149-1153.
68. Mitchell, J. S., and Wu, Y. (2010) Surface Plasmon Resonance Biosensors for Highly Sensitive Detection of Small Biomolecules, In *Biosensors* (Serra, P. A., Ed.), pp 151-168, InTech.
69. Homola, J., Yee, S. S., and Gauglitz, G. (1999) Surface plasmon resonance sensors: review, *Sensors and Actuators B: Chemical* 54, 3-15.
70. Kimmel, D. W., LeBlanc, G., Meschievitz, M. E., and Cliffler, D. E. (2012) Electrochemical Sensors and Biosensors, *Analytical Chemistry* 84, 685-707.
71. Lin, J. H., and Ju, H. X. (2005) Electrochemical and chemiluminescent immunosensors for tumor markers, *Biosensors & Bioelectronics* 20, 1461-1470.
72. Suman, and Kumar, A. (2008) Recent Advances in DNA Biosensor, *Sensors & Transducers Journal* 92, 122-133.
73. Schuvailo, O. M., Soldatkin, O. O., Lefebvre, A., Cespuglio, R., and Soldatkin, A. P. (2006) Highly selective microbiosensors for in vivo measurement of glucose, lactate and glutamate., *Analytica Chimica Acta* 573-574, 110-116.
74. Stöllner, D., Stöcklein, W., Scheller, F., and Warsinke, A. (2002) Membrane-immobilized haptoglobin as affinity matrix for a hemoglobin-A1c immunosensor, *Analytica Chimica Acta* 470, 111-119.
75. Erdem, A., Kerman, K., Meric, B., Akarca, U. S., and Ozsoz, M. (2000) Novel hybridization indicator methylene blue for the electrochemical detection of short DNA sequences related to the hepatitis B virus, *Anal. Chim. Acta* 422.
76. Shishkanova, T. V., Volf, R., Krondak, M., and Kral, V. (2007) Functionalization of PVC membrane with ss oligonucleotides for a potentiometric biosensor, *Biosens Bioelectron* 22, 2712-2717.
77. Grieshaber, D., MacKenzie, R., Voros, J., and Reimhult, E. (2008) Electrochemical biosensors - Sensor principles and architectures, *Sensors-Basel* 8, 1400-1458.
78. Ensafi, A. A., Taei, M., Rahmani, H. R., and Khayamian, T. (2011) Sensitive DNA impedance biosensor for detection of cancer, chronic lymphocytic leukemia, based on gold nanoparticles/gold modified electrode, *Electrochim Acta* 56, 8176-8183.
79. Waggoner, P. S., and Craighead, H. G. (2007) Micro- and nanomechanical sensors for environmental, chemical, and biological detection, *Lab Chip* 7, 1238-1255.
80. Corcoles, E. P., Deeba, S., Hanna, G. B., Paraskeva, P., Boutelle, M. G., and Darzi, A. (2011) Use of online rapid sampling microdialysis electrochemical biosensor for bowel anastomosis monitoring in swine model, *Analytical Methods* 3, 2010-2016.
81. Deeba, S., Corcoles, E., Hanna, B., Pareskevas, P., Aziz, O., Boutelle, M., and Darzi, A. (2008) Use of Rapid Sampling Microdialysis for Intraoperative Monitoring of Bowel Ischemia, *Diseases of the Colon & Rectum* 51, 1408-1413.
82. Moscone, D., Pasini, M., and Mascini, M. (1992) Subcutaneous microdialysis probe

- coupled with glucose biosensor for in vivo continuous monitoring, *Talanta* 39, 1039-1044.
83. Yao, T., Yano, T., and Nishino, H. (2004) Simultaneous in vivo monitoring of glucose, l-lactate, and pyruvate concentrations in rat brain by a flow-injection biosensor system with an on-line microdialysis sampling, *Analytica Chimica Acta* 510, 53-59.
84. Yao, T., Nanjyo, Y., and Nishino, H. (2001) Micro-flow in vivo analysis of L-glutamate with an on-line enzyme amplifier based on substrate recycling, *Anal Sci* 17, 703-708.
85. Petrou, P. S., Moser, I., and Jobst, G. (2002) BioMEMS device with integrated microdialysis probe and biosensor array, *Biosens Bioelectron* 17, 859-865.
86. Clapp-Lilly, K. L., Roberts, R. C., Duffy, L. K., Irons, K. P., Hu, Y., and Drew, K. L. (1999) An ultrastructural analysis of tissue surrounding a microdialysis probe, *J Neurosci Methods* 90, 129-142.
87. Kotanen, C., Moussy, F. G., Carrara, S., and Guiseppi-Elie, A. (2012) Implantable Enzyme Amperometric Biosensors, *Biosensors and Bioelectronics*.
88. Netchiporouk, L. I., Shul'ga, A. A., Jaffrezic-Renault, N., Olier, R., and Cespuglio, R. (1995) Properties of carbon fibre microelectrodes as a basis biosensors, *Analytica Chimica Acta* 303, 275-283.
89. Gonon, F., Buda, M., Cespuglio, R., Jouvét, M., and Pujol, J. F. (1980) In vivo electrochemical detection of catechols in the neostriatum of anaesthetized rats: dopamine or DOPAC?, *Nature* 286, 902-904.
90. Pernot, P., Mothet, J. P., Schuvailo, O., Soldatkin, A., Pollegioni, L., Pilone, M., Adeline, M. T., Cespuglio, R., and Marinesco, S. (2008) Characterization of a yeast D-amino acid oxidase microbiosensor for D-serine detection in the central nervous system, *Anal Chem* 80, 1589-1597.
91. Najafi, K., Ji, J., and Wise, K. D. (1990) Scaling limitations of silicon multichannel recording probes, *IEEE Trans Biomed Eng* 37, 1-11.
92. Wise, K. D., Angell, J. B., and Starr, A. (1970) An integrated-circuit approach to extracellular microelectrodes, *IEEE Trans Biomed Eng* 17, 238-247.
93. Wise, K. D., and Angell, J. B. (1975) A low-capacitance multielectrode probe for use in extracellular neurophysiology, *IEEE Trans Biomed Eng* 22, 212-219.
94. Hoogerwerf, A. C., and Wise, K. D. (1994) A three-dimensional microelectrode array for chronic neural recording, *IEEE Trans Biomed Eng* 41, 1136-1146.
95. Burmeister, J. J., Moxon, K., and Gerhardt, G. A. (2000) Ceramic-Based Multisite Microelectrodes for Electrochemical Recordings, *Anal. Chem.* 72, 187-192.
96. Burmeister, J. J., and Gerhardt, G. A. (2001) Self-Referencing Ceramic-Based Multisite Microelectrodes for the Detection and Elimination of Interferences from the Measurement of L-Glutamate and Other Analytes, *Anal. Chem.* 73, 1037-1042.
97. Lin, C. W., Lee, Y. T., Chang, C. W., Hsu, W. L., Chang, Y. C., and Fang, W. L. (2009) Novel glass microprobe arrays for neural recording, *Biosensors & Bioelectronics* 25, 475-481.
98. Tijero, M., Gabriel, G., Caro, J., Altuna, A., Hernandez, R., Villa, R., Berganzo, J., Blanco, F. J., Salido, R., and Fernandez, L. J. (2009) SU-8 microprobe with microelectrodes for monitoring electrical impedance in living tissues, *Biosensors & Bioelectronics* 24, 2410-2416.
99. Cho, S.-H., Lu, H. M., Cauller, L., Romero-Ortega, M. I., Lee, J.-B., and Hughes, G. A. (2008) Biocompatible SU-8-Based Microprobes for Recording Neural Spike Signals From Regenerated Peripheral Nerve Fibers, *IEEE SENSORS JOURNAL* 8, 1830-1836.
100. Ensell, I., Banks, D. J., Richards, P. R., Balachandran, W., and Ewins, D. J. (2000) Silicon-based microelectrodes for neurophysiology, micromachined from silicon-on-insulator wafers, *Med. Biol. Eng. Comput* 38, 175-179.
101. Leong, K. H., Ensell, G., Wall, P., and Pickard, R. S. (1990) Multichannel microelectrode probes machined in silicon, *Biosensors and Bioelectronics* 5, 303-310.
102. Wassum, K. M., Tolosa, V. M., Wang, J. J., Walker, E., Monbouquette, H. G., and Maidment, N. T. (2008) Silicon wafer-based platinum microelectrode array biosensor for near real-time measurement of glutamate in vivo, *Sensors-Basel* 8, 5023-5036.

103. Herwik, S., Kisban, S., Aarts, A. A. A., Seidl, K., Girardeau, G., Benchenane, K., Zugaro, M. B., Wiener, S. I., Paul, O., Neves, H. P., and Ruther, P. (2009) Fabrication technology for silicon-based microprobe arrays used in acute and sub-chronic neural recording, *J Micromech Microeng* 19.
104. Norlin, P., Kindlundh, M., Mouroux, A., Yoshida, K., and Hofmann, U. G. (2002) A 32-site neural recording probe fabricated by DRIE of SOI substrates, *J Micromech Microeng* 12, 414-419.
105. Mugweru, A., Clark, B. L., and Pishko, M. V. (2007) Electrochemical sensor array for glucose monitoring fabricated by rapid immobilization of active glucose oxidase within photochemically polymerized hydrogels, *J Diabetes Sci Technol* 1, 366-371.
106. Rassaei, L., and Marken, F. (2010) Pulse-Voltammetric Glucose Detection at Gold Junction Electrodes, *Analytical Chemistry* 82, 7063-7067.
107. Day, B. K., Pomerleau, F., Burmeister, J. J., Huettl, P., and Gerhardt, G. A. (2006) Microelectrode array studies of basal and potassium-evoked release of L-glutamate in the anesthetized rat brain, *J Neurochem* 96, 1626-1635.
108. Moser, I., Jobst, G., and Urban, G. A. (2002) Biosensor arrays for simultaneous measurement of glucose, lactate, glutamate, and glutamine, *Biosens Bioelectron* 17, 297-302.
109. Llaudet, E., Botting, N. P., Crayston, J. A., and Dale, N. (2003) A three-enzyme microelectrode sensor for detecting purine release from central nervous system, *Biosensors and Bioelectronics* 18, 43-52.
110. Musallam, S., Bak, M. J., Troyk, P. R., and Andersen, R. A. (2007) A floating metal microelectrode array for chronic implantation, *J Neurosci Meth* 160, 122-127.
111. Netchiporouk, L. I., Shram, N. F., Jaffrezic-Renault, N., Martelet, C., and Cespuglio, R. (1996) In vivo brain glucose measurements: differential normal pulse voltammetry with enzyme-modified carbon fiber microelectrodes, *Anal Chem* 68, 4358-4364.
112. Oldenziel, W. H., Dijkstra, G., Cremers, T. I. F. H., and Westerink, B. H. C. (2006) In vivo monitoring of extracellular glutamate in the brain with a microsensor, *Brain Res* 1118, 34-42.
113. Lingane, J. J., and Lingane, P. J. (1963) Chronopotentiometry of hydrogen peroxide with a platinum wire electrode, *Journal of Electroanalytical Chemistry (1959)* 5, 411-419.
114. Wilson, G. S., and Johnson, M. A. (2008) In-Vivo Electrochemistry: What Can We Learn about Living Systems?, *Chemical Reviews* 108, 2462-2481.
115. Hall, S. B., Khudaish, E. A., and Hart, A. L. (1998) Electrochemical oxidation of hydrogen peroxide at platinum electrodes. Part II: effect of potential, *Electrochim Acta* 43, 2015-2024.
116. O'Connell, P. J., O'Sullivan, C. K., and Guilbault, G. G. (1998) Electrochemical metallisation of carbon electrodes, *Analytica Chimica Acta* 373, 261-270.
117. De Corcuera, J. I. R., Cavalieri, R. P., and Powers, J. R. (2005) Improved platinization conditions produce a 60-fold increase in sensitivity of amperometric biosensors using glucose oxidase immobilized in poly-o-phenylenediamine, *J Electroanal Chem* 575, 229-241.
118. Aggett, P. J. (1985) 1 Physiology and metabolism of essential trace elements: An outline, *Clinics in Endocrinology and Metabolism* 14, 513-543.
119. Vasylieva, N., Barnych, B., Meiller, A., Maucler, C., Pollegioni, L., Lin, J. S., Barbier, D., and Marinesco, S. (2011) Covalent enzyme immobilization by poly(ethylene glycol) diglycidyl ether (PEGDE) for microelectrode biosensor preparation, *Biosens Bioelectron* 26, 3993-4000.
120. Gregg, B. A., and Heller, A. (1991) Redox Polymer Films Containing Enzyme. 2. Glucose Oxidase Containing Enzyme Electrodes, *J. Phys. Chem* 95, 5976-5980.
121. Karyakin, A. A., Karyakina, E. E., and Gorton, L. (2000) Amperometric biosensor for glutamate using Prussian Blue-based "artificial peroxidase" as a transducer for hydrogen peroxide, *Analytical Chemistry* 72, 1720-1723.
122. Llaudet, E., Hatz, S., Droniou, M., and Dale, N. (2005) Microelectrode Biosensor for Real-Time Measurement of ATP in Biological Tissue, *Anal. Chem.* 77, 3267-3273.

123. Burmeister, J. J., and Gerhardt, G. A. (2003) Ceramic-based multisite microelectrode arrays for in vivo electrochemical recordings of glutamate and other neurochemicals, *Trac-Trend Anal Chem* 22, 498-502.
124. Poitry, S., Poitry-Yamate, C., Innocent, C., Cosnier, S., and Tsacopoulos, M. (1997) Detection of glutamate released by neurons with an enzyme-based microelectrode, *Electrochimica Acta*, 42, 3217-3223.
125. Pernot, P., Maucler, C., Tholance, Y., Vasylieva, N., Debilly, G., Pollegioni, L., Cespuglio, R., and Marinesco, S. (2012) d-Serine diffusion through the blood-brain barrier: Effect on d-serine compartmentalization and storage, *Neurochemistry International* 60, 837-845.
126. Errachid, A., Ivorra, A., Aguilo, J., Villa, R., N.Zine, and Bausells, J. (2001) New technology for multi-sensor silicon needles for biomedical applications, *Sensors and Actuators B* 78, 279-284.
127. Burmeister, J. J., Pomerleau, F., Palmer, M., Day, B. K., Huettl, P., and Gerhardt, G. A. (2002) Improved ceramic-based multisite microelectrode for rapid measurements of L-glutamate in the CNS, *J Neurosci Methods* 119, 163-171.
128. Tan, Y. M., Deng, W. F., Chen, C., Xie, Q. J., Lei, L. H., Li, Y. Y., Fang, Z. F., Ma, M., Chen, J. H., and Yao, S. Z. (2010) Immobilization of enzymes at high load/activity by aqueous electrodeposition of enzyme-tethered chitosan for highly sensitive amperometric biosensing, *Biosensors & Bioelectronics* 25, 2644-2650.
129. Luo, X. L., Xu, J. J., Du, Y., and Chen, H. Y. (2004) A glucose biosensor based on chitosan-glucose oxidase-gold nanoparticles biocomposite formed by one-step electrodeposition, *Anal Biochem* 334, 284-289.
130. Ryan, M. R., Lowry, J. P., and O'Neill, R. D. (1997) Biosensor for neurotransmitter L-glutamic acid designed for efficient use of L-glutamate oxidase and effective rejection of interference, *Analyst* 122, 1419-1424.
131. Foulds, N. C., and Lowe, C. R. (1986) Enzyme Entrapment in Electrically Conducting Polymers - Immobilization of Glucose-Oxidase in Polypyrrole and Its Application in Amperometric Glucose Sensors, *J Chem Soc Farad T* 1 82, 1259-1264.
132. Psoma, S. D., van der Wal, P. D., Frey, O., de Rooij, N. F., and Turner, A. P. F. (2010) A novel enzyme entrapment in SU-8 microfabricated films for glucose micro-biosensors, *Biosensors and Bioelectronics* 26, 1582-1587.
133. Yan, J., Pedrosa, V. A., Simonian, A. L., and Revzin, A. (2010) Immobilizing Enzymes onto Electrode Arrays by Hydrogel Photolithography to Fabricate Multi-Analyte Electrochemical Biosensors, *Acs Appl Mater Inter* 2, 748-755.
134. Strike, D. J., Derooij, N. F., and Koudelkahep, M. (1993) Electrodeposition of Glucose-Oxidase for the Fabrication of Miniature Sensors, *Sensor Actuat B-Chem* 13, 61-64.
135. Quinto, M., Koudelka-Hep, M., and Palmisano, F. (2001) Enzyme modified microband electrodes: cross-talk effects and their elimination, *Analyst* 126, 1068-1072.
136. Palmisano, F., Rizzi, R., Centonze, D., and Zambonin, P. G. (2000) Simultaneous monitoring of glucose and lactate by an interference and cross-talk free dual electrode amperometric biosensor based on electropolymerized thin films, *Biosens Bioelectron* 15, 531-539.
137. Suzuki, M., and Akaguma, H. (2000) Chemical cross-talk in flow-type integrated enzyme sensors, *Sensors and Actuators B: Chemical* 64, 136-141.
138. Yu, P., and Wilson, G. S. (2000) An independently addressable microbiosensor array: What are the limits of sensing element density?, *Faraday Discussions* 116, 305-317.
139. Jobst, G., Moser, I., Varahram, M., Svasek, P., Aschauer, E., Trajanoski, Z., Wach, P., Kotanko, P., Skrabal, F., and Urban, G. (1996) Thin-film microbiosensors for glucose-lactate monitoring, *Anal Chem* 68, 3173-3179.
140. Dempsey, E., Diamond, D., Smyth, M. R., Urban, G., Jobst, G., Moser, I., Verpoorte, E. M. J., Manz, A., Michael Widmer, H., Rabenstein, K., and Freaney, R. (1997) Design and development of a miniaturised total chemical analysis system for on-line lactate and glucose monitoring in biological samples, *Analytica Chimica Acta* 346, 341-349.



141. Wassum, K. M., Tolosa, V. M., Tseng, T. C., Balleine, B. W., Monbouquette, H. G., and Maidment, N. T. (2012) Transient extracellular glutamate events in the basolateral amygdala track reward-seeking actions, *J Neurosci* 32, 2734-2746.
142. Burmeister, J. J., Pomerleau, F., Huettl, P., Gash, C. R., Werner, C. E., Bruno, J. P., and Gerhardt, G. A. (2008) Ceramic-based multisite microelectrode arrays for simultaneous measures of choline and acetylcholine in CNS, *Biosens Bioelectron* 23, 1382-1389.
143. Stephens, M. L., Pomerleau, F., Huettl, P., Gerhardt, G. A., and Zhang, Z. M. (2010) Real-time glutamate measurements in the putamen of awake rhesus monkeys using an enzyme-based human microelectrode array prototype, *J Neurosci Meth* 185, 264-272.
144. Vaddiraju, S., Tomazos, I., Burgess, D. J., Jain, F. C., and Papadimitrakopoulos, F. (2010) Emerging synergy between nanotechnology and implantable biosensors: a review, *Biosens Bioelectron* 25, 1553-1565.
145. Dale, N., Hatz, S., Tian, F. M., and Llaudet, E. (2005) Listening to the brain: microelectrode biosensors for neurochemicals, *Trends in Biotechnology* 23, 420-428.
146. Wilson, R., and Turner, A. P. F. (1992) Glucose-Oxidase - an Ideal Enzyme, *Biosensors & Bioelectronics* 7, 165-185.
147. McMahan, C. P., Killoran, S. J., and O'Neill, R. D. (2005) Design variations of a polymer-enzyme composite biosensor for glucose: Enhanced analyte sensitivity without increased oxygen dependence, *J Electroanal Chem* 580, 193-202.
148. Tian, F., Gourine, A. V., Huckstepp, R. T., and Dale, N. (2009) A microelectrode biosensor for real time monitoring of L-glutamate release, *Anal Chim Acta* 645, 86-91.
149. Coche-Guerente, L., Cosnier, S., Innocent, C., and Mailley, P. (1995) Development of amperometric biosensors based on the immobilization of enzymes in polymer films electrogenerated from a series of amphiphilic pyrrole derivatives, *Analytica Chimica Acta* 311, 23-30.
150. Ohara, T. J., Rajagopalan, R., and Heller, A. (1993) Glucose electrodes based on cross-linked [Os(bpy)<sub>2</sub>Cl]<sup>+/2+</sup> complexed poly(1-vinylimidazole) films, *Anal Chem* 65, 3512-3517.
151. Gregg, B. A., and Heller, A. (1991) Redox Polymer Films Containing Enzyme. 1. A Redox-Conducting Epoxy Cement: Synthesis, Characterization, and Electrocatalytic Oxidation of Hydroquinone, *J. Phys. Chem.* 95, 5970-5975.
152. Kulagina, N. V., Shankar, L., and Michael, A. C. (1999) Monitoring glutamate and ascorbate in the extracellular space of brain tissue with electrochemical microsensors, *Anal Chem* 71, 5093-5100.
153. Oldenziel, W. H., Beukema, W., and Westerink, B. H. C. (2004) Improving the reproducibility of hydrogel-coated glutamate microsensors by using an automated dipcoater, *J Neurosci Meth* 140, 117-126.
154. McGarraugh, G. (2009) The chemistry of commercial continuous glucose monitors, *Diabetes Technol Ther* 11 Suppl 1, S17-24.
155. Zigah, D., Pellissier, M., Fabre, B., Barrière, F., and Hapiot, P. (2009) Covalent immobilization and SECM analysis in feedback mode of glucose oxidase on a modified oxidized silicon surface, *J Electroanal Chem* 628, 144-147.
156. Molla, G., Vegezzi, C., Pilone, M. S., and Pollegioni, L. (1998) Overexpression in Escherichia coli of a recombinant chimeric Rhodotorula gracilis d-amino acid oxidase, *Protein Expr Purif* 14, 289-294.
157. Hayashi, S., and Nakamura, S. (1976) Comparison of fungal glucose oxidases. Chemical, physicochemical and immunological studies, *Biochim Biophys Acta* 438, 37-48.
158. Nakamura, S., Hayashi, S., and Koga, K. (1976) Effect of periodate oxidation on the structure and properties of glucose oxidase, *Biochim Biophys Acta* 445, 294-308.
159. Szajani, B., Molnar, A., Klamar, G., and Kalman, M. (1987) Preparation, characterization, and potential application of an immobilized glucose oxidase, *Appl Biochem Biotechnol* 14, 37-47.
160. Kalisz, H. M., Hecht, H. J., Schomburg, D., and Schmid, R. D. (1990) Crystallization

- and preliminary X-ray diffraction studies of a deglycosylated glucose oxidase from *Aspergillus niger*, *J Mol Biol* 213, 207-209.
161. Demers, N., Agostinelli, E., Averill-Bates, D. A., and Fortier, G. (2001) Immobilization of native and poly(ethylene glycol)-treated ('PEGylated') bovine serum amine oxidase into a biocompatible hydrogel, *Biotechnol Appl Bioc* 33, 201-207.
  162. Pollegioni, L., Falbo, A., and Pilone, M. S. (1992) Specificity and kinetics of *Rhodotorula gracilis* D-amino acid oxidase, *Biochim Biophys Acta* 1120, 11-16.
  163. Buto, S., Pollegioni, L., D'Angiuro, L., and Pilone, M. S. (1994) Evaluation of D-amino acid oxidase from *Rhodotorula gracilis* for the production of alpha-keto acids: a reactor system, *Biotechnol Bioeng* 44, 1288-1294.
  164. Mikeladze, E., Collins, A., Sukhacheva, M., Netrusov, A., and Csoregi, E. (2002) Characterization of a Glutamate Biosensor Based on a Novel Glutamate Oxidase Integrated into a Redox Hydrogel, *Electroanal* 14, 1052-1059.
  165. Maalouf, R., Chebib, H., Saikali, Y., Vittori, O., Sigaud, M., and Jaffrezic-Renault, N. (2007) Amperometric and impedimetric characterization of a glutamate biosensor based on Nafion and a methyl viologen modified glassy carbon electrode, *Biosens Bioelectron* 22, 2682-2688.
  166. Leybaert, L. (2005) Neurobarrier coupling in the brain: a partner of neurovascular and neurometabolic coupling?, *J Cereb Blood Flow Metab* 25, 2-16.
  167. Malitesta, C., Palmisano, F., Torsi, L., and Zambonin, P. G. (1990) Glucose fast-response amperometric sensor based on glucose oxidase immobilized in an electropolymerized poly(o-phenylenediamine) film, *Anal Chem* 62, 2735-2740.
  168. Oldenzel, W. H., and Westerink, B. H. C. (2005) Improving glutamate microsensors by optimizing the composition of the redox hydrogel, *Analytical Chemistry* 77, 5520-5528.
  169. Okahata, Y., Tsuruta, T., Ijro, K., and Ariga, K. (1989) Preparations of Langmuir-Blodgett Films of Enzyme Lipid Complexes - a Glucose Sensor Membrane, *Thin Solid Films* 180, 65-72.
  170. Singhal, R., Takashima, W., Kaneto, K., Samanta, S. B., Annapoorni, S., and Malhotra, B. D. (2002) Langmuir-Blodgett films of poly(3-dodecyl thiophene) for application to glucose biosensor, *Sensor Actuat B-Chem* 86, 42-48.
  171. Hnaïen, M., Hassen, W. M., Abdelghani, A., Cotte, S., Leonard, D., Bessueille, F., and Jaffrezic-Renault, N. (2009) A conductometric biosensor for the estimation of the number of cleaving sites in peptides and proteins, *Electrochem Commun* 11, 165-168.
  172. Hu, Y. B., Mitchell, K. M., Albahadily, F. N., Michaelis, E. K., and Wilson, G. S. (1994) Direct Measurement of Glutamate Release in the Brain Using a Dual Enzyme-Based Electrochemical Sensor, *Brain Res* 659, 117-125.
  173. Vasylieva, N., Barnych, B., Meiller, A., Maucler, C., Pollegioni, L., Lin, J.-S., Barbier, D., and Marinesco, S. (2011) Covalent enzyme immobilization by poly(ethylene glycol) diglycidyl ether (PEGDE) for microelectrode biosensor preparation, *Biosensors and Bioelectronics* (submitted).
  174. Heller, A. (2006) Electron-conducting redox hydrogels: Design, characteristics and synthesis, *Curr Opin Chem Biol* 10, 664-672.
  175. Cui, J., Kulagina, N. V., and Michael, A. C. (2001) Pharmacological evidence for the selectivity of in vivo signals obtained with enzyme-based electrochemical sensors, *J Neurosci Meth* 104, 183-189.
  176. Walcarius. (2001) Electroanalysis with Pure, Chemically Modified, and Sol-Gel-Derived Silica-Based Materials, *Electroanal* 13, 701-718.
  177. Ciriminna, R., Sciortino, M., Alonzo, G., Schrijver, A. D., and Pagliaro, M. (2010) From Molecules to Systems: Sol-Gel Microencapsulation in Silica-Based Materials, *Chem Rev*.
  178. Sayen, S., and Walcarius, A. (2003) Electro-assisted generation of functionalized silica films on gold, *Electrochem Commun* 5, 241-348.
  179. Shacham, R., Avnir, D., and Mandler, D. (1999) Electrodeposition of methylated sol-gel films on conducting surfaces, *Adv Mater* 11, 384-388.

180. Rozhanchuk, T., Tananaiko, O., Mazurenko, I., Etienne, M., Walcarius, A., and Zaitsev, V. (2009) Electroanalytical properties of haemoglobin in silica-nanocomposite films electrogenerated on pyrolytic graphite electrode, *J Electroanal Chem* 625, 33-39.
181. Yang, S., Jia, W. Z., Qian, Q. Y., Zhou, Y. G., and Xia, X. H. (2009) Simple Approach for Efficient Encapsulation of Enzyme in Silica Matrix with Retained Bioactivity, *Analytical Chemistry* 81, 3478-3484.
182. Dale, N., Llaudet, E., and Droniou, M. (2004) COATINGS, C12Q 1/00 ed.
183. Tian, F. M., Wu, W. J., Broderick, M., Vamvakaki, V., Chaniotakis, N., and Dale, N. (2010) Novel microbiosensors prepared utilizing biomimetic silicification method, *Biosensors & Bioelectronics* 25, 2408-2413.
184. Cosnier, S., and Innocent, C. (1992) A novel biosensor elaboration by electropolymerization of an adsorbed amphiphilic pyrrole-tyrosinase enzyme layer, *Electroanal. Chem.*, 328, 361-366.
185. Coche-Guerente, L., Deronzier, A., Galland, B., Labbe, P., Moutet, J. C., and Reverdy, G. (1991) Immobilization of Redox Anions in Poly(Amphiphilic Pyrrolylalkylammonium) Using a Simple and Monomer-Saving One-Step Procedure in Pure Water-Electrolyte, *J Chem Soc Chem Comm*, 386-388.
186. Cosnier, S., Fombon, J.-J., Labbea, P., and Limosin, D. (1999) Development of a PPO-polyamphiphilic pyrrole/ electrode for on site monitoring of phenol in aqueous effluents, *Sensors and Actuators B* 59, 134-139.
187. Arima, J., Tamura, T., Kusakabe, H., Ashiuchi, M., Yagi, T., Tanaka, H., and Inagaki, K. (2003) Recombinant expression, biochemical characterization and stabilization through proteolysis of an L-glutamate oxidase from *Streptomyces* sp. X-119-6, *J Biochem* 134, 805-812.
188. Kusakabe, H., Midorikawa, Y., Kuninaka, A., and Yoshino, H. (1983) Occurrence of a New Enzyme, L-Glutamate Oxidase in a Wheat Bran Culture Extract of *Streptomyces* sp. X-1 19-6, *Agric. Biol. Chem.*, 47, 179-182.
189. Robinson, D. L., Hermans, A., Seipel, A. T., and Wightman, R. M. (2008) Monitoring rapid chemical communication in the brain, *Chemical Reviews* 108, 2554-2584.
190. Wisniewski, N., and Reichert, M. (2000) Methods for reducing biosensor membrane biofouling, *Colloid Surface B* 18, 197-219.
191. Gourine, A. V., Dale, N., Korsak, A., Llaudet, E., Tian, F., Huckstepp, R., and Spyer, K. M. (2008) Release of ATP and glutamate in the nucleus tractus solitarii mediate pulmonary stretch receptor (Breuer-Hering) reflex pathway, *J Physiol-London* 586, 3963-3978.
192. Dale, N., Gourine, A. V., Llaudet, E., Bulmer, D., Thomas, T., and Spyer, K. M. (2002) Rapid adenosine release in the nucleus tractus solitarii during defence response in rats: real-time measurement in vivo, *J Physiol-London* 544, 149-160.
193. Newman, L. A., Korol, D. L., and Gold, P. E. (2011) Lactate produced by glycogenolysis in astrocytes regulates memory processing, *PLoS One* 6, e28427.
194. Mateo, C., Palomo, J. M., Fernandez-Lorente, G., Guisan, J. M., and Fernandez-Lafuente, R. (2007) Improvement of enzyme activity, stability and selectivity via immobilization techniques, *Enzyme Microb Tech* 40, 1451-1463.
195. Mateo, C., Abian, O., Fernández-Lorente, G., Pedroche, J., Fernández-Lafuente, R., and Guisan, J. M. (2002) Epoxy Sepabeads: A Novel Epoxy Support for Stabilization of Industrial Enzymes via Very Intense Multipoint Covalent Attachment, *Biotechnol Progr* 18, 629-634.
196. Lopez-Gallego, F., Betancor, L., Mateo, C., Hidalgo, A., Alonso-Morales, N., Dellamora-Ortiz, G., Guisan, J. M., and Fernandez-Lafuente, R. (2005) Enzyme stabilization by glutaraldehyde crosslinking of adsorbed proteins on aminated supports, *J Biotechnol* 119, 70-75.
197. Bes, M. T., Gomez-Moreno, C., Guisan, J. M., and Fernandez-Lafuente, R. (1995) Selective oxidation: stabilisation by multipoint attachment of ferredoxin NADP+ reductase, an interesting cofactor recycling enzyme, *Journal of Molecular Catalysis A: Chemical* 98, 161-169.

198. Takahashi, H., Li, B., Sasaki, T., Miyazaki, C., Kajino, T., and Inagaki, S. (2001) Immobilized enzymes in ordered mesoporous silica materials and improvement of their stability and catalytic activity in an organic solvent, *Microporous and Mesoporous Materials* 44–45, 755-762.
199. Shepard, D., Donovan, M., Raghupathy, E., Yeung, K. K., Owen, A. J., and Dain, J. A. (1983) Effect of Immobilization on the Stability and Substrate-Specificity of Alpha-D-Galactosidase Isolated from the Invertebrate Turbo-Cornutus, *Carbohydr Res* 118, 239-245.
200. Palomo, J. M., Fernandez-Lorente, G., Mateo, C., Ortiz, C., Fernandez-Lafuente, R., and Guisan, J. M. (2002) Modulation of the enantioselectivity of lipases via controlled immobilization and medium engineering: hydrolytic resolution of mandelic acid esters, *Enzyme Microb Tech* 31, 775-783.
201. Shepard, D., Donovan, M., Raghupathy, E., Yeung, K.-K., Owen, A. J., and Dain, J. A. (1983) Effect of immobilization on the stability and substrate specificity of  $\alpha$ -d-galactosidase isolated from the invertebrate Turbo cornutus, *Carbohydrate Research* 118, 239-245.
202. Grossie, V. B., Yick, J., Alpeter, M., Welbourne, T. C., and Ota, D. M. (1993) Glutamine Stability in Biological Tissues Evaluated by Fluorometric Analysis, *Clin Chem* 39, 1059-1063.
203. Sauvinet, V., Parrot, S., Benturquia, N., Bravo-Moraton, E., Renaud, B., and Denoroy, L. (2003) In vivo simultaneous monitoring of gamma-aminobutyric acid, glutamate, and L-aspartate using brain microdialysis and capillary electrophoresis with laser-induced fluorescence detection: Analytical developments and in vitro/in vivo validations, *Electrophoresis* 24, 3187-3196.
204. Hu, Y., and Wilson, G. S. (1997) Rapid changes in local extracellular rat brain glucose observed with an in vivo glucose sensor, *J Neurochem* 68, 1745-1752.
205. Pazur, J. H., and Kleppe, K. (1964) The Oxidation of Glucose and Related Compounds by Glucose Oxidase from *Aspergillus Niger*, *Biochemistry* 3, 578-583.
206. Keilin, D., and Hartree, E. F. (1948) Properties of glucose oxidase (notatin): Addendum. Sedimentation and diffusion of glucose oxidase (notatin), *Biochem J* 42, 221-229.
207. Sols, A., and Crane, R. K. (1954) Substrate specificity of brain hexokinase, *J Biol Chem* 210, 581-595.
208. Viggiano, A., Marinesco, S., Pain, F., Meiller, A., and Gurden, H. (2012) Reconstruction of field excitatory post-synaptic potentials in the dentate gyrus from amperometric biosensor signals, *J Neurosci Methods* 206, 1-6.
209. Goldstein, L. (1972) Microenvironmental effects on enzyme catalysis. A kinetic study of polyanionic and polycationic derivatives of chymotrypsin, *Biochemistry* 11, 4072-4084.
210. Engasser, J. M., and Horvath, C. (1973) Effect of internal diffusion in heterogeneous enzyme systems: evaluation of true kinetic parameters and substrate diffusivity, *Journal of theoretical biology* 42, 137-155.
211. Bru, R., Sanchez-Ferrer, A., and Garcia-Carmona, F. (1990) The effect of substrate partitioning on the kinetics of enzymes acting in reverse micelles, *Biochem J* 268, 679-684.
212. Clark, D. S. (1994) Can immobilization be exploited to modify enzyme activity?, *Trends in Biotechnology* 12, 439-443.
213. Hecht, H. J., Kalisz, H. M., Hendle, J., Schmid, R. D., and Schomburg, D. (1993) Crystal structure of glucose oxidase from *Aspergillus niger* refined at 2.3 Å resolution, *Journal of molecular biology* 229, 153-172.
214. Kandel, E., Schwartz, J., and TMJessell (2000) *Principles of neural science*, fourth edition ed., McGraw-Hill, New York.
215. Ballini, C., Corte, L. D., Pazzagli, M., Colivicchi, M. A., Pepeu, G., Tipton, K. F., and Giovannini, M. G. (2008) Extracellular levels of brain aspartate, glutamate and GABA during an inhibitory avoidance response in the rat, *J Neurochem* 106, 1035-1043.
216. Hernandez, L. F., Segovia, G., and Mora, F. (2008) Chronic treatment with a

- dopamine uptake blocker changes dopamine and acetylcholine but not glutamate and GABA concentrations in prefrontal cortex, striatum and nucleus accumbens of the awake rat, *Neurochem Int* 52, 457-469.
217. Hugues, S., Garcia, R., and Lena, I. (2007) Time course of extracellular catecholamine and glutamate levels in the rat medial prefrontal cortex during and after extinction of conditioned fear, *Synapse* 61, 933-937.
218. Ferraro, L., Tomasini, M. C., Gessa, G. L., Bebe, B. W., Tanganelli, S., and Antonelli, T. (2001) The cannabinoid receptor agonist WIN 55,212-2 regulates glutamate transmission in rat cerebral cortex: an in vivo and in vitro study, *Cereb Cortex* 11, 728-733.
219. Rocha, L., Briones, M., Ackermann, R. F., Anton, B., Maidment, N. T., Evans, C. J., and Engel, J., Jr. (1996) Pentylentetrazol-induced kindling: early involvement of excitatory and inhibitory systems, *Epilepsy Res* 26, 105-113.
220. Boatell, M. L., Bendahan, G., and Mahy, N. (1995) Time-related cortical amino acid changes after basal forebrain lesion: a microdialysis study, *J Neurochem* 64, 285-291.
221. van der Zeyden, M., Oldenziel, W. H., Rea, K., Cremers, T. I., and Westerink, B. H. (2008) Microdialysis of GABA and glutamate: analysis, interpretation and comparison with microsensors, *Pharmacology, biochemistry, and behavior* 90, 135-147.
222. Borland, L. M., Shi, G., Yang, H., and Michael, A. C. (2005) Voltammetric study of extracellular dopamine near microdialysis probes acutely implanted in the striatum of the anesthetized rat, *J Neurosci Methods* 146, 149-158.
223. Hu, Y., Mitchell, K. M., Albahadily, F. N., Michaelis, E. K., and Wilson, G. S. (1994) Direct measurement of glutamate release in the brain using a dual enzyme-based electrochemical sensor, *Brain Res* 659, 117-125.
224. Okubo, Y., Sekiya, H., Namiki, S., Sakamoto, H., Iinuma, S., Yamasaki, M., Watanabe, M., Hirose, K., and Iino, M. (2010) Imaging extrasynaptic glutamate dynamics in the brain, *Proc Natl Acad Sci U S A* 107, 6526-6531.
225. Herman, M. A., and Jahr, C. E. (2007) Extracellular glutamate concentration in hippocampal slice, *J Neurosci* 27, 9736-9741.
226. Campbell, P. K., Jones, K. E., Huber, R. J., Horch, K. W., and Normann, R. A. (1991) A silicon-based, three-dimensional neural interface: manufacturing processes for an intracortical electrode array, *IEEE Trans Biomed Eng* 38, 758-768.
227. Bai, Q., Wise, K. D., and Anderson, D. J. (2000) A high-yield microassembly structure for three-dimensional microelectrode arrays, *Ieee T Bio-Med Eng* 47, 281-289.
228. Laszlo, G., Anita, P., Vazsonyi, E., Gergely, M., Guban, D., Fiath, R., Kerekes, B. P., Gyorgy, K., Istvan, U., and Gabor, B. (2011) A novel multisite silicon probe for high quality laminar neural recordings, *Sensor Actuat a-Phys* 166, 14-21.
229. Cosnier, S. (2003) Biosensors based on electropolymerized films: new trends, *Anal Bioanal Chem*, 507-520.
230. Walcarius, A. (1998) Analytical applications of silica-modified electrodes - A comprehensive review, *Electroanal* 10, 1217-1235.
231. Krajewska, B. (2004) Application of chitin- and chitosan-based materials for enzyme immobilizations: a review, *Enzyme and Microbial Technology* 35, 126-139.
232. PETER, M. G. (1995) Applications and environmental aspects of chitin and chitosan, *J Macromol Sci Pure Appl Chem* 32, 629-640.
233. Kang, X. H., Wang, J., Wu, H., Aksay, I. A., Liu, J., and Lin, Y. H. (2009) Glucose Oxidase-graphene-chitosan modified electrode for direct electrochemistry and glucose sensing, *Biosensors & Bioelectronics* 25, 901-905.
234. Norouzi, P., Pirali-Hamedani, M., Ganjali, M. R., and Faridbod, F. (2010) A Novel Acetylcholinesterase Biosensor Based on Chitosan-Gold Nanoparticles Film for Determination of Monocrotophos Using FFT Continuous Cyclic Voltammetry, *Int J Electrochem Sc* 5, 1434-1446.
235. Wan, D., Yuan, S., Li, G. L., Neoh, K. G., and Kang, E. T. (2010) Glucose biosensor from covalent immobilization of chitosan-coupled carbon nanotubes on polyaniline-modified gold electrode, *ACS Appl Mater Interfaces* 2, 3083-3091.

236. Li, Y., X, X. P., Epand, R., and Zhitomirsky, I. (2011) Electrodeposition of chitosan-hemoglobin films, *Materials Letters*.
237. Fellows, L. K., Boutelle, M. G., and Fillenz, M. (1992) Extracellular Brain Glucose Levels Reflect Local Neuronal Activity: A Microdialysis Study in Awake, Freely Moving Rats, *J Neurochem* 59, 2141-2147.
238. Silver, I. A., and Erecinska, M. (1994) Extracellular glucose concentration in mammalian brain: continuous monitoring of changes during increased neuronal activity and upon limitation in oxygen supply in normo-, hypo-, and hyperglycemic animals, *J Neurosci* 14, 5068-5076.
239. Ronne-Engström, E., Carlson, H., Yansheng, L., Ungerstedt, U., and Hillered, L. (1995) Influence of Perfusate Glucose Concentration on Dialysate Lactate, Pyruvate, Aspartate, and Glutamate Levels Under Basal and Hypoxic Conditions: A Microdialysis Study in Rat Brain, *J Neurochem* 65, 257-262.
240. Eklund, T., Wahlberg, J., Ungerstedt, U., and Hillered, L. (1991) Interstitial lactate, inosine and hypoxanthine in rat kidney during normothermic ischaemia and recirculation\*, *Acta Physiologica Scandinavica* 143, 279-286.
241. M Demestre, and, M. B., and Fillenz, M. (1997) Stimulated release of lactate in freely moving rats is dependent on the uptake of glutamate, *JOURNAL OF PHYSIOLOGY* 499, 825-832.
242. Harada, M., Sawa, T., Okuda, C., Matsuda, T., and Tanaka, Y. (1993) Effects of Glucose Load on Brain Extracellular Lactate Concentration in Conscious Rats Using a Microdialysis Technique, *Horm Metab Res* 25, 560-563.
243. Harada, M., Okuda, C., Sawa, T., and Murakami, T. (1992) Cerebral Extracellular Glucose and Lactate Concentrations during and after Moderate Hypoxia in Glucose- and Saline-infused Rats, *Anesthesiology* 77, 728-734.



# Annexes





## Annex 1. Microfabrication

### Microfabrication protocol

1. Double-side polished p-type, B-doped silicon wafers of  $250\pm 15\mu\text{m}$  thickness and double-side thermal grown  $1\text{-}2\mu\text{m}$   $\text{SiO}_2$  were used (Siltronix).
2. Prior to technological procedure, the silicon wafer were cleaned with acetone, ethanol and dried in nitrogen gas stream, if needed.
3. The lithography to define the electrodes pattern was done with photosensitive resist AZ 5214 (negative mode):
  - Spin-coating at acceleration/speed/time: (rpm=rounds per minute) 3000(rpm/sec)/3000rpm/30 sec;
  - Soft-bake at hot plate  $120^\circ\text{C}$ , 2min;
  - UV-light exposition  $35\text{ mJ/cm}^2$  under hard glass mask;
  - Reverse bake at hot plate  $120^\circ\text{C}$ , 1min 30sec;
  - Exposition  $150\text{mJ/cm}^2$  without mask;
  - Development in MIF726, 1min.
4. Substrate metallization by evaporation: Ti= 20nm, Pt=100nm.
5. Lift-off of metals at acetone/ethanol or Remover PG/acetone/ethanol.
6. The lithography of top isolator layer. To obtain  $3.5\text{-}4\mu\text{m}$  thickness the photoresist SU8-2 (negative) was used. Prior to resist spin-coating, it is indispensable to bake the substrate at  $150^\circ\text{C}$  for 10 min to eliminate the adsorbed  $\text{H}_2\text{O}$  on the  $\text{SiO}_2$ :
  - Spin-coating at acc/speed/time: 1) 100/500/1sec, 2) 300/2000/30sec;
  - Soft-bake at hot plate: 1)  $65^\circ\text{C}$ , 1min, 2)  $95^\circ\text{C}$ , 3min;
  - UV-light exposition  $150\text{ mJ/cm}^2$  under hard glass mask;
  - Post-exposure bake: 1)  $65^\circ\text{C}$ , 1min, 2)  $95^\circ\text{C}$ , 1min;
  - Development in PEGMA, 2min with intensive agitation.
7. The SPR 220-4.5 (positive) lithography at the back side of the wafer and then on the top side to define the membrane positions and needle shape, respectively. To obtain the resist layer of  $4\mu\text{m}$  the following parameters were used for both sides:
  - Spin-coating at acceleration/speed/time: 4000/4000/30 sec;
  - Soft-bake at hot plate  $115^\circ\text{C}$ , 1min 30sec;
  - UV-light exposition  $230\text{ mJ/cm}^2$  under hard glass mask;
  - It is advisable to leave the wafer for 10 min to repose at ambient conditions;
  - Post-exposure bake at hot plate  $115^\circ\text{C}$ , 1min 30sec;
  - Development in MIF726, 1min.
8. The SPR resist acts as a protection mask during wet etch of  $\text{SiO}_2$ . For  $\text{SiO}_2$  etch BOE (buffered HF solution,  $\text{NH}_4\text{F}/\text{HF}$ ) solution was used. The etch rate is about  $1\mu\text{m}$  for 6-8 min.
9. To determine final needle-shape of the microprobe, the DRIE was performed on the top side and back side consequently.
10. The design was considered so that each microprobe was break out of the bulk wafer

as “chocolate tablet”. In other cases, the probes were cut out by diamond saw.

11. Finally, the microprobe was glued on the home-made printed circuit board. The electrical contacts were made by microsolder with ultrasonic assistance.

### **SU8 patterning conditions**

#### SU8-2000.5 (0.8 $\mu$ m)

- Spin-coating at acc/speed/time: 1) 100/500/7sec,  
2) 300/2000/30sec;
- Soft-bake at hot plate: 95°C, 1min;
- UV-light exposition 140 mJ/cm<sup>2</sup> under hard glass mask;
- Post-exposure bake: 95°C, 1min 30 sec;
- Development in PEGMA, 1min with intensive agitation.

#### SU8-2010 (11 $\mu$ m)

- Spin-coating at acc/speed/time: 1) 100/500/7sec,  
2) 300/2000/30sec;
- Soft-bake at hot plate: 95°C, 2min 30 sec;
- UV-light exposition 250 mJ/cm<sup>2</sup> under hard glass mask;
- Post-exposure bake: 95°C, 3min30 sec;
- Development in PEGMA, 2-3min with intensive agitation.

#### SU8-2 (2 $\mu$ m)

- Spin-coating at acc/speed/time: 1) 100/500/1sec,  
2) 300/3000/30sec;
- Soft-bake at hot plate: 1) 65°C, 1min,  
2) 95°C, 1min;
- UV-light exposition 150 mJ/cm<sup>2</sup> under hard glass mask;
- Post-exposure bake: 1) 65°C, 1min,  
2) 95°C, 1min;
- Development in PEGMA, 1min with intensive agitation.

### **SU8 oxygen plasma etch conditions**

O<sub>2</sub> flow rate – 20 sccm

Total pressure – 100mTor

Plasma power – 540 W

## Design evolution within project

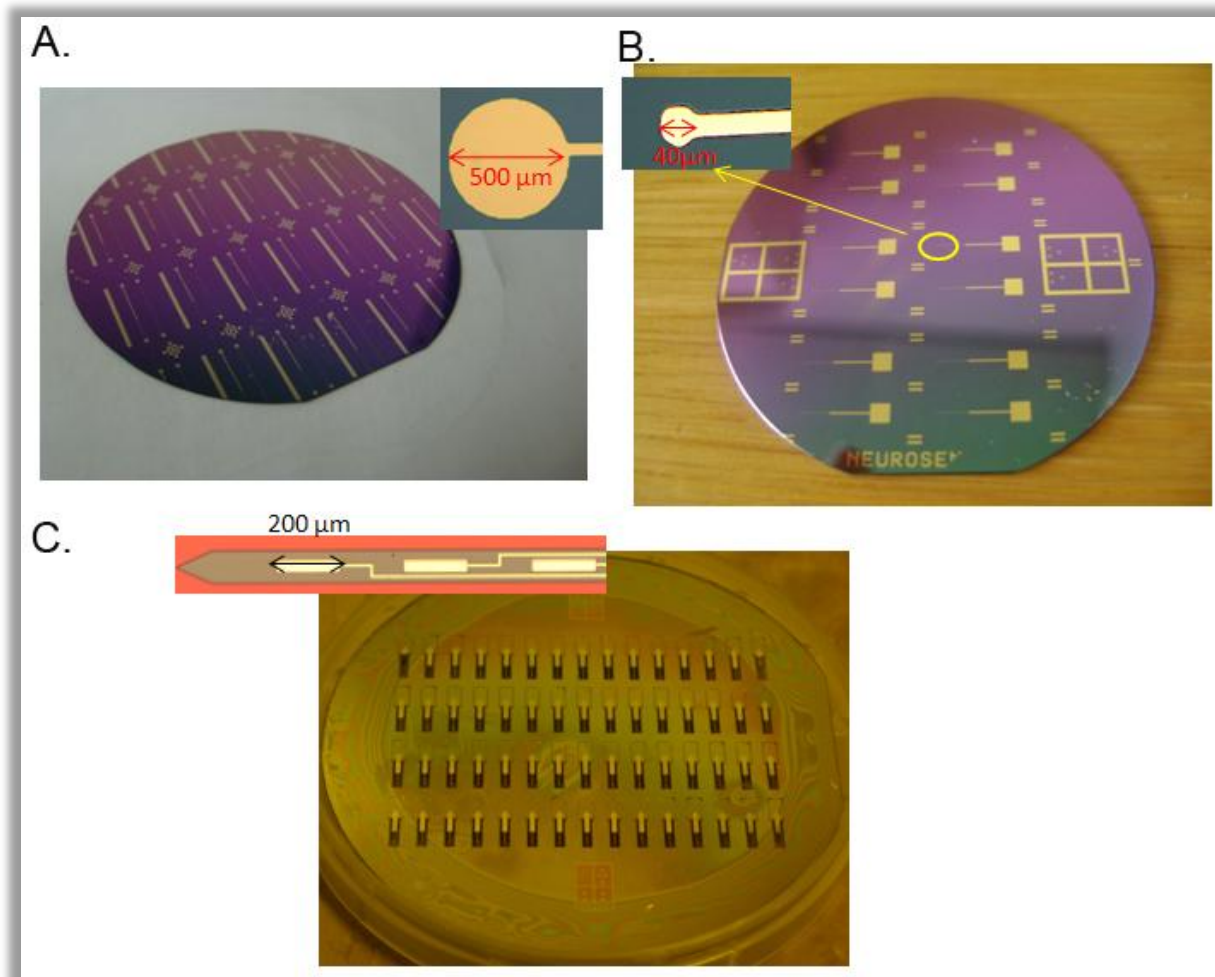


**Figure A. 1. Microprobe design:** A. The first design, a monoelectrode probe with circle electroactive site (500  $\mu\text{m}$  diameter); B. The second design – miniaturization of design A (40  $\mu\text{m}$  diameter); C. Final three-electrode microprobe design.



## Annex 2. Enzyme-immobilization protocols

### PEGDE

Oxidase	Enzyme, mg/mL	BSA, mg/mL	PEGDE, mg/mL	V <sub>aliqu.</sub> , $\mu$ L	T, °C	time
Glucose	60	30	20	5	55-57	2h
DAAO	58	25	5.9	8.5	55	1h45
Glutamate	100	150	100	5	45-47	1h30
Lactate	60	30/60	42.8	7	55	2h
Choline	60	30	10	5	55	2h
Glycine	30	15	10	5	45-47	1h
Histamine	60	30	20	5	45-47	1h-2h

### Glutaraldehyde

Oxidase	Enzyme, mg/mL	BSA, mg/mL	V <sub>protein aliqu.</sub> , $\mu$ L	time
Glucose	60	30	5	3min30sec
DAAO	58	25	8.5	2min30sec
Glutamate	100	150	5	3min30sec
Lactate	60	30/60	7	2min15sec
Choline	60	30	5	2min30sec
Glycine	30	15	5	3min
Histamine	60	30	5	2min



### Annex 3. Thesis summary in French

Les microcapteurs enzymatiques implantables sont des outils de choix pour l'étude du système nerveux central. Ils permettent d'analyser en temps réel la composition du milieu interstitiel du cerveau et les variations de concentration de neurotransmetteurs et de substrats métaboliques dans l'espace extracellulaire. Le diagnostic médical nécessite de plus en plus une détection et un suivi de biomarqueurs et d'autres molécules endogènes chez le patient pour comprendre l'évolution des maladies neurologiques. Dans les expériences sur les animaux de laboratoire, les microcapteurs utilisés sont généralement des microélectrodes en platine recouvertes d'une couche d'enzyme immobilisée. Leur fabrication est simple et ne nécessite pas d'équipement ni de matériaux coûteux. De plus, les microcapteurs sont peu invasifs ce qui minimise les lésions tissulaires. Cependant, pour pouvoir les intégrer dans la pratique médicale, les biocapteurs doivent répondre à un cahier des charges qui inclut des normes de sécurité, de biocompatibilité, de stabilité opérationnelle et posséder une forte spécificité chimique.

Les développements récents ont abouti à des sondes multisensibles contenant plusieurs électrodes et permettant le suivi simultané de neurotransmetteurs et/ou de métabolites dans le cerveau dans des conditions physiologiques ou pathologiques. Ces dispositifs peuvent également détecter et suivre la concentration d'une molécule dans des zones différentes du cerveau, en réponse à une stimulation électrique, chimique ou au cours de processus biologiques spontanés. A présent, ces sondes multisensibles n'ont que très rarement abouti à des applications *in vivo*. Le potentiel de ces techniques en pratique clinique a également été très peu exploré.

La procédure d'immobilisation de l'enzyme sur la microélectrode a aussi un impact important sur les performances des biocapteurs. Une large variété de méthodes d'immobilisation a été développée mais la plupart des protocoles utilisent des composants toxiques, ce qui limite leur application potentielle en clinique. Les composés chimiques nécessaires à l'immobilisation sont souvent chers ou demandent une synthèse organique. Il est donc indispensable de développer une méthode d'immobilisation d'enzyme non-toxique et simple à réaliser. Il est aussi primordial de préserver la sélectivité naturelle des enzymes après l'immobilisation, pour assurer la détection sélective de neurotransmetteur dans un milieu complexe comme le cerveau, où les molécules d'intérêt sont présentes en quantité très faibles.

L'objectif de ce travail de thèse est de réaliser un outil biomédical qui permette de détecter simultanément et de manière très sélective la variation de concentration de neurotransmetteurs et de molécules métaboliques tels que le glutamate, la D-sérine, le glucose, ou le lactate et de le valider dans le cerveau d'animaux de laboratoire. Le travail expérimental associe trois domaines : la microfabrication, la chimie analytique et la neurobiologie, pour développer un outil analytique possédant un potentiel d'applications cliniques. Dans un premier temps, nous avons cherché à développer une méthode d'immobilisation en utilisant l'agent de réticulation poly(éthylène glycol) diglycidyl ether (PEGDE), qui pourrait mieux répondre aux critères des applications cliniques. Ensuite, nous avons adapté les méthodes d'immobilisation d'enzyme les plus utilisées dans le domaine des neurosciences: immobilisation par réticulation dans des vapeurs de Glutaraldéhyde ou par PEGDE, piégeage dans une matrice de sol-gel ou de polypyrrole dérivé, ou immobilisation dans une matrice d'hydrogel. Nous avons effectué l'étude comparative des biocapteurs réalisés en termes de sensibilité, de stabilité *in vivo*, de temps de réponse et aussi de toxicité. Nous avons caractérisé l'effet de ces procédures de fixation de l'enzyme



sur la spécificité apparente du biocapteur.

Nous avons enfin développé des sondes multisensibles en utilisant les techniques de microfabrication en salle blanche sur silicium et en utilisant le PEGDE pour l'immobilisation d'enzyme. Cet outil a été utilisé pour le suivi simultané de glucose et lactate dans le SNC de rats anesthésiés.

Cette thèse contient 5 Chapitres. Le Chapitre 1 est une revue bibliographique générale et les Chapitres 2-5 rapportent sur les principaux résultats de ce travail.

Le **Chapitre 1** décrit l'organisation et les mécanismes de fonctionnement du cerveau ainsi que l'intérêt particulier pour le suivi de molécules dans le milieu interstitiel et les méthodes relatives couramment employées dans la recherche fondamentale et clinique. Cette revue bibliographique couvre les domaines de la neurochimie, de la chimie analytique et du génie biomédical mais aussi les technologies de micro-nanofabrication.

Le cerveau est l'organe biologique le plus complexe chez les mammifères, qui contrôle les fonctions essentielles de l'organisme vivant et peut être le siège de maladies neurologiques. Il est important d'étudier et de comprendre le rôle de la communication chimique dans le cerveau. Schématiquement, la communication cellulaire s'opère par le biais d'impulsions électriques nerveuses, suivies par la libération de neurotransmetteurs dans l'espace extracellulaire suivie de leur fixation sur des récepteurs membranaires et par des cascades biochimiques intracellulaires. Le suivi des neurotransmetteurs, des molécules métaboliques et des hormones pendant le fonctionnement physiologique ou pathologique du cerveau est une approche efficace pour comprendre les mécanismes de communication cellulaire neuronale et gliale et pour suivre l'évolution d'une maladie neurologique. En plus de neurotransmetteurs, le milieu extracellulaire du cerveau contient des molécules métaboliques comme le glucose ou le lactate qui constituent des sources d'énergie pour les réactions biochimiques. Les changements d'activité neuronale sont accompagnés par des variations de leur concentration dans le milieu interstitiel. Ainsi, l'espace extracellulaire représente un environnement chimique complexe contenant des diverses substances impliquées dans l'activité neuronale.

Il existe des techniques modernes permettant la détection non-invasive de biomolécules dans le cerveau et parmi elles, la spectroscopie de résonance magnétique de protons (<sup>1</sup>HMR) ou la spectroscopie proche infrarouge. Néanmoins, les méthodes non-invasives reflètent généralement la concentration globale des molécules d'intérêt. Elles ne permettent pas de différencier la répartition des molécules entre les milieux intracellulaire et extracellulaire. Par exemple, le glutamate, principal neurotransmetteur excitateur du cerveau, est stocké dans des vésicules neuronales qui forment un stock intracellulaire représentant plus de 99% du glutamate total présent dans le cerveau, tandis que les quantités effectivement libérées dans le milieu extracellulaire pour assurer des fonctions de signalisation sont comparativement infimes. Ainsi, malgré le grand intérêt des techniques non invasives, particulièrement dans le cas des études cliniques, il y a aussi besoin de méthodes et de techniques de détection locale de molécules extracellulaires.

Deux méthodes principales sont utilisées pour le suivi des molécules dans le SNC des animaux de laboratoire: l'analyse en temps réel au moyen de biocapteurs ampérométriques et le prélèvement de liquide cérébral au moyen d'une sonde de microdialyse. Malgré ses performances, la microdialyse est seulement une technique de dosage et elle exige une méthode de détection appropriée. La chromatographie liquide à haute performance (HPLC) ou l'électrophorèse capillaire (CE) sont des techniques de séparation associées avec des détecteurs sensibles. Elles sont souvent utilisées pour

l'analyse des échantillons biologiques complexes avec une sélectivité chimique maximale, des limites de détection basses et une forte sensibilité. Cependant, ces techniques exigent souvent une préparation complexe des échantillons avant leur analyse. Dans les unités de soin intensif, l'analyse rapide des échantillons biologiques peut avoir une importance vitale, car les résultats de microdialyse peuvent indiquer une situation d'urgence vitale. De plus, malgré les progrès dans la construction de sondes de microdialyse, leur diamètre reste d'environ 200-300  $\mu\text{m}$  au minimum, ce qui peut causer des lésions du cerveau et une réponse inflammatoire après l'insertion. Par conséquent, cette technique exige un temps de récupération d'au moins plusieurs heures. Enfin, la résolution spatiale et temporelle de la microdialyse est relativement basse (10-30min) ce qui limite le suivi des événements biologiques rapides de quelques secondes, comme par exemple une libération de neurotransmetteurs. Pour surmonter ces contraintes, les biocapteurs à base de microélectrodes ont été développés comme alternative à la microdialyse pour les études neurochimiques. C'est la raison pour laquelle les biocapteurs enzymatiques implantables sont le sujet principal de ce travail de thèse.

Avant leur application dans les études neurologiques, les biocapteurs implantables doivent répondre à plusieurs critères: (1) une petite taille d'électrode qui limite l'étendue des lésions. Les électrodes de plus petite taille ont aussi une meilleure résolution spatiale; (2) une bonne sensibilité est nécessaire pour la détection des molécules en faibles quantités en gardant le signal linéaire dans la gamme de concentrations étudiées (typiquement, une limite de détection de l'ordre de  $10^{-7}$  M est souhaitable) ; (3) la sélectivité du biocapteur doit être optimale pour une molécule d'intérêt, l'influence des molécules endogènes oxydables doit être éliminée par des méthodes appropriées; (4) le temps de réponse détermine la résolution temporelle. Le changement rapide de la composition du milieu interstitiel, particulièrement en cas de libération des neurotransmetteurs, exigeant une haute résolution temporelle (un temps de réponse d'au plus une à deux secondes est souhaitable); (5) la stabilité de la réponse du biocapteur dans les conditions opérationnelles est importante sur toute la durée de l'expérience, et la stabilité pendant le stockage permet l'exploitation optimale de l'enzyme; (6) la biocompatibilité de tous les composants du biocapteur est importante pour éviter l'inflammation et la perturbation du fonctionnement physiologique du cerveau.

La procédure d'immobilisation de l'enzyme influe considérablement sur les caractéristiques opérationnelles du biocapteur. Elle détermine la plupart des critères exigés pour les capteurs implantables. La méthode d'immobilisation doit assurer une fixation stable sur la surface d'électrode et garantir la sensibilité de la réponse. Elle ne doit pas faire intervenir de produits toxiques et respecter des conditions de biocompatibilité. Il est désirable de proposer une procédure simple et peu coûteuse. Or, malgré un large choix parmi les méthodes existantes, il n'y en a aucune qui peut satisfaire tous les critères. Par conséquent, nous avons commencé cette étude par le développement d'une méthode d'immobilisation d'enzyme qui pourrait être intégrée dans la fabrication de dispositifs orientés sur les applications cliniques.

Le **Chapitre 2** est un article paru dans la revue *Biosensors and Bioelectronics* (2011) qui présente les résultats importants obtenus avec la méthode de fixation par le poly(éthylène glycol) diglycidyl ether (PEGDE). Le PEGDE est un des composants impliqués dans la synthèse d'hydrogels qui est utilisé pour la fabrication de biocapteurs commerciaux sensibles au glucose. Néanmoins, la possibilité d'immobiliser l'enzyme par le PEGDE seul n'a jamais été étudiée.

Le PEGDE est une molécule bi-fonctionnelle, qui contient deux groupes époxydes et

peut réagir avec les groupes amine ( $-\text{NH}_2$ ), hydroxyle ( $-\text{OH}$ ) et carboxyle ( $-\text{COOH}$ ). Les groupes amines présents dans la structure des protéines réagissent avec le PEGDE en produisant une matrice enzymatique sur la surface d'électrode. La réaction entre l'époxyde et la protéine est lente à température ambiante ( $\sim 48$  h), mais elle peut être considérablement accélérée par l'augmentation de la température. Dans les préparations de biocapteurs, la température doit être suffisamment haute pour accélérer la réaction mais assez basse pour éviter la dénaturation et la désactivation de l'enzyme. Nous avons fixé la température à  $55^\circ\text{C}$  et généralement, 2h de réaction ont été suffisantes pour obtenir une matrice d'enzyme stable.

Dans un premier temps, la méthode d'immobilisation par PEGDE a été étudiée et optimisée pour fabriquer des biocapteurs sensibles au Glucose. La composition de la solution contenant la Glucose Oxydase, la protéine supplémentaire inactive (Bovine Sérum Albumine, BSA) et le PEGDE a été variée afin de trouver une proportion des composants qui permet d'obtenir une forte sensibilité du biocapteur. Nous avons démontré que la sensibilité du biocapteur dépend fortement de la concentration de PEGDE : la sensibilité est faible quand la concentration de PEGDE est basse, en augmentant la concentration de PEGDE, la sensibilité augmente également jusqu'à atteindre un maximum. Une augmentation supplémentaire de la concentration de PEGDE diminue la sensibilité de biocapteur, probablement à cause de la réticulation excessive de l'enzyme et de sa désactivation. La même optimisation a été effectuée pour deux autres enzymes : D-aminoacide Oxydase (DAAO) et Glutamate Oxydase, pour obtenir une immobilisation stable sur la surface de la microélectrode.

En utilisant les paramètres optimaux, une série de biocapteurs sensibles au glucose a été réalisée et caractérisée. Nous avons mesuré leur temps de réponse, la gamme de linéarité et la constante apparente de Michaelis-Menten  $K_m^{\text{app}}$ .

Pour étudier le temps de réponse du biocapteur, celui-ci a été rapidement transféré du tampon dans la solution de glucose générant un courant d'oxydation correspondant à la réaction enzymatique. Le temps de réponse a été estimé comme le temps nécessaire pour atteindre 90% du plateau de réponse.

Une calibration dans une large gamme de concentrations (1mM) a été effectuée pour déterminer une plage de linéarité de la réponse. Les paramètres cinétiques, en particulier, la constante apparente de Michaelis-Menten ( $K_m^{\text{app}}$ ) a été calculée à partir de courbes expérimentales en utilisant un modèle mathématique.

Finalement, les résultats obtenus par les biocapteurs construits en utilisant le PEGDE ont été comparés à ceux de capteurs où la Glucose Oxydase, la DAAO et la Glutamate Oxydase ont été immobilisées par réticulation dans les vapeurs de Glutaraldéhyde. En effet, immobilisation par Glutaraldéhyde est une méthode reconnue et largement utilisée pour la fabrication de biocapteurs. Elle est considérée comme une méthode de référence, malgré son caractère toxique.

La comparaison des résultats indique qu'en utilisant le PEGDE les capteurs de glucose et de D-sérine sont significativement plus sensibles que les capteurs à base de Glutaraldéhyde (Glucose :  $147 \pm 45$  vs  $106 \pm 29 \mu\text{A} \cdot \text{mM}^{-1} \text{cm}^{-2}$ , D-sérine :  $212 \pm 119$  vs  $87 \pm 27 \mu\text{A} \cdot \text{mM}^{-1} \text{cm}^{-2}$ ). Quand au glutamate, les deux types de capteurs ne diffèrent pas en sensibilité ( $173 \pm 63$  vs  $178 \pm 99 \mu\text{A} \cdot \text{mM}^{-1} \text{cm}^{-2}$ ). Le temps de réponse de biocapteurs à base de PEGDE et de Glutaraldéhyde sont similaires (environ 3.2 sec) à l'exception des capteurs de glutamate, qui sont plus rapides si l'enzyme est immobilisée par Glutaraldéhyde ( $3.6 \pm 0.5$  vs  $2.1 \pm 1$  sec). Enfin, généralement, les deux types de capteurs ne présentent pas de différence significative en  $K_m^{\text{app}}$ , sauf pour la D-sérine, pour laquelle les capteurs à base de PEGDE ont

montré un  $K_m^{app}$  plus faible ( $1.3 \pm 0.4$  vs  $3.6 \pm 0.4$  mM).

Les capteurs de glucose à base de PEGDE ont été également caractérisés en terme de stabilité dans les conditions opérationnelles et dans les conditions de stockage. Les capteurs ont été placés dans un bain-marie à 37°C pendant 3 jours, conditions proches des conditions physiologiques. Après 3 jours à 37°C, la sensibilité des capteurs a augmenté à  $23 \pm 17\%$ . Nous avons aussi démontré que les capteurs sont réutilisables pour les expériences in vivo de durée 5-8 h sans perte importante en sensibilité. Pour évaluer la stabilité à long terme, les capteurs ont été stockés dans un réfrigérateur à 4°C pendant 3 mois et testés tous les 20 jours. Dans ces conditions, la sensibilité des biocapteurs n'a pas diminué de façon significative.

Finalement, nous avons étudié la fiabilité de nos biocapteurs pour les études in vivo. Les capteurs à glucose ont été implantés dans le cerveau de rats anesthésiés et la concentration basale de glucose a été évaluée à  $0.68 \pm 0.15$  mM. Ce résultat est en accord avec les données publiées par des équipes indépendantes. Nous avons ensuite cherché à moduler la concentration de glucose dans le SNC de rat pour démontrer la capacité de nos capteurs à suivre les variations de concentration dans le temps réel. L'administration d'insuline a provoqué la diminution progressive du courant d'oxydation enregistré par le capteur à glucose mais pas de celui détecté par l'électrode de contrôle. L'injection de glucose 1h après administration de l'insuline a fait monter rapidement le signal au-dessus de sa valeur initiale. Les étalonnages de capteurs après expériences in vivo ont validé l'activité de l'enzyme et la stabilité du signal des biocapteurs. Les effets de l'insuline puis de l'injection de glucose sont bien connus et le fait que nos capteurs à base de PEGDE reproduisent ces données indique leur potentialité à être utilisés dans des études neurochimiques du cerveau. Cette conclusion est également confirmée par des expériences utilisant les capteurs à D-sérine, dont l'estimation de la concentration in vivo s'est révélée proche de celle donnée par des capteurs à base de Glutaraldéhyde.

Les résultats de ce chapitre confortent l'idée que le PEGDE est une solution pour l'immobilisation covalente d'enzymes sur des électrodes de biocapteurs. Plusieurs méthodes couramment utilisées, telles que la fixation par glutaraldehyde et le piégeage d'enzyme dans un sol-gel ou une matrice de polypyrrole dérivé utilisent des composants toxiques ce qui limite leur application clinique. Ainsi, le PEGDE offre une alternative propre, non-toxique à ces méthodes. Ses propriétés avantageuses –coût bas et facilité d'emploi, font du PEGDE une méthode prometteuse pour la fabrication de biocapteurs in vivo.

Le **Chapitre 3** est une adaptation d'un chapitre écrit pour l'ouvrage Microelectrode biosensors (Humana Press, N. Dale and S. Marinesco Eds.). Dans ce chapitre nous présentons l'étude comparative de cinq méthodes d'immobilisation d'enzyme couramment utilisées dans le domaine des Neurosciences: l'immobilisation par réticulation dans des vapeurs de Glutaraldéhyde ou par le PEGDE, greffage dans une matrice d'hydrogel, le piégeage dans une matrice de sol-gel ou d'un dérivé du polypyrrole. Nous avons effectué l'étude comparative des biocapteurs fabriqués par ces différents procédés en termes de sensibilité, de stabilité in vivo, de temps de réponse et de toxicité et de danger potentiel.

Les méthodes d'immobilisation par le Glutaraldéhyde et le PEGDE sont discutées dans le chapitre 2. Néanmoins, il faut préciser que ces méthodes produisent une immobilisation covalente en utilisant des molécules bi-fonctionnelles. Le PEGDE fait partie des composants utilisés pour la synthèse des hydrogels utilisés dans la construction de biocapteurs de glucose commerciaux. L'hydrogel est une matrice à base d'un polymère de polyvinylpyridine, soluble dans l'eau, mais qui, suite à la réaction avec l'enzyme par le

PEGDE, augmente sa masse molaire et forme une membrane enzymatique insoluble dans l'eau. Le rôle du PEGDE est de greffer l'enzyme aux groupes fonctionnels du polymère. L'hydrogel se présente comme une couche transparente capable d'augmenter considérablement sa teneur en eau, ce qui diminue les contraintes de diffusion de molécules dans son volume et facilite le transport du substrat enzymatique et des produits de réaction.

Le piégeage de l'enzyme dans une matrice de polymère qui retient la protéine par des forces physiques est une deuxième approche largement utilisée pour la construction de biocapteurs. Le principe consiste en la polymérisation de monomères sur la surface des microélectrodes. L'enzyme étant présente dans la même solution précipite sur la microélectrode au cours de la polymérisation et reste piégée dans la matrice de polymère. Les matrices sol-gel et polypyrrole sont les plus couramment utilisées.

Ces cinq procédés ont été adaptés dans le laboratoire et utilisés pour construire des biocapteurs de glucose et de glutamate. Ces biocapteurs ont été utilisés pour déterminer la relation entre la concentration de substrat et le courant d'oxydation détecté sur la microélectrode. Le courant a été mesuré après chaque injection de la solution de substrat en augmentant progressivement sa concentration. La courbe reconstituée ressemble à la cinétique enzymatique de Michaelis-Menten. Elle commence par une partie linéaire, qui correspond à une plage de linéarité du signal du biocapteur, puis s'incurve et atteint un plateau.

Une reconstitution mathématique nous a permis de calculer le  $K_m$  apparent du système constitué de l'enzyme immobilisée sur l'électrode. Nous avons obtenu des valeurs très variées de  $K_m^{app}$  des capteurs de glucose allant de  $1.1 \pm 0.2$  mM pour immobilisation par Glutaraldehyde à  $5.6 \pm 2$  mM pour l'immobilisation dans le sol-gel. Néanmoins, les valeurs sont considérablement plus faibles par rapport au  $K_m$  de la Glucose Oxidase libre (26-30 mM). En revanche, les  $K_m^{app}$  de capteurs de Glutamate sont plus importants par rapport enzyme libre allant de  $0.4 \pm 0.1$  mM pour l'hydrogel à  $0.9 \pm 0.5$  mM pour le glutaraldehyde par rapport aux 0.2 mM de glutamate oxidase libre. Ces effets peuvent venir en particulier, de la pré-concentration ou de l'exclusion du substrat de la matrice enzymatique. En effet, la pré-concentration peut diminuer le  $K_m^{app}$ , alors que l'exclusion de la membrane peut augmenter sa valeur.

Pour toutes les méthodes sauf la méthode sol-gel, les capteurs ont montré une linéarité de réponse dans une gamme de concentration allant de 0 à 100-300  $\mu$ M pour le glucose, et de 0 à 75  $\mu$ M pour le glutamate. Ces résultats sont en accord avec les calculs théoriques, qui prévoient la linéarité du signal jusqu'à une concentration d'environ  $K_m/10$ . Les capteurs préparés par la méthode sol-gel ne respectent pas cette règle, car la linéarité s'étend jusqu'à 2.5 mM pour le glucose et 140  $\mu$ M pour le glutamate. Ces résultats laissent supposer que l'enzyme piégée dans la matrice de sol-gel ne suit pas le modèle cinétique de Michaelis-Menten.

La sensibilité des biocapteurs a été estimée à partir des plages de linéarité et exprimé en pA/ $\mu$ M de substrat. Pour les capteurs de glucose la sensibilité a varié entre  $12.2 \pm 3.7$  pA/ $\mu$ M (pour PEGDE) et  $1 \pm 0.1$  pA/ $\mu$ M (pour sol-gel); et pour les capteurs de glutamate entre  $21.6 \pm 3.1$  pA/ $\mu$ M et  $14.4 \pm 8.2$  pA/ $\mu$ M sans différence significative pour les capteurs à base de glutaraldehyde, PEGDE ou hydrogel. Les capteurs à base de sol-gel ont montré une sélectivité significativement plus basse à  $7.8 \pm 3.5$  pA/ $\mu$ M.

Le temps de réponse des biocapteurs a été également mesuré. Parmi les capteurs de glucose, ceux à base de polypyrrole se sont révélés plus lents avec un temps de réponse à  $4.8 \pm 0.7$  sec (par rapport 2-3 sec). Parmi les capteurs de glutamate, les plus lents étaient les capteurs de PEGDE, avec un temps de réponse de  $3.6 \pm 0.5$  sec, par rapport 1.5-2.1 sec

par les autres méthodes. Néanmoins, ces valeurs sont acceptables pour assurer le suivi des événements biologiques en temps réel.

Les capteurs implantables doivent assurer la stabilité de réponse dans le cerveau pendant plusieurs heures, voire même plusieurs jours. La stabilité du signal dépend de la stabilité de la couche enzymatique, mais aussi de ses propriétés biochimiques. La biocompatibilité des matériaux utilisés dans la fabrication de biocapteurs peut avoir un impact important sur la stabilité de la réponse du biocapteur. Dans la littérature cet effet est connu et il a été rapporté que les biocapteurs avec l'enzyme immobilisée dans les matrices de sol-gel ou de polypyrrole subissent une désactivation partielle ou complète après implantation dans les tissus cérébraux. Dans notre étude, nous avons testé la stabilité des biocapteurs à 37°C dans un bain-marie pendant 2-3h. A l'exception de la matrice sol-gel, toutes les autres méthodes ont montré une bonne stabilité dans ces conditions. Le signal des capteurs à base de sol-gel a été dégradé considérablement au cours des premières heures et ensuite le signal est resté stable pendant plusieurs jours ou semaines. Les capteurs à base de PEGDE, Glutaraldéhyde et hydrogel ont ensuite été testés dans les expériences in vivo. Nous avons pu détecter la D-sérine ou le glucose pendant ou moins 5h dans le cortex de rats anesthésiés avec une bonne stabilité du signal.

Cette étude comparative des méthodes nous a permis de conclure que les méthodes d'immobilisation covalentes (par Glutaraldéhyde, PEGDE et hydrogel) sont préférable pour la fabrication des capteurs implantables car elles assurent une bonne stabilité de la couche enzymatique avec une meilleur sensibilité. L'immobilisation covalente est plus robuste et elle peut s'appliquer à une grande variété d'enzymes. Quant au polypyrrole, il n'a pas permis d'immobiliser la glutamate oxidase. Cette méthode s'est avérée très délicate et très sensible aux conditions expérimentales utilisées. De plus, la synthèse du monomère de pyrrole dérivé est complexe et longue. Les capteurs avec l'enzyme immobilisée dans une matrice de sol-gel ont été utilisés dans les expériences in vivo. Cependant leur faible sensibilité et stabilité limitent leur utilisation pour la détection des molécules présentes en faible concentration et sur de longues durées. Parmi les méthodes covalentes, le PEGDE est préférable au Glutaraldéhyde ou hydrogel, car il ne demande pas de synthèse organique des composants supplémentaires. Le fait qu'il soit non-toxique et bon marché est un argument supplémentaire pour cette méthode d'immobilisation de l'enzyme.

L'étude comparative a mis également en évidence l'effet de la procédure de fixation de l'enzyme sur la spécificité du biocapteur. Le **Chapitre 4** est principalement dédié à ce sujet.

L'étude de la composition du milieu interstitiel du cerveau, qui contient une large variété de molécules, est une tâche difficile qui demande des techniques très sélectives pour obtenir des données fiables. Il est donc important que le procédé d'immobilisation utilisé pour fabriquer les biocapteurs préserve la spécificité de l'enzyme pour son substrat. Les enzymes immobilisées sont largement utilisées dans la synthèse organique et dans l'industrie. Beaucoup de travaux ont été réalisés pour comprendre l'effet de l'immobilisation sur les propriétés de l'enzyme telles que la stabilité, l'activité, la sélectivité pour les molécules souhaitées etc. Suite à l'immobilisation, l'enzyme se trouve dans une matrice polymérique qui forme une barrière de diffusion. Le changement de coefficient de diffusion entre la solution et la matrice, ainsi que l'affinité de la molécule pour cette matrice peut provoquer une répartition inégale du substrat à l'intérieur et à l'extérieur de la matrice (« partitioning effect »), qui mène à la pré-concentration ou à l'exclusion de cette molécule de la membrane enzymatique. La spécificité naturelle de l'enzyme peut aussi être modifiée par la rigidité induite par la fixation de la protéine à la matrice, ou par des changements de la

mobilité ou de la géométrie du site actif. Cet effet de l'immobilisation sur la sélectivité de l'enzyme est parfois mis à profit dans le cadre de la catalyse enzymatique. Dans le domaine des biocapteurs, en revanche, cet effet a été très peu étudié. La sélectivité de l'enzyme doit toujours être préservée par l'immobilisation pour assurer une sélectivité optimale pour le biocapteur. Cette caractéristique est extrêmement importante pour la détection des neurotransmetteurs qui sont présents en faibles quantités dans le milieu extracellulaire du cerveau, comme par exemple le glutamate. Nous avons caractérisé l'effet des méthodes d'immobilisation les plus utilisées pour fabriquer des biocapteurs implantables sur les performances de ces dispositifs et particulièrement sur la sélectivité au substrat. Des capteurs de glucose et de glutamate ont été utilisés pour cette étude.

La Glucose Oxydase libre oxyde préférentiellement le glucose en gluconolactone, mais présente aussi une activité significative pour les autres substrats, par exemple le 2-déoxy-D-glucose (2-DG), le mannose, le galactose et le xylose. Elle est aussi légèrement sensible au lactose mais insensible au fructose. Nous avons mesuré l'activité de la Glucose Oxydase libre ou après fixation par Glutaraldéhyde, PEGDE, hydrogel, sol-gel et polypyrrole dérivé, pour le glucose et les substrats secondaires. Nous avons démontré que l'activité de l'enzyme a augmenté significativement pour tous les substrats secondaires après immobilisation par le Glutaraldéhyde. Les capteurs PEGDE et hydrogel ont présenté une activité significativement plus élevée pour la 2-DG et pas pour les autres substrats. Quand aux capteurs à base de sol-gel, leur activité a significativement augmenté pour le 2-DG et le Fructose. La matrice de polypyrrole dérivé n'a pas eu d'influence considérable sur la spécificité naturelle de la glucose oxydase.

Nous avons ensuite déterminé l'effet de l'immobilisation sur la spécificité de la Glutamate Oxydase, souvent utilisée dans la fabrication de biocapteurs de glutamate pour les études dans le système nerveux central. Seuls les capteurs à base de PEGDE et de Glutaraldéhyde ont été utilisés car la méthode par sol-gel n'assure pas la stabilité du signal des biocapteurs et nous n'avons pas réussi à immobiliser la glutamate oxydase dans une matrice de polypyrrole dérivé. Les capteurs de glutamate ont été testés pour le glutamate et pour les substrats secondaires potentiels: la glutamine, l'asparagine, l'aspartate et l'histidine. La Glutamate oxydase libre est une enzyme très spécifique au glutamate. Nous n'avons détecté aucune activité pour ces quatre acides aminés. En revanche, une faible activité de 0.03 à 0.3% pour les acides aminés secondaires (par rapport au signal de glutamate) a été mesurée sur les capteurs PEGDE. Cette perte de sélectivité a été largement aggravée dans le cas de l'immobilisation par Glutaraldéhyde avec l'activité pour les substrats secondaires allant jusqu'à 15%.

Il est possible que cette perte de sélectivité soit due à la rigidification de la structure de l'enzyme, et/ou à une distorsion de son site actif suite à la procédure de fixation. De ce point de vue, le procédé à base de PEGDE est plus avantageux pour l'immobilisation de l'enzyme, car la cinétique de réaction est plus lente, et permet à l'enzyme de prendre sa conformation la plus favorable en préservant son site actif. De plus, la molécule de PEGDE est plus longue en comparaison du Glutaraldéhyde (4nm vs 0.7 nm), ce qui laisse plus de liberté de mouvement à l'enzyme au cours de la catalyse.

Les milieux biologiques tels que le sérum, le liquide céphalo-rachidien, les homogénats de cerveau ou les microdialysats sont des mélanges complexes contenant de nombreuses molécules. Par conséquent, la perte de sélectivité du biocapteur peut considérablement altérer la détection et la quantification de molécules d'intérêt.

Pour évaluer l'impact potentiel de cette perte de sélectivité, les concentrations des substrats secondaires de Glucose et Glutamate Oxydase dans le sérum, les homogénats

tissulaires et les microdialysats de cerveau de rats ont été quantifiés. Les concentrations de sucres ont été dosées par HPLC. La concentration de D-Galactose s'est révélée très faible dans les homogénats de cerveau ( $0.5 \pm 0.07 \mu\text{g/g}$ ) et indétectable dans le sérum. La concentration significative de D-Mannose a été mesurée dans le sérum ( $0.03 \pm 0.01 \text{ mM}$ ) et l'homogénat ( $19 \pm 4 \mu\text{g/g}$ ) de cerveau. Néanmoins, la concentration de glucose est beaucoup plus élevée que celle des autres sucres dans les milieux biologiques ( $11 \pm 2 \text{ mM}$  dans le sérum,  $81 \pm 8 \mu\text{g/g}$  de tissu dans l'homogénat de cerveau). L'HPLC a été également utilisé pour quantifier la concentration d'acides aminés dans les homogénats et microdialysats de cerveau. Nous avons mesuré la concentration de 20 acides aminés protéinogéniques à l'exception de l'hydroxyproline. Dans les homogénat de cerveau le glutamate était présent en quantité plus élevée ( $1980 \pm 434 \mu\text{g/g}$ ) que la glutamine ( $1044 \pm 244 \mu\text{g/g}$ ) et l'aspartate ( $426 \pm 100 \mu\text{g/g}$  de tissu). En revanche, dans les microdialysats, le glutamate était présent en quantité beaucoup plus faible que la glutamine ( $4 \pm 1 \mu\text{M}$  vs  $41 \pm 15 \mu\text{M}$ ), la proline ( $12 \pm 8 \mu\text{M}$ ) ou la lysine ( $9 \pm 2 \mu\text{M}$ ). Par conséquent, contrairement aux capteurs de glucose, les capteurs de glutamate risquent de surestimer la concentration de glutamate dans le milieu extracellulaire en raison de la perte de la spécificité de l'enzyme suite à son immobilisation sur la surface de la microélectrode.

Pour vérifier la validité des mesures sur nos capteurs, nous avons mesuré la concentration de glucose et de glutamate dans les échantillons biologiques et comparé les résultats avec ceux obtenu par HPLC ou électrophorèse capillaire (CE-LIF) (pour les acides aminés). L'HPLC et les capteurs avec Glucose Oxidase immobilisée par Glutaraldéhyde ou PEGDE ont donné les mêmes estimations de la concentration de glucose dans le sérum (PEGDE  $100.1 \pm 6.0\%$ , Glutaraldéhyde  $107.1 \pm 4.4\%$  de valeur HPLC) les homogénats de cerveau (PEGDE  $102.8 \pm 4.1\%$ , Glutaraldéhyde  $92.1 \pm 5.2\%$  de valeur HPLC). Ceci confirme que la réponse des capteurs de glucose n'a pas été influencée par les substrats secondaires de la Glucose Oxidase. De même, l'estimation du glutamate dans les homogénats de cerveau n'a pas été différente entre les capteurs préparés avec PEGDE ou le Glutaraldéhyde, et la CE-LIF (PEGDE  $101.7 \pm 7.5\%$ , Glutaraldéhyde  $97.6 \pm 2.1\%$  de valeur CE-LIF). En revanche, dans les microdialysats, les capteurs à base de Glutaraldéhyde ont détecté une concentration de glutamate significativement plus élevée ( $145.1 \pm 43.0\%$  de valeur CE-LIF,  $F(2,68)=6.20$ ,  $p < 0.01$ ) que les capteurs PEGDE ( $108.7 \pm 46.1\%$  de valeur CE-LIF). Ces résultats confirment notre hypothèse que la procédure d'immobilisation peut avoir un impact important sur la spécificité de l'enzyme et la quantification des molécules in vivo.

Nous avons effectué une série d'expériences pour étudier les conséquences de l'immobilisation de la Glutamate Oxidase par le Glutaraldéhyde et le PEGDE sur la détection de glutamate dans le SNC du rat. Le glutamate a été déjà détecté in vivo en utilisant la microdialyse. La concentration extracellulaire a été évaluée dans la gamme  $0.9$  à  $3.7 \mu\text{M}$ . Cependant, cette technique souffre d'une résolution temporelle basse et elle cause des lésions cérébrales locales par l'insertion de la sonde de microdialyse dans le cerveau. Le glutamate a été aussi détecté par les biocapteurs, mais des résultats très variables ont été rapportés allant de  $1.6$ - $4 \mu\text{M}$  (immobilisation par Glutaraldéhyde) à  $19$ - $29 \mu\text{M}$  (hydrogel) dans les rats anesthésiés et à  $19$ - $45 \mu\text{M}$  dans les rats éveillés (Glutaraldéhyde). En plus de leur variabilité, ces données sont problématiques car des concentrations aussi élevées de glutamate sont en général toxiques pour les cellules. Notre étude montre que la méthode d'immobilisation utilisée pour la construction de biocapteurs peut impacter significativement la quantification de la concentration de glutamate dans le milieu extracellulaire. En utilisant le Glutaraldéhyde pour l'immobilisation de la Glutamate Oxidase, l'enzyme perd sa spécificité menant à la surestimation significative du glutamate.



En utilisant les capteurs PEGDE la concentration de glutamate a été évaluée à  $1.16 \pm 0.34 \mu\text{M}$  vs  $16.4 \pm 8.4 \mu\text{M}$  (estimée par capteurs Glutaraldéhyde). Contrairement aux données bibliographiques, le glutamate basal n'a pas varié en fonction de l'anesthésie utilisée (uréthane ou isoflurane), ainsi que chez les rats éveillés. Nous avons également démontré que seulement 35% de glutamate basal est d'origine neuronale (par administration de tétradotoxine, un bloqueur de l'influx nerveux. Finalement, les stimulations électriques des terminaisons synaptiques n'ont pas permis de détecter un débordement (« spillover ») de glutamate depuis les fentes synaptiques vers l'espace extrasynaptique où est effectuée la mesure. Nos résultats contredisent les études précédentes utilisant les biocapteurs à base de Glutaraldéhyde, qui semblent indiquer la présence de glutamate en concentration plus élevée chez le rat éveillé par rapport au rat anesthésié, ou que le glutamate diffuse dans milieu interstitiel suite la stimulation électrique. De plus, des données très variables ont été rapportées à propos de l'origine du glutamate extracellulaire indiquant 25-90% (hydrogel) ou même 100 % (Glutaraldéhyde) de glutamate neuronale. Ces résultats de la littérature obtenus avec des biocapteurs à base de Glutaraldéhyde sont à interpréter avec prudence à cause de la perte de sélectivité de la glutamate oxidase et les interférences possibles de la glutamine et des autres substrats secondaires de la glutamate oxydase. Les résultats obtenus avec les biocapteurs PEGDE sont, elles, plus conformes avec les données issues d'autres méthodes d'investigation. Ainsi, nous avons estimé à 35 % la diminution du glutamate extracellulaire suite à l'injection de tétradotoxine, ce qui est en accord avec le modèle actuel de régulation de glutamate extracellulaire par l'échangeur cystéine-glutamate. L'absence de « spillover » suite la stimulation électrique est aussi en accord avec les études récentes par imagerie, qui ont rapporté un « spillover » d'environ  $2 \mu\text{M}$  de glutamate pendant moins de 300 ms après la stimulation. Les biocapteurs ne sont pas capables de détecter de tels changements rapides de la concentration en raison de leur temps de réponse de l'ordre 2-3 s.

Nos résultats indiquent donc que l'immobilisation d'enzyme par PEGDE est une méthode optimale pour la fabrication de microbiocapteurs. Cette étude montre que l'immobilisation PEGDE est assez douce pour préserver la spécificité naturelle de l'enzyme. Le PEGDE est une méthode avantageuse qui permet l'immobilisation non seulement de la Glucose Oxidase et de la Glutamate Oxidase, mais aussi d'une vaste gamme d'autres enzymes d'intérêt potentiel pour les études neurochimiques. Cette méthode permet de développer les outils justes et précis pour l'étude des communications cellulaires et du fonctionnement du cerveau plus généralement.

**Chapitre 5.** Actuellement, deux configurations d'électrode sont fréquemment utilisées pour la conception des biocapteurs implantables. L'électrode cylindrique constituée d'un fil de platine (ou autre métal noble ou carbone) inséré dans un capillaire en verre était un des premiers dispositifs implantables présentés dans les années 1950 et il reste toujours le plus utilisé dans ce domaine. Les électrodes de ce type sont très faciles à fabriquer et à manipuler, leur taille et forme permettent un accès facile dans les structures les plus profondes du cerveau avec une altération minimale du tissu nerveux. Cependant, leur fabrication est manuelle et donc couteuse, et conduit à une mauvaise reproductibilité de la surface de l'électrode. Par ailleurs, le dosage simultané de plusieurs molécules ou de la même molécule dans des structures différentes du cerveau est d'un grand intérêt pour la compréhension du métabolisme et de la signalisation cellulaire du cerveau. Ceci exige l'implantation de plusieurs biocapteurs cylindriques qui est non seulement d'une haute difficulté technique mais s'accompagne de lésions plus importantes que lors de l'implantation

d'une seule électrode. La détection simultanée devient possible avec l'introduction des microsondes à plusieurs électrodes intégrées sur une seule aiguille.

Les progrès dans le domaine de la microfabrication en salle blanche a permis de réaliser des dispositifs destinés à l'analyse multicomposante dans un milieu complexe. Les sondes multisensibles portant plusieurs électrodes ont été fabriquées pour la première fois par l'équipe de Wise par des procédés de microfabrication. La technologie consiste en un dépôt de métal sur la surface d'un support, généralement en silicium, puis à sa gravure pour créer un motif correspondant à la forme désirée des électrodes. Des pistes conductrices et des plots de contact électrique sont également réalisés par gravure sélective. L'isolation externe de l'ensemble du dispositif est indispensable. Une couche de passivation recouvre des pistes conductrices en laissant les électrodes et les zones de contact exposés. Le nitrure de silicium est généralement utilisé pour la passivation à cause de ses excellentes propriétés d'isolation électrique et de barrière de diffusion aux molécules d'eau et aux ions de sodium. Après dépôt en film mince sur tout le substrat les ouvertures sont réalisées par gravure ionique réactive (Reactive Ion Etching ou RIE) sur les zones d'électrodes et les contacts. Cependant, l'épaisseur de nitrure de silicium est limitée par le temps de dépôt, approximativement 200-300nm par heure, rendant le procédé cher et coûteux. Le pyralène et le polyimide sont des matériaux alternatifs au nitrure de silicium. Ils permettent d'obtenir une couche de passivation dont l'épaisseur est de l'ordre du  $\mu\text{m}$ . La disponibilité de résines photosensibles SU8 a ouvert de nouvelles voies pour la microfabrication. En particulier, ces résines ont montré de bonnes propriétés isolantes avec une épaisseur facilement modulable dans la gamme 1-100  $\mu\text{m}$ . De plus, la résine SU8 a été reconnue comme étant biocompatible, ce qui la rend particulièrement adaptée à la fabrication de microsondes implantables. L'utilisation de techniques de microfabrication est avantageuse car elle permet la fabrication de plusieurs dispositifs en parallèle avec une excellente reproductibilité et un bon rendement économique (coût unitaire).

Au début de nos travaux, fin 2008, très peu de publications étaient dédiées aux microsondes enzymatiques implantables pour la détection et le contrôle simultanés de marqueurs biologiques. Ceci s'explique par la difficulté de miniaturiser tous les procédés de fabrication de biocapteurs, de la conception de l'électrode à la mise au point du dépôt d'enzyme et de couches protectrices. En effet, la conception des électrodes doit limiter la superposition des zones de diffusion d'électrodes adjacentes. De plus, la méthode de dépôt d'enzyme doit permettre l'application locale en évitant la contamination croisée entre les électrodes.

Dans ce travail de thèse nous avons développé un procédé de fabrication en salle blanche de sondes multisensibles pour la détection simultanée de glucose et lactate. Des sondes à trois électrodes ont été fabriquées sur des plaques de silicium de  $250\mu\text{m}$  d'épaisseur recouvert d' $1\mu\text{m}$  d'oxyde thermique. Une couche de métallisation (20nm Ti et 150nm Pt) a été structurée par la procédure de lift-off sur de la résine AZ5214 pour réaliser le design à trois électrodes. La résine photosensible SU8 d'une épaisseur de  $4\mu\text{m}$  a été utilisée pour l'isolation du dispositif. Ensuite, le motif des microsondes a été transféré en face avant du substrat par lithographie, suivi par la lithographie en face-arrière pour permettre la gravure de substrat en face arrière. Le film de  $\text{SiO}_2$  a été gravé en face arrière et en face avant simultanément par le mélange de  $\text{NH}_4^+/\text{HF}$ . Afin de donner aux microsondes une forme d'aiguille, la gravure ionique réactive profonde (DRIE) a été réalisée en face avant, puis en face-arrière pour déterminer l'épaisseur finale des microsondes. Pendant la DRIE le Pt et la SU8 ont été protégés par de la résine épaisse SPR 220-4.5. Enfin, les microsondes ont été libérées du substrat de silicium par cassure manuelle. Une fois les électrodes

libérées de leur substrat et avant tous les tests in vitro, les biosondes ont été montés sur un circuit imprimé et traitées électro-chimiquement dans l'acide sulfurique 1M en balayant le potentiel de -1V au +1V pendant 15-25 min.

Tout d'abord, nous avons quantifié l'effet de contamination croisée («cross-talk») lié à la diffusion de molécules entre électrodes adjacentes en utilisant le système électrochimique réversible  $K_3[Fe(CN)_6]/K_2[Fe(CN)_6]$ . Le principe de ce test consiste à réduire  $K_3[Fe(CN)_6]$  en  $K_2[Fe(CN)_6]$  sur une électrode maintenue à -500mV et de suivre la diffusion de molécules réduites, par l'enregistrement du courant d'oxydation de  $K_2[Fe(CN)_6]$  en  $K_3[Fe(CN)_6]$  sur une électrode adjacente maintenue à +500mV. Les résultats obtenus indiquent que le «cross-talk» ne dépend pas de la profondeur du puits formé sur la SU8 dans la gamme d'épaisseurs de la résine SU8 0.8-11 $\mu$ m. En revanche, le «cross-talk» est apparemment plus prononcé quand la surface du dispositif est plus hydrophile (par exemple, si la résine SU8 a été traité par plasma d'oxygène). Nous avons ensuite estimé le «cross-talk» après immobilisation de glucose oxidase sur une des microélectrodes. Deux techniques ont été testées : le dépôt manuel de petites gouttes d'enzyme ou le dépôt par précipitation locale dans une matrice de chitosan. Nous avons démontré que le «cross-talk» varie entre 15% et 50% sur l'électrode adjacente quand l'enzyme était immobilisé dans la matrice de chitosan. Seulement 2.46 $\pm$ 1.43% ont été détecté quand la Glucose Oxidase a été déposée en goutte localement sur une électrode. Nous supposons que pendant le dépôt par électro-précipitation dans la solution de chitosan, l'enzyme adhère non spécifiquement sur les électrodes adjacentes et que l'augmentation du courant d'oxydation (cross-talk) est lié à l'activité de l'enzyme accidentellement déposée.

Avant de pouvoir utiliser les microsondes multisensibles pour des expériences dans le SNC d'animaux de laboratoire, en plus de l'absence de cross-talk, la technique d'immobilisation doit assurer la stabilité de la couche enzymatique sur la surface de la microélectrode, et les capteurs doivent avoir bonne sensibilité pour la molécule d'intérêt et présenter une réponse linéaire dans la gamme de concentrations estimée dans le cerveau. Les microsondes multisensibles ont été développées pour la détection simultanée de glucose et de lactate. La méthode PEGDE développée aux chapitres 1 et 3 a été utilisée pour immobiliser la glucose oxydase et Lactate Oxidase La solution enzymatique optimale pour la Lactate Oxydase contient 20 mg/mL de Lactate oxydase, 20 mg/mL de BSA et 80 mg/mL de PEGDE, pour une immobilisation à 55°C pendant 2h. Nous avons obtenu des biocapteurs présentant une sensibilité de 44.8 $\pm$ 37.4  $\mu$ A.mM<sup>-1</sup>cm<sup>-2</sup> (n=9) pour le glucose et de 140.4 $\pm$ 113.5  $\mu$ A.mM<sup>-1</sup>cm<sup>-2</sup> (n=11) pour le lactate.

Finalement, nous avons utilisé des sondes multisensibles pour détecter le glucose et lactate dans le cortex de rats anesthésiés, ainsi que les courants non-spécifiques de la troisième électrode recouverte par une couche de protéine non active (BSA). Avant implantation, les capteurs ont été recouverts par une membrane de polyuréthane pour obtenir un signal linéaire dans la gamme 0-1mM de glucose et de lactate. Nous avons enregistré un courant d'oxydation dans le cerveau qui correspond à concentration basale de glucose et lactate de 1.2mM et de 400 $\mu$ M respectivement. La concentration basale de glucose mesurée dans le cortex est différente par rapport la valeur présentée dans le chapitre 2, mais elle reste en accord avec les données bibliographiques allant de 0.47 $\pm$ 0.18 à 2.4-3.3 mM. Nous avons ensuite administré de l'insuline et détecté une diminution du courant d'oxydation sur le biocapteur de glucose, mais pas sur le capteur de lactate ou sur l'électrode de contrôle. Une solution de glucose a été injectée en intrapéritonéal 30 minutes après l'administration de l'insuline et l'augmentation de courant d'oxydation a été observée seulement sur le capteur à glucose. Ces résultats indiquent que la mesure du glucose est

bien indépendante de celle du lactate. Ces microsondes multisensibles sont appropriées pour enregistrer en temps réel le changement de la concentration de molécules dans le milieu interstitiel et elles peuvent être utilisées pour les études neurochimiques in vivo.

Les sondes à multi-capteurs développées dans cette thèse en utilisant les techniques de microfabrication et la méthode d'immobilisation de l'enzyme par PEGDE, pourront à l'avenir être utilisées dans les études neurochimiques destinées à améliorer notre compréhension des communication chimiques entre les cellules cérébrales par : (1) la suivi de la concentration de neurotransmetteurs et de métabolites, et (2) l'étude des variations de leur concentration en réponse à un traitement pharmacologique, ou une stimulation électrique ou biologiques, pour comprendre leur rôle dans le fonctionnement physiologique et pathologique du cerveau. Cette compréhension est indispensable pour concevoir des stratégies pharmacologiques appropriées et le traitement médical efficace de nombreuses maladies neurologiques. Une des perspectives à long terme de cette thèse est l'application clinique des microsondes multisensibles pour le suivi de patients en état de conscience minimal, afin de prévoir les complications secondaires comme le vasospasme cérébral après un traumatisme crânien ou une hémorragie subarachnoïdienne. Les données issues de ce nouveau type de monitoring permettraient de prendre les mesures appropriées pour améliorer la prise en charge des malades.



## **Annex 4. List of publications related to the thesis project**

### ***Publications***

1. Vasylieva, N., Maucler, C., Meiller, A., Barbier, D., Marinesco S. (2012) Implantable enzymatic biosensors for neurotransmitter detection: effects of immobilization method on enzyme selectivity and consequences on glutamate detection in the brain (submitted).
2. Vasylieva, N., and Marinesco, S. (2012) Enzyme immobilization on microelectrode biosensors, In MICROELECTRODE BIOSENSORS, Humana Press (accepted).
3. Vasylieva, N., Sabac, A., Marinesco, S., and Barbier, D. Simple and non toxic enzyme immobilization onto platinum electrodes for detection of metabolic molecules in the rat brain using silicon micro-needles, *Procedia Engineering* 2011, 25, 1361-1364.
4. Vasylieva, N., Barnych, B., Meiller, A., Maucler, C., Pollegioni, L., Lin, J.S., Barbier, D., Marinesco S. Covalent enzyme immobilization by poly(ethylene glycol) diglycidyl ether (PEGDE) for microelectrode biosensor preparation. *Biosens Bioelectron* 2011, 26(10), 3993-4000.

### ***Lecture communication***

1. N. Vasylieva, Simple and non toxic enzyme immobilization onto Platinum electrodes for detection of metabolic molecules in the rat brain using silicon micro-needles, 4-7 September 2011, EUROSENSORS XXV, Athens, Greece.
2. N. Vasylieva. Enzymatic biosensor performance optimization depending on applied enzyme immobilization technique. XIII<sup>ème</sup> seminar of French Bioelectrochemistry Society, 17-20 May 2010, Lacanau-Océan, France.

### ***Poster communication***

1. N. Vasylieva, Implantable enzymatic biosensors for neurotransmitter detection: effects of immobilization method on enzyme selectivity and consequences on glutamate detection in the brain, symposium "Molecule imaging in the organism". Lyon, France, 25-26 June 2012.
2. N. Vasylieva, Implantable enzymatic biosensors for neurotransmitter detection: effects of immobilization method on enzyme selectivity and consequences on glutamate detection in the brain. Biosensors, Cancun, Mexico, 15-18 May 2012.
3. N. Vasylieva, Simple, non-toxic enzyme immobilization on microelectrode biosensors using PEGDE, 21st International Symposium on Bioelectrochemistry and Bioenergetics of the Bioelectrochemical Society (BES), Cracow, Poland, 8-12 Mai 2011.
4. A. Meiller, N. Vasylieva, S. Marinesco, Innovative microbiosensors for in vivo brain glucose monitoring, 10<sup>ème</sup> Seminar of French Neuroscience Society, Marseille 24-27 Mai, 2011.
5. N. Vasylieva, Enzymatic biosensors for the neurotransmitter detection: immobilization effect on enzyme selectivity, Ecole thématique CNRS "Fonctionnalisation de surfaces et méthodes de détection pour les biocapteurs", 8-12 Février 2010, les Houches, France.



FOLIO ADMINISTRATIF

THESE SOUTENUE DEVANT L'INSTITUT NATIONAL DES SCIENCES APPLIQUEES DE LYON

NOM : Vasylieva

DATE de SOUTENANCE : 11/09/2012

Prénoms : Natalia

TITRE : Implantable microelectrode biosensors for neurochemical monitoring of brain functioning

NATURE : Doctorat

Numéro d'ordre : 2012 ISAL 0078

Ecole doctorale : EEA

Spécialité : micro et nano technologies

RESUME : Identification, monitoring and quantification of biomolecules in the CNS is a field of growing interest for identifying biomarkers of neurological diseases. Implantable enzymatic microelectrode biosensors are a unique minimally invasive tool for real-time monitoring. Progress in microfabrication technologies has opened new possibilities in the preparation of complex biosensor architectures with numerous electrodes to respond to the needs of neurobiologists and neurochemists for simultaneous monitoring of numerous biomarkers.

In this thesis, silicon needle-shaped multisensing microprobes were developed. Our microelectrode array design comprises a needle length of 6mm with 100x50  $\mu\text{m}^2$  cross-section bearing three platinum electrodes with a size of 40x200  $\mu\text{m}$  and 200 $\mu\text{m}$  spacing between them. We have used these microprobes for simultaneous glucose and lactate monitoring, using the third electrode for control of non-specific current variations. Local microdroplet protein deposition on the electrode surface was achieved using a pneumatic picopump injection system.

Enzyme immobilization on the electrode surface is a key step in microelectrode biosensor fabrication. We have developed a simple, low cost, non-toxic enzyme immobilization method employing poly(ethyleneglycol) diglycidyl ether (PEGDE). Successful biosensor fabrication was demonstrated with glucose oxidase, D-amino acid oxidase, and glutamate oxidase. We found that these biosensors exhibited high sensitivity and short response time sufficient for observing biological events in vivo on a second-by-second timescale. PEGDE-based biosensors demonstrated an excellent long-term stability and reliably monitored changes in brain glucose levels induced by sequential administration of insulin and glucose solution. We then carried out a comparative study of five enzyme immobilization procedures commonly used in Neuroscience: covalent immobilization by cross-linking using Glutaraldéhyde, PEGDE, or a hydrogel matrix and enzyme entrapment in a sol-gel or polypyrrole-derived matrices. Enzymatic microelectrodes prepared using these different procedures were compared in terms of sensitivity, response time, linear range, apparent Michaelis-Menten constant, stability and selectivity. We conclude that PEGDE and sol-gel techniques are potentially promising procedures for in vivo laboratory studies. The comparative study also revealed that Glutaraldéhyde significantly decreased enzyme selectivity while PEGDE preserved it. The effects that immobilization can have on enzyme substrate specificity produce dramatic consequences on glutamate detection in complex biological samples and in the CNS. Our biosensor's results were systematically controlled by HPLC or capillary electrophoresis. The highly selective PEGDE-based biosensors allowed accurate measurements glutamate concentrations in the anesthetized and awaked rats at physiological conditions and under pharmacological and electrical stimulations.

The microfabricated multielectrodes based on silicon needles coupled to the simple, non-toxic and mild immobilization method based on PEGDE, opens new possibilities for specific neurotransmitter detection in the central nervous system and the study of cell-cell communication in vivo.

MOTS-CLES : biocapteur, électrochimie, amperometry, enzyme, immobilisation, PEGDE, microaiguille, silicium, MEMS, in vivo, rat, glucose oxidase, glutamate oxidase.

Laboratoire (s) de recherche : Institut des Nanotechnologies de Lyon, INL - Site INSA INSA-CNRS, UMR 5270,  
7, avenue Jean Capelle, Bât. Blaise Pascal, 69621 VILLEURBANNE Cedex, France

Inserm U1028, CNRS UMR 5292, Physiologie Intégrée du Système d'Eveil,  
Centre de Recherche en Neurosciences de Lyon, 8 avenue Rockefeller, UCBL, 69373 Lyon cedex 08 France

Directeur de thèse: Daniel Barbier,  
Stéphane Marinesco

Président de jury Eliane Souteyrand

Composition du jury: Eliane Souteyrand Daniel Barbier  
Christian Amatore Stéphane Marinesco  
Olivier Frey Andrei Sabac  
Pierre Temple Boyer  
Alain Walcarius